DOCTOR OF PHILOSOPHY

The Effects of Haptic Feedback on a Pilot Monitoring's Performance, Workload and Situation Awareness on Passive Sidestick Aircraft

Wolfert, Floris

Award date:
2024

Awarding institution:
Coventry University

Coventry University

Institute for Future Transport and Cities

The Effects of Haptic Feedback on a Pilot Monitoring's Performance, Workload and Situation Awareness on Passive Sidestick Aircraft

Ing. Floris Wolfert

A thesis submitted in partial fulfilment of the University's requirements for the degree of Doctor of Philosophy

December 18, 2023

Certificate of Ethical Approval

Applicant:

Floris Wolfert

Project Title:

The effects of Haptic Feedback on Pilots performance, workload and situation awareness, Experiment 1

This is to certify that the above named applicant has completed the Coventry University Ethical Approval process and their project has been confirmed and approved as Medium Risk

Date of approval:

15 January 2019

Project Reference Number:

P76095

Declaration of Authorship

The work presented in this thesis has been published and presented at an international conference. The content of that work has contributed towards the thesis in Chapter 2 (Literature Review) & Chapter 4 (Effects of Coupled Sidesticks on Pilot Monitoring Awareness during Hard Landings).

I declare that the paper detailed below is the original work and that I was the primary and lead author, with my supervisors as my co-authors providing contributions through study supervision and editorial direction.

Name:	**Signature:**	**Date:**
Floris Wolfert	This item has been removed due to third party copyright. The unabridged version of the thesis can be viewed at	14/01/22

Paper 1: Wolfert, F., Bromfield, M.A., Scott, S. and Stedmon. S., (2019) "Passive Sidesticks and Hard Landings – Is there a Link?", (AIAA 2019-3611), 2019 Aviation Technology, Integration, and Operations Conference, Dallas, Texas, USA, 17-21 June 2019, https://doi.org/10.2514/6.2019-3611

I agree that Floris was this article's primary and lead author with our contributions from study supervision and editorial direction.

Co-authors	**Signature**	**Date**
Name: Mike Bromfield	This item has been removed due to third party copyright. The unabridged version of the thesis can be viewed at the	13/01/22
Name: Steve Scott	This item has been removed due to third party copyright. The unabridged version of	14/01/22
Name: Alex Stedmon	This item has been removed due to third party copyright. The unabridged version of the thesis can be viewed at the Lanchester	13/01/22

Declaration

All sentences or passages quoted in this document from other people's work have been specifically acknowledged by clear cross-referencing to author, work and page(s). Any illustrations that are not the work of the author of this report have been used with the explicit permission of the originator and are specifically acknowledged. I understand that failure to do this amounts to plagiarism and will be considered grounds for failure.

Name: Floris Wolfert

Signature: This item has been removed due to third party copyright. The unabridged version of the thesis can b i d t th

Date: 17-01-2022

Acknowledgement

This PhD has been an incredible journey, and throughout the process I have received a great deal of support and assistance. I would first like to thank my supervisors. Dr Mike Bromfield's expertise was invaluable in formulating this research project. His insightful feedback pushed me to sharpen my thinking and brought my work to a higher level. Even after leaving Coventry University, he continued to voluntarily provide support. I thank Dr Steve Scott for his endless optimism and support. His aviation experience and expertise in human factors lent immense realism to the project. I would also like to thank Professor Stewart Birrell for his valuable contributions and guidance towards submitting this document. A final thanks to Professor Alex Stedmon for his help in shaping research and designing a rigorous methodology.

I would like to thank Steve Moody for volunteering his time to act as pilot flying during the majority of the simulator experiments. Without his help, the fidelity of the experiment would not be as high as it is now. An immense thanks to all participants who volunteered their time and travelled to Coventry at their own expense to participate in this research project. Their contribution was indispensable.

Additionally, I would like to thank my PhD colleagues: Samuel Everet, Thomas Milward, Osita Ugwueze and Antoine Peltier. They were always there to provide emotional support and share in my challenges throughout the entire PhD process. Also, a huge thanks to my close friends Lennert Hoogduin and Boris Boïng for their friendship, their critical proofreading and for all the interdisciplinary meetings we had to cancel. Finally, I would like to thank my colleagues at ProRail, especially Mylene Malipaard and Bruno van Touw, for providing a generous amount of leave, understanding and support in the final submission phase.

A huge thanks also to my family. My parents, Ton and Laura, and my brothers Casper and Jochem for always supporting me. A big thanks to Frank and Joke for their endless amount of babysitting throughout the amendment phase. To Suze, our daughter, who joined our family during the write-up of this thesis.

Finally, I would like to thank Eva. Eef, words cannot express how much your endless support and belief has meant to me. You have been my biggest cheerleader throughout this challenging and sometimes trying process. I couldn't have done it without you!

Abstract

The research presented in this thesis focuses on the evaluation of haptic feedback through coupled flight control inceptors on monitoring pilots on the flight deck. The study has three main objectives. The first is to evaluate the effects of haptic feedback on the flight deck in the literature. The second is to determine whether there is a statistical association between the number of accidents/incidents and the presence of haptic feedback on the flight deck. The third and final objective is to evaluate the effects of haptic feedback on pilots' monitoring ability on a multi-crew jet aircraft in an experimental setting.

In the last 15 years, there has been a notable rise in the integration of fly-by-wire control systems by aircraft manufacturers, with a particular emphasis on the incorporation of passive sidesticks lacking active control force feedback. This shift away from historically interconnected flight control inceptors has implications for the perception of flight control inputs between pilots. Field and Harris (1998) and Uehara (2014) concluded that the interconnection between flight controls is one of the essential ways in which pilots communicate. The static nature of passive sidesticks imposes limitations on the ability of the pilot monitoring (PM) to monitor the actions of the pilot flying (PF), potentially impacting performance and contributing to significant accidents, such as was the case in the AF-447 accident.

Two statistical studies were conducted to determine whether the considerations regarding the use of passive sidesticks were apparent in the number of accidents. Hard landing as well as tailstrike accident and incident reports have been retrieved from 72 national air accident investigating bodies, yielding a total of 514 air accident and incident reports, of which 40 qualifying hard landing reports and 129 qualifying tailstrike reports were used. Both studies show that hard landing and tailstrike accidents indicate a significant association between the number of accidents and the type of flight control. Although passive sidestick aircraft flew only 31% of all jet aircraft flight cycles in a ten-year time span, they were involved in 47.5% of the recorded hard landings and 41.8% of the tailstrikes. Although significant associations were found on the number of accidents, it remains uncertain what causes the elevated accident rates on passive sidestick aircraft.

Two human-in-the-loop simulator studies have been conducted with 20 commercial airline pilots in a fixed-base Airbus A320 simulator. The experiment compared monitoring on passive sidestick flight control configurations and active flight control configurations on several normal and abnormal flight scenarios. The participants were tasked with monitoring and intervening according to their company policy whilst a PF commenced normal take-off and normal landing scenarios, as well as non-flared landings and over-rotations during take-off in both passive and active flight control configurations. A large quantity of subjective, objective and physiological data was collected to determine performance, perceived workload and situation awareness (SA). The results showed that in 90% of scenarios, PMs on the active flight control configuration were effective in preventing the hard landing. By contrast, in the passive configuration, the PMs intervened successfully only 10% of the time. The results show that the active flight control configuration enables the pilots to anticipate an improperly initiated flare, thereby allowing them sufficient time to verbally and physically intervene successfully with less perceived workload and higher perceived SA. During the approaches flown in active configuration, pilots showed a significant increase in out-the-window (OTW) eye fixations, which strongly correlated with the perceived spare mental capacity, indicating a possible novel workload measure. During the over-rotation on take-off study, pilots showed similar improvements in successful interventions as in the hard landing study: In active configuration, 70% of the tailstrikes were successfully prevented, compared to 20% in passive configurations. In this study, pilots perceived significantly lower workload and greater SA.

In conclusion, the novel findings obtained from the literature, accident statistics and experimental studies presented in this thesis show that the passive configuration of the passive sidestick negatively affects a PM's ability to anticipate future aircraft states, negatively affects the quality of the take-over action, and causes higher levels of workload as well as lower levels of perceived SA. The experiments show that the implementation of a cross-coupling between the flight control inceptors allows the PMs to perceive information throughout their haptic channel, which drastically lowers their perceived workload and significantly increases their ability to successfully intervene.

Table of Contents

List of Figures

List of Tables

List of Graphs

List of Bar Charts

List of Equations

Nomenclature

μS	MicroSiemen
AAIB	Air Accidents Investigation Branch (UK)
AAIU	Air Accidents Investigation Unit (Ireland)
AF	Alpha Floor. Flight Envelope Protection on Airbus Aircraft
AGL	Above Ground Level
AI	Attitude indicator
ANOVA	Analysis of Variance
AoA	Angle of Attack
ATC	Air Traffic Control
ATSB	Australian Transport Safety Bureau
BEA	Bureau d'Enquêtes et d'Analyses pour la Sécurité de l'Aviation Civile (France)
BFU	Bundesstelle für Flugunfalluntersuchung (Germany)
CG	Centre of Gravity
CPLD	Coupled Flight Controls
DFDR	Digital Flight Data Recorder
DI	Dual Input
DoF	Degree of Freedom
EASA	European Union Aviation Safety Agency (EU)
ECAM	Electronic Centralised Aircraft Monitoring
ECG	Electrocardiogram
EDA	Electrodermal Activity
EHAM	ICAO Airport Code Amsterdam Schiphol Airport
EICAS	Engine Instrument and Crew Alerting System
ER-SCR	Event-Related Skin Conductance Response

ESC	European Society of Cardiology
FAA	Federal Aviation Administration (US)
FDM	Flight Data Monitoring
FEP	Flight Envelope Protection
FO	First Officer
HCD	Human-Centred Design
HF	High Frequency Power Band of HRV
HITL	Human-In-The-Loop
HRV	Heart Rate Variability
IATA	International Air Transport Association
ICAO	International Civil Aviation Organisation
ILS	Instrument Landing System
LF	Low Frequency Power Band of HRV
LOC-I	Loss of Control - In Flight
MCDU	Multi-Function Control and Display Unit
MCP	Mode Control Panel
MSL	Mean Sea Level - altitude with reference to the average sea level
NASA	National Aeronautics and Space Administration
ND	Navigation Display
NTSB	Nation Transportation Safety Board (US)
OTW	Out-The-Window
PDT	Proportional Dwell Time
PF	Pilot Flying
PFD	Primary Flight Display
PITL	Pilot-In-The-Loop
pNN50	Percentage of successive RR intervals that differ by more than 50 ms

PNS	Parasympathetic Nervous System
PSS	Passive SideStick
PPL	Private Pilot's Licence
RMSSD	Root Mean Square of successive differences for HRV
ROC	Rate of Climb
ROD	Rate of Descent
ROI	Region of Interest
RR	Heartbeat inter-beat interval between 'R' peaks
RWY	Runway
SA	Situation Awareness
SART	Situation Assessment Rating Technique
SCR	Skin Conductance Response
SDRR	Standard deviation of the RR interval
SDSD	Standard deviation of the successive differences of the RR interval
SME	Subject Matter Expert
SNS	Sympathetic Nervous System
SPSS	Statistical Package for the Social Sciences
SVS	Synthetic Vision Systems
TLX	NASA Task Load Index
TPB	Take-Over Push Button
TSB	Transport Safety Board (Canada)
Vapp	Approach speed
VMC	Minimum Control Speed
VLF	Very Low Frequency
Vr	Rotation speed on take-off

Chapter 1 Introduction

1.1 Motivation

The flight deck of a modern jet aircraft is an environment where information is transferred dynamically from the aircraft to the pilots. Pilots receive and process this information, operating in accordance with company policies and standard operating procedures. Proper presentation of this information is a cornerstone of safe operations, as perceiving accurate and correct information is key to building adequate situational awareness. Information perception relies entirely on the sensory capabilities of the flight crew, and the current layout of all modern jet aircraft flight decks depends mainly on transferring information throughout pilots' visual sensory channels.

During emergencies or sudden unforeseen events, the need for greater information transfer may exceed the pilot's capacity to perceive accurate information through their visual information channel – which can have fatal consequences, as in the case of the Air France 447 accident. Distributing information via more sensory channels, such as aural or haptic sensory channels, can mitigate sudden information overload on pilots and may thereby improve overall human–machine interaction to reduce the risk of accidents.

Research in the automotive domain using the haptic sensory channel as an additional information-transfer channel has shown promising results, and implementing haptics as another information channel in the flight deck may be especially beneficial for aircraft equipped with passive sidestick flight control inceptors. Passive sidestick aircraft have no cross-coupling between the two inceptors, which means the other sidestick will remain static when a pilot moves his sidestick. The static nature of this sidestick removes the haptic information channel present on aircraft equipped with either mechanical or electronically coupled flight controls. Even though passive sidesticks have been used in aviation for more than 40 years and have proven suitable for safe operations, it can be hypothesised that the application of haptic or proprioceptive feedback would distribute the aircraft's information among several sensory channels, thereby facilitating greater information transfer whilst also decreasing the load on the visual information channel.

At the time of writing this thesis, no research has yet investigated the differences in safety performance between aircraft with and without cross-couple flight controls. Only limited simulator studies have been conducted, none of which have involved a multi-crew flight deck. The research project described in this thesis aims to answer both previously mentioned research gaps by following three steps: First, evaluate the effects of haptic feedback on the flight deck in the literature. Second, determine whether there is a statistical association between accident and incident rates and the type of flight control. Third and finally, evaluate the effects of haptic feedback on a pilot in an experimental set-up.

1.2 Research objectives

As mentioned, this thesis has three sections: a literature review, a statistical study and an experimental study. Each section has its own aims and objectives

Overall aims for the thesis:

1) Evaluate the effects of haptic feedback on the flight deck in the literature.
2) Determine whether there is a statistical association between the number of accidents/incidents and the presence of haptic feedback on the flight deck.
3) Evaluate the effects of haptic feedback on pilots' ability to monitor on a multi-crew jet aircraft.

Literature review objectives:

1) Gain an understanding of existing research in the domain of haptic feedback and passive sidesticks on the flight deck.
2) Gain an understanding of the experimental human factors research domain.
3) Analyse air accident reports in which haptic feedback has played an essential role.

Statistical study objectives:

1) Statistically compare aircraft types with and without haptic feedback on the number of accidents and incidents in recent history.
2) Determine if any of the potential differences in the number of accidents between the aircraft types are due to design characteristics.

Experimental study objectives:

1) Conduct a human-in-the-loop experiment evaluating the effects of passive sidesticks on a pilot's ability to accurately monitor in a multi-crew flight simulation.
2) Conduct a human-in-the-loop experiment evaluating the effects of providing a haptic cross-coupling between the flight control inceptors on a monitoring pilot in a multi-crew flight simulation.

1.3 Thesis structure

This thesis consists of several chapters, each beginning with a brief explanation of how its content contributes to one or more research aims or objectives, as well as to the overall research project. A schematic overview of each chapter can be seen in **Figure 1.1**. This thesis begins by defining the research motivation, aims and objectives in Chapter 1. Chapter 2 contains a literature review of research covering the human on the flight deck, aviation flight controls and the use of haptics in aviation, and it closes with a review of aviation accidents related to haptics. Chapter 3 lays out the research methodology of this thesis. Chapter 4 presents a statistical analysis study on hard landing accidents in commercial aviation. Chapter 5 follows a procedure similar to that of Chapter 4 to statistically analyse the effects of passive sidesticks on aviation tailstrike events. Chapters 6 and 7 consist of two human-in-the-loop simulator studies that place the results of the previous chapters in an experimental set-up. Chapter 8 delivers the overall thesis summary and reflects on the study's limitations as well as prospects for future work.

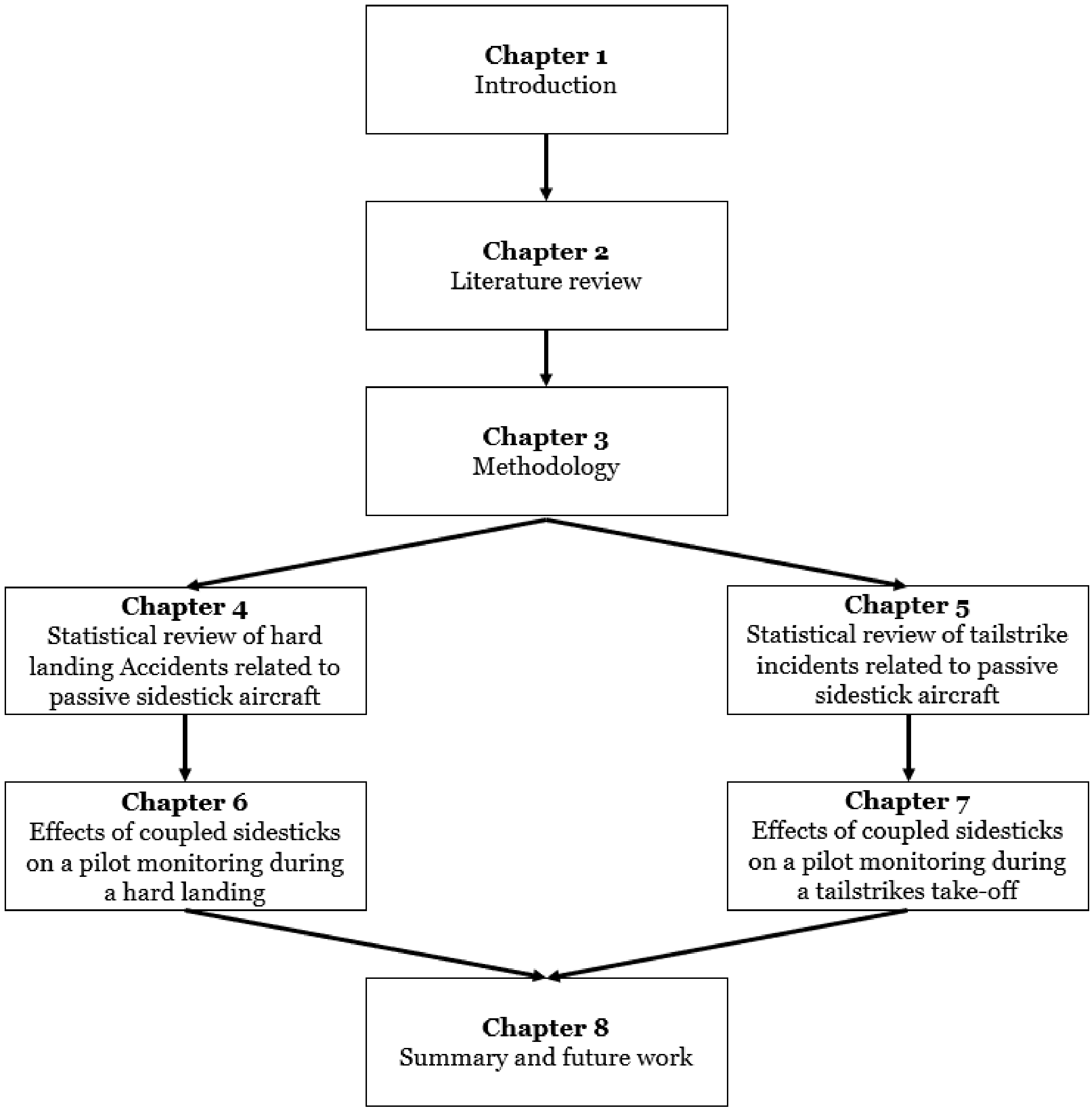

Figure 1.1 Thesis structure

Chapter 2 Literature Review

This chapter reviews the pertinent literature surrounding the topics of the human factors, aircraft flight controls and the application of haptics. This Chapter starts with a review of the human factor on the flight deck, followed by a paragraph focused on the theory of flight controls and the application of haptic feedback in aviation. This chapter closes with a review of three relevant air accidents involving passive sidesticks.

2.1 The human on the flight deck

This paragraph will review and discuss research methods and conclusions from literature related to various cognitive ergonomics subjects in aviation. Therefore providing a human factors background for the experimental chapters that follow.

2.1.1 Human information processing

Human information processing is a mechanism essential to the understanding of the world around us and for transforming information into subsequent actions. Information processing has a close relationship with both situation awareness and workload, and it is therefore critical to human performance. The cognitive engineering model, as outlined by Wickens and Carswell (2021) in **Figure 2.1**, serves as a framework that incorporates elements of understanding of the task and environment as well as modelling and understanding knowledge structures of the system involved. The model's key components encompass sensing the world, perception of that information, selecting responses based on stored knowledge, and executing chosen actions. The components relevant for information processing, such as senses, perception, working memory and long-term memory, will be discussed in this section.

Figure 2.1 Model of information processing (Wickens & Carswell, 2021)

The sensory register is a high-capacity, short-term storage unit specific for each sensory modality. The basic sensory modalities are: vision, aural, pressure (or tactile), temperature, taste and smell. Other sensory modalities include: balance, (angular momentum and acceleration), proprioception, nociception (pain) and chronoception (passage of time). According to Lee et al. (2003), there are three basic functions of the sensory register:

- **Limitations of sensory input:** The sensory register stops the information processing upon becoming overwhelmed by a multitude of inputs.
- **Buffer function**: The sensory register allows the information processing to determine whether an input needs to be processed further.
- **Stability:** The buffer function has as a side effect in which the delay of information (for example, in visual images) makes the visual perception appear smoother and continuous despite interruptions (such as eye blinking).

'Perception' refers to the way in which information processing system interprets information originating from the sensory register. Although a large amount of information runs through the sensory register at any given time, the amount of information that is perceived is relatively small. Sensing can be seen as a passive process, whereas perception very much is an active process. Perception involves selecting, organizing and interpreting information for processing and is dependent on learned processes, relying on working memory and long-term memory for interpretation (Harris, 2012). The role of working memory, previously called 'short-term memory', is to store information for a relatively longer period of time (roughly 30 seconds) (Wickens et al, 2015). Working memory can be seen as a central processing unit that requires attention resources. According to Baddeley, working memory consists of multiple components, including the central executive and two subsystems: the phonological loop for verbal information and the visuospatial 'sketchpad' for visual and spatial information (2000). The central executive coordinates information flow. Long-term memory functions as long-term storage for information and involves the encoding, consolidation, and retrieval of knowledge and experiences, contributing to learning and behaviour. Neuroscientific studies have identified brain structures, including the hippocampus and cortex, as integral parts of long-term memory (Squire et al., 2004). Long-term memory has two basic types of memory: procedural and declarative. Procedural memory contains knowledge of skills, strategies and procedures concerning how to undertake tasks. Procedures are stored as a series of steps (stimulus–response pairings) which, when activated, trigger subsequent steps. Declarative memory has two further sub-components that are readily available:

– **Episodic memory:** The ability to recall past experiences and events, including information related to those events. Episodic memory is stored as images (Pihlajamäki et al., 2003).

– **Semantic memory:** The memory section for facts, rules, concepts, principles and problem-solving skills. Memories are stored as networks or schemes.

2.1.2 Situation awareness

The subject of situation awareness (SA), sometimes referred to as 'situational awareness', has been of increasing interest for human factors engineers over the years. There are various definitions of SA. Smith and Hancock (1995) defined it as the up-to-the-minute comprehension of task relevant information. Boy and Ferro (2004) stated that SA is a function of several quasi-independent situation types: the available situation, perceived situation and expected situation. Bell and Lyon (2000) defined SA as working-memory knowledge about elements of the environment. However, the most commonly used definition of SA is likely that of Mica Endsley, who describes a SA as 'the perception of critical elements in the environment, the comprehension of their meaning, and the projection of their status into the future' (Endsley, 1988).

Endsley's three-stage model of SA is based on the previously discussed information processing approach seen in **Figure 2.2**. This model suggests that situation awareness begins with goal specification, at level one, where the human operator (or pilot) is perceiving the status, dynamics and attributes of relevant data. Level one is therefore the 'perception of the elements', wherein Endsley concludes that if one does not perceive fundamental data, one cannot be situationally aware. Once information is perceived, the information must be 'comprehended' at level two. At the second level, the perceived data is comprehended and turned into information – in other words, what it means. If the information is perceived and comprehended, the third level of SA is reached when a human operator can project the information on future status. This is the stage where information becomes knowledge. SA is believed to exist inside working memory, making it an active process that costs attentional resources (Harris, 2012). According to Harris (2012), SA is not 'achieved'; rather, it is a cyclical process that continues throughout the task. Possessing good levels of SA is essential to efficient task performance within safety-critical operations, including the work of air traffic controllers, pilots, surgeons, nuclear power plant operators, and military commanders (Endsley, 1995a; Durso & Hackworth, 1999). Even minor problems encountered can quickly snowball into disasters when operators do not fully comprehend the evolving situation. For example, Air France Flight 447 stalled at 38,000 feet over the Atlantic and crashed, killing all 228 persons on board, which will be discussed in section 1.4 of this chapter. Although most human factors researchers acknowledge the presence of some form of SA in the working memory, some critics fully reject the subject's scientific validity. Dekker and Hollnagel (2004) disparaged SA as one of a series of 'folk models' used in human factors and particularly in studies of human error and accident causation.

Figure 2.2 Endsley's three-stage model of situation awareness (Endsley 1998)

2.1.2.a Situation awareness in a team

The previous section discussed SA as part of an individual. In large jet aircraft, pilots are usually working in a team with two, and sometimes three, pilots on the flight deck. This introduces the complexity of having multiple human operators, each with their individual SA, although there is usually a great overlap among them. Three types of teams SA can be distinguished:

Shared SA: Both team members are equally or near-equally aware of their situation – such as during critical flight phases like take-off, approach or landing, where both crew members should have a great understanding of the current situation.

Overlapping SA: Overlapping SA can be defined as shared SA but to a lesser degree. During flight phases that are less safety-critical, each crewmember is tasked with their own role on the flight deck. The pilot flying (PF) is responsible for flying the aircraft, whilst the pilot monitoring (PM) is handling the radios. There is sufficient understanding of each other's tasks (i.e. there some certain degree overlap in SA of the overall flight status), but to a greater degree of individual SA toward each individual's tasks.

Distributed SA: Whereas shared and overlapping situational awareness imply the same collective requirements and purposes among the humans in a system – who all share the same understanding of the situation – distributed SA implies different requirements and purposes. In a distributed setting, team members may have access to diverse sources of information and can, for example, operate in different physical locations. Distributed SA involves the continuous exchange of relevant information among these team members to create a collective awareness of the overall situation. This shared understanding enables a team to respond to changes in the environment, make informed decisions, and coordinate their actions seamlessly without the need to have each individual team member be fully situationally aware of all aspects of the tasks.

2.1.2.b Measuring situation awareness

Measuring SA is primarily aimed at evaluating new systems of equipment in terms of helpful to the human operator. Especially in aviation human factors research, it has become standard to evaluate novel flight deck systems while considering the effect the novelty has on SA (Harris,2012). There are two types SA measurement approaches: behavioural and scale-based rating approaches. Behavioural SA measurements probe human operators with questions or prompts; their answers determine the scale of their SA. A commonly used behavioural measure according to Endsley's three-level model is the SAGAT (Situation Awareness Global Assessment Technique) (Endsley, 2000). During simulations or evaluation tests, the simulation is stopped to probe questions related to levels one, two or three of Endsley's SA model. Using these freeze and probe techniques frequently interrupts the simulations, constantly pulling participants out of the loop. Researchers who criticise Endsley's model also criticise the SAGAT method, claiming that it only tests memory performance, which is very much individually based (Hollnagel & Amalberti, 2001).

The other approach type – the rating scale – is less interfering than the behavioural approaches. The most commonly used scale-based rating for SA is the SART

(Situation Awareness Rating Technique) (Taylor, 1995). This self-rating approach consist of three dimensions: attentional demand, attentional supply, and understanding – each containing several sub-scales. The advantages of this test are that it is non-intrusive in research experiments, and that is it easy to administer. The disadvantage is that the SART has proven be inaccurate in test-retest reliability (Vidulich, Crabtree, & McCoy, 1993). Also, the validity of self-administered post-trial questionnaires can be diminished by subjects' imperfect memories. Events that occurred at the beginning of the experiment might not be taken into consideration during the post-trial self-rating (Selcon et al, 1998).

2.1.3 Mental workload

Mental workload is one of the most commonly recurring topics in human factors research (Hancock & Desmond, 2000; Moray, 1979), and is often related to questions such as: *How busy is the operator? Can any additional tasks be performed?* Research shows that high workload is connected to more mistakes, reduced safety margins, lower productivity, and increased perceived stress (Wickens et all, 2015; Moray, 1979; Salvendy, 1997). Although there is no consensus definition of mental workload, it is generally seen as the 'cost' (in terms of information processing) of performing a specific task (Harris, 2012). It is closely tied to human information processing theory, focusing on the limited capacity of our thinking abilities, as discussed in the previous section (Wickens, Hollands, Banbury, & Parasuraman, 2015). Theories about handling two tasks at once aim to explain the limits of a pilot's workload in terms of the number and types of tasks they can handle within a certain timeframe. The main idea is that cognitive workload is the product of competition for limited information processing resources. Chiles and Alluisi (1979) posited that workload has three defining features:

Input load: the amount of work needs to be done or its difficulty

Operator effort: the effort the operator puts in to meet task demands

Task performance: the actual results of their efforts

Input load is influenced mainly by the task requirements and how they are translated into the operators' control actions. Training is one aspect that somewhat increases the cognitive capacity available, although factors like stress and fatigue still negatively affect it. Task performance depends on the demands of the task versus the available cognitive capacity. However, workload is different from performance, as shown when considering primary task measures. Two pilots performing the same task can achieve the same results, but one may have more cognitive resource capacity left for other tasks (Vidulich & Wickens, 1986; Yeh & Wickens, 1984). Therefore, workload can be seen as a personal experience of task load and is affected by individual differences. However, the effort needed for successful task completion also depends on task requirements, which is influenced by how well the materials used are designed. In aviation, this translates to how well the flight deck is designed and how the flight deck supports the pilot in their task. It is a common misconception that increasing flight deck automation always reduces workload; however, it often does the opposite. As research by Wiener and Curry (1980) showed, automation only changes the nature of task requirements, which then affects the workload experienced by the crew. Moray (1979) makes a distinction between cognitive workload ('thinking') and perceptual motor load ('doing'). Automation on the flight deck may increase cognitive workload because it relieves the pilot from motor tasks like flying the aircraft, as will be discussed in the next paragraph. However, reducing workload through improved automation may come at the cost of SA. Mental workload measurement is associated with attention resource theories (Wickens, 1981) and influences the allocation of cognitive resources. As individuals invest more cognitive resources in a demanding task, fewer resources remain for secondary tasks, eventually reaching a cognitive resource limit. Eye-tracking systems leverage this connection to assess mental workload. Assessment methods encompass subjective measures, such as NASA TLX (Hart & Steveland, 2006), secondary tasks (Young & Stanton, 2005; Gawron, 2008), and eye-tracking systems (Xiao, Wanyan, & Zhuang, 2015; Diaz-Piedra et al., 2017; Babu et al., 2019).

2.1.3.a Maximum capacity

The well-known arousal curve, a bell curve linking individual arousal with performance, is a concept the human factors domain. This concept traces its roots to Yerkes and Dodson (1908), despite their original investigation focusing on stimulus strength and habit formation in mice. Criticisms by Dekker and Hollnagel (2004) caution against over-generalization and confusion between arousal and stress based on folk models. Regardless of the accuracy of the Yerkes and Dodson arousal curve, the notion of maximum pilot capacity aligns with the LOC-I analysis of Belcastro et al. (2016). Maximum capacity, expressed in terms of performance, highlights errors arising from mismatches between task demands and a pilot's ability to execute them (Zeller, 1978). Shelnutt et al. (1980) extend this concept as a pilot performance model, emphasizing the need for adjustments in task demands and/or pilot capabilities to address incongruities.

2.1.4 Measuring mental workload via physiological measures

2.1.4.a Eye tracking

Flying a modern aircraft is a highly visually demanding task. In order to adequately perceive information, pilots must actively search for information, either on flight deck displays or from available cues outside. During every phase of flight, the information being presented changes in real time and requires extensive monitoring. Over the last 20 years, more research has confirmed the relationship between eye movements on the flight deck and a pilot's cognitive state. This section first focusses on the various published studies on the subject of eye tracking and the relationship between human-in-the-loop experiments. The main appeal for monitoring eye movements on the flight deck, according to several studies (Ellis, 2009; Faulhaber et al., 2020; Glaholt, 2014), is the possibility of a so-called 'window view' into a pilot's cognitive state. This pan window view provides a quantification of an operator's 'mental workload', which is defined as the difference between the cognitive demand of a task and the spare mental capacity of the human operator (Glaholt, 2014). The cognitive demand of a task on the flight deck can be derived from performance variables. Tracking eye movements provides a direct measure of a pilot's attention and information processing, thereby providing insight into the pilot's mental capacity.

2.1.4.b Proportional dwell time

Proportional dwell time (PDT) is simplest eye-tracking parameter to record. The most common method of computing PDT is to define different flight deck areas of interest and calculate the percentage of eye fixation relevant to each area, such as primary flight display (PFD), navigation display (ND), mode control panel (MCP) and out-the-window (OTW) view. PDT is calculated by dividing the total dwell time (or all eye fixations) by the sum of the dwell time across all areas; this is quite common when measuring PDT across different flight instruments. PDT is not evenly distributed across all facets of the flight deck (Colvin & Dodhia, 2003). Instruments that require more monitoring due to their importance for safe flight, as well as instruments for which the information changes frequently, often have more eye fixations. It also depends on the task of the pilot. A pilot flying a visual approach will tend to look more OTW than inside (Harris et al., 1986). Focussing on military aircraft in tactical air-to-air movements, Svensson et al. (1997) compared the amount of time pilots spent looking at instruments versus the amount of time spent looking OTW. They concluded that the amount of time spent OTW or on the instrument depends on the amount of information displayed on the tactical display. Other studies focussed on PDT on flight instruments found a relationship between the amount of experience a pilot has on the flight deck and the amount of time they spend looking at their instruments. Li, et al. (2013) reported that the more experienced a pilot is, the more often they look at relevant flight deck areas during failures. Several studies have been conducted on the defining different parts of OTW PDT in single-engine airplanes (e.g. Colvin & Dodhia, 2003). However, flying a small general aviation aircraft usually requires many OTW fixations because a great deal of essential information is perceived by looking outside, such as navigation, orientation, airspace and maintaining separation from other aircraft.

Interestingly, no study has yet compared the amount of OTW fixation and a pilot's perceived workload on a modern jet aircraft. Even though the relationship between PDT and cognitive workload on OTW fixations has not yet been established, some research show that there is a side note to make when measuring PDT. Research by Glaholt (2014), complementing that of Li et al. (2013), concluded that there is a relationship between eye fixations and relative aircraft experience on that specific aircraft type. More notably, however, Glaholt suggest that fixation frequencies and duration of the fixation are interacting with each other. Pilots with fewer fixations tend to have lower dwell times. In order words, by fixating for longer, pilots can perceive the same amount of information with fewer fixations. This means that there may be a link to overall duration of dwell. Other studies have shown that dwell time and fixation duration can be linked to the mental demand of the task. De Rivecourt et al. (2008) found that, in a simulated flight, when the mental demand of the task increased, the duration of the fixation decreased.

2.1.4.c Pupil dilation

The diameter of the pupil is capable of dilation and contraction by muscles that control the amount of light entering the eyeball. Pupil diameter can also be affected by factors other than light, including substances such as coffee or sedative drugs. Although these factors complicate the measurement of pupil diameter and make it difficult to isolate the variables causing its dilation or contraction, a robust body of research has confirmed a relationship between pupil diameter and mental workload (Causse et al., 2010; Dehais et al., 2014; Ho et al., 2016).

2.1.4.d Heart rate variability

The physiological phenomenon of heart rate variability (HRV) refers to variations in time between heartbeats. The sympathetic and parasympathetic nervous systems control the cardiovascular system of the human body, and a heartbeat is the result of the combination of their influences. A heartbeat is measured using an electrocardiogram (ECG), an electrogram that plots the electrical activity of the heart versus time using electrodes. The electrical activity measured is the changes of the cardiac muscle being cyclically depolarised and repolarised (De Rivecourt et al., 2008). This cycle is called the cardiac cycle, or heartbeat. Heart rate or cardiac cycles can also be measured using blood pressure; however, the use of ECG is more common because it provides a clear waveform for analyses (Kim et al., 2017). HRV is measured by the variation in RR interval within the QRS complex of the ECG waveform, as illustrated in **Figure 2.3**.

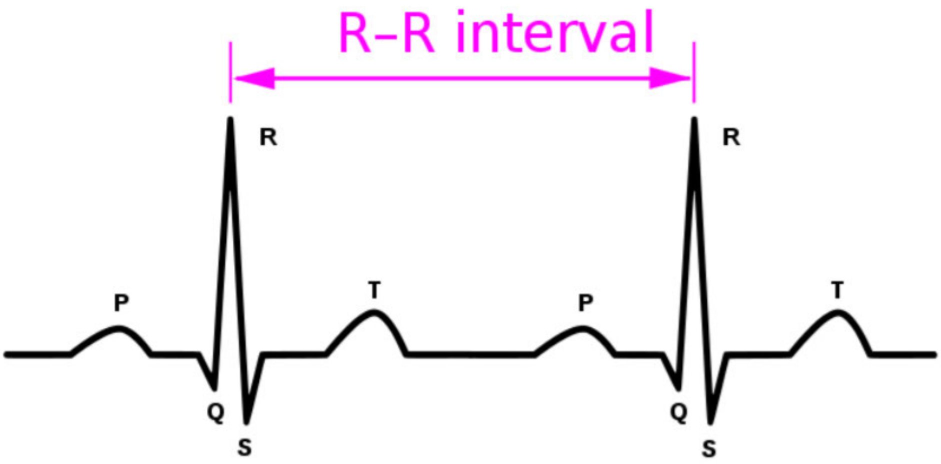

Figure 2.3 Schematic example of an electrocardiograph with QRS complex and RR interval highlighted

A normal cardiac cycle consists of multiple different waves that can be identified. The P-wave, usually 0.11 seconds in wavelength, represents the depolarisation of the left and right atria. The P-wave is followed by the QRS complex, which consists of the Q-wave, R-wave and S-wave, which follow one another in relatively rapid succession. The QRS complex represents the electrical impulse immediately before contraction. The Q-wave represents the a negative deflection before the main positive wave (the R-wave) of the complex. The S-wave is the first negative deflection after the R-wave. The QRS complex is followed by a T-wave, representing ventricular repolarisation. HRV can be measured and expressed in a number of ways; the most frequently used are time-domain methods, which measure heartrates using an ECG whereby each QRS complex is detected so the normal-to-normal interval (NN) can be detected. Another measurement calculated on the NN interval is the standard deviation of the NN interval (SDNN), or the so-called square root of variance. SDNN is usually calculated over a longer period (24 hours) (Shaffer & Ginsberg, 2017). The most frequently used time domain measure for HRV is the root of the mean squared successive differences of the NN interval (RMSSD), which is obtained by calculating each successive time difference between heartbeats in milliseconds (ms), followed by squaring each value, averaging it over the entire epoch, and then square-rooting it. The most commonly used timeframe is 5 minutes, although several studies have used times of 30 seconds (Baek et al., 2015) and 60 seconds (Esco & Flatt, 2014; Stuiver et al., 2014). However, claims of accurately measuring HRV using time-domain methods with time periods shorter than 5 minutes are controversial, having been called into question by some studies (Lehrer, 2013).

There is a variety of research showing the difficulties in comparing heart rate variability (HRV) between simulated and laboratory environments and in real test scenarios. A review of the use physiological measurements for measuring mental workload by Charles and Nixon (2019) has compared, among other physiological measurements, 52 studies using electrocardiographic measures. Some of the studies mentioned in their review state that heart rate (HR) can change up to 50% in applied environments, whereas they are only up to 10% in laboratory studies (Wilson, 1992). When investigating the electrocardiographic correlation between different tasks in laboratory environments and in-the-field environments, it showed a reduced correlating result, mainly for passive coping tasks and exercises (Johnston et al., 1990). Nickel and Nachreiner (2003) concluded that the medium-range frequency domain in HRV lacked the necessary sensitivity to properly assess mental workload. They stated that electrocardiographic measures are suitable only for distinguishing between levels of work and levels of rest, or that differences in task demand need to be high in order to be reflected in HRV, as seen in the research of Veltman and Gaillard (1998). However, a later study conducted by Veltman observed no differences in HR and HRV in comparing simulated and real flight scenarios (Veltman, 2002). The difficulties shown in the above-mentioned studies mainly show difficulties in achieving a measurable outcome of electrocardiographic measures in simulated environments.

2.1.4.e Electrodermal activity

Electrodermal activity (EDA), also referred to as galvanic skin response (GSR), is the activity of the electrical conductance of the skin in response to sweat secretion. Human sweat is secreted by the eccrine sweat gland, which is controlled by the sympathetic nervous system (SNS), and acts as a body temperature regulator. When the body's internal temperature rises, the eccrine sweat glands secrete water to the skin surface where heat is removed by evaporation. The water on the skin changes the conductance level of the skin, which can be measured by applying a low, undetectable and contestant voltage to the skin between two electrodes (Benedek & Kaernbach, 2010; Posada-Quintero & Chon, 2020). This measurement of the conductivity of the skin is called skin conductance response (SCR). Even though

EDA is directly linked to the regulation of body temperature, research has shown a strong association between EDA and emotional arousal (Geršak, 2020; Posada-Quintero & Chon, 2020; Zangróniz et al., 2017). Signals of emotional arousal are linked with the activation of the SNS, which leads an increased activity of the eccrine sweat glands, which on their turn affect the SCR (Geršak, 2020). It should be noted that either positive or negative stimuli can result in an increased arousal, and therefore increased SCR. EDA is therefore not capable of distinguishing different emotions, only the intensity. Skin conductance is measured in microsiemens (μS) and is usually captured using conductive electrodes. The skin conductance signal consists of two components; A tonic skin conductance level and a phasic skin conductance response. The tonic SCL is a slowly fluctuating baseline, whilst the phasic response is vastly fluctuating. Phasic responses have steep inclines and a distinctive peak, followed by a slow decline to the tonic baseline level. Therefore the focus on EDA measurements lies in the latency and amplitude of this phasic response. A phasic increase of SCR in response to a provided stimulus is called event-related skin conductance response (ER-SCR). For example, the amplitude of ER-SCR is used to infer sympathetic arousal (Bach et al., 2010). The amplitude is the increase of conductance level from the point of the waveform onset, typically a 10% increase of μS within a 1- to 5-second time period after a stimulus is given, until the peak. The time between the given stimulus and the waveform onset is called 'latency'. Typically it takes a minimum of 1 second for the SCR to react to a given stimulus (Dawson et al., 2016). An example of a phasic SCR can be seen in **Figure 2.4**.

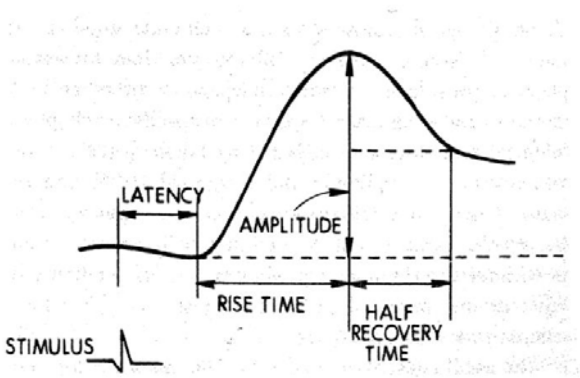

Figure 2.4 Example of phasic skin conductance response

In the review study of physiological measurements conducted by Charles and Nixon, mentioned in the previous section, seven studies have been included that compared EDA. In this review, a study conducted by Wilson (2007) showed a strong correlation between EDA and heart rate during a real flight task, but not during the flight simulations. Research conducted by (Fairclough & Venables, 2006) showed high levels of skin conductance increase in a computer-based task with 35 participants. These results indicated that EDA is sensitive to sudden stimuli but shows little reliability when measuring gradual changes in mental workload (Charles & Nixon, 2019).

2.1.5 Multiple resource theory

Multiple resource theory (MRT), first developed by Christopher Wickens provides a framework for understanding how human operators allocate and manage resources when engaged in complex tasks. In an aviation environment such as the flight deck, pilots have a multitude of responsibilities that include communication, navigation, monitoring instruments and decision making. This chapter focuses on the principles of MRT and its application to flight crew tasks, investigating how resource overlap, compatibility, competition and capacity impact cognitive resource allocation – and thereby influence pilots' performance. MRT posits that the separation of resources used for perceptual and cognitive activities is different from that of the resources involved in response, selection and execution. The MRT model defines four dichotomous dimensions: stages, processing codes, input (modalities) and visual channels (Wickens et al., 2015). A computational model of MRT can be seen in **Figure 2.5**.

The risk of dual-task interference can depend on whether the multiple tasks require cognitive/perceptual activities or response activities. These activities represent the *stages* of the MRT model, and they are relevant in that dual tasks requiring the same stages are more vulnerable to interference than those requiring one cognitive activity and one response. Various experiments manipulating task difficulty have shown that the difficulty of response-related tasks does not necessarily affect the performance of perceptual-cognitive tasks, and vice versa (Kessel & Wickens, 1980). In some instances, this can be explained by the fact that different tasks utilise different parts of the brain. For example, speech and motor activities tend to be controlled by frontal regions in the brain, whereas perceptual and language comprehension activities tend to controlled by the mid-aft section of the brain (Isreal et al., 1980; Wickens et al., 2015).

The *processing codes* dimension refers to the separation of resources used in analogue/spatial processes and verbal processes (C. Wickens, Hollands, Banbury, & Parasuraman, 2015). Wickens and Liu state that the separation of these resources may account for the lack of interference that occurs when manual and vocal responses are utilised simultaneously (time-shared). In the MRT model, manual responses (e.g. tracking or steering tasks) are classified as spatial processes, whereas vocal responses (e.g. speaking) are verbal processes (Wickens & Liu, 1988). Wickens and Liu concluded that manual control may disrupt performance in a task environment due to the extra demands on spatial working memory, whereas voice control may disrupt performance of a task with heavy verbal demands.

The *input* dimension refers to the perceptual modalities – visual, audio and tactile – in time-sharing tasks. The MRT model predicts that there will tend to be less interference when using cross-modalities (compared to intra-modalities) because separate perceptual resources are being used simultaneously (Wickens, 2008; C. Wickens et al., 2015). The role of tactile channels in presenting information, such as a buzz on the wrist of a pilot to alert them to a visual change on the display (Moacdieh et al., 2013; Sarter, 2006), suggests that the tactile modality acts as another resource channel that enhances the visual modality in much the same manner that the auditory channel enhances does so.

The final dimension is the *visual channel*. MRT posits that two visual channels are used in visual processing: the focal visual channel and ambient visual channel. These channels use separate resources characterised by the location within the brain where processing occurs as well as by the type of processing. The MRT model predicts that dual tasks involving one focal and one ambient process will result in minimal interference (Wickens, 2005; Wickens et al., 2015). Focal vision, linked to eye movement, is adept at perceiving fine details and pattern recognition. It is used in tasks involving visual search, object recognition and other tasks requiring high visual acuity. Ambient vision, on the other hand, uses peripheral vision to sense orientation and motion in the environment. Examples of dual tasks that use both visual channels include keeping a car in the centre of a lane (ambient) whilst reading a road sign or looking in the rear-view mirror (focal).

Figure 2.5 A three-dimensional cube of the MRT model cited from Wickens et al. (2015)

2.2 Aircraft flight controls

2.2.1 Historical overview of flight control inceptors

It is often thought that Airbus was the first manufacturer of Fly-by-Wire (FBW) aircraft. However, before Airbus's flight control design, several manufactured aircraft had FBW technology incorporated into their systems. The first non-experimental aircraft that had FBW flight controls dates to 1958. This aircraft was the CF105 Arrow, a supersonic delta-wing aircraft manufactured by Avro Canada. This dynamically unstable aircraft needed an analogue conversion of the flight control inputs to fly safely. This was established by developing a system which can be seen as the earliest form of FBW.

When the Concorde was introduced in 1970, it faced similar problems with implementing flight controls for that time, which also has been overcome by an analogue conversion of its flight control inputs whilst stabilising terms were added (Palmer, 2017). In the 1980s, Airbus Industries manufactured the first commercial subsonic aircraft without a conventional flight control inceptor system. Aircraft in that period usually had mechanical flight controls connected to servos and hydraulic pumps using pulleys and pushrods to move the flight control surfaces on the wings. Airbus replaced this mechanical system with a purely electrical control system (hence the name ‘fly by wire’). The flight control inputs in this system are converted into electrical signals processed by flight control computers that send corresponding signals to the flight control actuators. Removing the mechanical components in this flight control system made the system a lot less sensitive for maintenance. It reduced weight and increased reliability because there were fewer mechanical components that could fail. However, the original mechanical coupling also provided a haptic feedback loop because both conventional flight control inceptors were mechanically linked to each other. Also, the direct mechanical linkage between the flight control inceptor and the flight control actuators provided direct haptic feedback to the pilots about the state of the flight control surfaces.

On a conventional flight control system or a mechanical control column, the limited freedom of physical cables determines the forced displacement. **Figure 2.6** is a component breakdown of a conventional flight control inceptor of a Boeing 737-700

NG, designed in the 1990s (Boeing Aircraft Industries, 1998). What can be seen here is that the control columns are mechanically linked to each other by a coupling rod, which means the other control column mimics each movement of any flight control column. This mechanical rod is connected to a set of springs and cables connected to the flight control surfaces. This mechanical link to the flight control servos provides additional haptic feedback on the position of the flight control surfaces, which means that if a flight control surface is deflected, the control columns are in a position that reflects this control surface deflection. Another benefit of mechanical linkages between the flight control servos is their feedback on flight control surface movements, which means that a movement of the flight control surface due to turbulence results in a movement of the control columns.

Figure 2.6 Schematic component assembly conventional flight control system Boeing 737-800 (Boeing Aircraft Industries, 1998)

2.2.1.a Passive sidestick technology

The main feature of a passive sidestick is that the forced displacement on the flight control inceptor is converted into an electrical signal; by doing so, the majority of mechanical and moving components are eliminated. According to Corps (1989), the main reason was to avoid friction and backlash and to reduce the chance of a single-point failure that could affect both control inceptors. Another benefit of passive sidesticks is that they are relatively small and thus easy to incorporate into the flight deck. This results in more physical space on the flight deck and an unlimited view of the flight deck instruments, as shown in **Figure 2.7**. The current design of a passive sidestick consists only of a set of springs and dampers, which means there is no haptic feedback provided besides the spring loading. In addition to this, sidesticks are not coupled, which means that if one pilot moves their sidestick, the other will remain static.

Figure 2.7 Component breakdown of an Airbus A320 passive sidestick (Airbus SE, 2017)

2.2.1.b Active sidestick technology

The main difference between passive and active sidesticks is that, as the name suggests, active sidesticks actively provide haptic force feedback onto the stick. This is done by connecting force feedback actuators to the flight control inceptor. Currently, there are only a limited number of companies manufacturing active sidesticks. The most notable is BAE Systems, which has designed an active sidestick for the development of the Lockheed Martin Joint Strike Fighter (BAE, 2009) A component breakdown of their design can be seen in **Figure 2.8**. This system design is created so that force feedback can be artificially applied to the control inceptors in a similar way to a conventional flight control system. Besides the 'conventional' force feedback, this type of system provides much more feedback than passive sidesticks. Through the computer-controlled actuators, the sticks can be allocated a precise location with a precise force, allowing the system to accurately provide a feel characteristic of this flight control inceptor. The forces inside the servo actuator units are electromagnetically produced. This type of active sidestick has been developed only for military aircraft; consequently, publicly available information is scarce. However, some of the capabilities developed for the F35 programme are made available throughout BAE Systems and its developer Joseph Krumenacker (2008). Some of the known capabilities are detailed below.

Figure 2.8 Schematic component breakdown of a Lockheed Martin F35 Joint Strike Fighter active sidestick (Krumenacker, 2008)

2.2.1.c Current active sidestick development

An overview paper from the German Luft- und Raumfahrt institute in Braunschweig published summarised the difference between passive and active sidesticks (Hanke & Herbst, 1999). Next to the above-mentioned added functionalities in comparison to passive sidesticks, active sidestick require a different system lay-out. **Figure 2.9** shows a system overview of both passive and active sidesticks. The main difference in system lay-out is that passive sidesticks are only providing an input to the fly-by-wire computer whilst active sidesticks are an integrated part of the feedback loop.

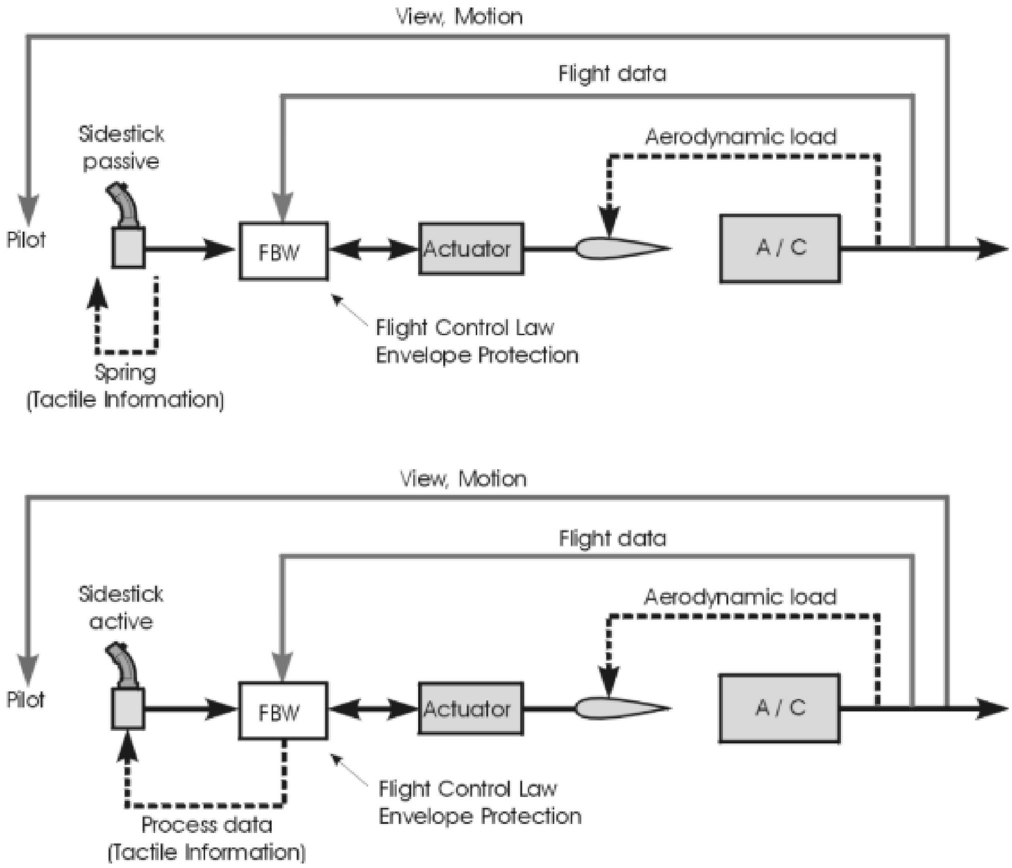

Figure 2.9 Systematic difference between passive and active sidesticks adapted from Hanke and Herbst (1999)

2.2.2 Aircraft types equipped with active sidesticks

In the aviation industry, several operational aircraft are already equipped with active sidesticks. The following section is a summarised overview of aircraft types that fly with active sidesticks.

2.2.2.a Gulfstream G500

The Gulfstream G500 is a twin-engine turbofan, long-range business jet manufactured by Gulfstream Aerospace Corporations. The G500 is one of the first business jets to be equipped with BAE systems active inceptor sidesticks offering simultaneous stick movement whilst using a fully FBW flight control system. There is no published research or motivation on why Gulfstream choose active sidesticks.

2.2.2.b Embraer KC-390

The Embraer KC-390 Millennium is a mid-sized cargo and military transport aircraft designed and developed jointly by Embraer and the Brazilian Air Force (FAB). The aircraft, equipped with two turbofan engines, can be used for a wide variety of missions, ranging from aerial firefighting and air-to-air refuelling to airlifting military equipment. The state-of-the-art FBW flight control system uses active control sidesticks provided by BAE Systems which are designed to improve pilot to pilot awareness through electrical linking. The KC-390 made its first flight on 3rd of February 2015. According to BAE systems, the reason for Embraer to implement Active Inceptor Systems is to implement variable gradients, force breakouts, detents, ramps, gates, and soft stops – to warn of mode engagements or impending flight envelope limits (BAE, 2016).

2.2.2.c IRKUT MC-21

The Irkut MC-21 is a medium-size commercial twin jet designed and built in Russia. This aircraft made its maiden flight in 2019 and is expected to enter commercial service beginning 2022. According to Roman Taskaev, chief test pilot for the MC-21 programme, the reason for implementing active sidesticks is: ‘Active sidesticks significantly improve the level of safety, making evident control inputs of pilots to one another and allowing prompt recovery actions’. As part of the development programme of the MC-21, Irkut collaborated research with the Moscow Aviation Institute. A recent published study by Savelev and Neretin (2019), as part of the MC-21 development programme, investigated the effects of active sidesticks for tracking automated flight controls; they reported that ‘the advent of sidesticks, instead of yokes, a problem began to arise due to the lack of tactile feedback to the flight crew about the attitude of the aircraft. Such problems are associated with this, as indicated in Wolfert, Bromfield, Scott, & Stedmon, (2019)’. This research will be elaborated in Chapter 4.

2.2.3 Aircraft control and automation

2.2.3.a Aircraft flight control problem

According to Harris (2012), an aircraft's flight path can be controlled by the pilot in three different modes:

Manual control: In this mode, the pilot flies the aircraft by hand, using the control stick, throttles and pedals.

Tactile control: In this mode, the pilot controls the aircraft through the autopilot flight control module. Instead of flying by hand, adjustments to the flight path are made on a merely strategic level by commanding specific flight path changes in heading, altitude or speed.

Strategic control: In most modern aircraft, a flight plan is entered into the flight management system, allowing aircraft to follow a long-term pre-programmed flight path using the autopilot. Changes made to the flightpath are at the long-term level.

Manually controlling an aircraft involves dealing with a hierarchical control problem (Harris, 2012) . In other words, the main parameter a pilot wants to control (e.g. the flight path of the aircraft) can be influenced only indirectly through other lower-level parameters such as pitch rate, roll rate or heading. Directly manipulating altitude is not possible; instead, a pilot uses pitch rate control, adjusting the pitch attitude to make the aircraft climb. Changing the heading involves rolling the aircraft to the right roll attitude, altering the rate of change of heading, and consequently adjusting the heading.

Flight controls for the primary axes of an aircraft are therefore interconnected, meaning that a change in one parameter affects others. A clear example is the connection between speed and pitch. In conventional aircraft, altering the pitch attitude impacts the vertical position or airspeed. For instance, increased speed causes the aircraft to climb due to added lift over the wings unless the trimmed angle of attack (AoA) is reduced. Similarly, pitching up without boosting thrust leads to a decrease in airspeed. Additionally, when rolling the aircraft for lateral control, there is a simultaneous downward pitching moment as some lift is lost on the slower-moving wing inside the turn. Yaw inputs also interact with the roll and pitching axes, influencing operator control strategies and skill acquisition. This shows that even though the AoA response remains constant, the pilot is experiencing a pitch rate response in which larger stick displacements result in larger pitch rate. A widely used model to assist in pilot control strategy, explaining the pilot/aircraft system as a whole, is the McRuer flight control model (1982). An adapted version from Field (2004) can be seen in **Figure 2.10**.

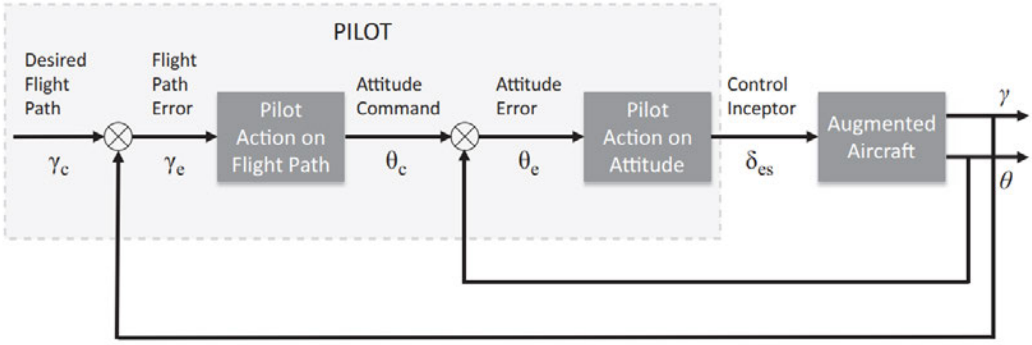

Figure 2.10 The McRuer series pilot model illustrating a response in pitch adapted from Field & Harris (2004)

Controlling an aircraft in general involves a compensatory tracking task wherein the goal is to minimise deviations from the desired three-dimensional flight path. However, it is crucial to note that the pilot cannot directly control the flight path. Instead, they use surrogates – for instance, in the vertical axis, the pilot manages pitch rate in the short term and AoA in the longer term, as previously described. However, the pilot can't directly observe flight path or AoA but can see only the aircraft's pitch attitude. McRuer's pilot flight control model breaks down the flight control problem into short-term and long-term challenges. In the vertical axis, the short-term issue is controlling pitch attitude, because the pilot can't directly observe AoA, the parameter affecting flight path. The long-term challenge involves flight path or altitude control. The short-term (pitch attitude) control problem is nested within the longer-term (flight path angle or altitude) control problem. The pilot aims to close the inner control loop to manage the actual problem of altitude/flight path angle control. In the horizontal plane, a similar control problem exists: The pilot uses aircraft roll attitude as a first approximation (inner loop parameter) to control the aircraft's heading. Similar to the vertical control problem, the pilot lacks direct control over the aircraft's heading, having control only over roll attitude. Automation has made it possible to take the dynamic tracking tasks and related problems away from the human, as will be described in the following section.

2.2.3.b Role of automation

Automation in flight control design has changed the execution of dynamic tracking tasks, as previously described, replacing them with flight path management-oriented tasks; the pilot has gone from a manual controller to a system manager (O'Leary & Chappell, 1996). Despite this shift, even experienced pilots may exhibit monitoring deficiencies (Sarter 2006). Depending on the type of input, the feedback available may be nothing more than a changing number on a display. Low-technology aircraft have direct responses from inputs, whereas in larger, more high-tech aircraft, there is a significant delay between input and aircraft response (Chappell, 1996; Harris, 2011). Aviation automation encompasses three principal types: information automation, control automation, and management automation (Woods & Billings, 1997). *Information automation* involves the management and presentation of information to pilots, *control automation* pertains to the automation of control surfaces influencing the flight path directly, and *management automation* focuses on strategic control rather than tactical control. The implementation of aviation automation has brought benefits such as reduced fuel consumption, all-weather operations, and enhanced aircraft handling (Parasuraman et al., 1992). Automation mitigates manual handling errors, especially in repetitive tasks, contributing to a substantial improvement in safety in air transport (Billings, 1996). However, the reliance on automation can introduce unsafe conditions when pilots are unaware of its current state or set of tasks. Task automation effectively takes pilots 'out of the loop' (Woods & Billings), as can be seen in **Figure 2.11**, which compromises a pilot's awareness of the system (Perry et al., 1997). In the event of sudden automation failure, humans are rushed back into the inner control loop without adequate time to prepare for the task and build SA, particularly if the system has not assisted pilots in maintaining their SA during automated control (Mouloua et al., 2010).

Figure 2.11 Management Automation removes the pilot from the inner control loop (Woods & Billings 1997)

2.2.4 Difference in flight control automation philosophy

The term 'fly-by-wire' is a common name for the type of automation involved, detailing the fact that flight control surface actuations are converted into electrical signals instead of push and pull rods. It is important to note that different manufacturers uphold different types of flight control automation philosophies. This subsection discusses the two different flight control configurations of the two most common manufacturers: Airbus and Boeing.

2.2.4.a Airbus flight control laws

Airbus flight control surfaces are hydraulically operated by an electronically controlled flight control input. At Airbus, there are three primary flight control laws: Normal Law, Alternate Law, and Direct Law (Corps, 1989). However, for this section only Normal Law operation will be discussed. Flight control in Normal Law provides three-axis control, flight envelope protection (FEP) and manoeuvre based on maximum load factor. Normal Law operates in three different modes depending on the stage of flight:

- **Ground mode:** Ground mode is active whilst the aircraft is on the ground. The autotrim feature is turned off and there is a direct relationship between sidestick deflection and elevator response (direct control). Immediately after the wheels are of the ground, flight mode takes over from ground mode; the reverse occurs after touch down during the landing phase.
- **Flight mode:** Flight mode provides five types of protection: pitch attitude, load factor limitations, high speed, low-speed high-AoA, and bank angle, as seen in **Table 2.1**. Flight mode is active for almost the entire flight, except for the final 100 ft before landing, where flight mode gives way to flare mode. Whereas conventional aircraft flight control inceptors command a certain flight control surface deflection, resulting in a certain roll rate, the Airbus flight control inceptors command roll or pitch input by a roll or pitch rate. As a result, a given sidestick deflection always results in the same roll rate, regardless of airspeed or attitude. Former Airbus pilot Bjorn Fehrm describes the Airbus flight control as follows: 'Point the aircraft's nose in a certain direction and the aircraft steadily keeps it there' (Fehrm, 2016). This rate command partially resolves the flight control problem mentioned in the previous section. On one hand, an automated and standardised roll or pitch rate allows for a very predictable control output, and therefore allows for direct and accurate flight path control by the flight control inceptor (Thomas & Ormsby, 1994). On the other hand, such high levels of automation can lead to grave difficulties in situations where automation fails. The Airbus flight control system degrades to Alternate Law, in which the pitch and roll rate demand is missing and is changed to direct control. Meaning, that a sidestick control input will command a specific control surface deflection, allowing the flight control problem to become apparent again.

Protection system	*Description*
Load factor protection	Limits the control inputs so that the aircraft remains within design limitations, not exceeding 1.33 g of load

	factor.
Pitch attitude protection	Limits the aircraft attitude to a maximum of 30° nose-up or 15° nose-down pitch attitude.
High-speed protection	High-speed protection limits the flight control inputs of the sidestick in order to prevent the airspeed from exceeding design limitations. High-speed protection will intervene with a nose-up movement in order to reduce airspeed.
Low energy protection	The low energy protection warning indicates that the total aircraft energy has become too low, computed on airspeed, descent rate and flight path angle. Depending on the situation, the Alpha Floor modus is engaged, which initiates maximum take-off thrust by the auto-thrust system. This is combined with an aural 'speed speed speed' warning.
Bank angle protection	Bank angle protection limits the bank angle of the aircraft. Depending on the situation, the aircraft will provide a maximum allowed bank angle of 67°. With the sidestick released, the bank angle will automatically return to 33°. If either Alpha Floor, high-speed protection or AoA protection is effective, bank angle protection does not allow for more than 45° of bank angle.
High AoA protection	Protects against aerodynamic stall. Protection is engaged when maximum AoA is reached and limits the full aft deflection of the sidestick when engaged. If the aircraft's AoA exceeds the maximum AoA, the aircraft engages Alpha Floor.

Table 2.1 Airbus flight envelope protection functions

- **Flare mode:** Flare mode is initiated upon achieving an altitude of 100 ft as measured by the radio altimeter. Flare mode changes the elevator control input from a pitch rate demand to a direct command to the position of the elevator. This means that at 100 ft altitude, the sidestick no longer commands a specific rate, but instead directly commands elevator deflection. A given sidestick deflection now reflects a specific elevator deflection. Also at this time, the aircraft slightly trims the nose down, requiring the pilot to move the sidestick rearward to initiate a flare (Airbus, 2017). The approach phase is normally flown with the help of flight guidance equipment, such as autopilot engagement, radio altimeter call-outs and instrument landing systems. Flare mode is initialised at the point where – with the exception of automated landings – the pilot has physically initiated the flare, requiring a manual flight control input, deviating from the flight path. This manual control input occurs at the same time as the transition to flare mode.

2.2.4.bBoeing flight control system

The Boeing 777 flight control system is designed to restrict control authority beyond a certain range by increasing the back-pressure once the desired limit is reached. It allows the pilot to exceed this limit, but alerts them that a critical limit has been exceeded via aural warnings and increased stick pressure. This is done via electronically controlled back-driven actuators. This type of FEP is called a 'soft stop' protection (Bartley, 2001). The FEP systems on the 777 are: bank angle protection, turn compensation, stall protection, over-speed protection, pitch control, stability augmentation and thrust asymmetry compensation (Boeing, 2003). The FEP system provides information on envelope margins and limitations by means of tactile, visual and aural cues and warnings. However, the protection functions of the system do not reduce or limit pilot control authority. The primary flight computers (PFCs) verify process signals and information from other airplane systems in order to compute control surface commands; these commands are then sent to the flight control surface actuators, which convert them into analogue servo commands. On Boeing aircraft, he flight control inputs being made by the pilot are directly linked to the flight control surfaces. The deflections of the control surfaces are filtered only on airspeed or flap configuration (Boeing, 2003). When the autopilot is engaged, the autopilot system sends commands to the PFCs, which, in turn, generate control surface commands that are sent to the ACEs in the same manner as pilot control inputs. The autopilot commands move the flight deck controls to provide autopilot feedback to the pilots. If a pilot overrides the autopilot with control inputs, the PFCs will disengage the autopilot and utilise the pilot control inputs.

2.3 Haptic feedback in aviation flight controls

2.3.1 Haptic feedback and general applications

2.3.1.a Proprioceptive and haptic feedback

'Haptic feedback' is a broad term that describes technologies that engage a human tactile senses. This sensory modality involves the use of touch to communicate information to users. Haptic feedback can be classified into several types, each with distinct mechanisms and applications. One of the most common forms of haptic feedback is vibrotactile feedback, which involves the use of vibrations to convey information. Vibrations can vary in frequency, intensity, and duration, providing users with different sensations. This type of feedback is widely used in mobile devices, gaming controllers, and wearable technologies (Grushko et al., 2021). Another haptic application is force feedback, also known as resistive or tactile feedback, which involves the application of forces or resistances to mimic the sense of touch. This type of haptic feedback is prevalent in virtual reality (VR) and gaming applications, as well as in-flight envelope protection systems in aviation (Ellerbroek et al., 2016; Lombaerts et al., 2017; Van Baelen et al., 2021) or automotive. Force feedback is commonly used to inform the operator of an approach limitation, such as flight envelope protection systems in aviation, or lane guidance in automotive. Section 2.3.2 will elaborate more on such applications. Another application is surface haptics, which focuses on creating the perception of textures on smooth surfaces. Electrostatic or ultrasonic technologies are used to generate friction or vibrations, simulating the feel of different textures. This type of haptic feedback is relevant in touchscreens and touch-sensitive interfaces (Hannaford, 2001). Proprioceptive (or kinaesthetic) feedback is defined as that of one's body motion or position. Proprioception is a neural representation of body parts to the central nervous system (Oxford University Press, 2018).

2.3.1.b Automotive applications of haptic feedback

A pilot and the driver of a car have similar objectives; the car driver seeks to operate a vehicle within the allowable limitations of the road, other cars and the environment. In order to stay within these limitations, haptic feedback is sometimes used to enhance safety and driver comfort. In order to avoid a head-on collision, haptic feedback can be provided through the gas pedal by increasing the stiffness when driving closer to the car in front, Mulder et al. (2010) showed it to increase car-following performance whilst reducing control activity. The lateral axis can be protected by providing haptic feedback through the steering wheel in order to keep the operator aware of the physical limitations of the road. Steering-wheel vibrations are a widely used method of providing warnings and directions via haptic feedback. Active feedback that is more involving can be provided by using an offset force to indicate a required deflection, and changing the stiffness to indicate a criticality of the action (Shi et al., 2023; Xu et al., 2023). This type of feedback can be used to provide support to either steer the car away from the boundaries, or to steer the car toward one specific path. The literature review found no research on haptic feedback in cross-coupled steering wheel control.

2.3.2 Use of haptic feedback in aviation

2.3.2.a Haptic feedback in variability in range axis

Variability in the range of the axis in the active sidestick is used for the multi-purpose take-off configuration of the F-35. This aircraft is capable of vertical take-off and landing (V-TOL). However, because the flight envelope and handling qualities during V-TOL differ entirely from those during normal flight, the F-35 active sidestick adjusts the motion range on the two flight control axes, limiting the stick in specific ways. This haptic cue also provides better awareness to the pilot whilst flying V-TOL.

2.3.2.b Simulating dynamic pressure

Earlier aircraft with conventional flight controls had dynamic pressure on their flight controls. When flight controls are mechanically connected to flight control surfaces, control surface deflection becomes heavier when airspeed increases. As a result, the flight controls stiffen up when airspeed increases. This dynamic pressure can be artificially applied on active sidesticks, resulting in a stiffening of the stick when flying at higher airspeeds. Boeing has implemented this type of dynamic pressure force feedback on their Boeing 777 and 787 models (The Boeing Company, 2007).

2.3.2.c Simulating stick shaker

On smaller aircraft with mechanical linkages between the flight controls and the flight control surfaces, the control column (or stick) provides a feedback force on the current position of the flight control surfaces. A positive side effect of this linkage is that in these aircraft a flight control inceptor will shake, sometimes violently, if the aircraft is nearing stall conditions. This is because during the stall of the main wings, turbulent airflow is striking the horizontal stabiliser and elevators, which can be felt on the flight control inceptor. The benefit of this is that it provides an additional haptic cue to the pilot that their aircraft is entering a stall. This aerodynamic stick shaking cannot be felt on larger aircraft and is therefore artificially applied on most modern aircraft.

2.3.2.d Autopilot back drive

Another aspect of passive sidesticks is that movements of the control inceptors are not back-driven by the auto-flight systems. Conventional back-driven flight controls move in accordance with the inputs made by the autopilot. Most of these aircraft also have a back drive on their throttles, providing the pilots with cues that indicate what the autopilot system is doing. This auto-flight back drive indicates to the pilots that the auto-flight system is performing as expected. A study conducted by Summers et al. (1987) suggested that a back-driven system is essential in intervening in time when the auto-flight system is failing. A survey conducted by Field and Harris (1998) indicated that the removal of this back drive has degraded communication lines in the cockpit.

2.3.2.e Asymmetrical axis force displacement

Another functionality of active sidesticks is their capability to provide asymmetrical load on the control inceptor. According to several studies (e.g. Joslin, 2017; Karim et al., 1973), the maximum load a pilot can apply on the control inceptor depends on the direction of the stick towards this force is applied. According to the above-mentioned studies, on average, pilots can apply a much higher force on the forward and aft direction of the stick than to the left and right aileron input. In addition, the location of the stick also influences the maximum force that can be applied to either left or right. In the above-mentioned studies, a pilot flying a centre-stick control inceptor with his right hand can apply much greater force on the stick towards the left (pushing) than towards the right (pulling). This maximum force also differs between male and female pilots; an active sidestick can be programmed so that the maximum force displacement can vary on each axis, taking human ergonomics into account.

2.3.2.f Use of haptic feedback on flight envelope protection

Several studies by the University of Delft (Lombaerts et al., 2017; Van Baelen et al., 2018; Van Baelen et al., 2021) focussed on the design and evaluations of flight envelope protection by using haptic feedback. These studies focus on two different types of haptic feedback: generating feedback through vibration (stick shaker) and generating feedback by control stiffness. If the aircraft is approaching its flight envelope limits, the sidestick will initiate a continuous vibration to alert the pilot that the aircraft is about to exceed its flight envelope. The stiffness of the sidestick is used to indicate to the pilots that the maximum load factor is reached. These studies conclude that haptic feedback provides fast, accurate and intuitive information during safety critical situations. Van Baelen et al. (2021) reported that one participant inadvertently stalled and crashed the aircraft whilst using the haptic system, but the article does not elaborate as to whether the stall was linked to the haptic feedback system.

2.3.2.g Use of cross-coupling helicopter flight controls

A recent study investigated the effect of helicopter cross-coupling cyclics (Berger et al., 2023) by configurating a simulator with two side-by-side pilot stations with sidestick controllers that could be configured to operate in either a linked or unlinked configuration. During each task, a control transfer from the pilot flying to the pilot not flying was either forced or induced, after which the pilots were asked to answer a series of questions and rating scales related to predictability, awareness, and acceptance. The study showed that in all cases, pilots preferred the linked cyclic controller configuration, rating it higher on predictability, awareness and acceptance. In addition, the linked cyclic controller configuration had no simultaneous input events, unlike the unlinked cyclic controller configuration.

2.3.3 Limitations of passive sidesticks

Although passive sidesticks are commonly used in commercial aviation, this system has certain limitations, which will be discussed in this section.

2.3.3.a Communication breakdown

Due to the increased amount of automation introduced in modern fly-by-wire aircraft, it is no longer necessary to link the flight control inceptors directly from the cockpit to the flight control surfaces. Instead of running physical cables from the cockpit to the control surfaces, the control surfaces are now electronically driven by the flight computer, which is commanded by the flight control inceptors. This situation requires fewer physical components, saves weight, allows for a more reliable system (Corps, 1989) and generates a more simplified system architecture. However, with the removal of these flight control linkages, the cross-coupling between the two inceptors has been lost as well. Several authors have suggested that the elimination of this physical interconnection removes one of the lines by which pilots communicate (Field & Harris, 1998; Taylor, 1988). Field and Harris described the four channels by which pilots communicate with one another, the aircraft, and the environment, and posited that pilots perceive information from one another via central visual cues, peripheral visual cues, auditory cues and proprioceptive cues. The removal of the interconnection between the control inceptors removes the proprioceptive cues for the pilot monitoring (PM). Pilots use proprioceptive cueing to perceive and feel flight control movements. Field and Harris illustrated these four communication channels in **Figure 2.12**. This paper stated that cues perceived by the peripheral view are still a way in which pilots communicate. However, in terms of passive flight control inceptors, it has become nearly impossible. The passive inceptors are located on the outboard side of the cockpit, making the other inceptor difficult to perceive throughout peripheral view. In relation to yokes and centre-stick flight inceptors, whose movements are much more easily captured simply because these movements occur within the peripheral view. Furthermore, the deflection of these passive inceptors is much smaller in comparison to yokes and centre-sticks, making their movement even harder to perceive. For these reasons, Field and Harris concluded that pilots of passive sidestick aircraft are much more dependent on central vision and auditory cues than pilots of conventional flight-controlled aircraft. According to Mica Endsley, this type of situation can lead to a decreased level of situation awareness (SA); in an earlier paper, Endsley concluded that the utilisation of several sensory modalities for conveying information, enhances SA (1988). If that is true, then the opposite can be concluded as well: The removal of several sensory modalities could lead to a degradation of SA. Therefore, it is possible that the removal of these two communication channels between pilots can lead to a decrease in SA. As Schmidt-Skipiol and Hecker concluded in their study, 'The removal of the cross-coupling between the flight controls, makes the flight crew more depending on visual and auditory cues, which are already extensively used when flying a modern aircraft' (2015). Again according to Endsley (1988), this is the opposite of enhancing SA because overburdening one sensory channel is not conducive to SA.

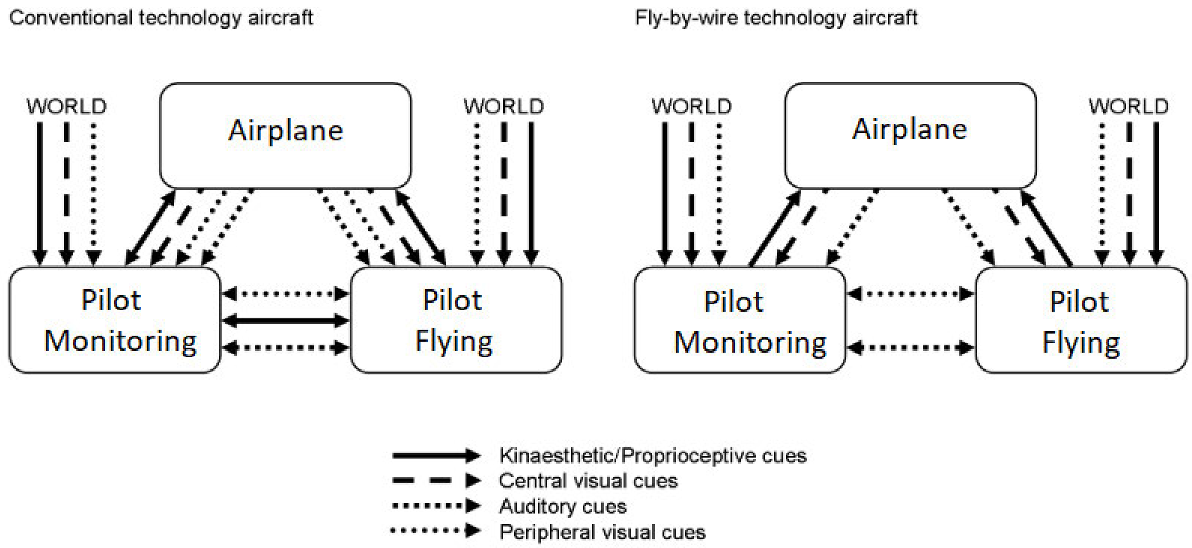

Figure 2.12 Information transfer between the airplane and its flight crew, adapted from Uehara (2014). Original source: Field and Harris (1998)

2.3.3.b Dual input logic

The passiveness of the sidestick enables the possibility of a 'DUAL INPUT' (DI), which occurs when both pilots are using the sidestick at the same time. Currently, all passive sidestick aircraft deal with this by algebraically summing up both inputs to generate a signal output with a maximum of a single stick deflection. For example, if both pilots push the sidestick halfway forward, the output will be equivalent to a full forwarded stick deflection. This is also true for conflicting commands: If one pilot pushes the stick fully forwards and the other pilots pulls the stick fully backwards, the resulting command is zero. The issue with this system logic is that the summation of the inputs generates a flight control deflection that neither of the pilots wants. To notify the pilots of a dual control input, the flight control system generates the acoustic alert: 'DUAL INPUT'. It should be noted that this aural alert will be suppressed when a warning with a higher precedence is sounding, such as: 'SINK RATE' or 'PULL UP', as was the case in the Air Afriqiyah accident in Tripoli (Libyan Civil Aviation Authority, 2015). Research by Dehais et al. (2014) concluded that in many situations, pilots are susceptible to inattentional deafness during high-stress situations in the cockpit.

According to Uehara and Niedermeier (2013), dual inputs in fly-by-wire aircraft often occur after the sudden evolution of a situation leading to manual input corrections. To avoid a dual input situation, most aircraft with passive sidesticks are equipped with a 'priority take-over push button' located on each sidestick. When this button is pressed, the other sidestick's control inputs are cancelled out. According to ICAO Annex 2 (ICAO, 2005), the commander should always be in command, stating: 'The pilot-in-command of an aircraft shall have final authority as to the disposition of the aircraft while in command'. Thus, if both pilots push the priority take-over button, the captain's side will overrule. If a pilot presses the priority take-over button, an aural alarm sounds and a visual signal is illuminated. (A summary of these warnings can be seen in **Figure 2.13**.) As mentioned by Uehara, dual inputs often occur when a sudden situation occurs. The question is, how instinctive is the priority push button when the other pilot wants to take control? According to some accident reports, the priority switch button is not instinctive at all (AAIB, 2006, 2008). The AAIB concluded several times that in certain situations in which the PM is forced to suddenly intervene, pressing the priority push button is not an instinctive response; rather, it is much more instinctive to move the sidestick. In such situations, a dual input occurs, in which the output of the flight controls is a summation of the inputs – which in many instances results in a combined output that none of the pilots initiated. Additionally, the AAIB concluded that the take-over push button is a highly cognitive action, instead of instinctive (AAIB, 2008).

Captain's side		First Officer'side	
Sidestick	Annunciation	Annunciation	Sidestick
Take-over button depressed	CPT Green	Red	Sidestick deflected
Take-over button depressed	"Light off"	Red	Sidestick in neutral
Sidestick deflected	Red	F/O Green	Take-over button depressed
Sidestick in neutral	Red	"Light off"	Take-over button depressed

Figure 2.13 Sidestick priority logic adapted from AIRBUS SE (2004)

2.3.3.c Unlinked flight controls on flying skill development

As stated above, the removal of the cross-coupling between the control inceptors also removed one of the lines by which pilots communicate. Research by Rees and Harris concluded that the physical linkage between the control inceptors also contributes to the development of flying skills (1995). In their study, 20 ab-initio pilots flew a series of approaches in linked and unlinked flight-control inceptor configurations. The results suggest that unlinked control inceptors are hindering the development of psychomotor control skills. Throughout proprioceptive cues, the ab-initio pilot gets a better sense of how to fly an approach, simply by feeling the cues from the flight instructor. This missing learning channel may also be affecting currency levels of passive sidestick pilots. Research by Haslbeck and Hoerman (2016) showed differences in manual flying skill degradation between long-haul pilots and short-haul pilots. They attributed the difference to the lack of practice of long-haul pilots, who conduct only a few flights a month. If the limited amount of flying degrades the psychomotor skills of long-haul pilots, the lack of proprioceptive cuing for passive sidestick pilots could perhaps have the same effect.

2.4 Relation to accidents

Over the last two decades, several aviation incidents involving FBW transport aircraft with uncoupled sidesticks have been investigated; the findings of these investigations support the provide additional evidence that the lack of sidestick coupling is a factor contributing to aviation incidents. This section provides an analysis of three investigation reports and highlights the human factors implications.

2.4.1 Near-collision during Simultaneous Runway Operations, (ATSB, 1993)

Sydney Airport was operating under simultaneous runway operations and both Runways 34 and 25, which intersect, were used for landing. A DC-10 landing on Runway 34 was instructed by ATC to stay clear of the intersecting Runway 25 because of an A320 that was on final approach of that runway. The commander of the A320, whilst observing the landing roll of the DC10, estimated that the aircraft would not come to a stop before the intersection. The commander, acting as PM, took over control from the first officer (FO) and initiated a go-around from low altitude. During the go-around, the digital flight data recorder (DFDR) recorded conflicting attitude command inputs from the sidesticks of both the commander and FO. The aircraft transitioned to a nose-up attitude and overflew the intersection of Runways 34 and 25 at an altitude of approximately 50 ft. The subsequent investigation of the incident found that as the go-around commenced, both pilots were making dual control inputs over a period of 12 seconds. The FO was changing between pitch-down and neutral sidestick inputs whilst the commander was making pitch-up sidestick commands. It was noted that the FO was not consciously aware of the control inputs he made after the initiation of the go-around. The investigators found that the dual inputs were the result of crew coordination breakdown, which most likely occurred due to the use of non-standard terminology during the hand-over/take-over procedure. The investigation report also states that had there been tactile feedback to one pilot to inform him about the sidestick control inputs of the other pilot, the dual input situation would almost certainly have been identified and corrected instantly.

2.4.2 Tailstrike on landing, Airbus A321, London Heathrow Airport, 21st of June 2000 (AAIB, 2000)

After receiving radar vectors to the ILS approach on Runway 27R, the Airbus A321 started its final descent towards London Heathrow. The FO, who was acting as pilot flying (PF), disconnected the autopilot and auto-throttle after establishing visual contact with the runway. The ILS approach was flown mostly manually and stable until an altitude of about 300 ft AGL. From this moment on, the aircraft destabilised and deviated above the glideslope as the rate of descent reduced substantially. The FO, in an attempt to correct the aircraft's trajectory, applied forward sidestick input. As a result, the rate of descent increased to approximately 800 ft/min. At an altitude of 60 ft AGL, the FO applied aft sidestick input, with a nose-up demand of 92.5%, until touchdown. However, this input was not sufficient and the touchdown that followed was hard. The aircraft subsequently bounced back, lifting the main landing-gear wheels off the ground. After the initial touchdown, the ground spoilers were deployed, and the nose of the aircraft continued to rise. On the second touchdown, the aft section of the fuselage contacted the runway. The commander applied forward sidestick input (56.3% nose-down), and the remainder of the landing was uneventful. In their investigation, the Air Accident Investigation Branch (AAIB) stated that the commander, in the capacity of PM, did not foresee any problems with the final stages of the approach until initial touchdown. The AAIB concluded that the commander 'could not have been aware of the sidestick control inputs made by the FO', especially the continued aft sidestick inputs from 60 ft AGL onwards, because his sidestick did not mirror the control inputs of the FO. In addition, the AAIB notes that, given the stage of the flight, it is unlikely that the commander had sufficient information available to assess the situation and to intervene successfully. Remarkably, the effectiveness of his intervention, as can be seen by the commander's control inputs after the second touchdown, would have been reduced because the take-over push button was not pressed.

2.4.3 Loss of control in flight, Airbus A330-203 (BEA, 2012)

The Airbus A330 was cruising at FL350 near the TASIL waypoint when ice crystals obscured the Pitot probes. As a result, the presented speed indications in the cockpit became unreliable, and several of the onboard automatic systems disconnected. During the subsequent manual flight, inappropriate sidestick control inputs made by the flight crew resulted in a destabilisation of the aircraft's flightpath. Following a late identification of the flight path deviation, the flight crew's attempts to correct it were insufficient. The aircraft approached a stall condition and subsequently departed controlled flight from which recovery was unsuccessful. The aircraft impacted the sea and all occupants perished. With respect to the destabilisation of the flight path, the accident investigators noted that the PF applied various nose-up sidestick control inputs. Either the PM was not verbally made aware of these inputs and intentions, or objectives related to the stabilisation of the aircraft's flight path were not relayed. Therefore, the investigators consider it unlikely that the PM could have identified what the PF flight path stabilisation targets were. Furthermore, the report mentions that it is difficult for one pilot to monitor the sidestick control inputs of the other pilot and that, especially in night-time conditions or in IMC, the aircraft's attitude is difficult to monitor.

2.5 Discussion

The introduction of fly-by-wire flight control technology with uncoupled sidesticks in modern commercial aircraft has been a topic of concern among human factors specialists. Studies by Field and Harris (1998), Savelev and Neretin (2019), Summers et al. (1987) and Uehara (2014) have addressed human factors implications regarding the absence of tactile feedback in these systems. They note that non-linked sidesticks may have degraded the lines of communication in the cockpit, thereby overburdening pilots' sensory systems and adversely affecting SA (Hanke & Herbst, 1999; Schmidt-Skipiol, 2013). When relating the tasks of a PM to Endsley's three-level SA model (Endsley, 1988), it can be stated that the passiveness of the sidestick limits the PM's ability to perceive flight control inputs being made, thereby negatively affecting level one. Endsley also concluded that SA is enhanced when utilising multiple sensory modalities for conveying information (Endsley, 1988).

A similar conclusion can be made regarding the multiple resource theory, where Wickens posited that there tends to be less interference in the input dimension in time-sharing tasks when using cross-modalities, due to the use of separate perceptual resources (Wickens, 2014). Wickens et al. concluded that haptics act as a resource to enhance the visual modality (2015).

The conclusions of both Endsley and Wickens corroborate the results of the cross-coupling flight control survey by Field and Harris (1998), which demonstrated the importance of interconnection in a flight control inceptor and strongly suggested that a coupled flight control inceptor configuration has much to recommend. With regards to the accidents discussed in paragraph **2.4**, it can be stated that the limitations on monitoring duties introduced by the passive sidestick system are not the root cause of those accidents. However, the removal of the cross-coupling causes difficulties in monitoring manual flight control inputs by the PF, resulting in the loss of an essential safety barrier – namely, effective monitoring – could negatively affect flight safety.

Chapter 3 Methodology

This chapter will describe all of the general equipment, data collection, data analyses and procedures used in Chapters 4 to 7, in addition to presenting a justification for the methodology chosen. Chapters 4 and 5 of this thesis describe statistical studies investigating the relationship between the number of hard landings or tailstrikes and the type of aircraft involved in these incidents. The same general methods and data analysis tools were used throughout these chapters. Chapters 6 and 7 describe simulator-based studies investigating the effects of haptic feedback on previously mentioned hard landings and tailstrike accidents. The same participants, equipment, data acquisition and data analysis tools were used in these simulator studies.

3.1 General methodology statistical studies

3.1.1 Experiment design

The studies undertaken in Chapters 4 and 5 are designed to compare the number of accidents and incidents between passive sidestick aircraft and aircraft with coupled flight controls. The number of accidents are compared to the total number of flight cycles per aircraft type to measure significant associations.

3.1.2 Timeframe

The most crucial data used in these studies were the accident and incident reports, which were retrieved from registered air accident investigation authorities by ICAO according to Annex 13 (ICAO Standards and Recommended Practices for aircraft accident and incident investigation). An Annex 13 investigation has a maximum duration of 18 months. At the start of the data retrieval in June 2019, the most recent reports dated from 2018. Therefore, a ten-year time span is chosen from 2018 backwards to 2009.

3.1.3 Flight cycles per aircraft type

In the statistical studies, aircraft accident and incident reports were compared to the number of flight cycles flown within a ten-year time span. The flight cycle dataset is constructed based on the number of flight cycles per aircraft type as reported in the International Air Transport Association (IATA) annual safety reports (IATA, 2010, 2010, 2011, 2012, 2013, 2014, 2015, 2016, 2017, 2018, 2019). The passive sidestick aircraft included in this flight cycle database are: the Airbus types A318, A319, A320, A321, A330, A340, A350 and A380; Bombardier CS 100 and CS 300; COMAC ARJ 21; and Sukhoi SJ-100. All commercial jet aircraft with conventional flight controls are calculated by subtracting these passive sidestick cycles from the IATA total calculated number of cycles by jet aircraft. The number of flight cycles per flight-control type per million cycles per year can be found in **Table 3.1**. The total amount of flight cycles and percentages per flight control type can be found in **Table 3.2**.

	2009	*2010*	*2011*	*2012*	*2013*	*2014*	*2015*	*2016*	*2017*	*2018*
PSS	6.93	7.55	8.34	9.03	9.84	10.6	11.41	12.24	12.817	13.772
Cpld	19.69	19.42	18.93	19.53	19.63	20.01	19.98	21.56	22.182	23.927

Table 3.1 Flight cycles (in millions) for passive sidestick aircraft (PSS) and coupled flight control aircraft (CPLD) derived from IATA (2010–2019)

	Total flight cycles in millions	*Percentage*
Passive Sidestick	94.98	31.67%
Coupled flight control	204.87	68.33%
Total	299.85	100%

Table 3.2 Flight cycles (in millions) divided between passive sidestick aircraft (PSS) and coupled flight control aircraft derived from IATA (2010–2019)

3.1.4 Defining a hard landing and tailstrike accident

3.1.4.a Hard landing definition

For the purposes of these statistical studies, a hard landing is defined as 'a symmetrical and conventional landing or de-rotation with hard contact to the ground that resulted in damage to the aircraft'. Commercial aircraft are equipped with flight data recorders capable of measuring vertical acceleration, but due to a number of inaccuracies regarding the accelerometer, this research does not use acceleration exceedance in its definition of hard landings. First of all, accelerometers are used to measure in-flight accelerations and are therefore not suitably positioned within the aircraft to properly measure landing accelerations; these inaccuracies can be as great as 0.4g during landing (Aigoin, 2012). Second, accelerations vary in magnitude and acceleration. Because the average accelerometer captures data 16 times per second, it is impossible to determine whether the recorded value is the actual maximum, minimum, or some intermediate value (Matthews et al, 2004). Finally, this research compares different aircraft makes and models, each of which differ in their maximum allowed landing acceleration. According to Aigoin (2012), the best way to determine a hard landing is to calculate the true vertical speed, which can be derived from flight data parameters. Because most accident reports do not provide sufficient data to perform such a calculation, this study does not attempt it. As indicated by the definition given in the first sentence of this paragraph, damage will be the leading factor in this study's definition of a hard landing. Any landing harder than the type-specific maximum allowed landing acceleration which results in damage will be considered a hard landing.

3.1.4.b Tailstrike definition

The general definition of a tailstrike is quite broad. According to SKYbrary, any contact between the tail section of an aircraft and the ground is defined as a tailstrike (SKYbrary, 2018). This definition includes so-called 'tail-stands', which are incidents where stationary aircraft suffer from tailstrikes due to wind or incorrect loading. Thus, for these studies, a tailstrike will be defined as: 'Any section of the aft fuselage of the aircraft that came in contact with the runway during take-off, landing or go-around which resulted in damage which is reported in an accident or incident report'.

3.1.5 Accident and incident reports

The accident and incident reports used for the statistical studies were retrieved from registered air accident investigation authorities by ICAO. According to the ICAO website (ICAO, 2012) there are 204 national aviation accident investigating authorities. Of these 204 authorities, 119 were found to have accessible websites, of which 72 published reports on those websites. A total of 225 hard landing and 289 tailstrike accident and incident reports were obtained that fit this study's hard landing and tail strike definitions. In order to make a reliable comparison, some reports are excluded from this study. First, turboprop aircraft are not included. Currently, no turboprop aircraft within commercial aviation are equipped with passive sidesticks. Second, events that occurred due to contributing weather will not be taken into account. Examples include wind shear, microbursts, and sudden turbulence drops. Third, events that occurred due to mechanical failures will be excluded. Examples include flight control malfunctions, autopilot malfunctions, runaway trim/elevators, and erroneous flight instrumentation. Finally, events that occurred during abnormally high workload situations are also excluded. Examples include inoperative engine, damage due to bird strikes, and landing gear failures. In the final tally, 40 qualifying hard landing reports and 129 qualifying tailstrike reports are used in the statistical studies.

3.1.6 Statistical methods used for data analysis

3.1.6.a Chi-square test for independence

The chi-square test for independence is used to explore the relationship between two categorical variables (Pallant, 2013). This test compares observed frequencies in each categorical variable and compares that with the values that would be expected if there were no association between them. The chi-square test is based on a cross-tabulation table; when using only two categorical variables (i.e. a 2 x 2 table), an additional 2 x 2 correction value – the Yates correction for continuity – is used (Giannini, 2005). For a reliable outcome, the lowest expected value in any cell should be at least 5; when working with a 2 x 2 table, this should be at least 10. When violating the lowest expected frequencies, the Fisher's exact probability test should be used instead of the Yates correction (Giannini, 2005). The effect size of a chi-square test depends on the size of the table. For a 2 x 2 table, it is recommended to express the effect size via the phi coefficient (Guilford, 1941), which is a coefficient expressed in a value between zero to one, indicating a stronger association between the variables when the phi coefficient is higher. To determine the meaning of the effect size, Cohen's criteria to assess effect sizes are used (Cohen, 1988). Cohen states that an effect size value below 0.1 is considered small, an effect size value of 0.3 is considered medium, and an effect size value above 0.5 is considered large.

3.1.6.b Independent t-test

The independent t-test is a statistical method used to determine if there is a significant difference between the means of two independent groups. It assesses whether the observed differences between the group means are likely to be due to random chance or if they reflect a true difference in the populations being studied. The effect size of a paired-samples *t*-test is calculated according to Cohen's *d* (Cohen, 1988) which can be seen in **Equation 3.1**.

This item has been removed due to third party copyright. The unabridged version of the thesis can be viewed at the Lanchester library, Coventry University

Equation 3.1 Cohen's d calculation (Cohen 1988)

3.1.6.c Pearson product moment correlation

The Pearson product moment correlation coefficient, often denoted as *r*, is a statistical measure that quantifies the strength and direction of a linear relationship between two continuous variables. It is widely used for assessing the degree to which two variables are linearly related, but it is reliable only if the variables are normally distributed. The Pearson product moment correlation coefficient is susceptible to outliers and can provide misleading results if the data is not accounted for extreme values (Shaughnessy et al., 2000). According to Cohen (1988), the r value below 0.1 is considered a small effect size, r values of 0.3 are considered medium, and r values above 0.5 are considered large.

3.1.7 Ethical approval on statistical studies

The research methodology described in this paragraph has been submitted to the Coventry University Ethics Commission and has been confirmed and approved under Project Reference Number P62546.

3.2 General methodology simulator studies

3.2.1 Experiment design

The aim of this study is to evaluate the effects of haptic feedback on monitoring duties during hard landing and tailstrike events. The experiment was conducted using an Airbus A320 fixed-base simulator at Coventry University. Pilots with an Air Transport Pilot Licence where invited to participate. During the experiments, pilots were sat in an Airbus A320 static simulator next to a retired A320 flight instructor. This instructor acted as the PF for the experiments, whilst the participants where tasked to act as a PM. During six flight scenarios, the participants monitored three flights with passive sidestick flight controls and three flights with active sidestick flight controls. During these six flights, four scenarios involved an improper manoeuvre deliberately initiated by the flight instructor, acting as PF. These manoeuvres involved not initiating the flare and excessive rotation during the take-off roll. Several quantitative and qualitive data points were gathered, which will be discussed in the following sections.

3.2.2 Participants

The preference was to have a fully Airbus-rated sample group. Unfortunately, this turned out to be extremely difficult to obtain. Thus, at a later stage the sample group was opened up to all type-rated airline pilots holding an Airline Transport Pilot Licence and experienced on modern twin-jet aircraft. Twenty-one ATPL-rated airline pilots volunteered to take part in this experiment. The participant group varied in age and experience, expressed in logged flight hours. Experience on all modern transport aircraft was accepted, but experience on passive sidestick aircraft was preferred. Participants were contacted by advertisements in various airline pilot magazines and were approached based on word-of-mouth. This resulted in a group of 21 pilots, of whom 16 had experience on passive sidestick aircraft. The original sample group consisted of one additional Airbus-rated participant. However, this person was close friends with the PF and showed a lot of trust in his competence – so much so that the participant did not intervene on any of the simulator runs. Therefore, the results of this participant were excluded. Before being invited over, the participants were asked to complete a survey regarding their recent experience.

Eligibility for the experiment was based on the answers provided in this questionnaire. All participant demographics can be found in **Table 3.3**.

Age	**20–29**	**30–39**	**40–49**	**50–59**	**60+**
No. pilots	3	8	2	3	4
Sex	**Male**	**Female**			
No. pilots	20	0			
Role	**Awaiting Role**	**First Officer**	**Captain**	**Training Captain**	**Recently Retired**
No. pilots	2	9	4	4	1
Type of ATPL	**Frozen**	**ATPL**	**ATPL FIC**		
No. pilots	2	14	4		
Flying hours	**Mean**	**Std. Dev.**	**Median**		
	7275	4059	4450		
Type rating	Airbus	Boeing	Other (coupled)		
	16	2	2		

Table 3.3 Participant demographic data

3.2.3 Hardware materials

The hardware materials used in these studies consisted of four distinct components: the flight simulator, eye-tracking system, BIOPAC physiological measurement system, and audio recording system. These last three hardware systems were standalone systems and were used alongside one another. A general overview of the different systems and their interconnections can be seen in **Figure 3.1**.

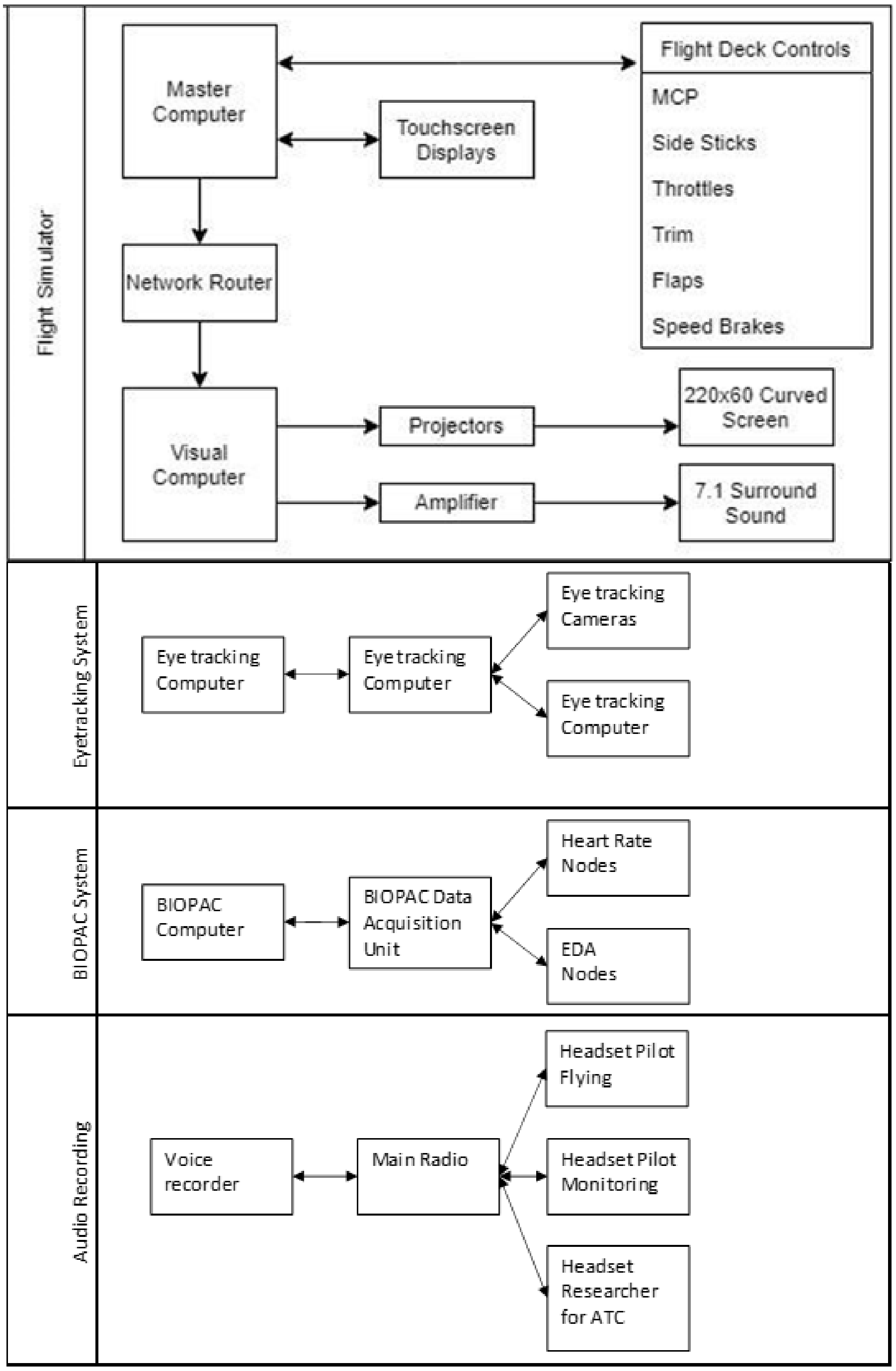

Figure 3.1 System hardware overview

3.2.3.a Coventry University flight simulator

Coventry University's human-in-the-loop flight simulator is a fixed-base flight simulator equipped with a wide projection screen providing a 220 x 60 degree curved projection. The flight deck lay-out consists of a generic jet transport aircraft with passive sidestick configuration based on the Airbus A320 flight deck. The passive sidesticks on both sides are interchangeable for active sidesticks. The participants were seated on the right side of the flight deck, whilst the PF for this experiment flew from the left side. A schematic overview can be seen in **Figure 3.2**, and photographs of the 220-degree screen can be seen in **Figure 3.3**.

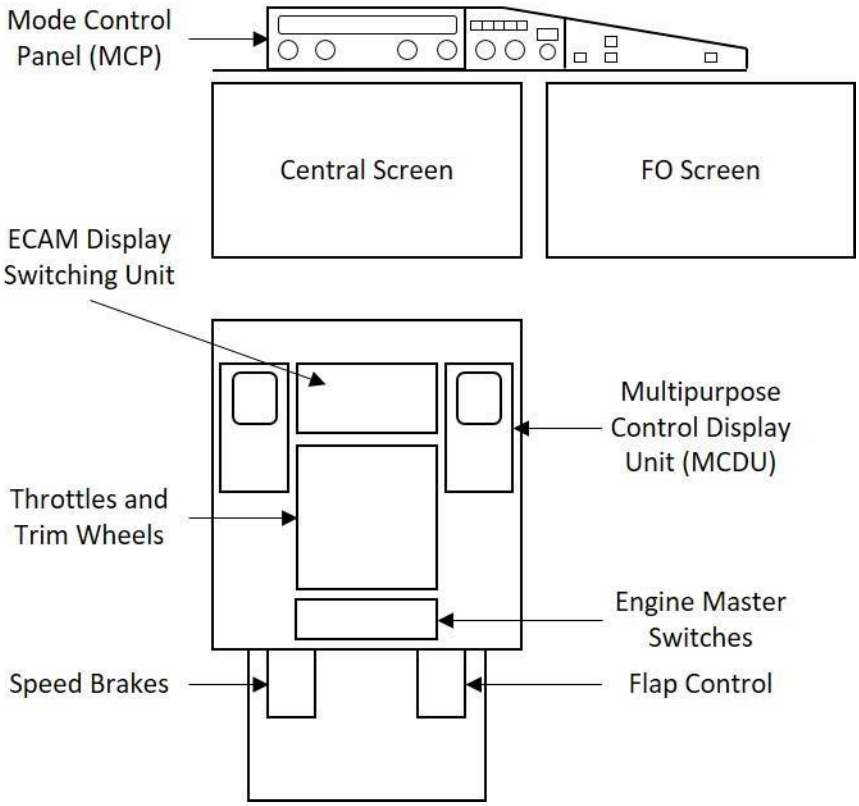

Figure 3.2 Schematic overview of the co-pilot's side of Coventry University's human-in-the-loop simulator

Figure 3.3 Photograph of Coventry University's human-in-the-loop simulator and 280-degree screen projection

3.2.3.b Flight control inceptors

These experiments use two different flight control inceptors. The standard flight control inceptors are Airbus lookalike passive sidesticks (**Figure 3.4**), which have the same spring-loaded force feedback as in a normal Airbus A320. Also, the flight control laws and take-over push buttons work accordingly. The priority light on the overhead panel illuminates when the take-over push button is pressed.

Figure 3.4 Airbus lookalike passive sidestick on Coventry University's human-in-the-loop simulator

The other half of the scenarios used an active sidestick system manufactured by Stirling Dynamics, as can be seen in **Figure 3.5**. This system consists of two sidesticks programmed to provide force feedback via electromagnets. The system is programmed such that the sticks are coupled, so if one pilot moves their stick, the other stick moves with it. This stick configuration lacks take-over priority; the buttons on the active stick were disengaged.

Figure 3.5 Stirling Dynamics Active Force Feedback Side Stick Plus

3.2.3.c Eye-tracking system

The eye-tracking data was collected using a SmartEye Pro system, which consisted of three eye-tracking cockpit mounted cameras and two infrared flashers. This standalone system consisted of a computer with the eye-tracking setup software, where the collected data was stored. Before the start of this experiment, various camera positions were tested. Because the simulator is shared with other researchers and because changing and calibrating different cameras' locations is labour-intensive, the choice was made to place the cameras among the FO's screen. Placing two cameras above the screen ensured a high accuracy of out-the-window eye fixations as well as high accuracy on the participant's display. The set-up can be seen in **Figure 3.6**.

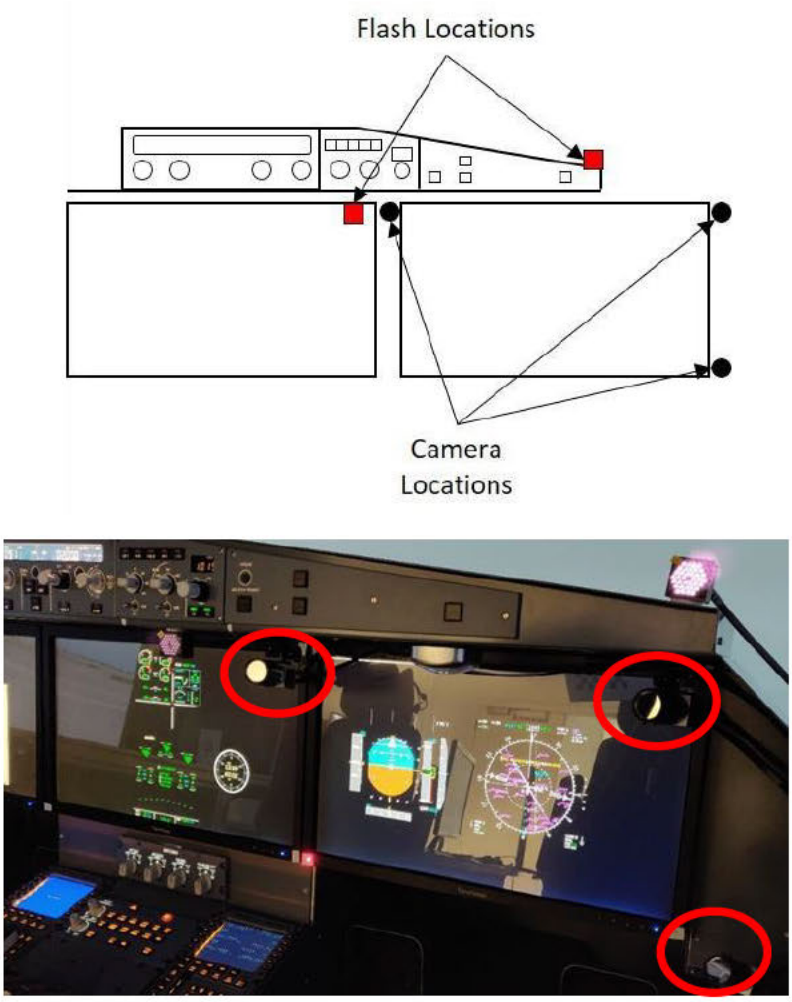

Figure 3.6 SmartEye eye-tracking system set-up

3.2.3.d BIOPAC data acquisition

The physiological data was acquired using a BIOPAC MP36 Data Acquisition Unit as can be seen in **Figure 3.7**. The metrics recorded during this experiment were: heartrate, heartrate variability, and electrodermal activity (EDA). The data was acquired with a frequency bandwidth between 0.5 Hz and 3.5 Hz with a band-stop filter. Heartrate and heartrate variability were measured using three nodes; two of these three nodes were placed on the participants' ankles, and the third was placed on their neck, as suggested in the BIOPAC guidelines (BIOPAC Systems Inc., 2015). This set-up is used to minimise interference by hand movement. During briefing, all participants were informed that they would not be required to operate the rudder and could therefore hold their feet still. The EDA nodes were attached to the fingers of the participants' left hands, whose movement was minimal during the experiment. The nodes were attached to the middle and ring finger, so that the autopilot could still be operated with the index finger and thumb, as suggested by the accompanying BIOPAC guidelines (BIOPAC Systems Inc., 2015). An example of this set-up can be seen in **Figure 3.8**.

Number of Channels	4 channels
A/D Sampling resolution	24-bit
Gain ranges	5x to 50,000x (13 steps)
Input Voltage Range	Adjustable from ± 200 µV to ± 2 V
Hardware filters	Low pass – 20 KHz (MP36); High pass – DC, 0.05 Hz, 0.5 Hz, 5 Hz
Sample rate	100,000 samples/sec each channel

Figure 3.7 BIOPAC MP36 Data Acquisition Unit and details

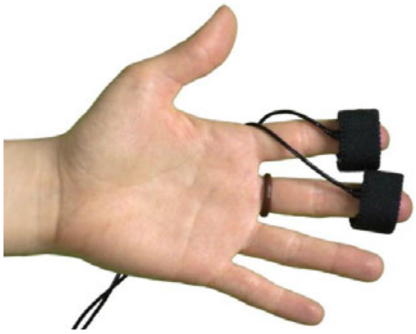

Figure 3.8 Example of EDA nodes applied to index and middle fingers, adapted from BIOPAC (2021)

3.2.4 Audio recordings

For communication between pilots and ATC simulation, a PA 400T Intercom unit was used. During the experiment, both pilots wore David Clark H10 Aviation headsets; the researcher wore a similar headset to mimic Air Traffic Control commands. A Philips DVT1100 audio recorder was attached to the intercom and recorded all communication. Before the start of the experiment, the researcher counted down from three in order to align the audio with the other data acquisition systems. An example of this equipment can be seen in **Figure 3.9**.

Figure 3.9 *Left:* PA400t intercom; *Right:* David Clark H10 aviation headset

3.2.5 Software materials

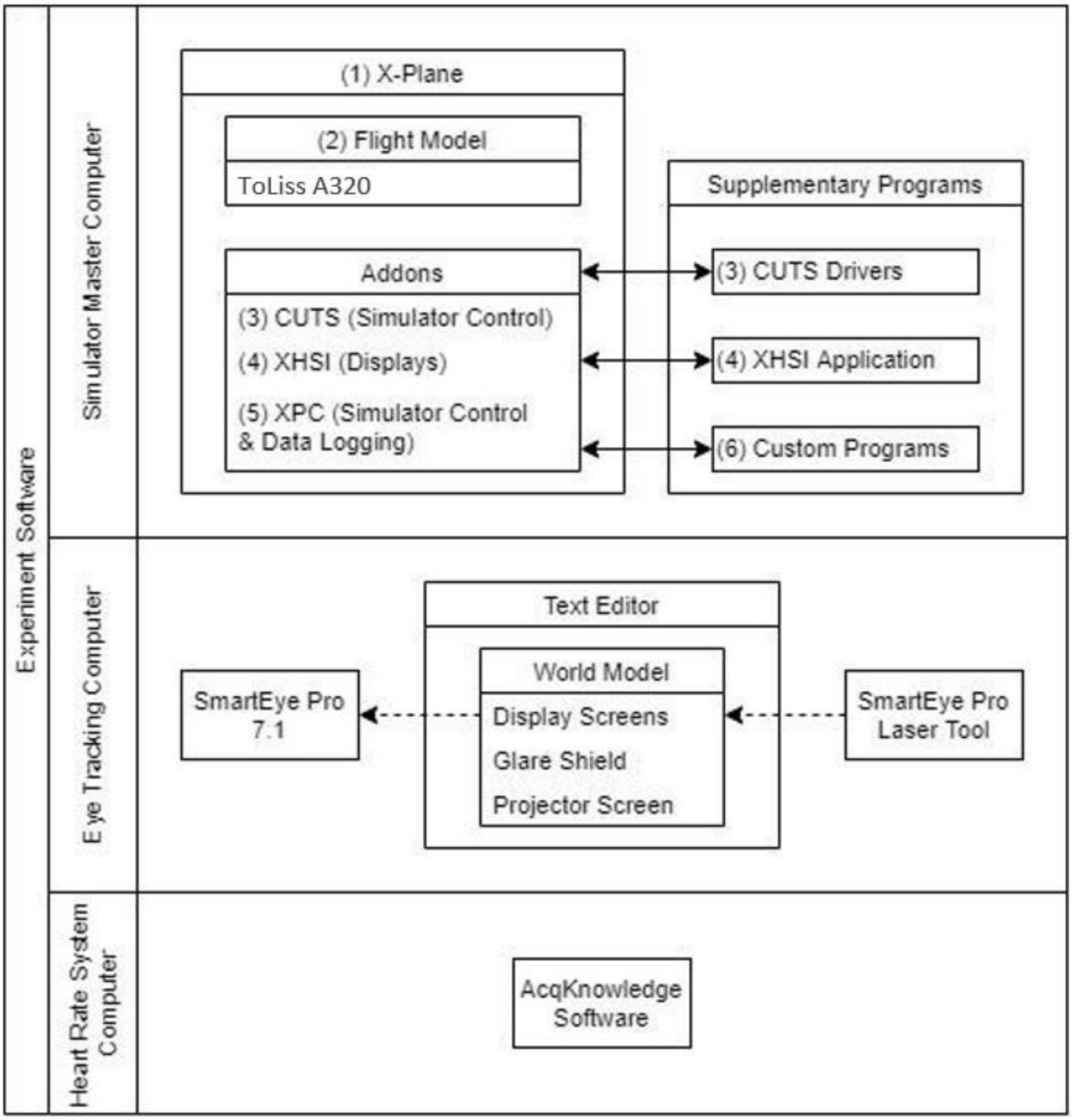

The software on which Coventry University's human-in-the-loop simulator runs consists of several components:

- Liminar Research X-plane version 10.5
- X-plane flight model of a Toliss A320-200 used for Airbus Flight Control Laws and systems
- Custom-made programme for data storage and scenario setting (XPC)
- Coventry University Transport Simulator (CUTS) drivers and operating software

- Stirling Dynamics plug-in for connection between X-plane and the sidesticks

Open-source plug-in for Airbus-style EICAS screen, primary flight display and navigation display (**Figure 3.10**)

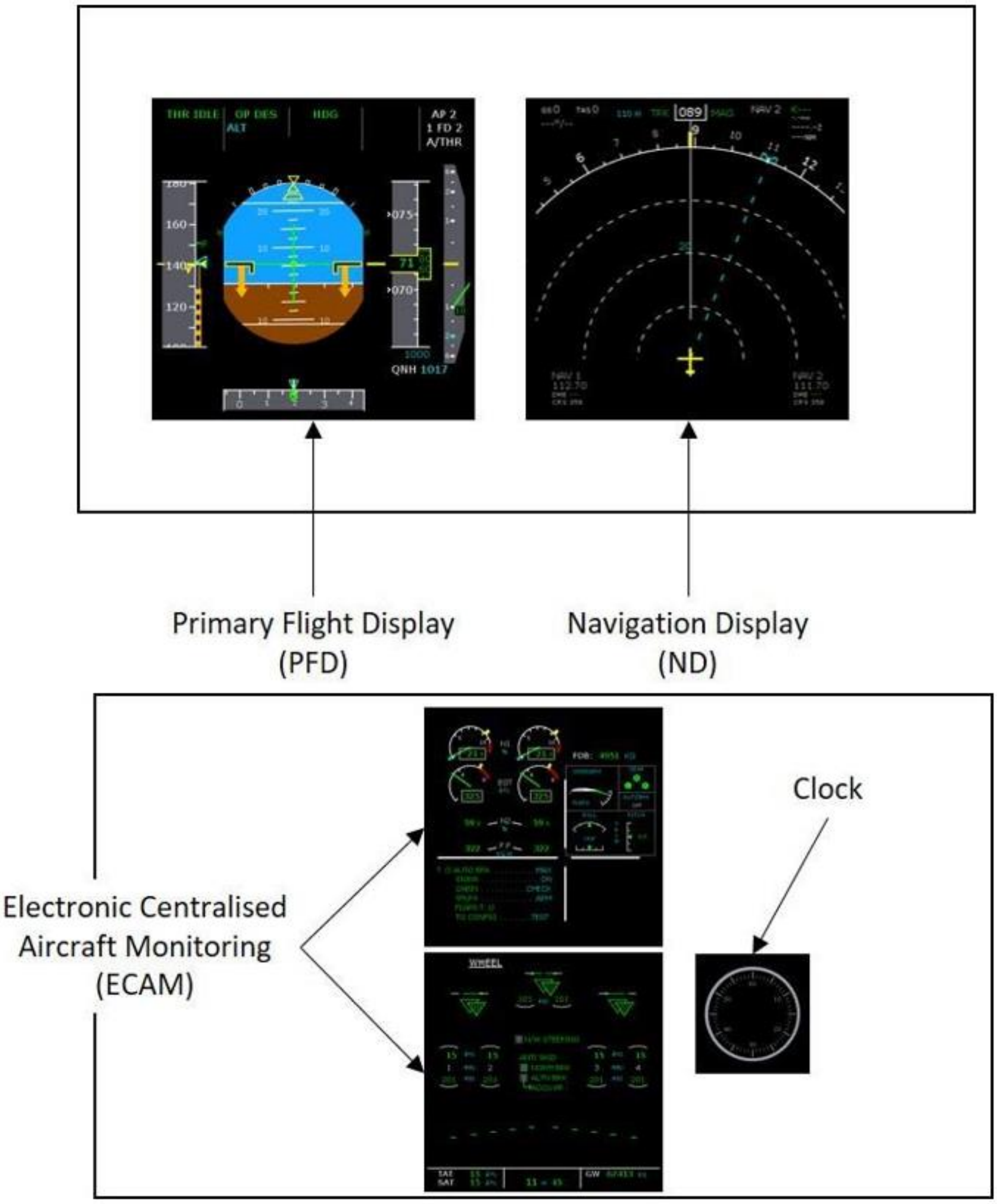

Figure 3.10 Primary flight display, navigation display and ECAM display used in simulator

3.2.5.a Eye-tracking software

The SmartEye eye-tracking software required extensive set-up. In order to accurately monitor eye-tracking fixations, each individual tracked object needed to be defined in the software. The software works based on a world model coordination system. The dimensions of each real-world object and its relative three-coordinate distance from each camera needed to be accurately programmed. By doing so, the eye-tracking system automatically tracked and linked eye fixations to real-world objects. The objects programmed in this coordinate can be seen in **Figure 3.11** and consisted of the following:

- Primary flight display (on FO's screen)
- Navigation display (on FO's screen)
- ECAM screen (central screen)
- Outside view far left
- Outside view middle left
- Outside view middle right
- Outside view far right
- Camera positions
- Camera calibration points

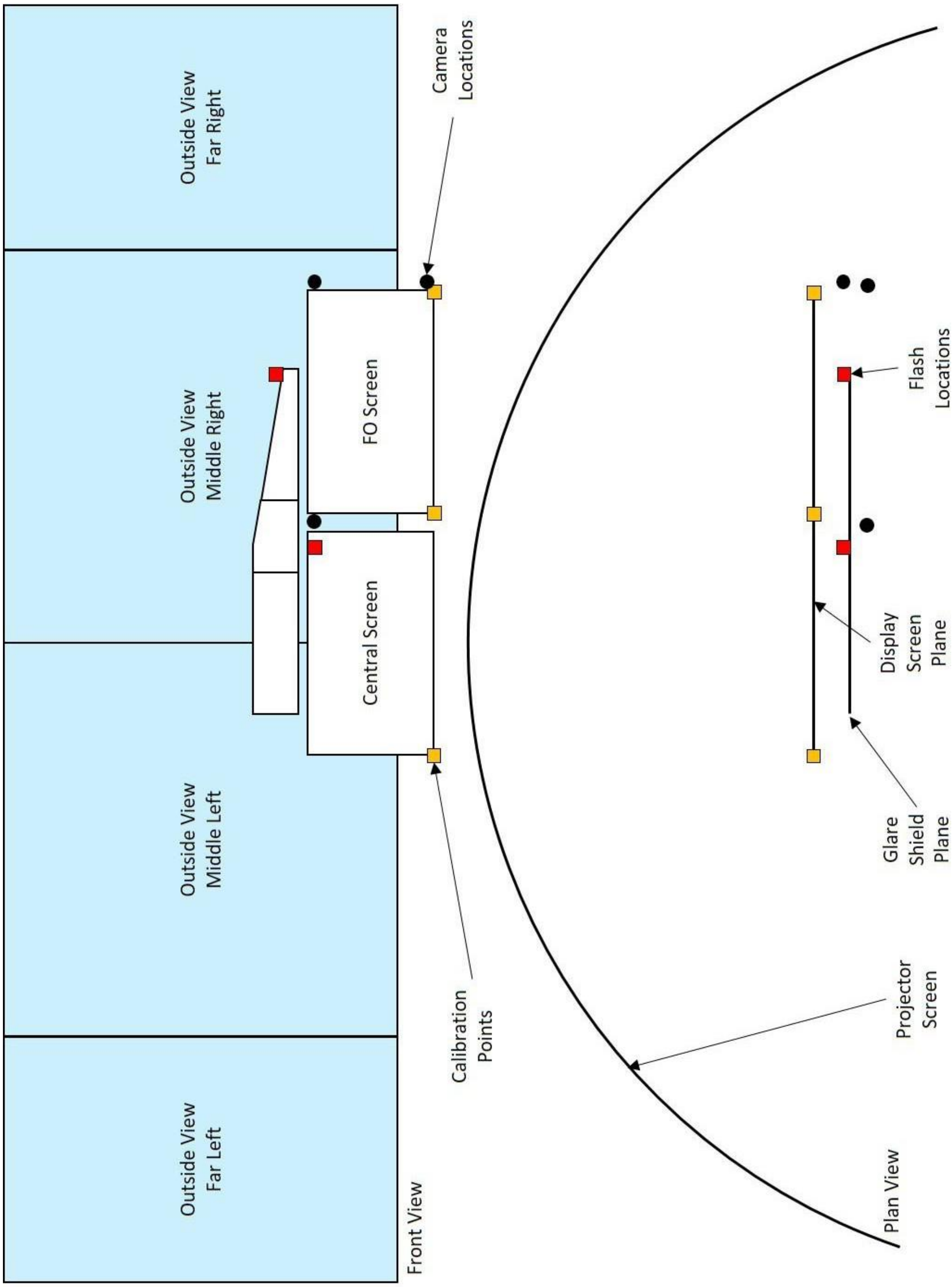

Figure 3.11 Schematic overview of objects programmed in the eye-tracking world coordinate system

3.2.5.b Overall quality of the eye-tracking data

In order to verify the quality of the eye-tracking data, a simplified analysis method is used to exclude unreliable eye-tracking data. The SmartEye system used to capture the eye-tracking data includes a quality metric for each fixation. This quality number per fixation ranges from 0 to 1, where which 1 represents the highest-quality fixation. The quality metric is calculated based on quality of gaze direction, gaze origin, head position quality, eye position, and whether the fixation occurred at a pre-defined intersection (area of interest). In order to assign a quality number to each simulation scenario, a mean quality number per scenario is used. This metric is devised by excluding all the zero points (i.e. fixations that could not be tracked), and by calculating a mean quality number per flight scenario. The formula used is:

$$Eye\ Tracking\ quality\ per\ scenario\ =\ 1-\frac{zero\ point\ fixations}{total\ eye\ tracking\ fixations}$$

Equation 3.2 Eye-tracking quality calculation

A histogram plot of all scenarios categorised by quality can be seen in **Graph 3.1**. Of the 120 flown scenarios, 55% have a quality of 90% or higher. The threshold for a reliable data point is set to an overall quality number of 75% or higher; all scenarios for which the overall quality was less than 75% are discarded. This yielded 18 scenarios that would not be taken into account whilst analysing the results. Of these 18 scenarios, four were approach scenarios, whereas the other 14 were take-off scenarios. The take-off scenarios' notably lower eye-tracking quality may potentially be attributable to the greater number of physical actions be undertaken during the scenario. Actions such as raising the landing gear, as well as many autopilot inputs, required the participant to bend forward, thus diminishing eye-tracking quality. The 102 scenarios used in the eye-tracking data analysis have a combined mean quality number of 91.3%.

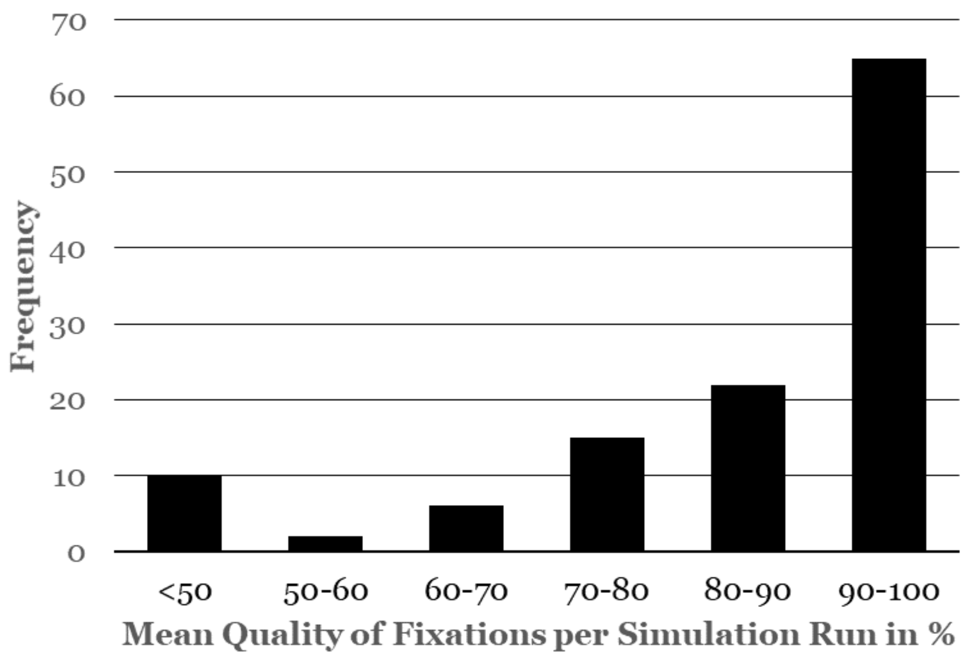

Graph 3.1 Mean quality of eye-tracking data per simulation run

3.2.5.c BIOPAC software

To acquire the physiological data, standard BIOPAC Student Lab software is used; this is a free data acquisition software from BIOPAC (2019). The configurations were during the experiment were as follows: Heartrate and EDA data were captured with a frequency of 1000 Hz. Both parameters were filtered using a band-stop filter. These configurations were pre-set before each experiment run, and are in line with the guidance provided by BIOPAC industries (BIOPAC, 2021). BIOPAC Acqknowledge software is used to analyse EDA and heart rate measures.

3.2.5.d Stirling Dynamics active sidestick software

The active sidesticks from Stirling Dynamics have a separate configuration programme whereby the active sticks and X-plane are linked by a separate connectivity programme, although it has no influence on the experiment. The force feel configuration on the active sidesticks is based on the Airbus force feel on the passive sidestick. The same amount of force feedback is provided, albeit on a large range of stick deflection. The Airbus A320 sidesticks deflect only up to 13 degrees, whereas the Stirling Dynamics sidesticks have a maximum deflection of 20 degrees.

Therefore, the maximum stick deflection of the active sidesticks was limited to 15 degrees with the same 10 lbs force as the Airbus Passive sidestick. The 2-degree difference in maximum stick deflection between the two different types of flight control inceptors is not considered noticeable by the participants.

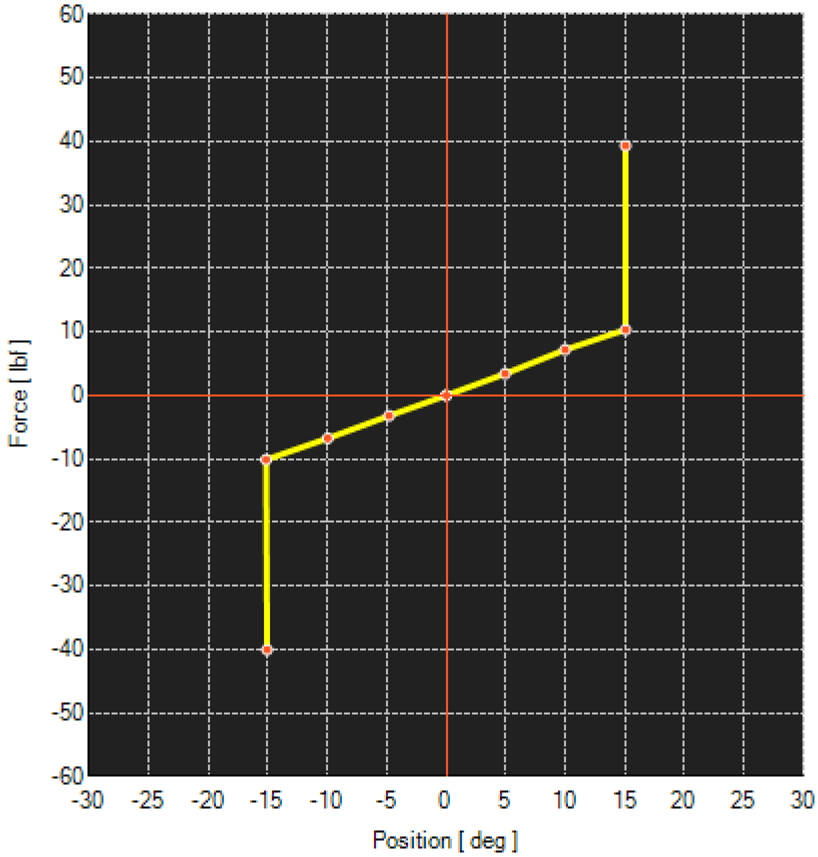

Figure 3.12 Programmed force feedback per degree of stick deflection active sidesticks

3.2.6 Scenario design

The study consisted of a total of six flown scenarios; three in a passive sidestick configuration, and three in an active sidestick configuration. During these scenarios, the participant is tasked with radio communications and monitoring the flight according to their company's standard operating procedures. The participants acted as PM. The flight scenarios were manually flown by members of the research staff, a former Boeing 777 captain and a retired training captain on the Airbus A320. These persons acted as captain and PF for all six scenarios. Each scenario lasted approximately 6 minutes and after each scenario, three questionnaires were completed by the participant. Halfway through, the participants received a 15-

minute break during which the flight control systems were swapped. The sequence of the scenarios was semi-randomised. However, all scenarios in the same flight control configuration were consecutive and were changed halfway through. Half of the participants started with the active sticks, and the other half started with the passive sidesticks. There were four different type of scenarios (normal take-off scenarios, normal landing scenarios, tailstrike scenarios, and hard landing scenarios), all of which took place on Amsterdam Schiphol's Runway 27. The normal take-off and tailstrike scenarios are discussed in Chapter 6. The normal landing and hard landing scenarios used for this experiment are discussed below.

3.2.6.a Normal approach scenario

The normal approach scenario of Amsterdam Schiphol's Runway 27 is simulated. The participant is briefed on the aircraft position by the use of the Jeppesen Airport Approach Chart for Runway 27. The aircraft is placed on a 10 nm approach with a 30-degree heading difference relative to the runway, as can be seen in **Figure 3.13**. The aircraft is flying a manual instrument landing approach. During the approach, the PF's task was to intercept the ILS and manually fly the approach and landing. At the start of the experiment, the aircraft is configured according to **Table 3.4** and the weather is set according to **Table 3.5**.

This item has been removed due to third party copyright. The unabridged version of the thesis can be viewed at the Lanchester library, Coventry University

Figure 3.13 Approach scenario Runway 27 at Schiphol Airport

Scenario	*Approach*
Location	Amsterdam Schiphol RWY 27
Position (Lat/Long)	52.36 Lat / 5.06 Long
Heading (degree)	240
Altitude (feet)	2000
Landing Gear Position	Down and Locked
Flap Setting	3
Aircraft Weight (in tonnes kg)	56
Airspeed (in Kts)	160
Autopilot	Off
Autothrottle	Off

Table 3.4 Aircraft configuration in approach scenario

Scenario	*Approach*
Time of day	13:00 GMT
Wind Direction (in degrees)	260
Wind Speed (in kts)	15
Wind Gusts (in kts)	2
Turbulence setting (X-plane configuration)	0.05
Cloud coverage	Overcast at 1000 feet,
Runway Visible Range	10+ kilometres

Table 3.5 Weather conditions in approach scenarios

3.2.6.b Normal take-off scenario

The normal take-off scenario is simulated on Amsterdam Schiphol's Runway 27. Each participant is briefed on the aircraft position by the use of the Jeppesen Airport Departure Chart for Runway 27. The Aircraft is placed on the runway threshold of Runway 27 and configured according to **Table 3.6** and weather conditions configured to **Table 3.7**. Once the participant and the PF were ready, they were given an ATC wind callout and take-off approval. The participants were asked to monitor in accordance with their company regulations. The participants were tasked with radio communications with the simulated ATC. After take-off, the participants received three ATC commands containing altitude and heading directions. There were three different headings, either a left climb-out with followed by a left turn, a right climb-out followed by a left turn and finally a right climb-out with a right turn. In order to avoid repetitive simulations the decision is made to adjust each take-off with different headings and different altitudes. The three different planned climb-out routes can be seen in **Figure 3.14**.

Figure 3.14 Expected flight paths during take-off scenarios

Scenario	*Take-off*
Location	Amsterdam Schiphol RWY 27 Threshold
Position (Lat/Long)	52.31 Lat / 4.79 Long
Heading (degree)	267
Altitude (feet)	0
Landing Gear Position	Down and Locked
Flap Setting	1
Aircraft Weight (in tonnes kg)	56
Airspeed (in Kts)	0
Vrotate (in Kts)	122
V1 (in Kts)	122

Table 3.6 Aircraft configuration in take-off and tailstrike scenarios

Scenario	*Approach*
Time of day	13:00 GMT
Wind Direction (in degrees)	260
Wind Speed (in kts)	15
Wind Gusts (in kts)	2
Turbulence setting (X-plane configuration)	0.05
Cloud coverage	Overcast at 1000 feet,
Runway Visible Range	10+ kilometres

Table 3.7 Weather conditions in take-off scenarios

3.2.6.c Hard landing scenario

The hard landing scenarios followed the exact same configurations as in the normal approach scenario discussed above. The difference in this scenario is that the PF does not initiate the flare. Normally, at an altitude of roughly 50 ft the pilot would start pitching the nose up, starting the pre-flare. At 30 ft, the throttles should be set to idle and the full flare should be commenced. However, in this scenario, the PF stops controlling the aircraft at the altitude of 50 ft over the pitch axis. No flare is initiated, nor is there any verbal cue from the PF. In this scenario, the airplane hits the ground with a vertical speed of roughly 900 ft per minute. If the PM does not intervene, a crash landing will result.

3.2.6.d Tailstrike scenario

The aim of this experiment was to see whether the PM could intervene correctly during a deliberately initiated wrong take-off rotation with two different flight control configurations: uncoupled flight control inceptors (used by Airbus) and coupled flight control inceptors. In order to do so, the PF excessively over-rotates during the take-off rotation, forcing the tail of the aircraft to touch the ground. During normal take-offs, a maximum of 75% aft stick deflection is used. During the tailstrike take-off scenarios, the PF applies a 100% aft stick deflection for a duration of 10 seconds, causing the aircraft to reach an approximate angular velocity of 9 degrees per second. The aft stick deflection is continued during the climb-out until the Airbus Flight Envelope Protection system kicks in. This Alpha Floor Protection prevents the aircraft from stalling by limiting the angle of attack and providing full take-off/go-around settings. Alpha Floor is accompanied with an aural warning, an EICAS notification, and the sound of the engines spooling up.

3.2.6.e Excessive rotation on take-off

During the tailstrike scenarios, the PF begins deliberately over-rotating once the Vr call is made, applying a 100% aft stick deflection for a period of 10 seconds. Normal operating procedure during take-off rotation is to aim for a maximum rotation speed of 3 degrees per second (Airbus SE, 2017). In the trial scenarios, it has become apparent that, on average, a tailstrike occurs when the control inceptor is deflected with a 100% aft input for a duration of 2.42 seconds. As discussed in the methodology, this is too short a period for a pilot to accurately intervene. In order to give the PM sufficient opportunity to intervene, the Vr (the indicated airspeed at which the PF should commence the take-off rotation) is lowered with 20 kts. By lowering the Vr, the PF can apply a 100% aft stick deflection for a longer time; the trials showed that a 100% stick deflection can be applied for 3.4 seconds, which will give the PM more time to detect, decide and act on the incorrect rotation. A tailstrike on an Airbus A320 occurs at 11.7 degrees of pitch attitude with the main landing gear compressed. The PF will implement an aft stick deflection of 100% within a timeframe of 1 second. The trial scenarios showed that this is an easy practice for the PF. This make sure that there is constancy among all tailstrike scenarios. **Graph 3.2** shows the stick deflection in percentage of maximum stick deflection over time during the scenario trials.

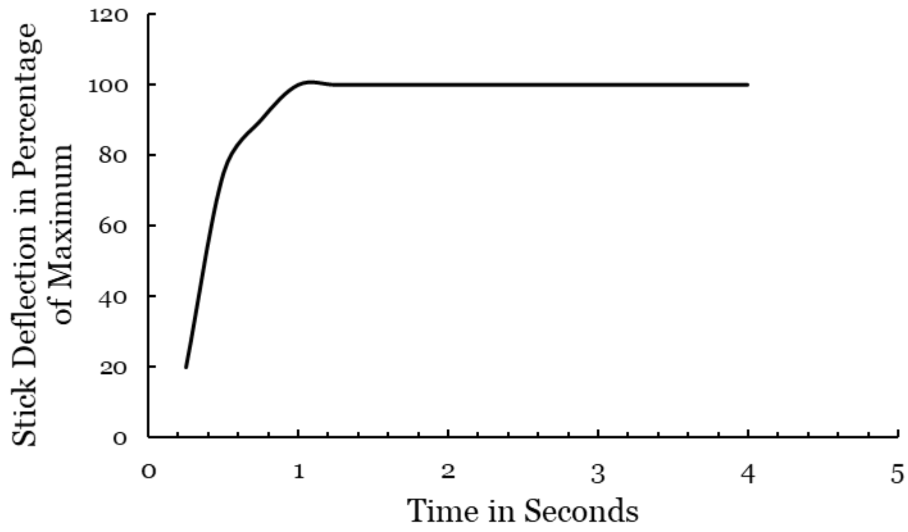

Graph 3.2 Mean stick deflection over time during tailstrike scenario trials

The lower Vr speed and the reaction time of the elevator deflection result in the change in movement of the pitch attitude; the change in pitch attitude over time can be seen in **Graph 3.3**. As previously mentioned, the tailstrike occurs at a pitch attitude of 11.7 degrees; this is clearly visible in the data as well. However, the pitch attitude continues to increase over time because the airplane is still rotating; due to the relatively high angular momentum, the airplane rotates over the tail section, lifting up the main landing gear. This explains the dip in the graph seen at approximately 3.5 seconds.

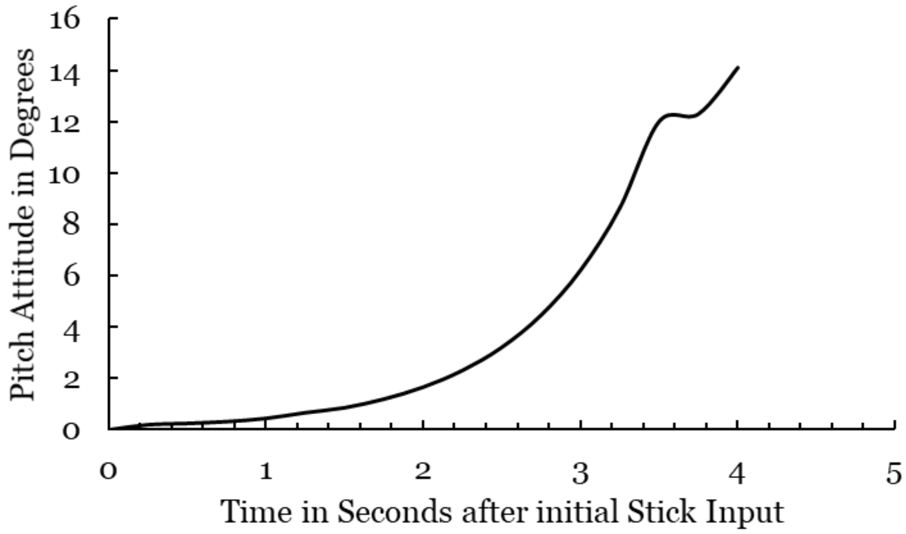

Graph 3.3 Mean pitch attitude in degrees with main landing gear compressed during tailstrike scenario trials

According to the Airbus Flight Crew Operating Manual, the overall aim is to achieve a maximum of 3 degrees per second rotation rate (Airbus SE, 2017). This is achieved by deflecting the stick to a maximum of 75% of the aft. Once the desired pitch attitude is reached, the PF returns the control inceptor to the neutral position. By lowering the Vr, the maximum rotation rate of 3 degrees per second is initially lower. Normally, with a stick deflection of 75%, the angular speed of 3 degrees per second is reached in 1.8 seconds. In this experiment, this angular velocity is reached in 2.35 seconds. However, due to the 100% aft stick deflection, this velocity is increasing sharply, reaching 9 degrees per second immediately before the tailstrike as can be seen in **Graph 3.4**. By keeping an aft stick applied and thereby increasing the angular velocity, it will become more evident to the PM that the rotation is excessive, which compensates for the lack of vestibular information due to the fixed-base simulator.

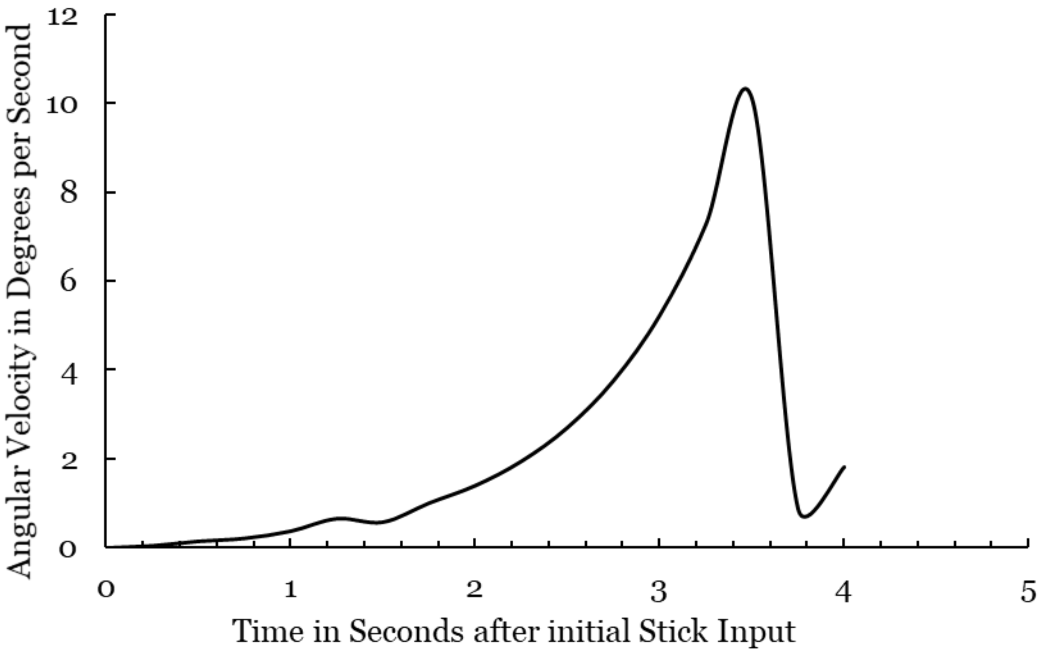

Graph 3.4 Mean pitch rate in degrees per second during the tailstrike trials

3.2.6.f Scenario order

The entire study consisted of six scenarios. Due to a maximum time restraint of 1.5 hours per participant, the normal scenarios were split up. This means that each participant would not simulate a normal approach and a normal take-off on each sidestick configuration. Uneven numbers of participants would fly the normal take-off scenario uncoupled and the normal approach scenarios in coupled configuration. Each participant flew both the hard landing and tailstrike scenarios in both configurations. An overview of the scenario order can be seen in **Table 3.8.**

Scenario Order per Participant	*Normal Take-off*	*Normal Take-off*	*Tailstrike Take-off*	*Tailstrike Take-off*	*Normal Landing*	*Normal Landing*	*Hard Landing*	*Hard Landing*
Participant Number	Uncoupled	Coupled	Uncoupled	Coupled	Uncoupled	Coupled	Uncoupled	Coupled
1	1	X	2	5	X	4	3	6
2	X	1	5	2	4	X	6	3
3	X	4	2	5	1	X	3	6
4	4	X	6	2	X	1	5	3
5	1	X	3	6	X	4	2	5
6	X	1	6	3	4	X	5	2
7	X	4	3	5	1	X	2	6
8	4	X	6	3	X	1	5	2
9	1	X	2	5	X	4	3	6
10	X	1	5	2	4	X	6	3
11	X	4	2	5	1	X	3	6
12	4	X	6	2	X	1	5	3
13	1	X	3	6	X	4	2	5
14	X	1	6	3	4	X	5	2
15	X	4	3	5	1	X	2	6
16	4	X	6	3	X	1	5	2
17	1	X	2	5	X	4	3	6
18	X	1	5	2	4	X	6	3
19	X	4	2	5	1	X	3	6
20	4	X	6	2	X	1	5	3

Table 3.8 Experiment scenario order per participant

3.2.7 Procedure

When a participant entered the simulation room, they were provided with a

Participant Information Sheet (Appendix I), which they signed to confirm that they understood the information as well as the goal and aims of this experiment. After that, the participant was asked to complete an Informed Consent Agreement (Appendix II). By signing this form, the participant consented to the recording of different data types for academic uses. Once the forms were signed, the physiological base rate of each participant was recorded: the participant was connected to the heart rate and EDA nodes and was asked to sit still for 2 minutes. This baseline is later used for analyses purposes. After obtaining the physiological baseline, the eye-tracking calibration process was initiated. During this process, the camera's position was calibrated based on the participant's physical dimensions. Once the physiological data calibration had been completed, the participant was given two practice runs on the simulator: a take-off followed by a 5-minute free flight, and a normal approach scenario towards Runway 27. During these familiarisation flights, all the data acquisitions were tested and adjusted if needed. All participants were briefed before the start of each scenario. Sufficient time was given before the start of each scenario to allow participants to fully familiarise themselves with the current configuration of the aircraft. Every briefing explained that pilots should act according to their current companies' standard operating procedures and intervene if they deemed it necessary.

3.2.8 Independent measures

The experiments had only one independent variable: the configuration of the flight control stick. Half of the scenarios were flown with a passive sidestick configuration (providing no feedback), and the other half were flown with an active sidestick configuration providing flight control inputs. This variable was a within-participant variable.

3.2.9 Dependent measures

A large volume of data was collected during the experiment, and this section describes each measured parameter. An overview of the types of data gathered can be found in **Table 3.9**. The dependent variable can be divided into objective/subjective measures and qualitative/quantitative measures.

Mode	*Type of data*		*No. Parameters*
Audio	Objective	Quantitative	***1***
Video	Objective	Quantitative	***2***
NASA Task Load Index (TLX)	Subjective	Qualitative	***7***
Situation Awareness Rating Technique (SART)	Subjective	Quantitative	***3***
Startle & Surprise Questionnaire	Subjective	Qualitative	***4***
Simulator Data	Objective	Quantitative	***44***
Eye-Tracking Data	Objective	Quantitative	***33***
Electrodermal Activity	Objective	Quantitative	***1***
Heart Rate	Objective	Quantitative	***2***

Table 3.9 Overview of parameters per measurement

3.2.10 Subjective measurements

3.2.10.a NASA Task Load Index

After each scenario, the participant was asked to complete three questionnaires. The first was the weighted NASA Task Load Index, or TLX (Hart et al., 1988), which is administered via a tablet using the official NASA TLX application. It measures subjective workload over six subsections: mental demand, physical demand, temporal demand, performance, effort and frustration. The first part of the TLX involves assigning the weighting to each subsection. This was done by presenting two subsections at the same time and asking the participant to rate which subsection was more relevant to the scenario; the number of times which subsection is chosen is the weighted score. The second part of the TLX is the subscale, a 100-point scale by which each subsection is rated. When combined, these two parts form a calculated TLX score. Thus, the TLX provides 7 parameters: one total TLX value and six TLX subsections scores.

3.2.10.b Situation Awareness Rating Technique

The Situation Awareness Rating Technique (SART) (Endsley, 1998) is a post-trial rating technique that uses nine dimensions to measure the participants' level of SA divided over three subdomains: attentional demand, which is the demand of attentional resources (complexity, variability and instability of the situation); attentional supply, which is the supply of attentional resources (division of attention, arousal, concentration and spare mental capacity); and understanding of the situation (information quantity and familiarity). Using paper and a pencil, the participant rates each dimension on a 7-point scale. The ratings are combined to calculate the measure of SA according to Equation 3.3. During the first trial sessions, it became clear that the participants had difficulties understanding the ratings. In response, the SART administered in this experiment has been elaborated with the meaning of the scale. An example of the adjusted SART can be found in Appendix III.

$$SA = Understanding - (Attentional\ Demand - Attentional\ Supply)$$

Equation 3.3 SART score calculation

3.2.10.c Startle and surprise questionnaire

After each scenario, a startle and surprise questionnaire was administered via a tablet. The questionnaire items assessed the participants' perceived surprise and startle, as well as how successful they perceived their responses in each scenario to have been. All questions are answered with a Likert-scale response. In recent startle and surprise research reports (EASA, 2018), Landman's (2019) self-assessment questionnaires are used to indicate a level of perceived startle and surprise. The questionnaires used in beforementioned startle and surprise research all use Likert-scale questions to indicate perceived effects. The response to each question is scored on a 10-point Likert scale. In both coupled and uncoupled flight control configurations, the following questions have been administered:

Question 1: Were you surprised by the events in the previous scenario?

	1	2	3	4	5	6	7	8	9	10	
Not at all	☐	☐	☐	☐	☐	☐	☐	☐	☐	☐	Very much

Question 2: Were you startled by the events in the previous scenario?

	1	2	3	4	5	6	7	8	9	10	
Not at all	☐	☐	☐	☐	☐	☐	☐	☐	☐	☐	Very much

Question 3: Did you immediately know how to respond when an event occurred?

	1	2	3	4	5	6	7	8	9	10	
Not at all	☐	☐	☐	☐	☐	☐	☐	☐	☐	☐	Very much

Question 4: Was or were your action(s) successful?

	1	2	3	4	5	6	7	8	9	10	
Not at all	☐	☐	☐	☐	☐	☐	☐	☐	☐	☐	Very much

Participants could read the definitions of the words 'surprise' and 'startle' by clicking them, which accessed hyperlinks with the following definitions:

- *Surprise* is defined as an emotional state which is the result of a mismatch between expected and perceived information.
- *Startle* is defined as a brief physiological response to a threatening stimulus.

3.2.11 Objective measurements

3.2.11.a Simulator data

The main objective data obtained is the output of the flight simulator, which records 44 flight parameters with a frequency of 50 Hz. A list of all recorded parameters is shown in Appendix IV. The output of the simulator is a text file containing all parameters with a timestamp, which is used to align the data with other metrics.

3.2.11.b Audio and video recordings

All experiments were recorded using four wall-mounted cameras, which were fixed so their position could not be altered. The timestamp on the top of each video is the leading timestamp on which all other analyses are based. An example of the four different camera angles is displayed in **Figure 3.15**. The video recordings were used to analyse precise timestamps and flight control input in combination with the audio recordings. The audio recordings were also used to determine the time at which the pilot verbally intervened.

Figure 3.15 Example of wall-mounted video camera recordings of all four angles

3.2.11.c Heart rate

Heart rate data metrics were chosen based on the guidance of the European Society of Cardiology (ESC) and the North American Society of Pacing and Electrophysiology (NASPE) (ESC & NASPE, 1996) and Shaffer and Ginsberg (2017). Due to the length of the scenarios being 5 minutes, only time domain heart rate measurements are chosen. The measurements used are root mean square of successive differences (RMSSD) between normal heartbeats and the percentage of adjacent NN intervals that differ from each other by more than 50 ms (pNN50). All ECGs were manually checked for artefacts using the Acqknowledge software. According to several studies (Esco & Flatt, 2014; Jelinek et al., 1996; Shaffer & Ginsberg, 2017) the use of RMSSD and pNN50 is reliable for epoch lengths of 60 seconds and longer. After using Acqknowledge's pre-set function to detect and classify heartbeats, each ECG was manually checked for correct detection of the QRS complex and, if needed, manually adjusted. An example of an ECG output with the detected QRS complexes can be seen in **Figure 3.16**. Once all QRS complexes had been determined, the RMSSD, SDSS and p50NN could be automatically extracted using Acqknowledge's 'Single Epoch HRV – Statistical' function.

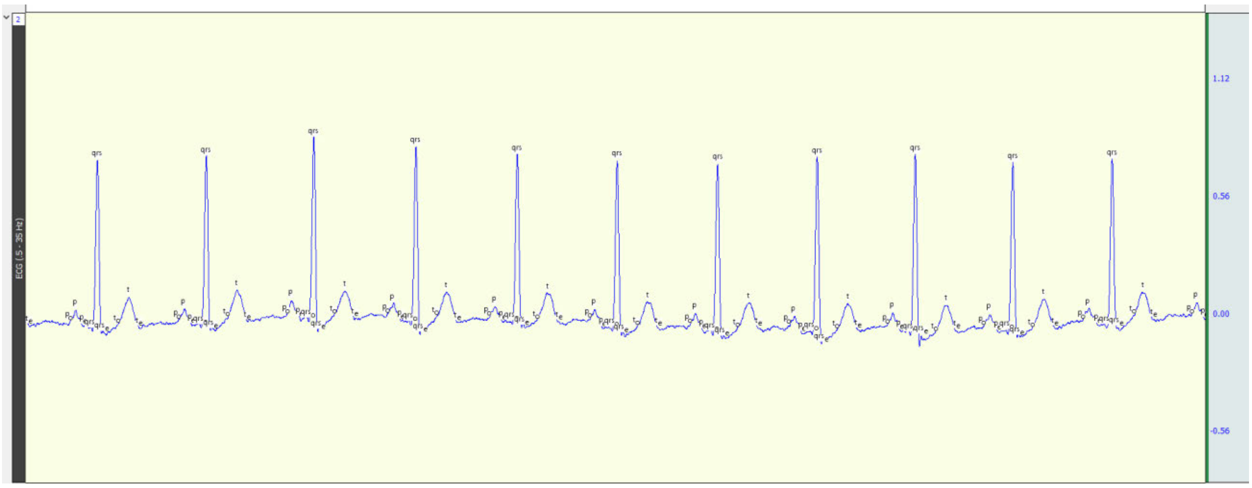

Figure 3.16 Example of 'Detect and Classify Heartbeat' function in Acqknowledge

3.2.11.d Electrodermal activity

As covered in section 2.1.4.e, SCR amplitude is a well-established method for comparing emotional arousal between different stimuli. The EDA data was analysed using the pre-set SCR detection function of BIOPAC's Acqknowledge software. The waveform onset value was set to 10% increase in microsiemens in order to qualify as SCR. ER-SCR is quantified as an SCR between 1 and 5 seconds after the given stimulus. The Acqknowledge software has a built-in function to detect ER-SCR and marks them with a flag; an example of an ER-SCR can be seen in **Figure 3.17**. For the hard landing scenarios, the event was any type of intervention, either verbal or physical. In case no intervention took place, the oncoming hard landing would be quantified as a stimulus, set to 2 seconds before touchdown.

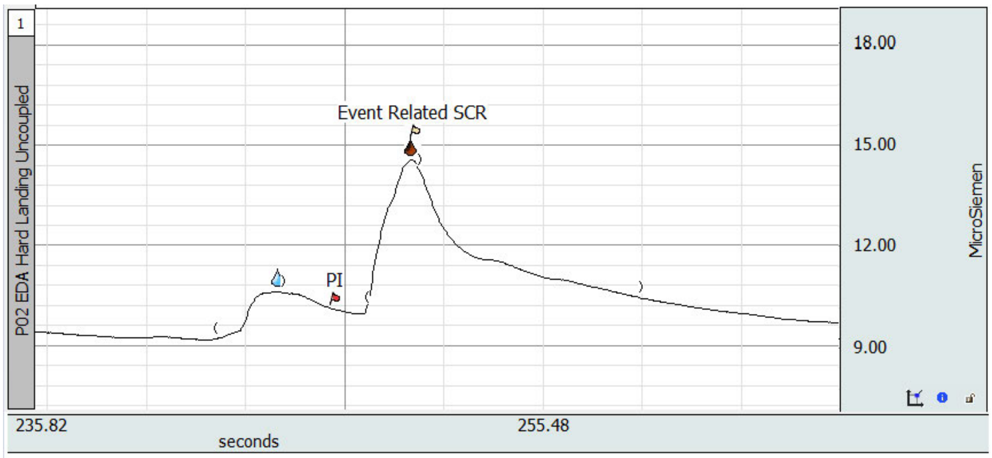

Figure 3.17 Example of Acqknowledge's event-related skin conductance response

3.2.12 Statistical methods used for data analysis

3.2.12.a Paired-samples *t*-test

The paired-samples *t*-test is used to compare means within one group of people. Data is collected from each participant twice, under two different conditions. A paired-sample *t*-test indicates whether there is a statistically significant difference between the mean scores per participant. The paired-samples *t*-test is a parametric test and is valid only if the data is normally distributed. The effect size of a paired-samples *t*-test is calculated according to Eta squared following **Equation 3.4**. The guidelines for interpretating Eta squared are: 0.01=small effect, .06=moderate effect, .14=large effect (Cohen, 1988)

$$Eta\ squared = \frac{{t_{value\ paired\ sampled}}^2}{{t_{value\ paired\ sampled}}^2 + (number\ of\ pairs - 1)}$$

Equation 3.4 Eta squared calculation for effect size

3.2.12.b Wilcoxon signed rank test

The Wilcoxon signed rank test is designed for the use of repeated measures, such as participants measured on two occasions. It is the non-parametric alternative to the paired-samples t-test. The outputs of the Wilcoxon test are a value, z, and a significance value (two-tailed). The effect size of the Wilcoxon signed rank test can be calculated according to **Equation 3.5**.

$$Effect\ size_{Wilcoxon} = \frac{z}{\sqrt{N}}$$

Equation 3.5 Effect size calculation Wilcoxon signed rank test (Cohen, 1988)

3.2.12.c Pearson product moment correlation

The Pearson product moment correlation coefficient, often denoted as r, is a statistical measure that quantifies the strength and direction of a linear relationship between two continuous variables. It is widely used for assessing the degree to which two variables are linearly related, but it is reliable only if the variables are normally distributed. The Pearson product moment correlation coefficient is susceptible to outliers and can provide misleading results if the data is not accounted for extreme values (Shaughnessy et al., 2000). According to Cohen (1988), the r value below 0.1 is considered a small effect size, r values of 0.3 are considered medium, and r values above 0.5 are considered large.

3.2.12.d Spearman rank correlation coefficient

The Spearman rank correlation coefficient, denoted as ρ (rho), is a non-parametric measure of statistical dependence between two variables. It assesses how well the relationship between two variables can be described using a monotonic function. Rather than dealing with the variables' actual values, Spearman's correlation works with the ranks of the values, calculating the correlation based on the difference between the ranks of corresponding values in the two variables. Spearman's correlation coefficient ranges from -1 to 1, where -1 indicates a perfect negative monotonic relationship, 1 indicates a perfect positive monotonic relationship, and 0 indicates the total absence of a monotonic relationship (A. Field, 2009; Pallant, 2013). According to Cohen (1988), the rho value below 0.1 is considered a small effect size, rho values of 0.3 are considered medium, and rho values above 0.5 are considered large.

3.2.12.e Multivariate analysis of variance

The above-described tests analyse variance to compare groups on a single variable. In this experiment, however, the data will be compared on a range of different characteristics. The multivariate analysis of variance (MANOVA) is an analysis of variance involving more than one dependent variable. MANOVA compares the groups' mean differences on a combination of dependent variables by creating a new summary dependent variable: a linear combination of each original dependent variable (Pallant, 2013). It then analyses variance using this combined dependent variable and tests whether there is a significant difference between the groups on this composite variable. Because the MANOVA test is sensitive to outliers, univariate and multivariate outliers should be excluded. The test for multivariate normality is performed by calculating the Mahalanobis distance, which refers to the distance of a particular case from the centroid of the remaining cases, where the centroid is the point created by the means of all the variables (Tabachnick & Fidell, 1996). Finally, before MANOVA can be conducted, the data should be tested for multicollinearity. If dependent variables are strongly correlated (more than .8), as can be the case when variables are a combination of other variables used in the MANOVA, they should not be included in the MANOVA (Pallant, 2013). The effect size of a MANOVA is calculated via a partial eta squared.

3.2.13 Ethical approval of experimental studies

The research methodology and experimental set-up described in this paragraph have been submitted to the Coventry University Ethics Commission and have been confirmed and approved under Project Reference Number P76095.

Chapter 4 Statistical Review of Hard Landing Accidents Related to Type of Flight Control

Between 2008 and 2018, the number of commercial aircraft equipped with passive sidesticks more than doubled (CAPA, 2018). However, a passive sidestick may limit the ability of the PM to perceive the flight control inputs by the PF, therefore affecting monitoring duties. This chapter compares accident statistics and reports for hard landings involving jet aircraft fitted with conventional coupled control inceptors and passive sidesticks to investigate if there is a measurable difference between the two aircraft types.

4.1 Background

From a human factors point of view, the missing coupling between the sidesticks creates some considerations within a multi-crew flight deck. It restricts a pilot monitoring from perceiving the flight control inputs from the other pilot. Within a multi-crew flight deck is the pilot flying (PF), who flies the aircraft, and pilot monitoring (PM), who actively monitors the flight. The Federal Aviation Administration (FAA) defines the PM's tasks as follows: 'Monitoring includes the process of observing and creating a mental model by seeking out available information to compare actual and expected aircraft state' (FAA, 2011). In some situations, effective monitoring can be the last line of defence to prevent accidents from happening. However, on a flight deck equipped with passive sidesticks, it is hard to predict an aircraft's state when the flight control inputs are not directly available for the PM. This study focuses on the effects of passive sidesticks on hard landing accidents within commercial jet aviation. The first passive sidestick in commercial aviation was introduced in 1987 by Airbus on the Airbus A320 (*Aviation Week*, 1987). Nearly 20 years passed before the passive sidestick was introduced into business jet aviation, where it debuted on the Dassault Falcon 7X in 2005. By then, Airbus had gained a significant share of the commercial jet aviation market: in 2007, 18% of the worldwide commercial jet aircraft in operation were passive sidestick aircraft – all built by Airbus. However, over the last ten years, many more manufacturers have been converting to a passive sidestick system. In 2017, three other manufacturers (besides Airbus) were building commercial jet aircraft with passive sidestick flight controls: Comac, with their C919 aircraft; Bombardier, with their C series; and Sukhoi, with their 100-Superjet. The total number of passive sidestick aircraft has increased from roughly 4,000 aircraft in 2008 to 9,130 in 2018 (CAPA, 2018). In 2018, passive sidestick aircraft accounted for 35% of all commercial jet aircraft worldwide in 2017, and this percentage only predicted to steadily increase: in 2019, 51.6% of all commercial jet aircraft on order were passive sidestick aircraft (CAPA, 2018).

4.2 Methodology

4.2.1 Experimental design

The experiment described in this chapter aims to compare the number of hard landing accidents by aircraft with passive sidestick flight controls with those by aircraft with coupled flight controls. The two aircraft types are compared by number of accidents in relation to their number of flight cycles. Additionally, the two aircraft types are compared in terms of several other relevant data aspects, as described in this section. The general methodology, general data acquisition and statistical data analyses tools for this study have been described in Chapter 3, section 3.1. A summary of the number of hard landing reports and number of flight cycles per aircraft type used for this study can be found in Table 4.1.

	Number of hard landings	*% of hard landings*	*Flight cycles in millions*	*% of flight cycles*	*Million flight cycles per hard landing*	*Hard landings per million flight cycles*
P-SS	19	47.5%	94.98	31.67%	4.99	0.2
Cpld	21	52.5%	204.87	68.33%	9.75	0.1
Total	40	100%	299.85	100%	7.49	0.13

Table 4.1 Number of hard landings and flight cycles flown in the period between 2009 and 2018 for passive sidestick aircraft (P-SS) and coupled flight control aircraft (Cpld)

4.2.2 Hard landing data acquisition

The accident reports used in this study contain different types of data that can be used to compare the flight control types. The specific data collected for such comparison is discussed in the following section. Because a statistical comparison is made via a 2 x 2 chi-square test for independence, a maximum of 20% of the cells can have a value less than five. For relevant data to be taken into account for this study, at least 50% of the reports must report the data. A justification for this methodology has been provided in Chapter 3, section 3.1. An overview of all accident reports can be found in Appendix V.

4.2.2.a Daytime or night-time flight conditions

A number of studies indicate that pilots are more likely to make errors during daytime operations than during night-time operations. In particular, de Mello et al. (2008) found that airline pilots are most likely to commit errors during early morning operations, because these tend to be long-haul flights that began the night before. De Mello further points out that, for the same reason, morning flights are also the most disruptive of pilots' sleep patterns. Similar results from Wiegmann and

Shappell (2001) show that the majority of airline accidents occur at minimum control speed (Vmc) in daytime conditions. The time of day and type of visual flight condition at the time of the accidents are noted in all hard landing reports.

4.2.2.b Pilot experience

Of the 40 accident reports, 38 mentioned the PF's accumulated hours on the specific aircraft type, which is a commonly used parameter to measure a pilot's experience on particular aircraft. Recent studies have found a positive correlation between a pilot's total hours of flight experience and hazardous attitude, and a negative correlation between total flight hours and safety performance (Gao & Wang, 2023; Gautam & Garg, 2021).

4.2.2.c Stabilised or unstable approaches

The current literature indicates that half of all hard landings in commercial jet aviation are the result of an unstable approach (IATA, 2016; Matthews et al., 2004). Every one of the 40 hard landing reports mentioned whether the approach was either stabilised or unstable. Thus, an accurate comparison between the number of stabilised or unstable approaches can be made in this study.

4.2.2.d Damage classification

Of the 40 hard landing accident reports, 39 classify the severity of the hard landings by a standard damage classification. The damage categories defined by ICAO can be seen in **Table 4.2** (ICAO, 2012). Because none of the hard landing reports mentioned minor damage, only the 'substantial' and 'destroyed' damage classifications have been used for comparison in this study.

This item has been removed due to third party copyright. The unabridged version of the thesis can be viewed at the Lanchester library, Coventry University

Table 4.2 Aircraft accident damage classification as stated by ICAO (ICAO, 2012)

4.2.2.e Parameters with overall insufficient reporting

In order to make an accurate comparison between the two flight control types, a minimum of 20 reports should mention the specific parameter being compared. Several parameters that were of interest, but that either received insufficient mentions or did not occur at least 20 times, are therefore not taken into account. These excluded parameters were: normal acceleration, true vertical speed, and pilot's total hours on jet aircraft. The number of hard landings that occurred with wide-body aircraft within the dataset was also insufficient to make an accurate comparison.

4.3 Results

4.3.1 Number of hard landings per aircraft type related to respective flight cycles

Table 3.2 on page 75 shows an overview of the number of hard landing occurrences and flight cycles over the 2009–2018 period. A chi-square test for independence (Yates continuity correction) indicated significant association between the two flight control groups divided into passive sidestick and coupled flight control aircraft types, when the hard landing events are related to their respective flight cycles in the same time period: $\chi 2$ (1 *df*, n = 29996.2 * 10^4, phi = 0.02) = 0.00, p = 0.03. On average over these 10 years, there has been one hard landing event every 7.49 million flight cycles, which explains why the effect size for this chi-square test (phi = 0.02) is very small.

4.3.2 Daytime or night-time conditions

Twenty-eight hard landing accidents (73%) took place during daylight conditions, eight (21%) occurred during the night, and two occurred during meteorological twilight (5%). These numbers tend to be in line with the results of Shappell et al. (2007), who found that 70% of the accidents occurred during daytime conditions, 25% during night conditions and 5% during meteorological twilight.

4.3.3 Hard landing difference in pilot experience

An independent *t*-test was conducted to compare the flight experience of the PF on passive sidestick aircraft and conventional flight-controlled aircraft. Preliminary analyses were performed to avoid violating assumptions of normality. There was a significant difference in experience between pilots who suffered hard landings with passive sidestick aircraft (M = 939, SD = 865.91) and pilots who suffered hard landings with coupled flight control aircraft (M = 2660.2, SD = 2806.96); t = -2.28, p <= 0.02, (two-tailed). The effect size of the difference in the means is considered large (eta squared = 0.82). This difference in experience becomes more evident when the data is capped at 300 flight hours on aircraft type, as can be seen in Bar chart 4.1. A total of 37% of the hard landings with passive sidestick aircraft occurred with pilots flying with fewer than 300 hours experience on aircraft type. For coupled flight-controlled aircraft, this is only 16%. A chi-square test for independence (Yates continuity correction) indicated no significant association between the two groups with less than 300 hours on type $\chi 2$ (1 *df*) = 1.22, p = 0.27. Another finding is that of the 19 accidents with passive sidestick aircraft, five hard landings (26%) occurred during an instruction flight or line training flight. This means that in 26% of the cases, there was a valid flight instructor on the flight deck and a third safety pilot present. For conventional flight control aircraft, this was true in only one case.

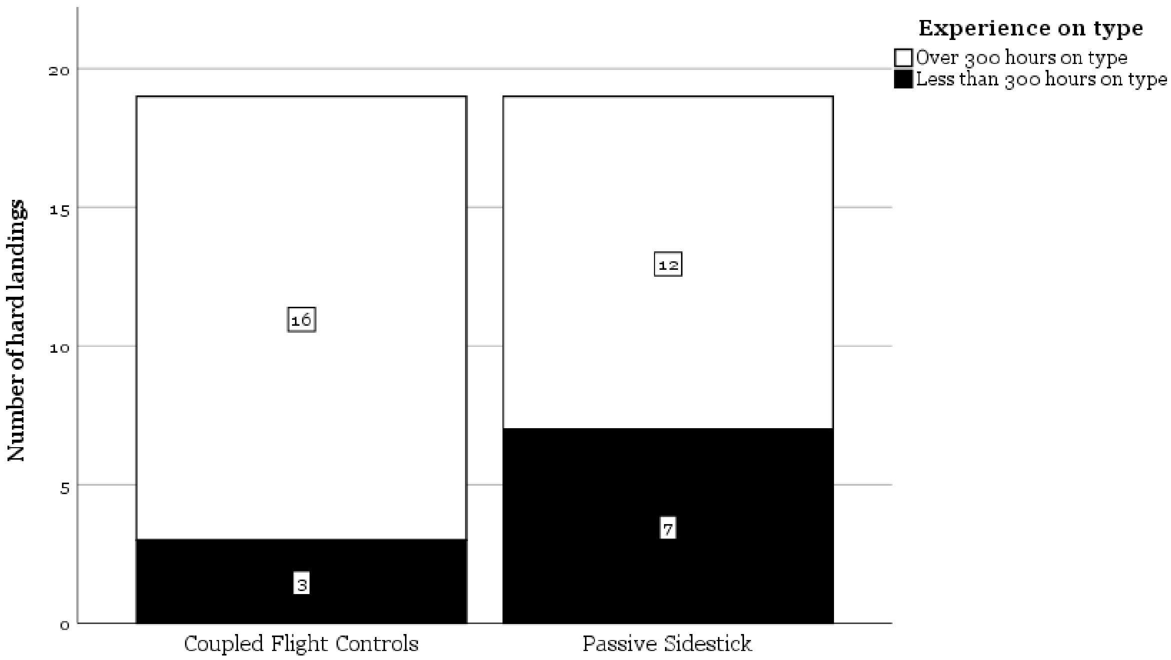

Bar chart 4.1 Number of hard landings divided by pilot flying hours of experience on aircraft type and type of flight control

4.3.4 Hard landings by damage classification

A chi-square test for independence (Yates continuity correction) indicated no significant association between the two flight control groups and the damage classification of the accident; $\chi2$ (1 *df*, n = 39, phi = -0.189) = 0.57, p = 0.45.

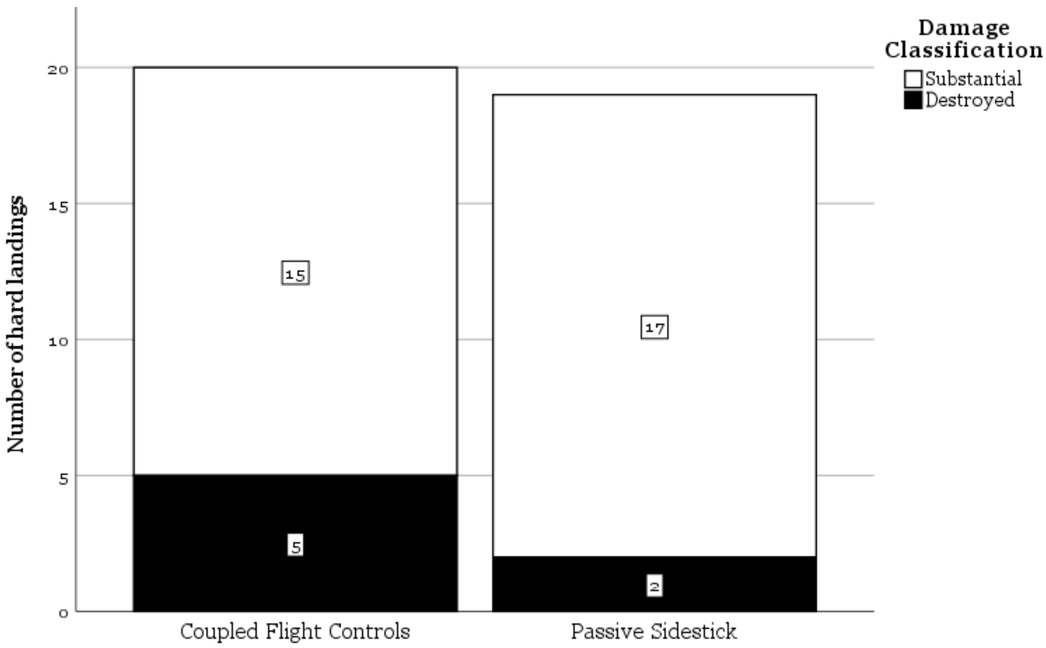

Bar chart 4.2 Number of hard landings divided by flight control type and damage classification

4.3.5 Hard landing by unstable approaches

The overall dataset showed that roughly half of the accidents followed an unstable approach. However, these numbers are not evenly distributed among passive sidestick and coupled flight-control aircraft. For the coupled flight-control aircraft, 74% of the hard landings were considered unstable approaches; for passive sidestick, aircraft this number is 21%. This means that 79% of the passive sidestick hard landings are stable approaches, but also that most were improperly initiated flare manoeuvres, as can be seen in **Bar chart 4.3**. A chi-square test for independence (with Yates continuity correction) indicated a significant association between the two groups $\chi 2$ (1 *df*, n = 38, phi = 0.52) = 8.55, p = 0.01. According to Cohen (1988), a phi coefficient value of 0.52 is considered large, which indicates a large and significant association between the type of flight control and the number of stabilised or unstable approaches.

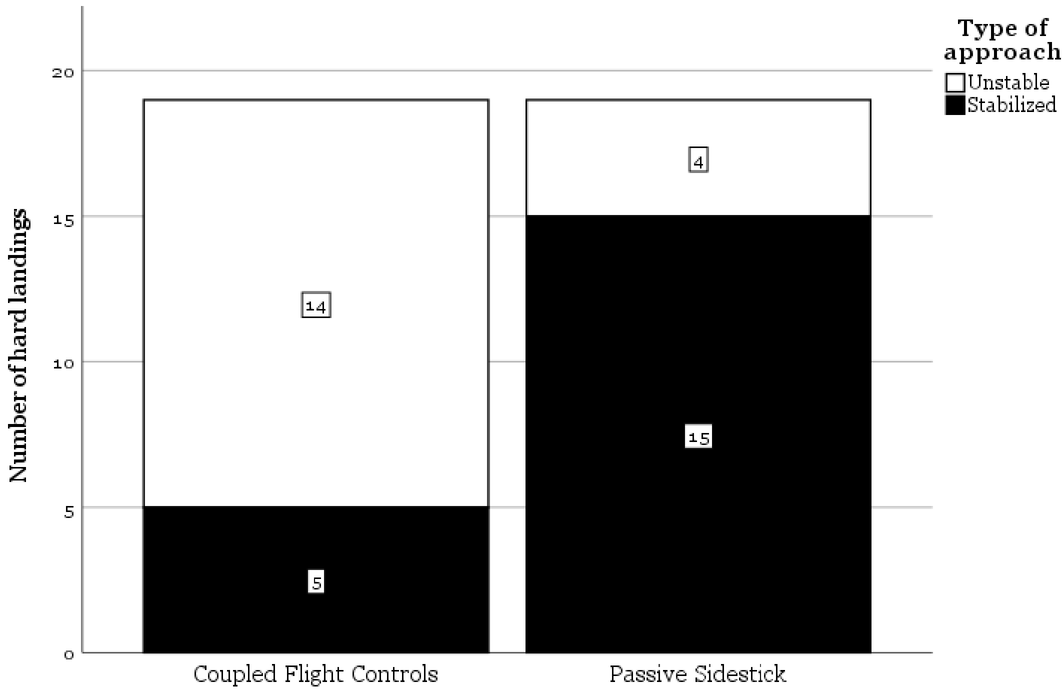

Bar chart 4.3 Number of hard landings divided by stabilized and unstable approaches

4.3.6 Passive sidestick system contributing to the hard landing

Of the 19 hard landings that occurred with passive sidestick aircraft, a multitude of reports mentioned the passive sidestick system logic to have contributed to the hard landing. In eight cases (42%) of the passive sidestick hard landings, a 'DUAL INPUT' occurred that worsened the situation. In five cases (26%), either the accident investigation authority or the PM identified the PM's inability to perceive flight control inputs from the PF as a factor contributing to the hard landing. In three cases (16%), the investigating authority cited the instinctiveness of the priority take-over push button as a factor contributing to the hard landing. For conventional flight control aircraft, none of these factors are relevant.

4.3.7 Single-aisle aircraft

Unexperienced pilots usually fly smaller aircraft; once they have gained more experience, they tend to fly larger aircraft. To account for this distinction, the two groups are also differentiated solely on the basis of experience flying single-aisle aircraft, to see whether the experience levels still differ. Even after filtering the dataset solely by single-aisle aircraft, all of the aforementioned results remained significant. First of all, the association between the flight cycles and the type of flight controls remains significant with a chi-square (with Yates continuity correction): $\chi 2$ (1 *df*) = 0.94, phi = 0.03, $p = 0.02$. The effect size phi remains very small due to the high number of normal landings. Second, the difference in flight hours (i.e. experience) on single-aisle aircraft between coupled flight controls (M = 2974.33, SD = 3607.27) and passive sidestick (M = 849.50, SD = 880.02) remains significant: $t = -2.21$, $p = 0.41$, (two-tailed). With an effect size of 0.81, the magnitude of this difference is considered to be large. If the number of flight hours are capped at 300, it still shows no significance: $\chi 2$ (1 *df*) = 0.41, $p = 0.11$. Finally, the association with stabilized and unstable approaches remains significant for single-aisle aircraft comparison ($\chi 2 = 19.95$, $p < 0.00$, phi = 0.83), also with a large effect size. (There have not been sufficient hard landing accidents to construct an accurate significance test on wide-body aircraft.)

4.4 Discussion

This study found that, compared to aircraft with coupled flight controls, passive sidestick aircraft are involved in twice as many hard landings per million flight cycles, as shown by **Table 3.2**. The significant association between the number of hard landing accidents and the type of flight controls in section **4.3.1** support the previous findings of (Alan F Uehara & Niedermeier, 2015), who concluded, based on a limited simulator study, that due to the missing coupling of the passive sidesticks, PMs were less likely to anticipate a hard landing and therefore less likely to take over control. Field and Harris (19980) concluded that the removal of the coupling between flight controls, as is the case for passive sidestick aircraft, is adversely affecting PM's SA. The findings of those two studies may explain the results in **Table 3.2** and section 4.3.1, which show a higher representation of passive sidestick aircraft in the hard landing data per flight cycle. However, the results of this study show only that there is a measurable association, without definitive evidence for the cause of that difference.

The results in section **4.3.3** show a significant difference in the mean hours of the PF's experience with the two aircraft types. Hard landings with passive sidestick aircraft occurred more often with PFs who had fewer flight hours. This finding may have several potential explanations. The first may be the PM's inability to perceive the flight control inputs, given that 26% of the hard landing accidents with passive sidesticks occurred during a line training flight with a flight instructor as PM. In combination with a PF with limited experience, this suggests that it may be more difficult for the PM to detect or intervene a hard landing on a passive sidestick aircraft. As (Rees & Harris, 1995) point out, it is more difficult to learn to fly without linked controls. In the light of these results, it may be that inexperienced pilots could also have more difficulties learning how to land on a passive sidestick aircraft. This introduces the possibility that the difference in flight hours may be attributable to pilot competency. If passive sidestick aircraft are harder to operate during the flare due to the aircraft switch from rate command to direct elevator control input in the flare mode, as discussed in section **2.2.4.a**, it follows logically that this increased difficulty would result in more accidents with less experienced pilots, as seen in this study.

At the moment of writing, the author knows of no research investigating the difference between handling qualities of passive sidestick aircraft and coupled flight control aircraft. However, an experimental set-up with airline pilots of different experience levels could provide an insight into the effects of pilot competency. Another key result from this study is the significant association between the number of unstable approaches and the type of flight controls. The results in section **4.3.5** support the previous findings of Matthews et al. (2004) and the IATA study on stabilised approaches (2016), where 50% of hard landings are caused by an unstable approach. Within the dataset, this is clearly the case: 50% of the hard landings follow an unstable approach. However, these 50% unstable approaches are not evenly divided among the different flight control types: for passive sidestick aircraft, 81% of the hard landings followed a stabilised approach path. The hard landing on these stabilised approaches went wrong during the initialisation of the flare. This again points in the direction of possible difficulties during the flare due to the change of flight modus, as explained in section **2.2.4.a**. The approach phase is normally flown with the help of flight guidance equipment, such as autopilot engagement, radio altimeter call-outs and instrument landing systems. The moment of the flare initialisation is the point where, with the exception of automated landings, the pilot has physically initiated the flare, requiring a manual flight control input, deviating from the flight path which, in combination with a mode change to direct elevator control, could possibly be linked to the flight control problem discussed in section 2.2.3.a. The results of this study are not sufficient to conclude that the elevated number of hard landings with passive sidestick aircraft is the result of neglecting to properly initiate the flare manoeuvre in time, as concluded by Uehara and Niedermeier (2015) and Uehara (2014), or that there is a more complex aircraft control problem involved regarding the sensitivity of flying passive sidestick aircraft. The results of this study are indicating that the limitations of effective monitoring for a monitoring pilot might be resulting in a higher number of accidents, especially in critical flight phases flown manually, such as the landing. This is supported by the fact that 26% of the passive sidestick hard landings either the PM involved or the investigating authority has stated that the inability to perceive flight control inputs as contributing to the hard landing. In order to come to an conclusion regarding the root cause of the elevated number of accidents, more research on the effects of passive sidesticks on accident rates is needed, as well an experimental study to investigate the effects of coupled flight controls on a PM's ability to successfully detect and prevent hard landings.

Chapter 5 Passive Sidesticks and Tailstrike Susceptibility: A Statistical Review

The previous chapter reported a statistically significant association between the number of hard landings and the type of flight controls. This chapter follows a similar methodology by comparing tailstrike events of both passive sidestick aircraft and coupled flight control aircraft to their respective flight cycles. Compared to hard landings, the frequency at which tailstrikes occur could be more dependent on aircraft-type-specific design parameters.

5.1 Background

A tailstrike occurs when the tail section of an airplane's fuselage comes into contact with the runway during take-off or landing. A tailstrike in itself is not a fatal accident; they are usually classified as an incident according to ICAO Annex 19 (ICAO, 2012) because they typically result in nothing more than damage to the airplane fuselage skin. However, fatal accidents have indeed occurred due to tailstrikes. China Airlines Flight 611 broke up mid-flight due to an undiscovered crack in the rear bulkhead as a result of a tailstrike 22 years prior, killing all 225 people on board (ASCT, 2002). In 1985, an aircraft of Japan Airlines broke up mid-flight due to a rapid decompression following the rear bulkhead's break-up due to damage incurred by a tailstrike seven years prior (JAAIC, 1987). Even though such fatal accidents are freak anomalies, rather than the most severe (but ultimately typical) results of a tailstrike, a tailstrike can still cost airlines a great deal of money. Depending on the damage, the aircraft is subjected to a rigorous tailstrike check, taking it out of service for at least two days. Although the main causal factors for tailstrike are related to pilot error (SKYbrary, 2017), environmental effects such as gusty winds can also contribute. Another major factor contributing to a tailstrike is an aircraft's specific geometrics and flight characteristics. For example, aircraft with long tail sections are more susceptible to tailstrikes than aircraft with shorter tails. During take-off, three main factors can cause a tailstrike (Airbus, 2017; Airbus Training & Flight Operations 2007; AAIB, 2006):

Early rotation: A rotation initiated at a lower speed during the take-off roll can cause a pilot to rotate whilst the aircraft generates insufficient lift to take off. When attempting to take off before the Vmc (or a so-called 'unstick' speed), the aircraft requires a larger angle of attack to provide sufficient lift with a lower speed to take off. This can cause pilots to deliberately apply a much larger aft stick deflection, leading to a higher pitch attitude, which can exceed the maximum pitch attitude, causing the tail to touch the runway (AAIB, 2006a; AAIB 2008). An early rotation can also occur when the pilot initiates a rotation before reaching the appropriate rotation speed (Vr). A more common cause for early rotation is incorrectly calculated rotation speed in the flight management system (FMS). If, for example, a lower take-off weight is entered into the FMS, the aircraft computes a lower rotation speed, leading to a rotation before the aircraft generates sufficient lift (Bernadin, 2003; Palomeque, 2008).

Excessive rotation rate at take-off: When take-off rotation is initiated, the pilot should apply a correct rotation rate. A too-slow rotation can cause the aircraft to overrun the runway (ATSB, 2009), whereas a too-fast rotation rate can cause the tail to strike the runway. Thus, the amount of control input being applied during affects the probability of a tailstrike. However, the proper rotation rate varies for each aircraft type.

Incorrect flap configuration: If the flaps are set incorrectly, especially if they are not sufficiently extended to the prescribed position, they can affect the aircraft's take-off and landing characteristics. In the context of a tailstrike during take-off, insufficient flap extension will result in insufficient lift at the predetermined rotation speed, resulting in a rotation with insufficient airspeed. In order to acquire sufficient lift to take off, the angle of attack must be increased, leading to a higher pitch attitude that increases the risk of the tail contacting the runway. Similarly, during the landing phase, incorrect flap settings can affect the approach and flare characteristics of the aircraft. If the flaps are not set properly during landing, the aircraft may have a higher approach speed, reducing the margin for a safe flare. This can result in a harder landing and increase the risk of a tailstrike.

With regards to the risk of a tailstrike occurrence during landing, many sources state that unstable approaches are the main reason for a tailstrike during landing (Bernadin, 2003; IATA, 2016; Matthews et al., 2004). These unstable approaches can be further divided into three different factors:

Approach speed below recommended approach speed: Flying an approach with a lower approach speed (Vapp) causes the aircraft to fly with a higher angle of attack (AoA) and therefore a higher pitch attitude, thus reducing ground clearance. When the flare is initiated, the aircraft pitch attitude is raised even more to reduce the vertical speed before touchdown and, in some cases, results in a tailstrike (AAIB, 2006b; National Transportation Safety Board, 2014)

Increased rate of descent: If the aircraft is approaching the runway with a much higher vertical velocity, the pilot will excessively increase the pitch attitude in order to avoid a hard landing. During this manoeuvre, the pilot can over-rotate, causing the tail to touch the runway (AAIB, 2000; Dutch Safety Board (OVV), 2017; Wang et al., 2016).

Incorrect flare initiation: When the flare manoeuvre is initiated too late, a greater aft stick deflection is required in order to avoid a hard landing. This results in an increased pitch attitude, narrowing the margins between the tail and the ground and increasing the risk of a tailstrike (ATSB, 2017; AAIB, 2006; OVV, 2017). Incorrect flare initiation can also lead to floated landings, a situation in which, on rotating the flare manoeuvre, the aircraft is gaining altitude instead of landing. In this situation, normal operating procedures for jet aircraft are to initiate a go-around. However, pilots sometimes decide to stay committed to the landing, often resulting in large control inputs in a situation where the aircraft is close to the ground with a high pitch attitude. This has led to multiple tailstrikes (AAIB, 2022; JTSB, 2014; NTSB, 2018).

5.2 Research questions

R5.1) Can the number of tailstrike incidents per aircraft type be related to their type-specific geometrics and flight characteristics?

R5.2) Does the number of tailstrike incidents for passive sidestick aircraft differ from that of aircraft with coupled flight controls?

5.3 Methodology

5.3.1 Design of Experiment

The study described in this chapter is aimed at comparing the number of tailstrike accidents and incidents between aircraft with passive sidestick flight controls and aircraft with coupled flight controls in the period between 2009 and 2018. In order to do so, the each specific aircraft sub-type is tested on their individual susceptibility to a tailstrike based on aircraft design parameters. For each aircraft type, the parameters that could influence the likelihood of a tailstrike are gathered and compared to the number of tailstrikes to investigate whether there is a statistically significant relationship between the number of tailstrikes and the design parameters. The general methodology, data acquisition and justification for statistical tests for this study have been described in Chapter 3 section paragraph 3.1.

5.3.2 Tailstrike data acquisition

5.3.2.a Tailstrike accident and incident data

The methodology to acquire and analyse the tailstrike accident reports has been described in Chapter 3 section 3.1.5, yielding 129 accident and incident reports used in this study. In comparison to the hard landing reports used in Chapter 4, many of the tailstrike reports are less detailed. The main reason is that, according to ICAO Annex 13 Aircraft Accident Damage Classification (ICAO, 2012), tailstrikes often resulted in minor damage; in such cases, the investigation reports are less thorough. Bar chart 5.1 shows the number of tailstrike accident and incident reports per aircraft type.

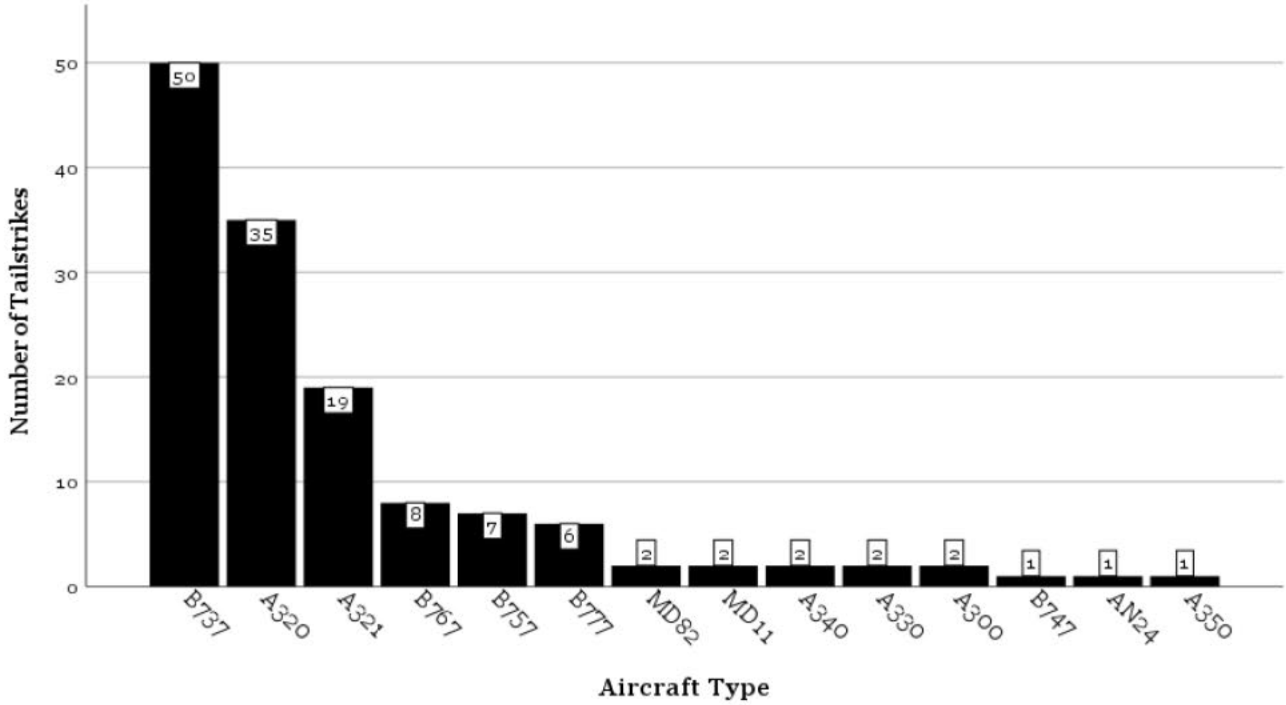

Bar chart 5.1 Histogram of tailstrike incidents and accidents per aircraft type

5.3.2.b Aircraft-specific design characteristics data

Various factors are involved in the occurrence of a tailstrike; some of these factors include aircraft-type-specific geometrics. These different aircraft design characteristics can create differences in the susceptibility of a tailstrike per aircraft type. The design characteristic that are of influence, as stated by Boeing (Bernadin, 2003; Brady, 1999), can be seen in **Table 5.1**. A schematic example of these design parameters can be seen in **Figure 5.1**. All aircraft characteristic data is gathered via the type-specific flight crew operating manual (FCOM) published by the aircraft manufacturer.

Aircraft de	***Description***
Tailstrike pitch attitude (MLG compressed)	The degree of pitch attitude per aircraft type required for the tail section to touch the ground with the main landing gear struts (MLG) compressed.

Length of aft fuselage	The length of the fuselage behind the MLG.
Ground clearance	The ground clearance of the tail section is the height of the aircraft's fuselage above the ground

Table 5.1 Aircraft-specific characteristics influencing tailstrike susceptibility (adapted from Bernadin, 2003; Brady,1999)

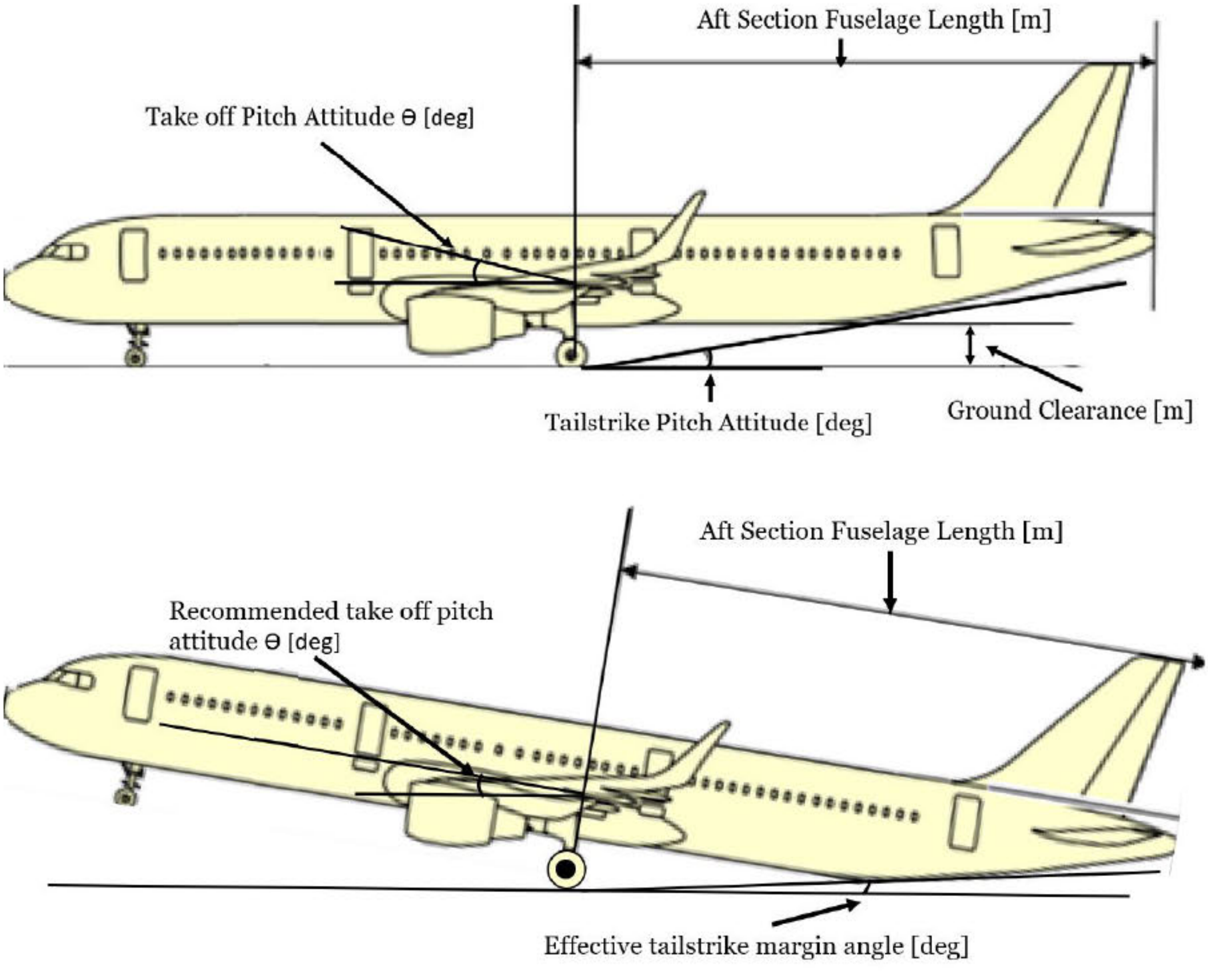

Figure 5.1 Schematic representation of aircraft design characteristics measured for tailstrike susceptibility during take-off and rotation

5.3.2.c Effective tailstrike margin angle

For an accurate comparison between different aircraft types, a new unit of comparison is proposed: the effective tailstrike margin angle, for which the equation can be found in Equation 5.1.

$$\begin{aligned} &Tailstrike\ pitch\ angle - Take\ off\ pitch\ attitude \\ &\qquad = Effective\ tailstrike\ margin\ angle \end{aligned}$$

Equation 5.1 Effective tailstrike margin angle

This unit is the degree margin between the manufacturer's recommended take-off pitch attitude and the tailstrike pitch attitude, and therefore represents the margin in degrees a pilot has between recommended take-off pitch attitude and tailstrike pitch attitude.

5.3.3 Tailstrike data processing

Chapter 3, paragraph 3.1 describes the data processing methodology for this study. To ensure statistical rigour in the comparison of the number of tailstrike incidents and the aircraft design characteristics, only aircraft types that suffered a minimum of five tailstrike incidents are considered. **Table 5.2** shows the type-specific aircraft characteristics, obtained from the manufacturers FCOMs, and effective tailstrike margin angle calculated according to Equation 5.1 for the aircraft types that had five or more tailstrikes within the dataset.

Type	***Tailstrike pitch angle in degrees***	***Take-off pitch attitude in degrees***	***Effective tailstrike margin angle in degrees***	***Length aft section fuselage in m***	***Ground clearance in m***
B737-700	14.7	9.1	5.1	16.2	1.40
B737-800	11.0	8.5	2.5	18.51	1.40
B737-900	10.0	8.0	2.0	19.61	1.43
B757-200	12.3	10.3	2.0	24.8	1.75

B767-300	9.3	7.1	2.1	27.2	1.78
B767-200	9.6	7.2	2.4	23.9	1.73
B777-200	12.1	8.5	3.6	37.8	2.19
B777-300	8.9	7.0	1.9	42.7	2.19
A320-200	11.7	8.1	3.6	19.87	1.79
A321-200	9.7	7.6	2.1	22.53	1.82

Table 5.2 Aircraft type specific design characteristic data and calculated effective tailstrike margin angle

5.4 Results

5.4.1 Aircraft design characteristics related to number of tailstrikes

Table 5.3 shows the ten aircraft types that experienced more than five tailstrikes alongside the number of tailstrikes and the number of flight cycles flown in the period between 2009 and 2018.

Type	***Number of tail-strikes***	***Total cycles flown***	***Cycles flown per tailstrike***	***Tailstrikes per million flight cycles***
B737-700	8	21,366,000	2.6 million	0.37
B737-800	36	60,384,000	1.6 million	0.59
B737-900	6	11,147,000	1.8 million	0.53
B757-200	7	7,202,000	1.0 million	0.97

B767-300	5	3,041,000	0.6 million	1.60
B767-200	3	4,562,000	1.5 million	0.65
B777-200	3	3,276,000	1.0 million	0.91
B777-300	3	5,345,000	1.7 million	0.56
A320-200	35	53,400,000	1.5 million	0.66
A321-200	19	13,977,000	0.7 million	1.36

Table 5.3 Number of tailstrikes and flight cycles per aircraft type

5.4.2 Effective tailstrike margin angle and number of tailstrikes per million flight cycles

The relationship between the effective tailstrike pitch margin angle per aircraft type (in degrees) and the frequency of tailstrike incidents (in tailstrikes per million flight cycles) was investigated using a Pearson product moment correlation coefficient. Preliminary analyses were performed to avoid violating assumptions of normality. A medium, non-significant correlation between the two variables was found, $r = -0.41$, $n = 10$, $p = 0.23$. The r^2 value is 0.168, meaning only 16% indicates a shared variance. A scatterplot of the effective tailstrike margin angle and number of tailstrikes per million flight cycles can be seen in Graph 5.1

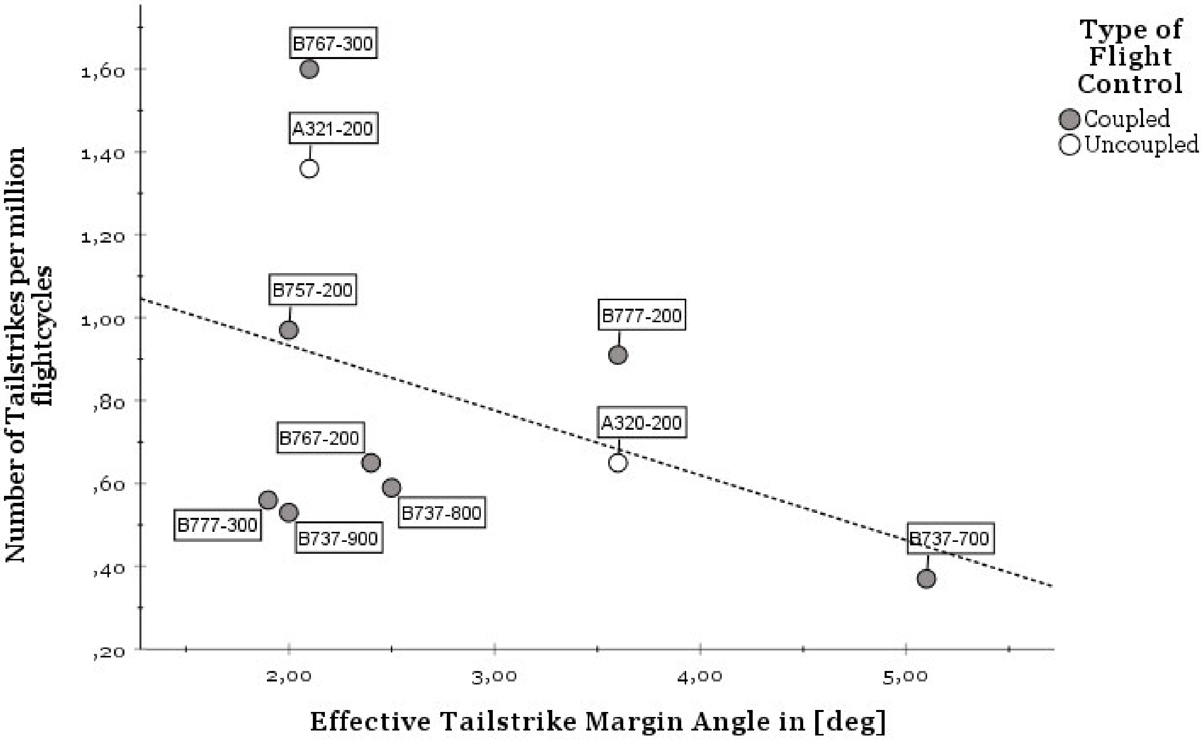

Graph 5.1 Scatterplot of effective tailstrike margin angle and number of tailstrikes per million flight cycles tailstrike with a dotted linear interpolation line

5.4.3 Length of aft fuselage section and number of tailstrikes per million flight cycles

The relationship between the length of the aft section of the fuselage per aircraft type (in meters) and the frequency of tailstrike incidents (in tailstrikes per million flight cycles) was investigated using a Pearson product moment correlation coefficient. Preliminary analyses were performed to avoid violating assumptions of normality. There was no significant correlation between the two variables, $r = 0.16$ $n = 10$ $p = 0.65$. The r^2 value is 0.02, which means that only 2% of the variables indicated a shared variance. A scatterplot of the length of the tail section per aircraft type and number of tailstrikes per million flight cycles can be seen in **Graph 5.2**.

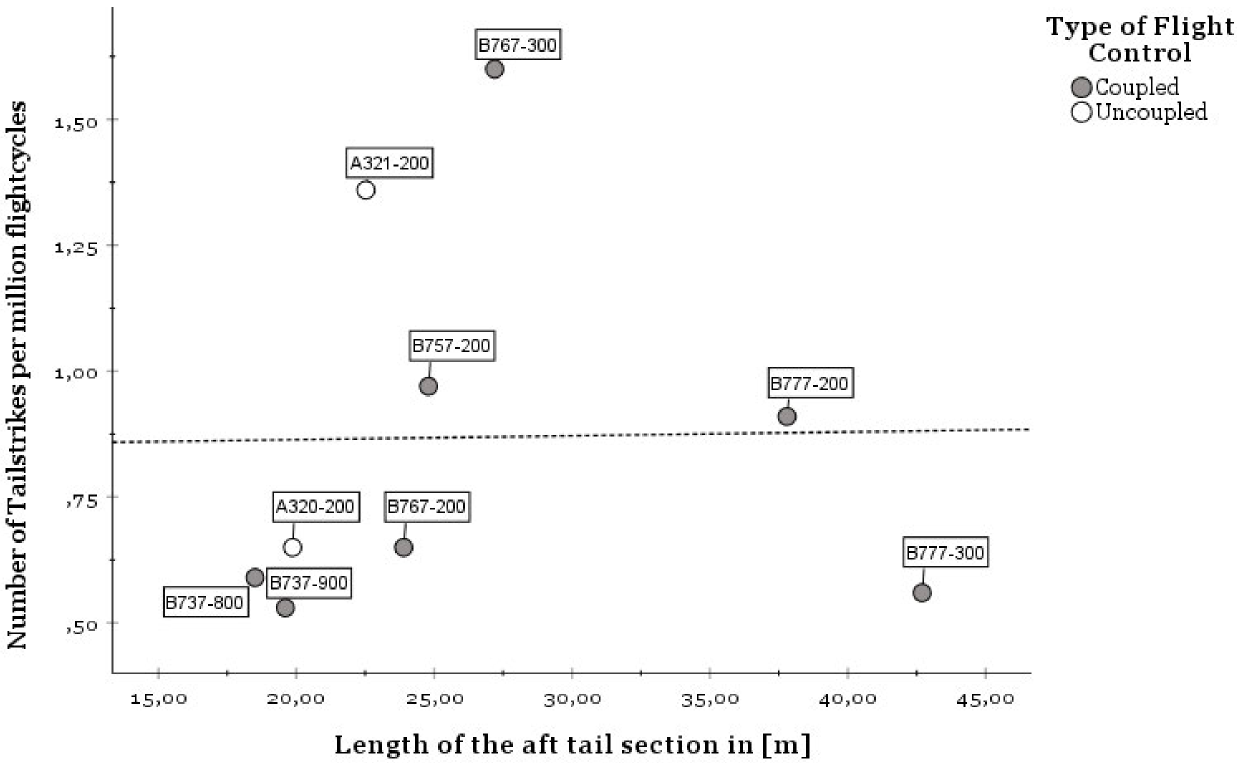

Graph 5.2 Scatterplot of aircraft-specific length of the tail section and number of flight cycles per tailstrike with a dotted linear interpolation line

5.4.4 Ground clearance and number of tailstrikes per million flight cycles

The relationship between ground clearance of the aft section of the fuselage per aircraft type (in meters) and the frequency of tailstrike incidents (in tailstrikes per millions flight cycles) was investigated using a Pearson product moment correlation coefficient. Preliminary analyses were performed to avoid violating assumptions of normality. A small, non-significant correlation between the two variables was found, $r = 0.28$ $n = 10$, $p = 0.38$. The r^2 value is 0.07, which means that only 7% of the data indicates a shared variance. Interestingly, the direction of this correlation is positive, which indicates the higher the ground clearance leading to a the higher number tailstrikes per million flight cycles. A scatterplot of the ground clearance in meters per aircraft type and number of tailstrikes per million flight cycles can be seen in **Graph 5.3**.

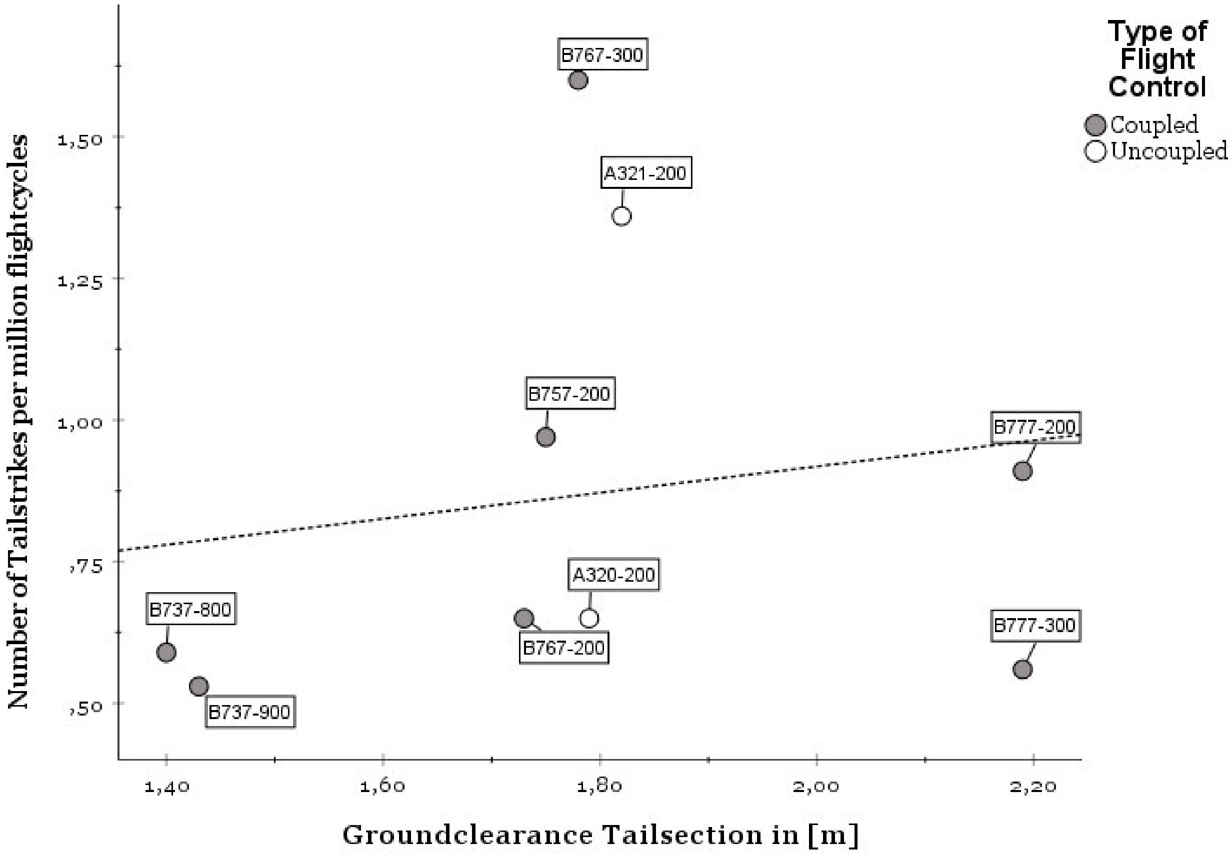

Graph 5.3 Scatterplot of aircraft-specific ground clearance of the tail section and number of flight cycles per tailstrike with a dotted linear interpolation line

5.4.5 Tailstrike comparison per flight control type

5.4.5.a Tailstrike difference on flight phase

The total number of tailstrikes divided by flight control configuration and phase of flight can be seen in **Bar chart 5.2**. A chi-square test for independence (Yates continuity correction) indicated no significant associations between the two flight control groups when grouped into passive sidestick aircraft and coupled flight control aircraft and the different flight phases at which the tailstrikes occurred; $\chi 2$ (1 *df*, n = 129, phi = -0.03) = 0.03, p = 0.83.

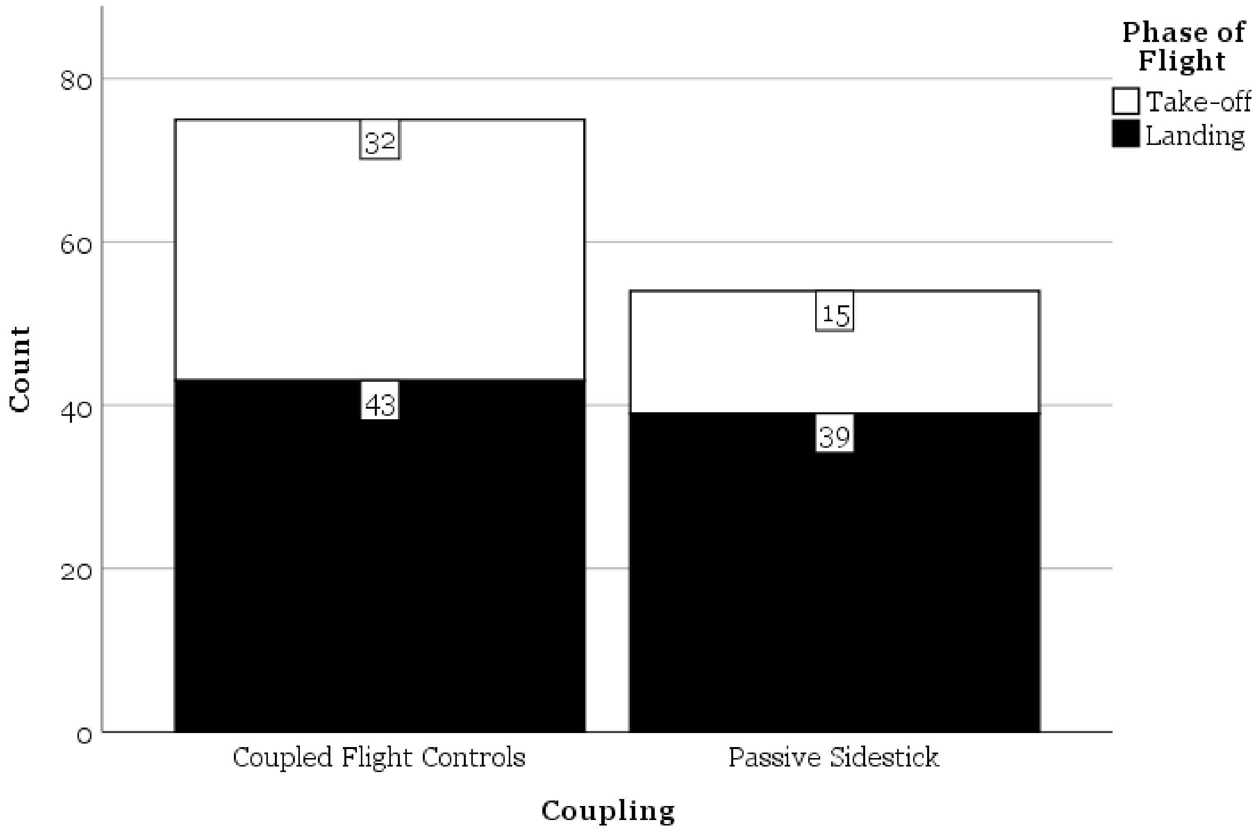

Bar chart 5.2 Number of tailstrikes divided by aircraft type and phase of flight

5.4.6 Number of tailstrikes per flight control type related to flight cycles

The database of 129 incident and accident reports comprises 54 tailstrikes by passive sidestick aircraft and 75 tailstrikes by coupled flight control aircraft. In order to test whether there is an association between number of tailstrikes that occurred with passive sidestick aircraft and the number of tailstrikes that occurred with coupled flight control aircraft in relation to the total amount of flight cycles, a chi-square test for independence (with a Yates continuity correction) is used. The chi-square test for independence indicated a significant association between the number of tailstrikes that occurred with passive sidestick aircraft and conventional aircraft type, when the number of tailstrike events are related to their respective flight cycles flown in the past 10 years; $\chi 2$ (1 *df*, n = 29984.1 * 10^4) = 9.16, p = 0.02, phi = 0.002. This means there is a statistically significant difference between the number of tailstrike events and the number of flight cycles flown. The data used for the chi-square test can be found in **Table 5.4**. Based on this dataset, a tailstrike occurs, on average, once every 2.32 million flight cycles. Therefore, the effect size is considered to be very small.

Type of Flight Control	***Tailstrikes***	***Tailstrikes % of total***	***Flight Cycles (x1000)***	***Flight Cycles % of total***
Passive Sidestick	54	42%	94,974	31.6%
Coupled Flight Controls	75	58%	204,867	68.4%
Total	129	100%	299,841	100%

Table 5.4 Number of tailstrike events by flight control type and number of flight cycles

5.5 Discussion

This chapter focuses on the relationship between flight control systems and tailstrike events. The results in paragraph 5.4.6 support the findings of Chapter 4, where a statistically significant overrepresentation of passive sidestick aircraft was observed in hard landing accident rates. The study in this chapter showed a similar significant association between the type of flight control and the number of accidents, this time on tailstrike incidents. No statistically significant association was found between the number of tailstrike incidents and specific design characteristics per aircraft type. Some design characteristics, such as 'length of aft tail section' and 'ground clearance', show a (non-significant) positive relation, meaning that the number of tailstrikes decreases as these criteria increase. One potential explanation is that crewmembers flying on aircraft types that are more vulnerable to tailstrikes, such as larger aircraft types, are often extensively trained in avoiding tailstrikes. Some aircraft types that were not included in the dataset have tailstrike notification systems to notify the pilot of a high pitch attitude during take-off; examples include the Airbus A380 and Airbus A350. If pilots are extensively trained on the avoidance of tailstrikes due to the susceptibility of the aircraft they are flying with, it could mean that in circumstances in which pilots are experiencing difficulties due to high stress levels or challenging weather conditions, these aircraft types are more likely to suffer a tailstrike. This hypotheses however is not investigated in this study.

Another limitation of this study is its use of incident reports, unlike in Chapter 4 where most of the reports used were accident reports following an ICAO Annex 19 report format. Incident reports are less extensive and contain less information. This is because a tailstrike often results in external damage on the fuselage skin, which is considered minor damage. Incident reports are more summarised and limited to a summary of the incident and some basic demographics. Extensive research on these reports, as has been done in the previous chapter, is therefore not possible. Parameters such as pilot experience, stabilised approaches, and angular rotation speeds are mentioned only sporadically, offering insufficient information for accurate comparison. Another limitation of this study is the severity of the tailstrike incidents, which determines whether an investigating body is involved. This study does not consider tailstrikes that incurred limited damage to the fuselage skin or tailstrikes that went unnoticed. Therefore, this research's significance is limited to the number of tailstrike reports published by investigating authorities.

5.6 Conclusions

This study found a strong association between the number of tailstrike occurrences and the type of flight control aircraft they involved. To accurately compare the susceptibility of each aircraft type, specific design criteria of each aircraft type are analysed and compared. The results show no statistically significant correlation between the number of tailstrike occurrences and specific design characteristics.

Therefore, the answer to Research Question 5.1 (Can the number of tailstrike incidents per aircraft type be related to their type-specific geometrics and flight characteristics?) is: No, there is no relationship found between the number of tailstrikes and the specific design characteristics of each aircraft type in this study. By concluding that design characteristics are not associated with the number of tailstrikes, the comparison can be made between flight control types with coupled and uncoupled flight controls. The results in section 5.4.6 show that there is a significant association between the number of tailstrikes and the type of flight control.

Thus, it can be concluded that the answer to Research Question 5.2 (Does the number of tailstrike incidents for passive sidestick aircraft differ from that of aircraft with coupled flight controls?) is: Yes, the number of tailstrike incidents is different for passive sidestick aircraft compared to aircraft with coupled flight controls. Within the dataset, passive sidestick aircraft are encountering 42% of the total number of tailstrikes despite flying only 31.6% of the total number of flight cycles.

These conclusions from this chapter and Chapter 4 are the foundation for the experimental research conducted in Chapters 6 to 7, where the effect of passive sidesticks is evaluated in simulator experiments.

Chapter 6 Effects of Coupled Sidesticks on Pilot Monitoring Awareness during Hard Landings

Taking cues from the results of the statistical review on hard landings in Chapter 4, This chapter describes the experimentation process in order to evaluate the contribution of haptic feedback cues for a PM during normal and hard landing scenarios. This experimental study is the culmination of the human factors considerations stated in Chapter 2 and the significant results in Chapter 4 and 5. The study is designed to resemble a normal multi-pilot flight deck of a representative transport jet aircraft. Because the simulator is shared with other research groups, the study was conducted in two phases. Phase one was conducted from May through October 2019, and phase two was conducted from November 2019 through January 2020.

6.1 Experimental method

The experimental methods for this study have been described in Chapter 3, paragraph 3.2. This section contains a brief summary of the experimental design of the study.

The aim of this study is to evaluate the effects of passive and active sidesticks on monitoring duties during hard landing and normal landing scenario's. The experiment was conducted using an Airbus A320 fixed-base simulator at Coventry University. Pilots with an Air Transport Pilot Licence where invited to participate. During the experiments, pilots were sat in an Airbus A320 static simulator with an Airbus 320 flight instructor who acted as PF for the scenario's and were tasked to monitor flights according to their company policies. During two of the landing scenarios the PF initiated an incorrect flare manoeuvre. Several quantitative and qualitive data points were gathered, which will be discussed in the following sections.

6.2 Objective results

6.2.1 Physical interventions: Pilot monitoring

Four parameters were measured for the non-flared landing scenarios: (1) whether an intervention took place; (2) time elapsed from when the PF stopped controlling the aircraft at 50 ft until the moment of intervention; (3) altitude at which the intervention took place, measured from ground level; and (4) projected time until touchdown from the moment of intervention. The number of physical interventions for both flight control configurations will be compared. Of the 40 non-flared landing scenarios, there were 25 physical interventions in which the PM took control. Nine of these 25 interventions occurred on the uncoupled flight control configuration, of which five were incorrect interventions. (In all of these incorrect interventions, the PM neglected to press the take-over push button, and in two cases the PM applied a stick-forward input, thereby worsening the hard landing.) This means that only 10% of the participants were able to prevent the hard landing with the passive sidestick configuration. The other 16 interventions (80% of the participants) occurred on the coupled flight control configuration. It should be noted that the four participants who did not physically intervene on the coupled flight control system did not intervene in any flight control configuration. (Two of these four participants were not accustomed to a sidestick system because they had no experience on passive sidestick aircraft.)

The time was measured from the moment of intervention from 50 ft, when the PF should start with a pre-flare manoeuvre, applying a small pitch-up movement to reduce vertical speed. If the PF did not intervene, the time of first contact to the ground was used to evaluate intervention time. Preliminary analyses were performed to avoid violating assumptions of normality. A paired-samples t-test was conducted to compare the time of physical intervention from 50 ft altitude for the different flight control configurations. There was no significant time difference in seconds between the uncoupled (M = 4.40, SD = 0.59) and coupled (M = 3.71, SD = 1.01) flight control configurations; $t = 1.64$, $p = 0.11$ (two tailed).

The time to touchdown from the moment of intervening was calculated using the vertical speed and altitude at the time of the intervention. This projected time until touchdown was compared to the different flight control configurations with a paired-samples *t*-test. Preliminary analyses were performed to avoid violating assumptions of normality. The time until touchdown when pilots intervened differed; intervention occurred significantly later (measured in time to touchdown) for the uncoupled flight controls (M = 0.56, SD = 0.92) than for coupled flight controls (M = 1.68, SD = 1.0); this difference was significant ($t(19) = -6.04$, $p = .001$) (two-tailed) The effect size, Eta squared, is 0.55 which is a large effect size. Third and finally, the altitude at which the intervention took place was measured and compared. A Shapiro-Wilks test for normality showed a violation of the assumption of normality p=0.005 , therefore a non-parametric test is used. A Wilcoxon Signed Rank test revealed a statistically significant reduction in altitude at the moment of physical intervention on the scenario's flown with passive sidestick configuration, z=-3,62, p<0.01 with a large effect size of 0.81.

It is noteworthy that these three parameters are closely related to one another. If a participant intervened earlier in the approach, it occurred at a higher altitude with more time until touchdown (**Figure 6.1**). However, the time in seconds measured from 50 ft altitude until the intervention is not significant, whereas the time to touchdown and the altitude are significant. The explanation for this effect is the relative point from which it is measured. The time until touchdown and altitude of intervention are both measured from a fixed point – the runway threshold – whereas the time from intervening measured from 50 ft is a relative point that is completely dependent on the current vertical speed. Therefore, a strong correlation is found between the time measured from 50 ft and the current vertical speed by using Pearson product moment correlation coefficient. There was a very strong correlation between the two variables, $r = 0.81$, $p = 0.03$, with a medium effect size of 0.41. This correlation was not found between the other two variables.

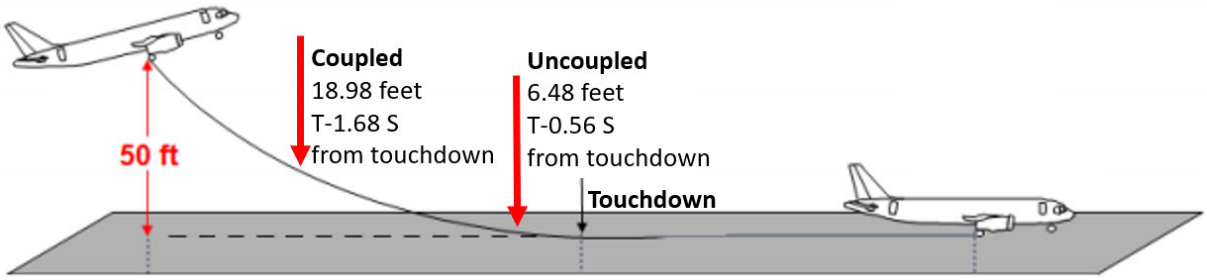

Figure 6.1 Physical intervention points on approach for coupled and uncoupled flight control configurations

6.2.2 Verbal interventions: Pilot monitoring

In addition to the physical interventions, the verbal interventions were captured as well. A verbal intervention is defined as any verbal action taken by the PM to prevent the hard landing, or to inform the PF that the flare maneuver was initiated incorrectly. The same parameters are measured for the verbal interventions as for the physical interventions. PMs verbally intervened during landings in only three of the 20 scenarios using the uncoupled configuration; in all three cases, the verbal and physical interventions occurred simultaneously. For the coupled configuration, the number of verbal interventions was much higher. In 15 of the 20 non-flared landings with the coupled configuration, the PM verbally intervened. In two of these fifteen verbal interventions, no physical intervention was initiated. In one of these 15 verbal interventions, verbal and physical interventions occurred simultaneously. The other 12 verbal interventions on the coupled configuration were followed by a physical intervention. These verbal interventions on the coupled configuration were, on average, initiated 0.83 seconds before the physical intervention was initiated. There have been insufficient verbal interventions on the uncoupled configurations (n = 3) to make an accurate comparison between the two systems; the means are displayed in **Figure 6.2**.

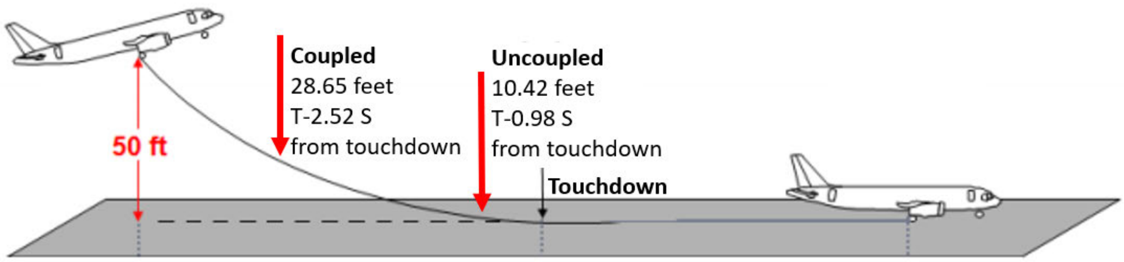

Figure 6.2 Verbal intervention points on approach for coupled and uncoupled flight control configurations

6.2.3 Landing acceleration

Normal acceleration is captured as part of the simulator data output. For reasons discussed in Chapter 3, normal acceleration is not commonly used to determine the acceleration on landing. However, because this study is conducted on a simulator, those real-life considerations do not affect the data acquisition. X-Plane calculates normal acceleration based on aircraft weight and is measured with a frequency of 50

Hz. The landing acceleration used in the results is the highest recorded value at the moment of touchdown or immediately afterward. A boxplot of the landing accelerations divided into the two different flight control configurations can be seen in **Graph 6.1**. This boxplot clearly shows different results for the two different flight control configurations. A paired-samples *t*-test was conducted to evaluate the impact of the coupling between the sticks on the landing acceleration. Preliminary analyses were performed to avoid violating assumptions of normality. There was a statistically significant decrease in normal acceleration from the uncoupled flight control configuration ($M = 2.71$, $SD = 0.69$) compared to the coupled flight control configuration active sticks ($M = 2.05$, $SD = 0.66$), $t\,(19) = 3.92$, $p = .01$ (two-tailed). The magnitude of the difference in means is considered large (Eta squared = 0.44). This significant difference can be explained by the previous results; the number of successful physical interventions on the coupled sidestick system were higher, resulting in a lower acceleration. However, the accelerations are highly dependent on the vertical speed at which the aircraft is landed. All scenarios are flown with an Airbus A320-200 flight model, for which the maximum allowed normal acceleration is 2.6 g. For the uncoupled flight control configuration, 65% of the hard landing scenarios exceeded this 2.6 g threshold, resulting in hard landings that exceeded design criteria. For the coupled flight control configurations, only 15% of the flown scenarios exceeded the 2.6 g normal acceleration threshold.

The results suggest that in 65% of the non-flared landing scenarios with uncoupled configuration, the aircraft landed hard enough to be considered an accident. In 80% of the non-flared landing scenarios with coupled configuration, the PM not only prevented the hard landing from occurring, but was also able to land within normal landing acceleration tolerances. The participants who intervened verbally before intervening physically landed the aircraft, on average, with a normal acceleration of 1.81 g. None of these landings exceeded the maximum landing acceleration tolerance of 2.6 g. All of these interventions were made on the coupled configuration.

Because all scenarios are flown manually by the PF without auto throttle or autopilot assistance, not all scenarios will encounter the exact same vertical speed. To rule out this potential explanation for the difference in landing acceleration, a paired-samples *t*-test was conducted to compare the mean vertical speed of the last 50 ft until touchdown or moment of intervention for the different flight control configurations. Preliminary analyses were performed to avoid violating assumptions of normality. No significant difference was found in the recorded vertical speed between uncoupled (M = -650.03, SD = 91.88) and coupled (M = -659.35, SD = 80.36); t = -.04, p = 0.66 (two-tailed). The relationship between landing acceleration and average vertical speed on the last 50 ft of the approach was investigated using Pearson product moment correlation coefficient, which found no correlation between the two variables, r = 0.05, p = 0.76. This means vertical speed was not a factor for the difference in acceleration values between the two types of control configuration.

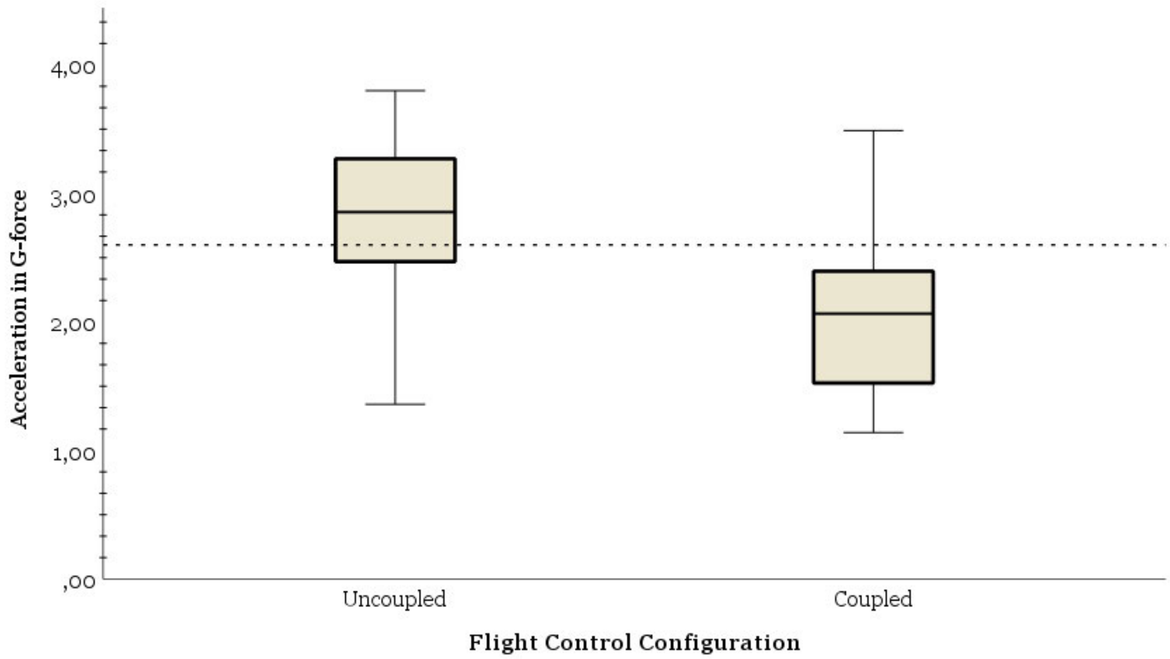

Graph 6.1 Boxplot of normal acceleration (g) on touchdown per flight control configuration with 2.6 g maximum allowable acceleration reference line

6.2.4 Hard landing results compared to Airbus rating

Not all participants who took part in this experiment were Airbus-rated. In this section, the difference between Airbus-rated and non-Airbus-rated pilots is investigated for two measures: (1) perceived workload on TLX and (2) landing acceleration. An overview can be seen in **Table 6.1**. An independent t-test is conducted to compare the difference in total hard landing TLX between Airbus-rated (M = 39.96, SD = 16.79) and non-Airbus-rated pilots (M = 35.77, SD = 9.15); t = -0.667, p = 0.54, which is not shown to be significant. There are not sufficient non-

Airbus-rated pilots to conduct an accurate test between the different flight coupling configurations. A significant difference is found in landing acceleration between Airbus-rated and non-Airbus-rated pilots. With an independent *t*-test, the difference in landing acceleration between Airbus-rated (M = 2.28, SD = 0.77) and non-Airbus-rated pilots (M = 2.89 SD = 0.58); t = 3.28, p = 0.45 is found to be significant.

	Airbus-rated	*N*	*Mean*	*Std Deviation*
Hard Landing Total TLX	No	4	35.77	9.15
	Yes	16	39.96	16.79
Landing Acceleration	No	4	2.89	0.58
	Yes	16	2.28	0.77

Table 6.1 Overview of Airbus-rated and non-Airbus-rated participants in mean TLX and landing acceleration

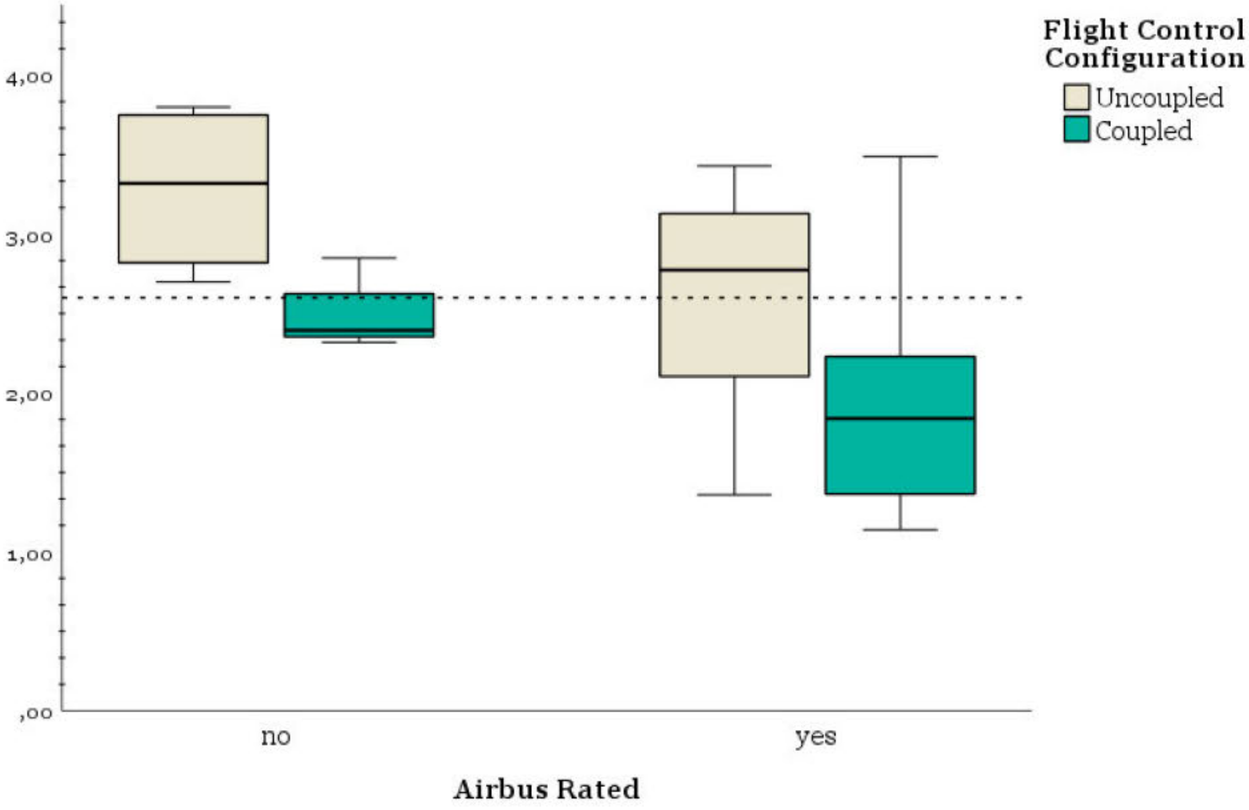

Graph 6.2 Boxplot of normal acceleration (g) on touchdown split in Airbus-rated participants and flight control configuration with 2.6 g maximum allowable acceleration reference line

6.2.5 Maximum achieved aft stick deflection on hard landing intervention

Only nine participants intervened on both systems, therefore the comparison can only be made between these nine participants. A Shapiro-Wilks test for normality showed a violation of the assumption of normality $p=0.008$, therefore a non-parametric test is used. A Wilcoxon Signed Rank test revealed a statistically significant reduction in the maximum achieved aft stick deflection during the intervention on the scenario's flown with coupled sidestick configuration, $z=-2,19$, $p=0.03$ with a large effect size of 0.73. The mean maximum stick deflection on the coupled flight control system ($m=64.4$, $SD=24,38$) was lower compared to the mean maximum stick deflection on the uncoupled flight control configuration ($m=87.5$, $SD=21,41$). Also it is noted that out of the nine interventions on the uncoupled flight control configuration, six pilots initiated a 100% stick deflection, some of which in multiple directions, resulting in a floated landing and in one case an engine pod strike.

6.3 Subjective results

6.3.1 Perceived workload

Each participant completed a digital weighted NASA-TLX at the end of each scenario. This digital survey focusses on six different subscales of perceived workload, all combined resulting in a total perceived workload. The mean weighted TLX score per scenario can be seen in **Graph 6.3**. As can be seen in this graph, the total weighted TLX score per scenario is lower for all scenarios flown in the coupled configuration. A paired-samples *t*-test was conducted to evaluate the impact of the coupling between the sticks on the normal scenarios. Preliminary analyses were performed to avoid violating assumptions of normality. The TLX scores from the uncoupled sticks ($M = 41.19$, $SD = 18.99$) were significantly lower than the TLX scores from the active sticks ($M = 30.33$, $SD = 15.30$), $t\ (19) = 3.6$, $p = 0.02$ (two-tailed). The magnitude of the difference in means is considered to be large (Eta squared = 0.40). For the non-flared landing scenarios, a paired-samples *t*-test was conducted to evaluate the impact of the coupling between the sticks on the hard landing scenarios. Preliminary analyses were performed to avoid violating assumptions of normality. Again, the TLX scores from the uncoupled sticks (M = 45.14, SD = 15.28) were significantly lower than the TLX scores from the active sticks (M = 36.66, SD = 14.39), t (19) = 3.68, p < .001 (two-tailed). The magnitude of this difference in means is large (Eta squared = 0.41). Therefore, we can conclude that the participants perceived a significantly lower overall workload when monitoring in a coupled configuration, regardless of the scenario.

These overall workload scores can be broken down into the six different subscales of the NASA TLX; the mean TLX breakdown can be seen **Bar chart 6.1**.

A Shapiro-Wilks test for normality showed a violation of the assumption of normality on the subscales 'physical demand' and 'frustration', therefore a non-parametric test is used for analysing these subscales. The subscales 'mental demand', 'temporal demand', 'performance' and 'effort' showed no violation of the assumption of normality. For each normally distributed subscale, a paired-samples *t*-test has been conducted, for the subscales 'physical demand' and 'frustration' a Wilcoxon Signed Rank test has been conducted. To avoid discussing twelve similar statistical comparisons, only the tests with significant differences will be discussed here. In the normal landing scenarios a paired samples *t*-test was conducted to assess the difference in perceived mental demand between uncoupled (M = 155.00, SD = 125.922) and coupled (M = 72.22, SD = 53.858); t = 1.81, p = 0.048 (two-tailed). The effect size is considered to be large (Eta squared = 0.15) For the hard landing scenarios a paired samples *t*-test showed significant differences between the mental demand on the uncoupled (M = 213.33, SD = 61.948) and coupled hard landing scenario's (M = 117.22, SD = 111.358); t = 2.26, p = 0.03 (two tailed). The effect size is considered to be large (Eta squared = 0.21). A paired samples t-test showed significant differences between the perceived effort in the hard landing scenarios between uncoupled (M = 156.11, SD = 46.420) and coupled flight controls (M = 101.67, SD = 64.614); t = 2.52, p = 0.041, (two tailed). The effect size is considered to be large (Eta squared = 0.25). An overview of the significant TLX subscales can be found in **Table 6.2**.

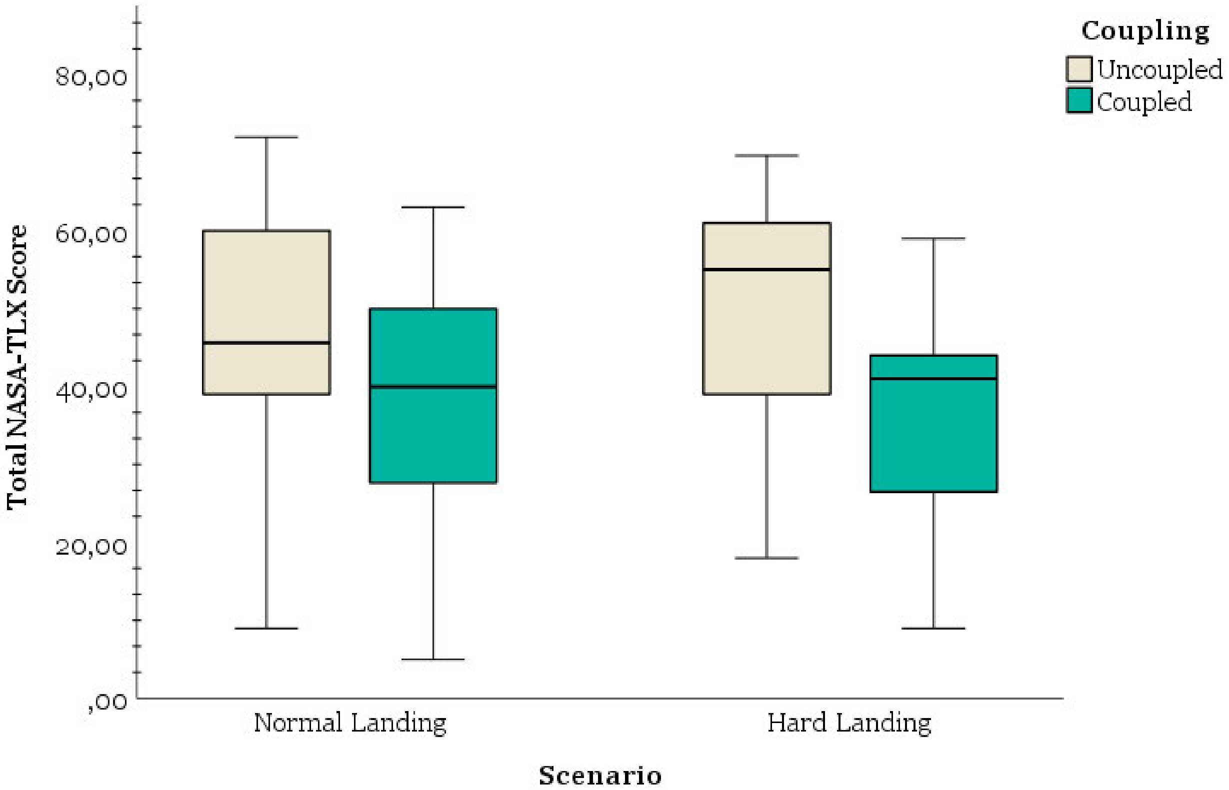

Graph 6.3 Boxplot of normal and hard landing scenarios and total NASA TLX scores by coupling

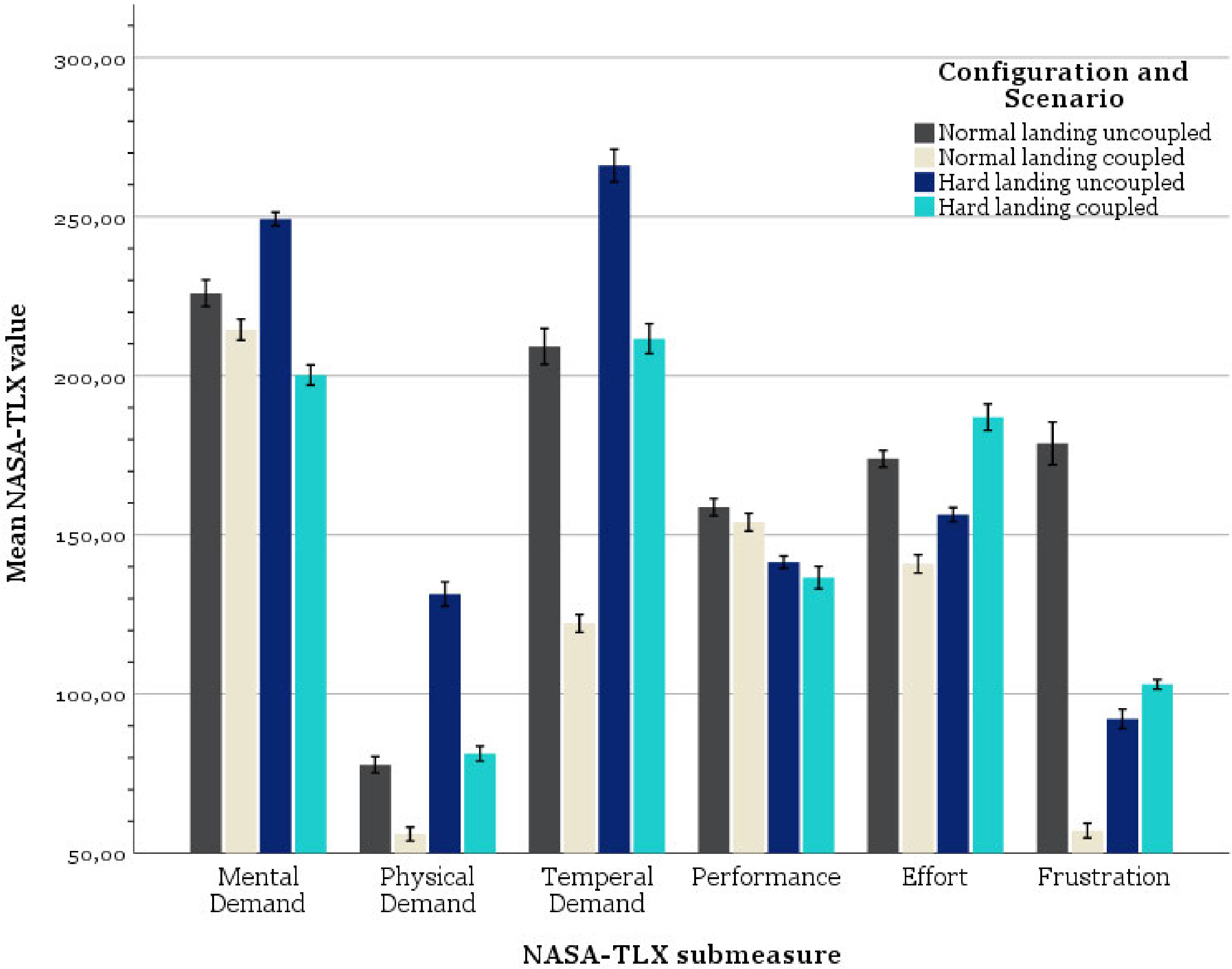

Bar chart 6.1 Mean NASA-TLX Subscale scores per landing scenario and flight control configurations with error bars representing 95% confidence interval

Scenario	*TLX Subsection*	*Configuration*	*M*	*SD*	*t (19)*	*Sig (2-tailed)*	*Effect Size (Eta squared)*
Normal Landing	Temporal Demand	Uncoupled	125.25	115.30	3.11	.006	0.15
		Coupled	72.25	63.04			
Hard Landing	Mental Demand	Uncoupled	216.75	88.42	3.16	.005	0.21
		Coupled	146.25	99.82			
Hard Landing	Effort	Uncoupled	154.25	63.08	4.29	<.001	0.25
		Coupled	75.50	55.27			

Table 6.2 NASA TLX significant scores between uncoupled and coupled configurations

6.3.2 Situation Awareness Rating Technique

Similarly to the TLX results, the results from the SART questionnaire showed differences in perceived SA between the two flight control configurations. The total SART score for the scenarios flown with the flight controls in the coupled configuration were higher (M = 19.00, SD = 5.43) than for the same scenarios flown in the uncoupled configuration (M = 16.2, SD = 8.35). This difference is analysed through a paired-samples *t*-test. Preliminary analyses were performed to avoid violating assumptions of normality. The test showed no significant difference (t = -2.8, p = 0.09). All other subdomains of the SART questionnaire have been analysed through a paired-samples *t*-test, for which the results can be found in **Table 6.3**. Preliminary analyses were on all subscales have been performed to avoid violating assumptions of normality. What becomes apparent in this table is the significant difference in the domain of attentional supply (t = -2.4, p = 0.02). The attentional supply score on the coupled flight control configuration (M = 23.8, SD = 3.15) is significantly higher than for the same scenarios flown on the uncoupled configuration (M = 17.5, SD = 4.50). This difference in score is mainly the result of a significant difference in the rated spare mental capacity. When the participants monitored the hard landing scenarios with the uncoupled flight control system, they rated their spare mental capacity lower (M = 4.8, SD = 1.36) compared to their rated spare mental capacity on the coupled flight control configuration (M = 5.5, SD = 1.05); this difference is significant (paired-sample *t*-test; $t = -2.7$, $p = 0.03$).

Scenario	*Configuration*	*M*	*SD*	*t (19)*	*Sig (2-tailed)*	*Effect Size (Eta squared)*
Total SART Score	Uncoupled	16.2	8.35	-2.8	.09	0.29
	Coupled	19.3	5.43			
Attentional Demand	Uncoupled	14.3	4.49	1.75	.09	0.14
	Coupled	12.9	4.25			
Attentional Supply	Uncoupled	17.5	4.50	-2.4	.02	0.23
	Coupled	23.8	3.15			
Understanding	Uncoupled	10.0	1.87	-3.0	.07	0.32
	Coupled	11.0	1.50			
Spare Mental Capacity	Uncoupled	4.8	1.36	-2.7	.03	0.27
	Coupled	5.5	1.05			

Table 6.3 SART subsection results of paired-samples *t*-test on hard landing scenarios

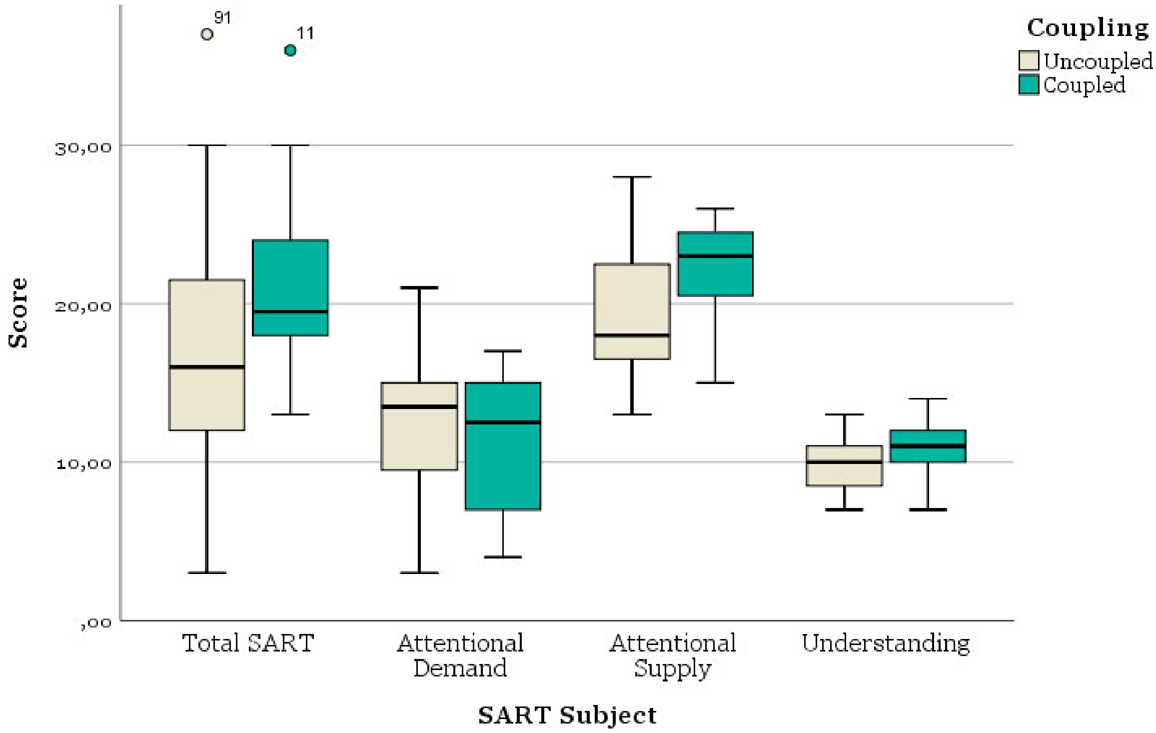

Graph 6.4 Boxplot of SART total score and SART subdomains during hard landing scenarios

6.3.3 Startle and surprise questionnaire

Because the sample size for statistical analyses is lower than 20, the required statistical power is calculated and taken into account before analysing. According to Cohen (1988), the minimal statistical power is 0.80. Therefore, all significant values with a statistical power lower than 0.80 will not be discussed. **Table 6.4** is a power table that provides an overview of the means and required statistical power.

Question	*Mean* *Uncoupled*	*Mean* *Coupled*	*Sigma*	*Sample size*	*Statistical Power*
Q1) Perceived Surprise	5.86	4.01	2.16	18	0.81
Q2) Perceived Startle	6.5	4.6	2.25	18	0.90
Q3) Perceived Response	6.33	7.55	2.06	18	0.55
Q4) Perceived Result	6.22	8.5	1.96	18	0.94

Table 6.4 Power table of startle and surprise questions

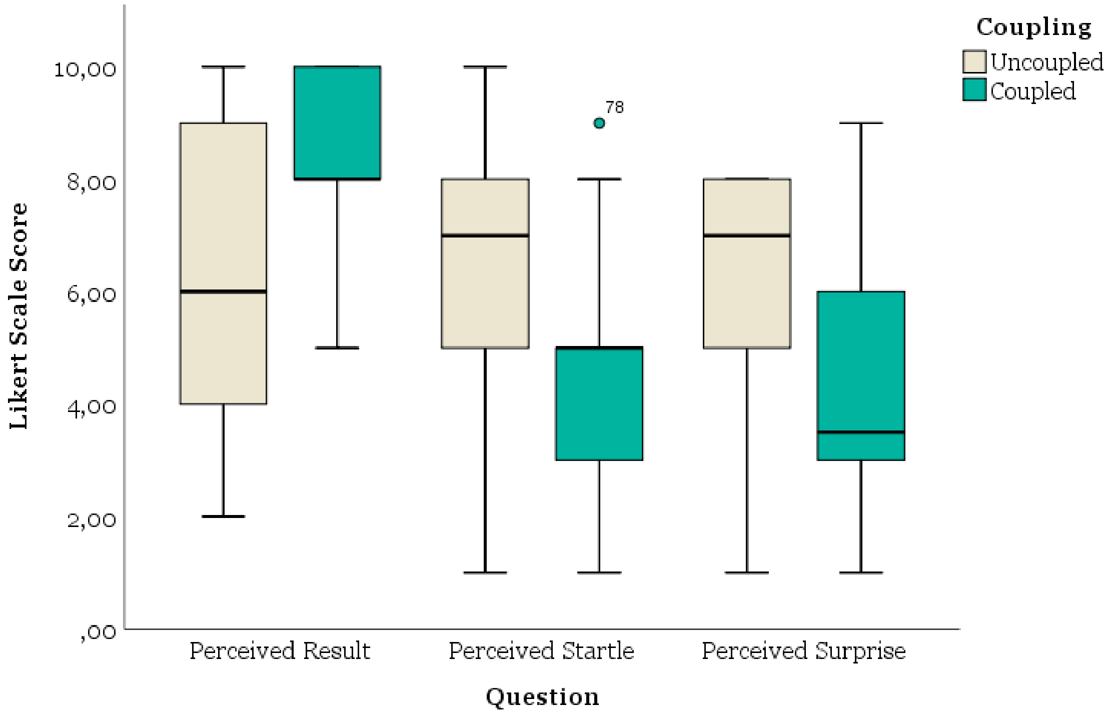

Graph 6.5 Boxplot of Likert-scale scores per questionnaire question divided by flight control coupling

6.3.4 Significance test for perceived surprise by flight control configuration

A paired-samples *t*-test was conducted to compare the perceived surprise Likert-scale scores for coupled and uncoupled flight control configurations during abnormal runway contact events. Preliminary analyses were performed to avoid violating assumptions of normality. There was a significant difference in scores for uncoupled (M = 6.00, SD = 2.35) and coupled flight control configurations (M = 4.16, SD = 1.91; *t* (2.531), *p* = 0.016, two-tailed). The effect size is considered large (Eta squared = 0.158).

6.3.5 Significance test for perceived startle by flight control configuration

A paired-samples t-test was conducted to compare the perceived startle Likert-scale scores for coupled and uncoupled flight control configurations during abnormal runway contact events. Preliminary analyses were performed to avoid violating assumptions of normality. There was a significant difference in scores for uncoupled (M = 6.52, SD = 2.56) and coupled flight control configurations (M = 4.32, SD = 2.00; *t* (2.03), *p* = 0.043, two-tailed). The effect size in means was moderate (Eta squared = 0.108).

6.3.6 Significance test for perceived result by flight control configuration

A paired-samples *t*-test was conducted to compare the perceived surprise Likert-scale scores for coupled and uncoupled flight control configurations during abnormal runway contact events. Preliminary analyses were performed to avoid violating assumptions of normality. There was a significant difference in scores for uncoupled (M = 6.22, SD = 2.55) and coupled flight control configurations (M = 8.50, SD = 1.38; *t* (-3.32), *p* = 0.03, two-tailed). The magnitude of the differences in means was moderate (eta squared = 0.24).

6.4 Physiological results

6.4.1 Proportional dwell time out-the-window view during approach

During all approach phases, a difference is found in the proportionate dwell time in percentage of out-the-window (OTW) eye fixations between coupled and uncoupled flight controls. Of the 56 approach scenarios taken into account in this analysis, a 12.4% mean OTW percentage for uncoupled flight controls was found; the same parameter for the coupled flight controls was 17.2%. Preliminary analyses were performed to avoid violating assumptions of normality. A paired-sample *t*-test was conducted to compare the percentage of OTW eye fixation between uncoupled (M = 12.4, SD = 5.77) and coupled (M = 17.2, SD = 4.35); *t* = 2.99, *p* = 0.007 (two-sided). which shows a significant difference in the percentage of OTW fixations. The effect size is considered to be large (Eta squared= 0,31).

Flight control configuration	*Number of approaches*	*Mean OTW dwell time percentage*	*Std Deviation*
Uncoupled	30	12.4	5.77
Coupled	26	17.2	4.35

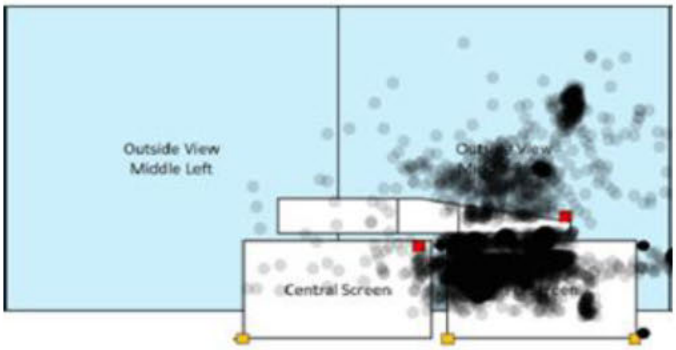

Figure 6.3 Example of eye fixation heath map during an uncoupled flight control approach: Participant no. 19

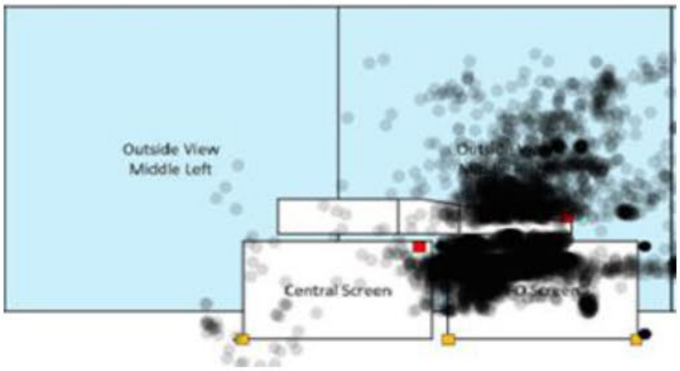

Figure 6.4 Example of eye fixation heath map during a coupled flight control approach: Participant no. 19

6.4.2 Fixation duration out-the-window view during approach

A paired-samples *t*-test was conducted to compare the duration of OTW eye fixation in ms for uncoupled (M = 210.94, SD = 71.91) and coupled (M = 199.05, SD = 63.87); $t = 0.539$, $p = 0.593$, which showed no significant differences in the duration of OTW fixations.

6.4.3 Pupil dilation

In addition to the overall quality of the eye-tracking data, SmartEye systems also record the specific quality of certain parameters, namely pupil dilation, heart rate variability, and electrodermal activity. Pupil dilation is scored from 0 to 1 based on the accuracy of the tracked parameter. During the initial simulation trials it became clear that the flight simulator lacks sufficient ambient light to track pupil diameter with high quality. More than half of the simulation scenarios flown lacked reliable pupil diameter data, setting the quality number to 0. For 90% of the data, the mean quality for pupil diameter has been less than 0.4. Therefore, the pupil diameter data has not been taken into account.

6.4.4 Heart rate variability

For heart rate measures, time domain heart rate variability (HRV) measurement is used. The root mean square of successive differences (RMSSD) between normal heartbeats and PNN50 (the percentage of adjacent NN intervals that differ from each other by more than 50 ms) are obtained using the BIOPAC MP36. Across the different hard landing scenarios, two types of RMSSD measurements are taken: the first are captured over the entire length of the flown scenario, and the second are taken within a 60-second interval across the hard landing event. A boxplot of the mean RMSSD results can be found in **Graph 6.6**. Of the 40 hard landing scenarios, 2 ECGs are deemed unsuitable for analysis purposes.

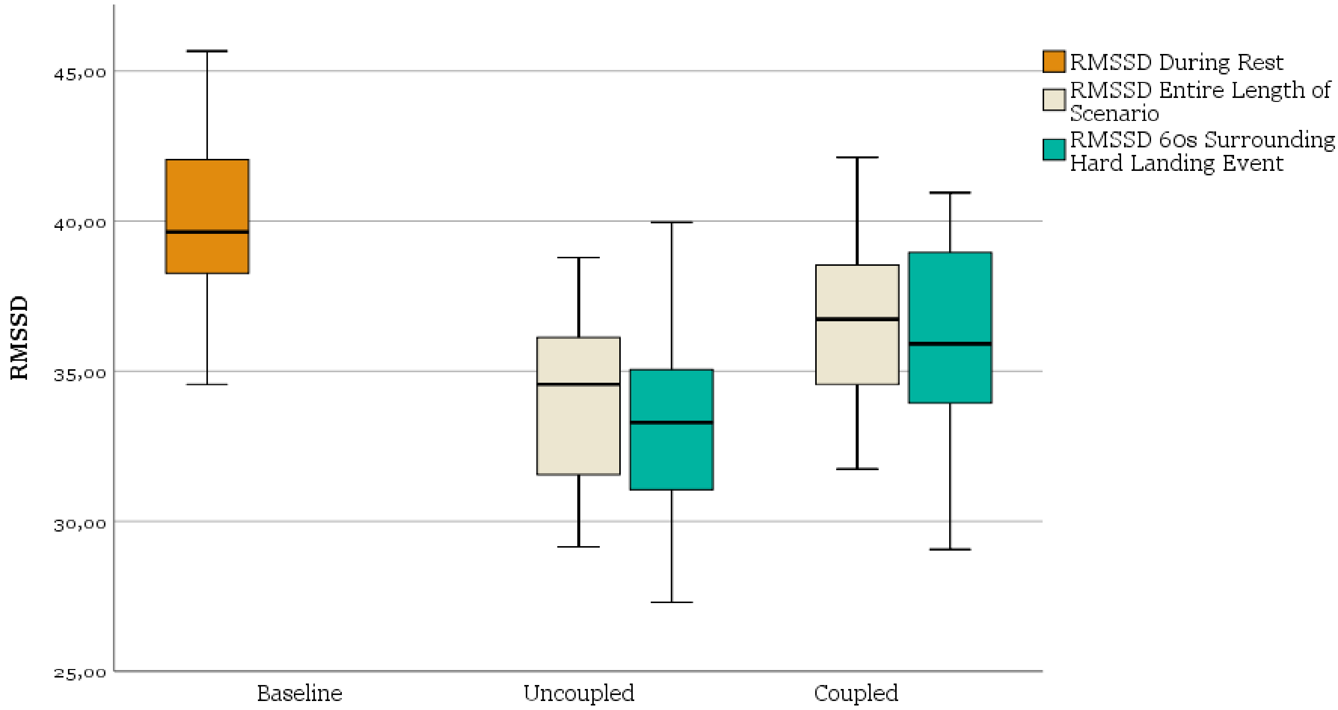

Graph 6.6 Mean RMSSD during resting conditions and hard landing events

The RMSSD measures were analysed using a paired-samples *t*-test to identify whether a statistically significant effect of the different flight control configuration is present. It is found that the RMSSD of participants during entire hard landing scenarios differed, with RMSSD increasing whilst using the coupled flight controls (M = 36.1, SD = 2.89) in comparison to the same scenario whilst using uncoupled flight controls (M = 34.5, SD = 2.97); this difference is significant (t = -4.17, p = 0.01). The effect size is considered to be large (Eta squared = 0.47). When the RMSSD is measured over only the 60 s surrounding the hard landing events, this difference becomes more apparent. The RMSSD of each participant during the hard landing event was higher for the coupled flight controls (M = 33.2, SD = 3.35) than for the same scenario whilst using uncoupled flight controls (M = 35.5 SD = 3.38); this difference is significant (t = -4.47, p = 0.00). The effect size is considered to be large (Eta squared = 0.51). The second HRV measure captured in this experiment is pNN50. This measure requires a 2-minute epoch (Shaffer & Ginsberg, 2017). p50NN was also analysed using a paired-samples *t*-test to identify whether the flight control coupling was of significant effect. It was found that the p50NN of the hard landing scenarios with uncoupled flight controls (M = 14.9, SD = 0.80) and coupled flight controls (M = 16.3, SD = 0.54) are not significantly different (t = -1.66, p = 0.12). A boxplot overview of the pNN50 values can be found in **Graph 6.7**.

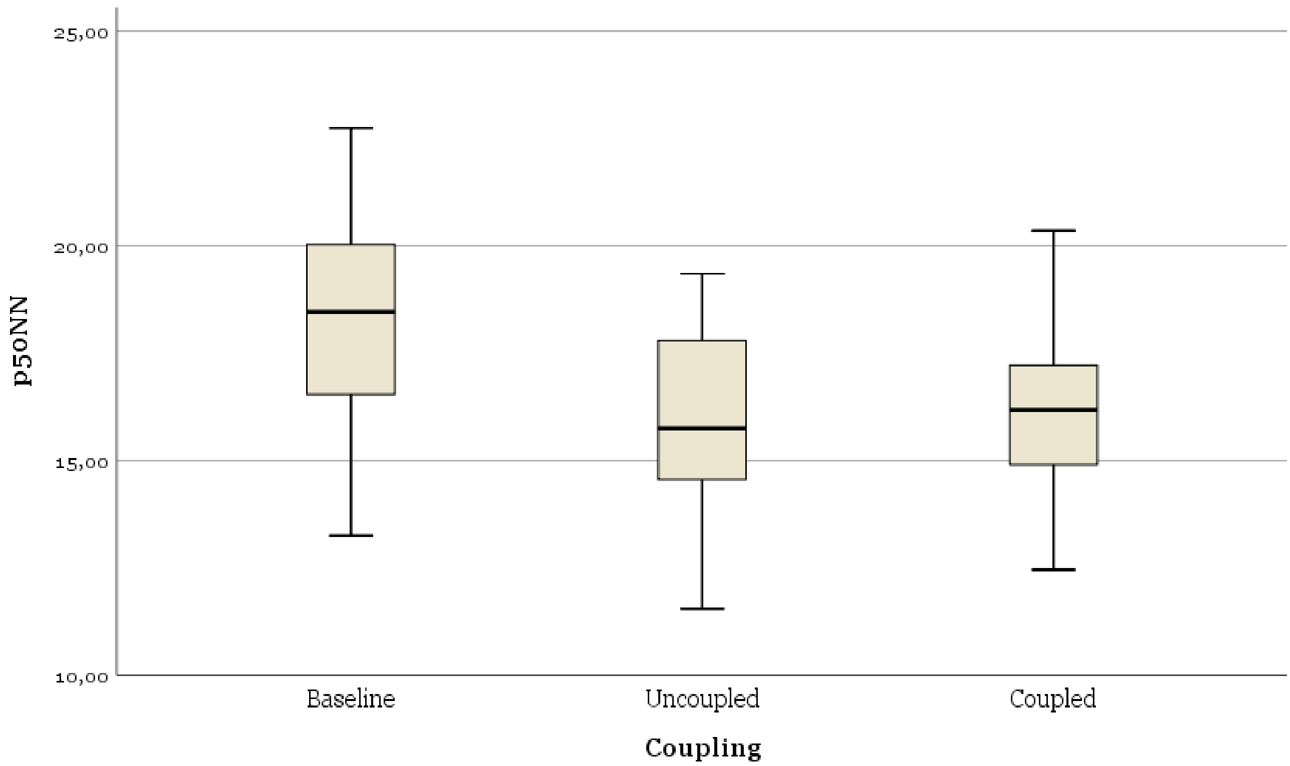

Graph 6.7 Mean p50NN during resting conditions (baseline) and hard landing scenarios

6.4.5 Electrodermal activity

Event-related skin conductance response (ER-SCR) is used to measure electrodermal activity. The SCR peak is taken into account if the waveform onset is at least 10% of the current skin conductance level and if the rise in conductance level occurs between 1 and 5 seconds after the stimulus is provided. In the hard landing scenarios, the stimulus is the moment when the participant provides any intervention, either verbal or physical. When no intervention is given, the stimulus is set to 2 seconds before calculated touchdown. The amplitude of the waveform onset determines the strength of the emotional arousal (Dawson et al., 2016); therefore, the amplitude of the waveform onset is used as a measurement. Because ER-SRC is dependent on a participant's perception of the situation, not all hard landing scenarios had an ER-SCR. Of the 40 hard landing scenarios, six runs had no ER-SCR; in two scenarios the data was unsuitable for analysis. An overview of the runs with suitable ER-SCRs can be seen in **Table 6.5**. Differences were identified in ER-SCR amplitudes during the hard landing scenarios: The ER-SCR amplitudes of the scenarios flown with the uncoupled flight control (M = 3.81, SD = 4.45) showed higher values than the scenarios flown with the coupled flight controls (M = 1.52, SD = 0.32). A Shapiro–Wilk test showed a violation of normality, therefore a non-parametric test is used. A Wilcoxon Signed Rank test revealed a statistically significant difference between the sidestick configurations, z=-2,34, p=0.01 with a large effect size of 0.63. An overview of the ER-SCR amplitudes can be seen in **Graph 6.8**.

Participant Number	*Normal Landing Uncoupled*	*Normal Landing Coupled*	*Hard Landing coupled*	*Hard Landing Uncoupled*
1		No ER-SCR	No ER-SCR	
2				
3				
4				
5		Bad data	Bad data	Bad data
6				
7	No ER-SCR		No ER-SCR	
8		No ER-SCR		
9				
10				
11	Bad data			
12				
13				
14			No ER-SCR	
15			No ER-SCR	
16				

17				No ER-SCR
18	No ER-SCR			
19				
20			No ER-SCR	
Total EDA data	7	7	14	18

Table 6.5 Overview of ER-SCRs on normal and hard landing scenarios

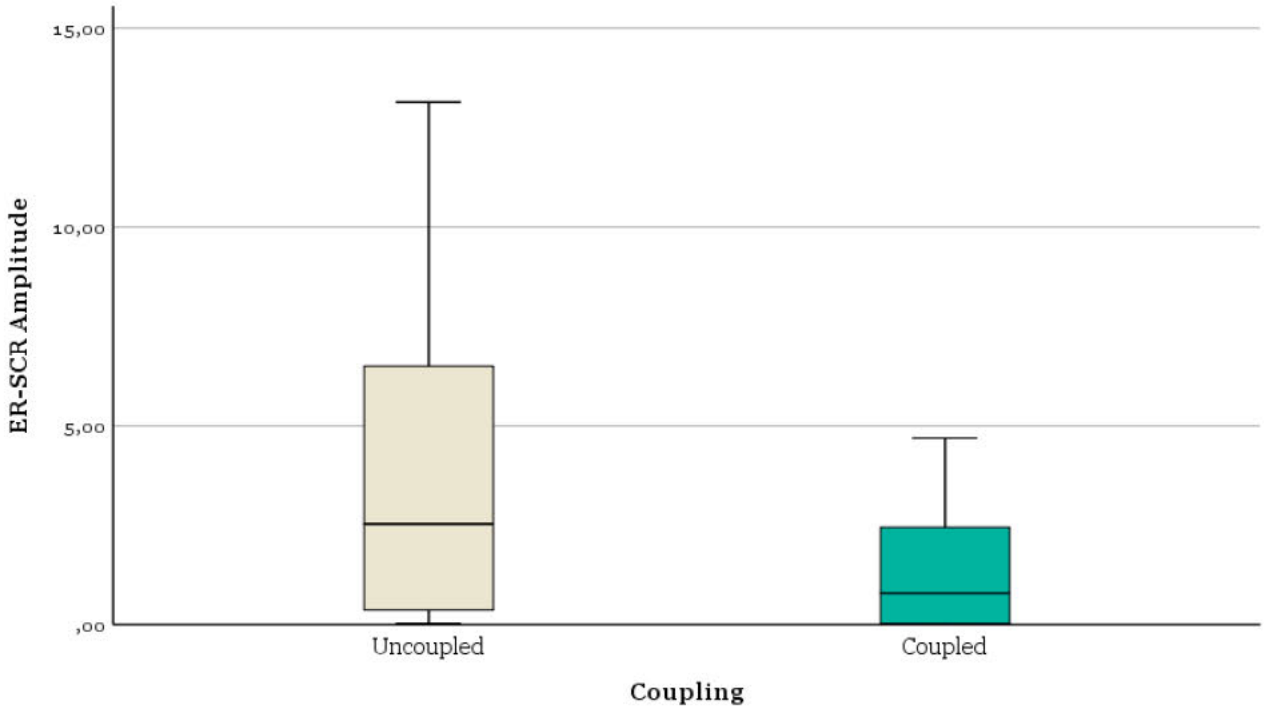

Graph 6.8 Boxplot of ER-SCR amplitudes during hard landing scenarios for uncoupled and coupled flight controls

6.5 Correlation between hard landing results

As described in the introduction of this chapter, the results are collected over three different domains – objective results, subjective results and physiological results – which form the pillars of this research. This section covers the linear relations among these three domains to determine coherence among the previous three paragraphs. Due to the large number of variables collected during this experiment, correlations between variables are investigated only where there is a suspected theoretical coherence.

6.5.1 Test for normality on hard landing correlating results

In order to accurately test for linear relations among the different results, a Shapiro–Wilk test is used. The results of this normality test can be found in **Table 6.6**. This resulted in four normally distributed variables, for which a parametric test will be used. All other variables in **Table 6.6** are not normally distributed; for these parameters a non-parametric test is used.

Shapiro–Wilk Normality Test	*Statistic*	*Degrees of Freedom*	*Significance*
Perceived Surprise	0.92	30	0.06
Perceived Startle	0.95	30	0.21
ER-SCR Amplitude	0.75	30	0.00
OTW Eye Fixations	0.97	30	0.56
Time Till Touchdown at moment of Intervention	0.90	30	0.01
Total TLX Hard Landing	0.96	30	0.39

SART Total Score	0.96	30	0.40
SART Mental Capacity	0.90	30	0.01
Landing Acceleration	0.92	30	0.07
RMSSD	0.90	30	0.05

Table 6.6 Shapiro–Wilk normality test results on hard landing scenario results

6.5.2 Correlations between objective and subjective hard landing results

The first correlation analysed is the relationship between the time until touchdown at the moment of intervening and perceived surprise and startle. It can be theorised that the less time before touchdown at the moment of intervening, the more surprised or startled the participant's reaction; this should result in a higher score on the Likert scale. Because preliminary analyses violated the assumption of normality, a non-parametric test was used. There was a moderate positive correlation between the time until touchdown and perceived surprise, rho = -0.33, n = 36 p = 0.049 analysed by a Spearman rank correlation coefficient. In other words, less time available to intervene (i.e. closer to the ground) is related to higher perceived surprise. The same non-parametric test was used to analyse the linear relation between the time until touchdown at the moment of intervening and perceived startle. Using a Spearman rank correlation coefficient, a very strong negative correlation is found between the two variables (rho = -0.91, n = 36, p =0.00).

6.5.3 Correlations between objective and physiological results

As shown in the previous section, the time until touchdown is significantly correlated with perceived startle and surprise. Therefore, it can be theorised that a linear relationship may exist between the ER-SCR of the hard landing and the time until touchdown. Because preliminary analyses violated the assumption of normality, a non-parametric test was used: A Spearman rank correlation coefficient found a strong negative relationship between available time until touchdown and ER-SCR amplitude (rho = -0.49, p = 0.007). This supports the significant subjective relation in section 6.5.2, which means that less time before touchdown results in higher ER-SCR amplitude, indicating higher emotional arousal. The same relationship can be theorised between the magnitude of the acceleration and the ER-SCR. Because preliminary analyses violated the assumption of normality, a non-parametric test is used: A Spearman rank correlation coefficient found a moderately strong positive correlation is found between the two variables (rho = 0.39, p = 0.03). This means that when the magnitude of the landing acceleration increases, the amplitude of the ER-SCR is increased as well.

6.5.4 Correlations between subjective and physiological results

In this section, the linear relations between the subjective and physiological results are analysed. According to various sources, a relationship exists between mental workload and time domain HRV measures (Mansikka et al., 2016; G. Matthews et al., 2015; Orsila et al., 2008; Wierwille, 1979). Therefore, it is reasonable to assume that a similar relation can be found in the hard landing dataset. The RMSSD and total TLX scores are compared to identify whether there is a significant relationship between the two variables. Because preliminary analysis shows that the RMSSD violates the assumption of normality, a non-parametric test (Spearman rank correlation coefficient) is used. This test shows a moderate negative correlation between the RMSSD and NASA TLX total score (rho = -0.46, p = 0.004). This means that a higher RMSSD value, associated with less perceived stress, results in a lower TLX score, which is a reflection of the perceived workload. As described in the previous section, a strong relation is found between the results of the startle and surprise questionnaire and the time until touchdown at the moment of intervention. Additionally, a relationship is found between time until touchdown at the moment of intervention and ER-SCR. To complete the circle, the relationship between the perceived startle and surprise and ER-SCR amplitude is investigated. Preliminary analyses showed that perceived surprise and ER-SCR amplitude are not normally distributed; therefore a non-parametric test (Spearman rank correlation coefficient) is used to analyse linear relationships. It is found no correlation between perceived surprise and ER-SCR amplitude (*rho* = 0.36, *p* = 0.007) and a moderate positive correlation between perceived startle and ER-SCR (*r* = 0.41, *p* = 0.03).

In terms of eye tracking, the results in section 6.4.1 showed an apparent difference between the amount of OTW eye fixations during the approach. According to various sources in both aviation and automotive industry, a higher OTW percentage is related to spare mental capacity, which in section 6.3.2 showed significantly different. Therefore, the relation between the OTW eye fixations and SART spare mental capacity score is investigated. Because the SART spare mental capacity score violates the assumption of normality, a Spearman rank correlation coefficient is used to test linear relations between the two variables. It is found a moderate positive correlation between the percentage of OTW eye fixations and the Likert-scale scores on the spare mental capacity question (*rho* = 0.47, *p* = 002). This means that a higher percentage of OTW eye fixations is correlating with a higher amount of perceived spare mental capacity.

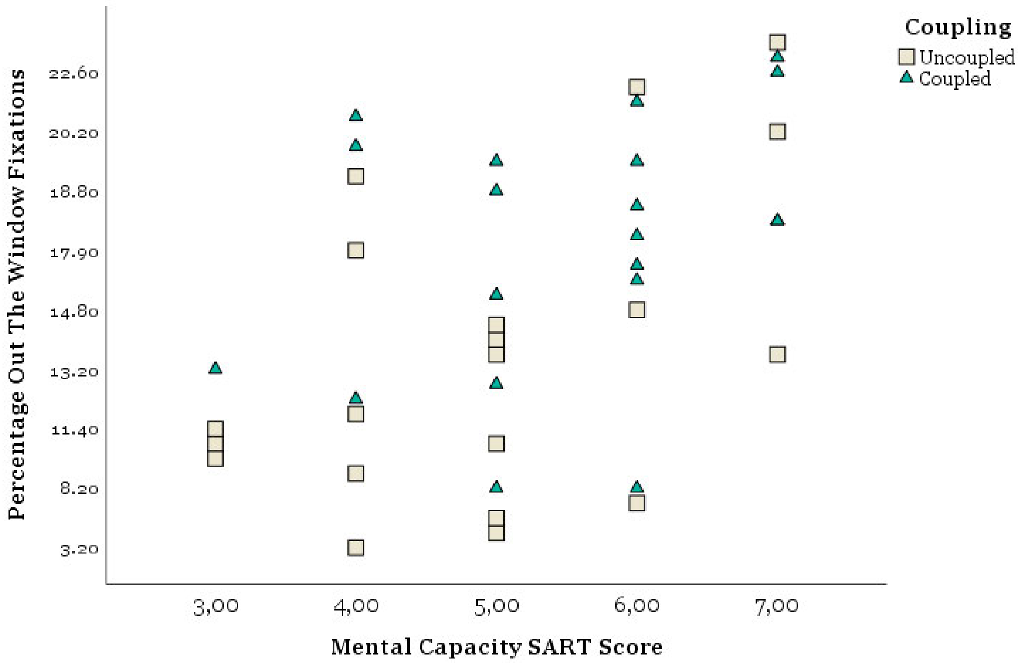

Graph 6.9 Scatterplot of the percentage of OTW eye fixations during approach and the perceived spare mental capacity on the SART questionnaire

6.6 Multivariate analysis of variance on hard landing results

In the previous sections of this chapter, the differences between coupled and uncoupled flight control configurations are compared on a single dependent variable. In this section, the differences are tested on the entire range of variables using a multivariate analysis of variance (MANOVA). The MANOVA controls for the risk of type 1 error (Pallant, 2013). Before the MANOVA is performed, a multivariate test for normality is carried out. The Mahalanobis distance is compared for each individual participant. According to Tabachnick and Fidell (1996), the critical Mahalanobis value for a MANOVA with nine dependent values should not exceed the critical value of 27.88; the test for multivariate normality shows no violation of this critical value. Some of the variables are a combination of other variables, such as TLX score and SART score; this is referred to as 'singularity' and as such the subscales are not taken into consideration by this analyses. The same is true for variables that are highly correlated, referred to as 'collinearity'. Variables such as RMSSD and p50NN or 'altitude of intervention' and 'time till touchdown at moment of intervention' are multicollinear variables and as such, some of these will not be taken into account in this MANOVA. The nine dependent variables that are included in the multivariate analyses are visible in **Table 6.7**. The independent variable in this test was flight control configuration (coupled and uncoupled). Preliminary assumption testing was conducted to check for normality, linearity, homogeneity of variance and multicollinearity; no violations were observed. The result of the MANOVA test can be seen in **Table 6.7**. There was a statistically significant difference between the results of the uncoupled and coupled flight control groups on the combined dependent variables: $F(9, 20) = 5.7$, $p = 0.001$; Pillai's trace = 0.72; partial eta squared = 0.72. When the results for the dependent values were considered separately, the only two variables to reach statistical significance (using a Bonferroni-adjusted alpha level of 0.0055) were ER-SCR amplitude ($F = 6.23$, $p = 0.005$, eta squared = 0.29) and time till touchdown at moment of intervention ($F = 23.4$, $p = 0.00$, eta squared = 0.45).

	F	*Significance*	*Bonferroni Adjustment*	*Eta Squared*
ER-SCR Amplitude	6.52	.005	.0055	.291
Percentage OTW Eye Fixations	5.43	.027	.0055	.162
RMSSD	6.47	.017	.0055	.188
Time Till Touchdown at Moment of Intervention	24.46	.000	.0055	.456
Acceleration	6.89	.014	.0055	.198
Total TLX Score	4.26	.032	.0055	.154
Total SART Score	5.08	.058	.0055	.132
Perceived Surprise	6.27	.018	.0055	.852
Perceived Startle	4.66	.032	.0055	.872

Table 6.7 Results of multivariate analysis of variance with Bonferroni adjustment on hard landing results

6.7 Discussion of the results

The discussion of the results is divided into objective measures, subjective measures, physiological measures and an overall conclusion.

6.7.1 Discussion of objective measures: Hard landing scenarios

Statistical analysis of results for the objective performance metrics indicated a multitude of significant differences between the same scenarios for different flight control configurations. The foremost result is the significantly higher number of hard landings prevented in coupled stick configurations. In coupled stick configurations, 80% of the hard landings were prevented by a correct take-over. By contrast, for the uncoupled configuration, only 10% of hard landings were prevented. The high number of prevented hard landings on coupled flight controls is supported by the research of Uehara (2013, 2015) who did not measure successful interventions, but rather measured improved take-over time. The high number of hard landings on uncoupled flight controls supports and explains the results of the statistical study in Chapter 4.

Another significant result is the high number of verbal interventions that occurred on the coupled flight control configuration. Of the 16 physical interventions on the coupled flight control configuration, 81% of the pilots verbally intervened an average of 0.84 seconds before physically intervening; this can be considered a crucial aspect of the take-over procedure. This outcome supports the claims by Field & Harris (1998) and Uehara (2013, 2015) that pilots are more aware of incorrect flight control inputs and anticipate a possible intervention. Besides that, it supports Field and Harris' explanation that the cross-coupling between the flight control inceptors is a way in which pilots communicate (Field & Harris, 1998). When related to the three-level SA model by Endsley, discussed in section 2.1.2, one possible explanation is that, due to the coupled stick configuration, pilots *perceive* and *comprehend* (level 1 and level 2) a wrongly initiated flare manoeuvre. Their *projection on future state* (level 3) for these pilots is that they anticipate the availability if sufficient time to verbally intervene and perceive if proper reaction is initiated by the PF (SA feedback loop). Anticipating that the flare is incorrectly initiated may also explain why take-over reactions in the coupled flight control configuration are less startled and have less extreme stick deflections. In six out of the nine physical interventions on the uncoupled flight controls, PMs initiated a take-over with a 100% stick deflection on touchdown; some pilots even put multiple 100% stick deflections in three different directions, which in many cases resulted in a floated landing – and in one case, an engine pod strike. This can be interpretated as a startled response and may the result of the pilot's inability to perceive what flight control inputs were being made. Following an analyses of multiple tailstrike incidents, the AAIB found that in such occurrences, the sidestick position was between 75% and 100%, whereas the average sidestick position during normal landing landings does not exceed 37%. In the light of the results, it can be stated that the application of coupled sidesticks not only reduces the number of hard landings; the extreme take-over reactions (100% aft stick deflection) seen on the uncoupled flight control hard landings are also a pre-cursor for potential tailstrike events on landing (AAIB, 2000). By providing haptic feedback through the use of coupling the sidesticks, the take-over reaction from the monitoring pilot shows much less extreme stick deflections during take-over.

Besides the high number of hard landings that occurred on the uncoupled flight control configurations, only nine participants physically intervened on the uncoupled flight control configuration, and three participants verbally intervened before the hard landing took place. Of these nine physical interventions, five (55%) were incorrect physical interventions. During these incorrect interventions, the take-over push button was not pressed, causing a dual input as explained in Chapter 2. This finding tends to support the hypotheses of the Air Accident Investigation Branch (AAIB), namely that use of the take-over push button is not instinctive during sudden take-over actions initiated by the PM (AAIB, 2006, 2008). All five of these incorrect interventions involved Airbus-rated pilots. There were no incorrect take-overs on the coupled flight control configuration because there is no procedure required, making the take-over in a sudden event much more intuitive.

Finally, one statistic showed significant differences between Airbus-rated and non-Airbus-rated pilots, namely hard landing acceleration. **Graph 6.2** shows that the landing acceleration was significantly higher for non-Airbus-rated pilots; however, it was higher on both uncoupled and coupled configurations. This difference can be explained by the pilots' lack of familiarity with Airbus systems. However, the paired samples *t*-test showed that both Airbus-rated and non-Airbus-rated pilots significantly improved on landing acceleration when flying with the coupled flight control configuration, as can be seen in **Graph 6.1**. This finding constitutes a major contribution to aviation safety because it shows that the application of coupled sidesticks improves landing acceleration, regardless of experience, potentially reducing the number of hard landings in commercial aviation.

6.7.2 Discussion of subjective measures: Hard landing scenarios

6.7.2.a NASA TLX

The NASA Task Load Index metric shows significant differences in perceived workload between the two flight control configurations. In section 6.3 it became apparent that for both the normal landing and hard landing scenarios, PMs' total perceived workload is significantly lower on the coupled flight control configuration. According to Hart and Staveland (1988), the mean TLX scores are considered to be 'somewhat high'. One possible reason for this fairly low overall TLX score is the fact that the entire experiment was conducted on a simulator, where there were no negative consequences for the participant if the flight scenario resulted in a crash. This is therefore a major limitation for this study. Even though the use of flight simulators is common practice in aviation and in aviation research, it does not provide the degree of realism an actual flight does. However, it is assumed that for these professional pilots, there is a social pressure to perform well to avoid losing face during a research study.

When the total TLX score is broken down in to the different subsections, three subsections emerge that differ significantly between the two flight control configurations. On the normal approach scenarios, the perceived temporal demand is significantly lower; the aviation literature offers no definitive explanation. However, research in the manufacturing field found that an increase in temporal demand is the main indicator for higher perceived mental workload (Puspawardhani et al., 2016). During the hard landing scenarios, the TLX subsections of mental demand and effort are significantly lower on the coupled flight control configuration, which tends to support the current literature (Field & Harris, 1998;

Summers et al., 1987; Uehara, 2014; Van Baelen et al., 2021) stating that the application of haptic feedback lowers the perceived mental demand and effort of a monitoring task in comparison to the uncoupled flight control configuration. In other words, accurate monitoring becomes less mentally demanding and requires less effort with the application of haptic feedback through the coupled flight controls. A lower experienced workload due to the application of information throughout the haptic channel is also supported by the multiple resource theory, as discussed in section 0.

6.7.2.b Situation Awareness Rating Technique

Perceived SA during this experiment is measured using the Situation Awareness Rating Technique (SART). The results show no clear significant difference between the two flight control configurations, although it can be seen in section 6.3.2 that there is a small, insignificant increase in SA on the total score. However, the subscale of spare mental capacity shows significantly more spare mental capacity on the coupled flight control configuration. SART is a relatively old method of assessing SA and dates back to 1990. The disadvantages of the SART are the participants capability of assessing their own SA (Endsley et al., 2000; Endsley et al., 1998; Salmon et al., 2009). Furthermore, participants are also prone to forgetting periods of lower SA, calling into question the test's validity on longer scenarios such as those in this study. However, the overall SART results correlate with the HRV measure RMSSD, which shows significantly longer time between heartbeats, indicating a less stressed participant. Additionally, a very strong correlation is found between the participants who rated high spare mental capacity and the percentage of OTW eye fixations, indicating a possible relation between OTW and workload.

6.7.2.c Startle and surprise questionnaire

All participants were subjected to a startle and surprise questionnaire after each scenario. There were significant differences found in the Likert-scale responses to several questions. First, a statistically significantly lower perceived startle was found on the hard landing scenarios flown in the coupled flight control configuration. A surprise in this study is defined as an emotional state which is the result of a mismatch between expected and perceived information. This lower score can be explained by the fact that during the coupled flight control configuration, more information is provided to the PM, which reduces the mismatch between expected and perceived information. Another reason for this significant difference is the fact that the majority of the physical take-overs were preceded by a verbal intervention. This means that the participant notices the incorrect flight control movements much sooner, leaving more time to process and react to the situation. Second, a statistically significant difference was found on the perceived startle scores, which were significantly lower on the scenarios flown with the coupled flight control configuration. This self-assessment is supported by the fact that in the uncoupled flight control configurations, a number of participants' take-overs were not in accordance with normal take-over procedures; furthermore, some participants made multiple 100% stick deflections in several directions, indicating a startled response.

The above finding is strengthened by the results from the ER-SCR amplitudes. As discussed in section 6.5.4, a strong correlation is found between the perceived startle and the magnitude of the ER-SCR amplitude (p = 0.007). These startle scores also strongly correlate with the measured landing acceleration and altitude of which participants intervened. This is mainly because participants are noticing the incorrect flare manoeuvre at an earlier stage of the landing phase, rendering the startle less intense. Finally, the perceived result of the situation has shown significant differences. Pilots on the coupled flight control configuration rated their actions as more successful than those on the uncoupled flight control configuration. This can be explained by the fact that 80% of the participants on the coupled flight control configuration intervened successfully, compared to only 10% on the uncoupled flight control configuration.

6.7.3 Discussion of physiological results

6.7.3.a Electrodermal activity

Based on the literature, analysing activation of sympathetic and parasympathetic nervous system via electrodermal activity is a common practice for measuring emotional arousal (Bach et al., 2010; Dawson et al., 2016; Posada-Quintero & Chon, 2020). The results discussed in section 6.4.5 showed a significant difference in ER-

SCR (p = 0.017). SCR magnitude on the uncoupled hard landing scenarios was significantly higher than on the coupled hard landing scenarios. This corroborates the finding that participants on the uncoupled flight control configuration reported higher levels of startle and surprise. The relationship between the ER-SCR and the startle and surprise questionnaire questions is therefore strongly correlated (p = 0.03). The relationship between ER-SCR and time till touchdown at which a physical intervention took place are also strongly correlated. This indicates that the physiological measurements support the theory that a reduction in perceived mental workload results in a measurable physical galvanic skin response (Benedek & Kaernbach, 2010; Charles & Nixon, 2019; Wang et al., 2012).

6.7.3.b Heart rate variability

Based on the literature review, the method of comparing root mean square of successive differences (RMSSD) in heart rate variability is a valid method for physiologically assessing a participant's mental workload. However, the major flaw in employing RMSSD is the duration over which it was used; this metric has been used only for short time domain areas. The results tend to be in line with other relevant research in the aviation (Borghini et al., 2014; Kim et al., 2017; Svensson et al., 1997) and automotive domains (Causse et al., 2010; Melnicuk et al., 2017; Mulder et al., 2004). The time domain measurements taken are the RMSSD p50NN, whose results show that the RMSSD is significantly lower on the scenarios flown in uncoupled flight control configuration. A lower RMSSD is associated with stress and an increase in mental demand. This finding is firmly in line with the current literature (Borghini et al., 2014; Causse et al., 2010; Kim et al., 2017; Kinney & O'Hare, 2020; Melnicuk et al., 2016; Saus et al., 2012). As discussed in Chapter 2 section 2.1.4.d, the HRV results in a simulator experiment do not differ significantly from HRV measurements in real aircraft experiments (Veltman, 2002; Veltman & Gaillard, 1996). The RMSSD value also correlates with the perceived workload measured in the NASA TLX; this correlation shows a close interconnection between the three domains of measurements: objective, subjective and physiological results correlate significantly with one another – all indicating that coupled sidesticks are more favourable during hard landing scenarios.

6.7.3.c Eye tracking

During all approach phases, the eye-tracking system recorded eye fixations based on the intersection of objects programmed in the world coordinate system of the eye-tracking system. A significant difference is found between the coupled and uncoupled flight control configurations in the number of OTW eye fixations: On the uncoupled system, the percentage of OTW eye fixations was measured at 12.2%, whereas on the coupled flight control configuration this percentage rose to 17.4%. Although the literature on this subject in aviation is limited, in automotive several studies have shown that OTW time is associated with lower mental workload (Chihara et al., 2020; Marquart et al., 2015; Young & Stanton, 1997). This is also supported by the strong correlation found between the percentage of OTW eye fixation and the scores on the SART subdomain Spare Mental Capacity. One study hypothesised that increased OTW fixations may be the result of a lower workload (Glaholt, 2014). This appears plausible, given that the TLX, SART and physiological measures all indicate a lower workload experienced by the pilots on the coupled flight control configuration. This could mean that because the participants are receiving more information through their haptic information channel, there is less need to accurately monitor their primary flight displays by actively seeking out information on the aircraft state. This means that participants experiencing a lower workload will have more spare mental capacity to focus on less relevant parameters, such as the state of the aircraft in relation to the runway, or looking for other OTW factors such as other traffic or the presence of birds. This is supported by the significant correlation between the percentage of OTW eye fixations and the results from the SART Likert-scale subdomain of spare mental capacity (p = 0.00). These results, in turn, are supported by Wickens's MRT (2008), whereby the use of multiple resources to perceive information increases spare mental capacity, thus improving task performance. These results combined to support the fact that PMs are experiencing a lower workload and therefore have more spare mental capacity to focus on other things, such as looking outside.

6.8 Conclusions

This study investigated the effects of coupled and uncoupled flight control configurations for PM during hard landing scenarios. Its results suggest a difference in awareness for the PM in objective, subjective and physiological data. As previous literature pointed out (Summers et al., 1987; Uehara & Niedermeier, 2015; Wolfert et al., 2019), passive sidestick control inceptors may limit the PM's ability to accurately monitor. Endsley (1995) stated that the utilisation of several sensory modalities enhances SA, and even though SART results did not show significant differences between the flight controls, it can be concluded that by providing tactile cues to the monitoring pilot, sensory modalities provide a substantial increase in SA. The high number of prevented hard landings, the high number of verbal interventions, and the reduced stick deflections for both Airbus-rated and non-Airbus-rated pilots show that providing haptic feedback allows the pilot to accurately anticipate future aircraft states, which, in combination with a perceived reduction of mental workload and a higher performance in terms of correct landings, shows that the cross-coupling of the flight controls has a major benefit for flight safety during the landing phase.

All these results combined suggest that the effect of proprioceptive cueing has a more powerful effect on the pilot's monitoring ability to act in a non-normal situation than previously thought. The leading factor for this case is the fact that the none of the pilots that participated have previously flown with coupled sidesticks in a commercial aircraft. However they are showing a significant increase in performances, subjective and physiological measurements in comparison to a system that that 80% of the participants had extensive experience on.

Chapter 7 Effects of Coupled Sidesticks on Pilot Monitoring Awareness during Take-off Tailstrike Scenarios

Taking cues from the results of the statistical review on hard landings in Chapter 5, Chapter 7 describes the experimentation process in order to evaluate the contribution of haptic feedback cues for a PM during normal and tailstrike take-off scenarios. This experimental study is the culmination of the human factors considerations stated in Chapter 2 and the significant results in Chapter 5 and 6. The study is designed to resemble a normal multi-pilot flight deck of a representative transport jet aircraft.

7.1 Experimental method

The experimental methods for this study have been described in Chapter 3, paragraph 3.2. This section contains a brief summary of the experimental design of the study.

The aim of this study is to evaluate the effects of passive and active sidesticks on monitoring duties during tail-strikes and normal take-off scenario's. The experiment was conducted using an Airbus A320 fixed-base simulator at Coventry University. Pilots with an Air Transport Pilot Licence where invited to participate. During the experiments, pilots were sat in an Airbus A320 static simulator with an Airbus 320 flight instructor who acted as PF for the scenario's and were tasked to monitor flights according to their company policies. During two of the take-off scenarios the PF initiated an incorrect flare manoeuvre. Several quantitative and qualitive data points were gathered, which will be discussed in the following sections.

7.2 Objective results

7.2.1 Tailstrike occurrences

This experiment aimed to see whether PMs could intervene correctly during a deliberately initiated improper take-off rotation, comparing their performance on two different flight control configurations. In order to determine whether the tail touched the ground, the design characteristics of the Airbus A320 are taken into account. According to the Airbus A320 FCOM, a tailstrike occurs when a pitch angle is reached of 11.7 degrees whilst the main landing gear struts are still compressed (Airbus SE, 2017). The parameters of pitch attitude and landing gear compression are measured by the simulator software. Therefore, any simulated take-off in which the main landing gear is compressed and a pitch attitude of 11.7 degrees or more is reached is classified as a tailstrike occurrence. Of the 40 tailstrike scenarios, there were 22 occurrences in which the tail came into contact with the ground. Of the 20 tailstrike scenarios in uncoupled configuration, 16 ended up in a tailstrike (80% of all uncoupled tailstrike scenarios). By contrast, for the coupled configuration, only six of the 20 scenarios resulted in a tailstrike. A histogram plot of these tailstrike occurrence numbers broken down in the two different flight control configuration can be seen in a chi-square test for independence (Yates continuity correction), which indicated significant associations between the two flight control groups, divided into coupled and uncoupled flight control configurations, compared to the frequencies of tailstrike occurrences during the scenarios; $\chi 2$ (1 *df*, n = 40, phi = 0.503) = 10.01, p = 0.01. The number of prevented and occurred tailstrikes can be seen in Bar chart 7.1.

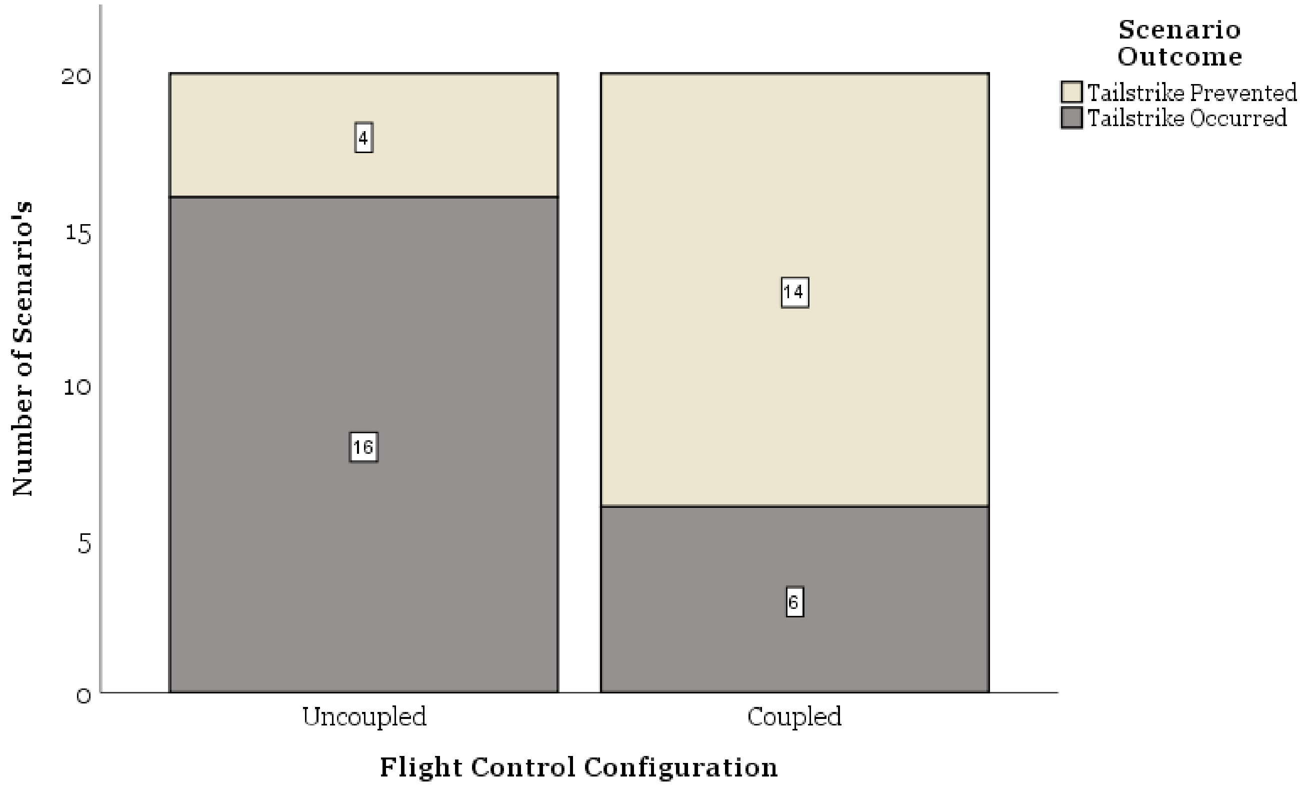

Bar chart 7.1 Histogram of tailstrike occurrence frequencies per flight control configuration

7.2.2 Tailstrike physical interventions: Pilot monitoring

During the tailstrike scenarios, several parameters were measured. One of the leading parameters in this study is the number of times each participant physically intervenes with the improperly initiated take-off rotation. This data is retrieved via the simulator's data-gathering software, which measures stick inputs from both sides. Video recordings are also gathered from the wall-mounted cameras, which capture the PM's flight control inceptor from four angles. In this study, a 'physical intervention' is defined as any manual control take-over intended to prevent a tailstrike. During the tailstrike scenarios, the PF will deliberately begin over-rotating once the Vr call is made. This is done by applying a 100% aft stick deflection for a period of 10 seconds. Of the uncoupled tailstrike scenarios, there were four successful physical interventions that prevented the aircraft from touching the ground. The mean time of these interventions was measured at 3.14 seconds after the rotation was initiated. Another five physical interventions occurred during or after the tailstrike. This sums up to a total of nine physical interventions on the uncoupled flight control configuration. The mean time of these combined interventions is 6.1 seconds, with an average maximum pitch attitude of 10.9 degrees. The other 11 participants either did not physically intervene, or else they intervened after Alpha Floor was initiated.

Figure 7.1 Mean physical interventions during tailstrike event on uncoupled configuration

For the tailstrike scenarios with the coupled flight control configuration, a total of 14 successful interventions occurred. The mean time of these interventions occurred at 2.4 seconds after the rotation was initiated. Another four physical interventions took place during the tailstrike or slightly afterward. This sums up to a total of 18 physical interventions on the coupled flight control flown scenarios with a mean intervention time of 2.7 seconds after the rotation was initiated. The mean value of the maximum reached pitch attitude during the coupled flight control tailstrike scenarios was 9.2 degrees. The remaining two participants did not physically intervene during the tailstrike scenario; one participant physically intervened after the initialisation of the Alpha Floor modus.

Figure 7.2 Mean physical interventions during tailstrike event on coupled flight control configuration

A paired-samples *t*-test found a significant difference between physical intervention times (in seconds) from the initialisation of the rotation for the uncoupled (M = 6.01, SD = 1.84) and coupled flight control configuration (M = 2.93, SD = 1.71); $N_{pairs} = 8$, $t = 2.82$, $p = 0.020$. Preliminary analyses were performed to avoid violating assumptions of normality. The effect size is considered to be large (Eta squared = 0.53).

7.2.3 Tailstrike verbal interventions: Pilot monitoring

Alongside physical interventions, the PM's verbal interventions are also considered crucial in answering the main research questions. A 'verbal intervention' is defined as any oral notification to the PF that either pitch or stick input is exceeding normal values. (Any sounds or expressions as a result of a startle or surprise reaction are not considered verbal interventions.) For the uncoupled flight control tailstrike scenarios, only one participant verbally intervened before the tail touched the ground; this participant verbally intervened whilst simultaneously initiating a physical take-over. A total of nine participants verbally intervened during or after the tailstrike occurred. These 11 verbal interventions combined resulted in a mean verbal intervention time of 6.3 seconds after the rotation was initiated. The mean value of the maximum reached pitch attitude on ground was measured at 11.5 degrees.

Figure 7.3 Mean verbal interventions during tailstrike event on uncoupled configuration

For the coupled flight control tailstrike scenarios, 12 participants verbally intervened before the tail touched the ground. Two of these participants intervened within half a second after the 100% stick deflection was reached by saying: 'watch stick' and 'too much'. Both of these participants physically intervened after another half second. Ten out of these 12 verbal interventions were followed by a physical intervention preventing the tail from touching the ground. Four physical interventions took place on the coupled flight control configuration without a verbal intervention. Another four participants verbally intervened during or after the tailstrike. These 16 verbal interventions combined had a mean intervention time of 2.4 seconds after the rotation was initiated. The mean value of the maximum reached pitch attitude on ground was measured at 8.9 degrees.

Figure 7.4 Mean verbal interventions during tailstrike event on coupled flight control configuration

A Shapiro-Wilks test for normality showed a violation of the assumption of normality (p=0.038) , therefore a non-parametric test is used. A Wilcoxon Signed Rank test revealed a statistically significant difference between verbal intervention times from the initialisation of the rotation for the uncoupled (M = 6.35, SD = 0.62) and coupled flight control configurations (M = 2.81, SD = 1.31); $N_{pairs} = 6$, z = -2.02 p = 0.028. The effect size is considered to be large (Eta squared = 0.81).

7.2.4 Maximum recorded pitch attitude on ground

As part of the simulator output, the pitch attitude of each flown scenario is registered. The pitch attitude discussed in this section is the highest recorded value for pitch attitude with the main landing gear struts compressed. The Airbus A320 used in this study has a tailstrike pitch attitude of 11.7 degrees with main landing gear struts compressed; on three occasions, the pitch angle exceeded this value. As discussed in section 7.2.1, the aircraft can reach a higher pitch attitude by rotating over the tail section. In such situations, the weight on wheel switch located in the main landing gear is still compressed, and is therefore still registered. A boxplot of all maximum reached pitch attitudes during the tailstrike scenarios can be found in **Graph 7.1** A paired-samples *t*-test was conducted to evaluate the impact of the coupling between the sticks on the maximum recorded pitch attitude during the tailstrike scenarios. Preliminary analyses were performed to avoid violating assumptions of normality. A statistically significant decrease is found in the maximum recorded pitch attitude on ground for the coupled flight control configuration (M = 9.50, SD = 1.72) in comparison to the maximum record values of the uncoupled control inceptor configuration (M = 11.47, SD = 0.51), $t\,(20) = 3.15$, $p = .005$ (two-tailed). The effect size is considered to be large (Eta squared = 0.66). This significant difference can mainly be explained by the previous results: The number of successful physical interventions on the coupled flight control scenarios was 14, compared to four for the uncoupled flight control scenarios.

The occurrence of a tailstrike is partially dependent on the stick inputs being made, and the PF is flying all scenarios by hand, without the use of auto-throttle or automated flight systems. In order to ensure that all scenarios are flown with a consistent angular velocity, both angular speeds over the last second are compared. The normal maximum allowed angular rotation speed on an Airbus A320 is 3 degrees per second. During the last second of the simulation trials, a mean angular velocity of 7.5 degrees per second was reached. However, the majority of the coupled flight control scenarios had a physical intervention, which often prevented reaching higher angular velocities. Thus, the average angular velocities are compared from the initialisation of the rotation towards 2.4 seconds in the rotation because the mean physical interventions on the coupled flight control scenarios occurred at this time. A paired-samples *t*-test was conducted to evaluate the effects on the angular velocity during the first 2.4 seconds of the rotation at all tailstrike scenarios. Preliminary analyses were performed to avoid violating assumptions of normality. No statistically significant difference is found in the recorded angular velocities between the uncoupled control inceptor configuration (M = 1.83, SD = 0.32) and the coupled flight control configuration (M = 1.79, SD = 0.36), t (20) = 0.82, p = 0.83 (two-tailed). The relationship between the average angular velocity over the first 2.4 seconds of each tailstrike scenario and the maximum recorded pitch attitude was investigated using Pearson product moment correlation coefficient, which found no significant correlation between the two variables, r = 0.03, p = 0.86.

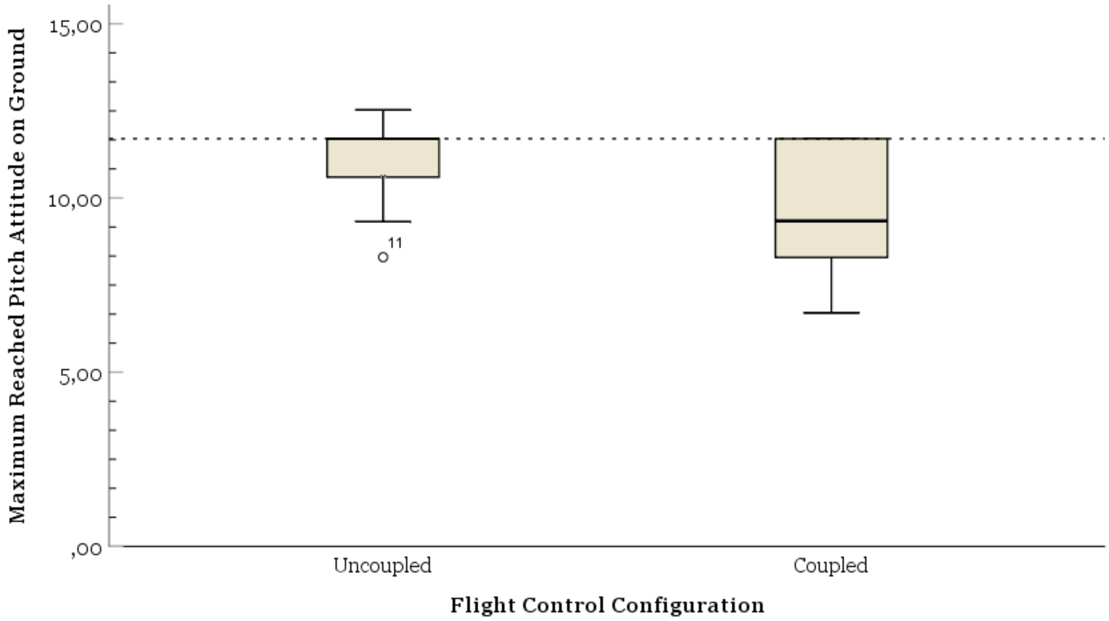

Graph 7.1 Boxplot of maximum recorded pitch attitude on ground per flight control configuration with a 11.7-degree reference line

7.2.5 Hours on type versus tailstrike

The relationship between maximum recorded pitch attitude on ground is compared to each participant's total flying hours. Because preliminary analyses violated the assumption of normality, a non-parametric test (Spearman rank correlation coefficient) was used, which found no significant correlation between the two variables, *rho* = 0.31, n = 40, p = 0.54.

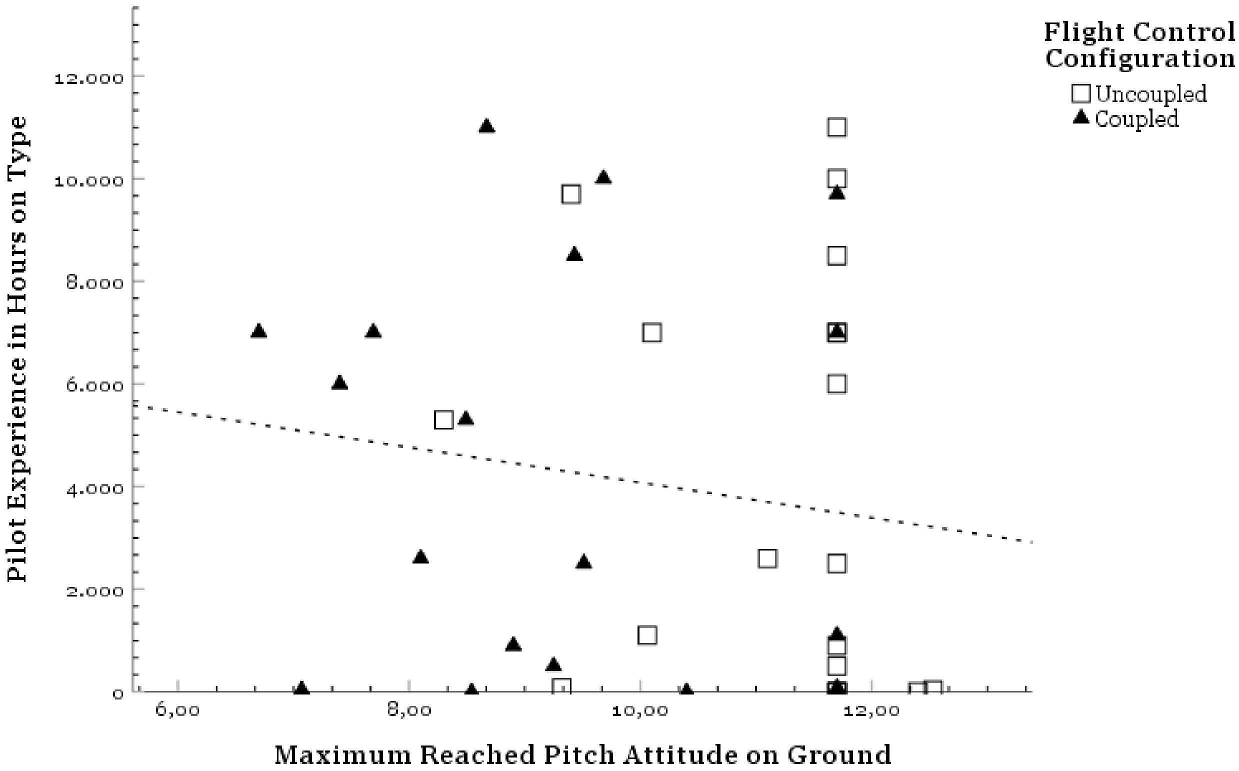

Graph 7.2 Scatterplot of pilot experience (in hours) on type and maximum reached pitch attitude on ground

7.3 Subjective results

7.3.1 Perceived workload tailstrike scenarios

Each participant completed a digital weighted NASA TLX at the end of each take-off scenario. This digital survey focusses on six different subscales of perceived workload which, together, constitute total perceived workload. The mean weighted TLX score per scenario can be seen in **Graph 7.3**, which shows that total weighted TLX score per scenario is lower for all scenarios flown in the coupled flight control configuration. A paired-samples *t*-test was conducted to evaluate the impact of the coupling between the sticks on the normal take-off scenarios. Preliminary analyses were performed to avoid violating assumptions of normality. No significant difference was found between TLX scores for take-off scenarios flown with the uncoupled flight control configuration (M = 34.00, SD = 17.12) and TLX scores for take-off scenarios flown with the coupled flight control configuration (M = 27.13, SD = 15.01), $t\ (19) = 1.7$, $p = 0.10$ (two-tailed).

For the tailstrike scenarios, a paired-samples *t*-test was conducted to evaluate the impact of the coupling between the two flight control configurations on the total TLX score. Preliminary analyses were performed to avoid violating assumptions of normality. A statistically significant difference was found between the TLX scores measured on the uncoupled flight control configuration (M = 51.17, SD = 17.84) and the TLX scores measured on the coupled flight control configuration (M = 40.50, SD = 14.37), $t\ (19) = 3.08$, $p < .005$ (two-tailed). The magnitude of this difference in means is large (Cohen's $d = 0.57$). As previously mentioned, these overall workload scores can be broken down into the six different subscales of the NASA TLX. Because the normal take-off scenarios showed no significant differences in total workload between coupled and uncoupled configurations, a significance test on the subscales is irrelevant. Therefore, a paired-sample *t*-test was conducted on all NASA TLX subscales for the tailstrike scenarios. This section will discuss only the significant results of the paired-samples *t*-test, which can be seen in **Table 7.1**.

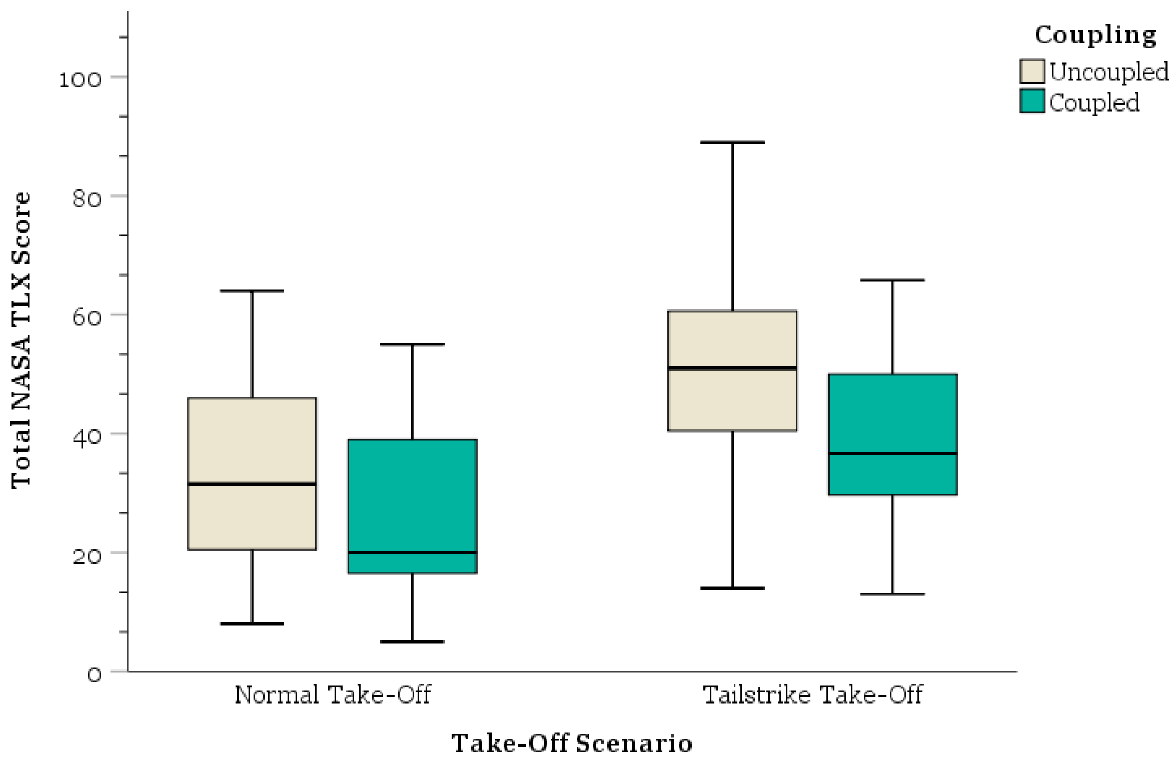

Graph 7.3 Boxplot of perceived workload measured by NASA TLX for normal and tailstrike take-off scenarios

Scenario	*TLX Subsection*	*Configuration*	*M*	*SD*	*t (19)*	*Sig (2-tailed)*	*Effect Size (Eta squared)*
Tailstrike	Total TLX	Uncoupled	51.17	17.84	3.07	.005	0.33
		Coupled	40.49	14.37			
Tailstrike	Mental Demand	Uncoupled	237.75	100.11	3.04	.006	0.32
		Coupled	160.75	89.00			
Tailstrike	Frustration	Uncoupled	113.50	116.38	3.09	.005	0.33
		Coupled	29.25	46.14			

Table 7.1 Significant outcomes of the paired-samples *t*-test of NASA TLX subscale scores between the uncoupled and coupled flight control configurations during tailstrike scenarios

7.3.2 Tailstrike perceived surprise and startle related to flight control configuration

Because the sample size for statistical analyses is lower than 20, the required statistical power is calculated and taken into account before analysis. According to Cohen (1988), the minimal statistical power is 0.80; therefore, any significant value with a statistical power lower than 0.80 will not be discussed. **Table 6.4** shows the calculated power per questionnaire item. A paired-samples *t*-test on each individual question was performed, which showed no significant differences between any of the flight control configurations. A boxplot of each Likert-scale value can be found in **Graph 6.8**. Preliminary analyses were performed to avoid violating assumptions of normality. A paired-samples *t*-test was conducted on all four questions of the startle and surprise questionnaire; none of its items showed significant differences between the coupled and uncoupled flight control configurations, as seen in **Table 7.2**.

Tailstrike Question	$Mean_{Uncoupled}$	Sd	$Mean_{Coupled}$	Sd	Sample size	Statistical Power	Paired-sample T-test P-Value	Effect Size (Eta squared)
Q1) Perceived Surprise	5.0	2.11	4.11	2.08	18	0.81	0.18	0.18
Q2) Perceived Startle	5.9	2.66	4.66	1.90	18	0.90	0.35	0.22
Q3) Perceived Response	6.00	2.55	7.44	1.55	18	0.84	0.45	0.31
Q4) Perceived Result	7.88	8.66	8.1	1.83	18	0.94	0.18	0.56

Table 7.2 Tailstrike scenarios startle and surprise questions paired-samples *t*-test results

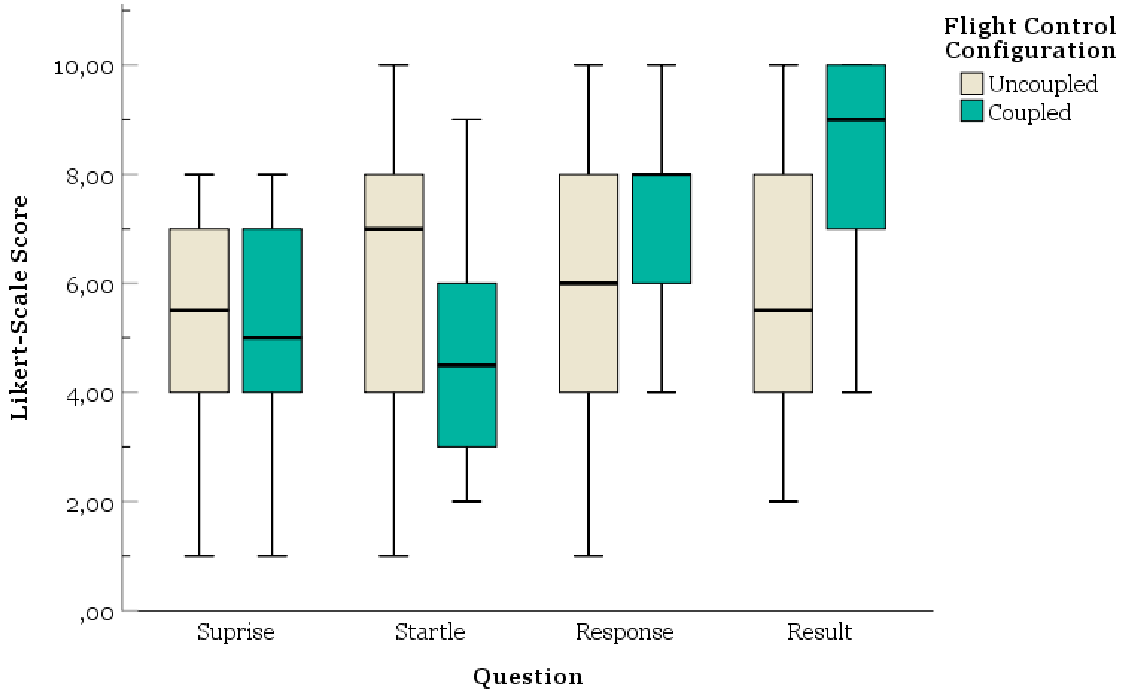

Graph 7.4 Boxplot of startle and surprise Likert-scale scores on tailstrike scenarios

7.3.3 Situation Awareness Rating Technique: Tailstrike scenarios

Differences were identified in the total SART score, which was higher for tailstrike scenarios with the coupled flight control configuration (M = 18.8, SD = 5.38) than for the same scenarios with the uncoupled configuration (M = 16.8, SD = 4.64). This difference was analysed through a paired-samples *t*-test, which showed that the difference was not significant (t = -2.0, p = 0.06). Preliminary analyses were performed to avoid violating assumptions of normality. All other subdomain of the SART questionnaire have been analysed through a paired-samples *t*-test, for which the results can be found in **Table 7.3**. The table shows a significant difference in the 'understanding' domain (t = -2.4, p = 0.02), which was significantly higher on the coupled flight control configuration (M = 10.5, SD = 1.98) than on the uncoupled configuration (M = 9.3, SD = 1.75). The effect size is considered to be large (Eta squared = 0.34). Preliminary analyses were performed to avoid violating assumptions of normality. This difference in score is mainly the result of a significant difference in the rated quantity of information section. The difference in the rated quantities of information between the scenarios flown with coupled flight control (M

= 5.5, SD = 1.19) and those with uncoupled flight controls (M = 4.5, SD = 1.27) is assessed using a paired-samples *t*-test, which shows that the perceived information quantity is greater (i.e. more information is received and understood) with the use of coupled flight controls; the difference is significant (t = -2.44, p = 0.025). The effect size is considered to be large (Eta squared = 0.23). Preliminary analyses were performed to avoid violating assumptions of normality.

Scenario	*Configuration*	*M*	*SD*	*t (19)*	*Sig (2-tailed)*	*Effect Size (Eta squared)*
Total SART Score	Uncoupled	16.8	4.64	-2.0	.06	0.17
	Coupled	18.8	5.38			
Attentional Demand	Uncoupled	12.9	4.00	.42	.68	0.009
	Coupled	12.6	3.70			
Attentional Supply	Uncoupled	20.4	3.76	-.73	.69	0.027
	Coupled	20.9	3.50			
Understanding	Uncoupled	9.3	1.75	-3.15	.005	0.34
	Coupled	10.5	1.98			
Quantity of Information	Uncoupled	4.5	1.27	-2.44	.025	0.23
	Coupled	5.5	1.19			
Familiarity of the situation	Uncoupled	4.75	1.51	-.042	.41	>0.001
	Coupled	5.05	1.46			

Table 7.3 Results of paired-samples *t*-test on SART scores and subdomains during tailstrike scenarios

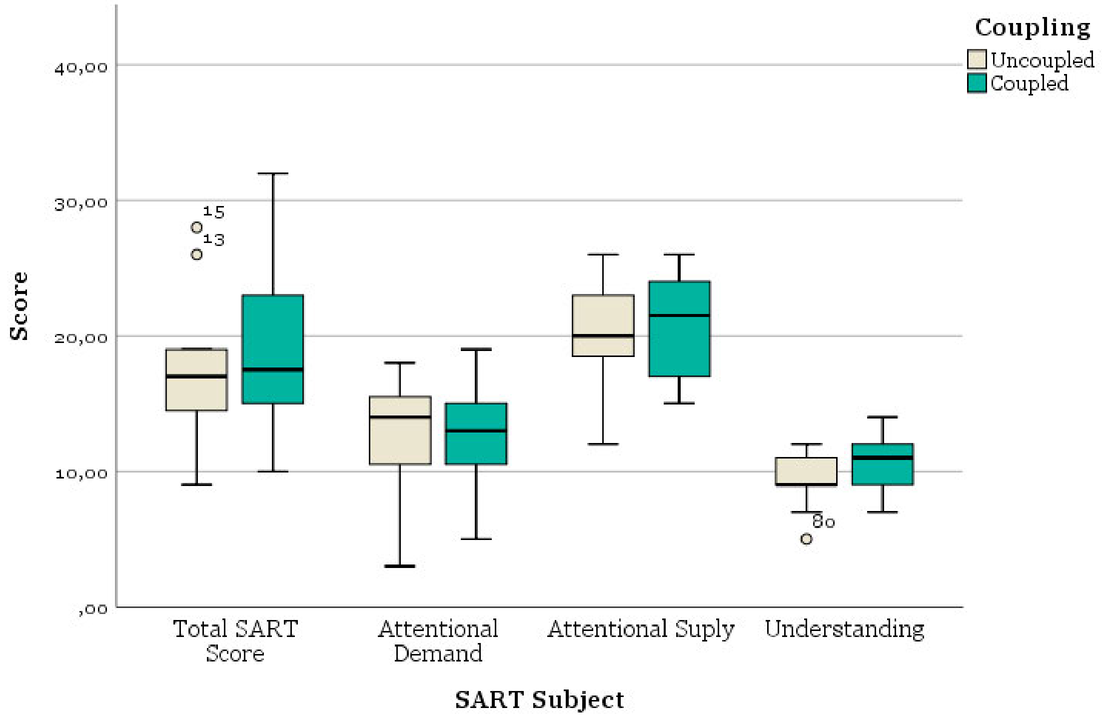

Graph 7.5 Boxplot of SART scores on different SART subdomains between coupled and uncoupled flight controls during tailstrike scenarios

7.4 Physiological results

7.4.1 Proportional dwell time OTW view during take-off

During all take-off phases, no difference is found in the proportionate dwell time in percentage of OTW eye fixations between coupled and uncoupled flight controls. Of the 46 take-off scenarios considered in this analysis, a mean OTW percentage of 6.4% was found on uncoupled flight controls, whereas the same parameter for the coupled flight controls was 5.2%. Preliminary analyses were performed to avoid violating assumptions of normality. A paired-samples *t*-test was conducted to compare the percentage of OTW eye fixation between uncoupled (M = 6.4, SD = 1.68) and coupled (M = 5.2, SD = 1.31); $t = 0.639$, $p = 0.393$; it did not show a significant difference in the percentage of OTW fixations.

Flight control configuration	*Number of take-offs*	*Mean OTW dwell time percentage*	*Std Deviation*
Uncoupled	20	6.4	1.68
Coupled	26	5.2	1.31

Table 7.4 Tailstrike and take-off scenarios OTW eye fixations whole length of the scenario

For accurate comparison to determine whether there is any significant difference in OTW eye fixations during the take-off rotation, the data is capped at the first 2 minutes of the take-off scenario. Of the 46 take-off scenarios considered in this analysis, a mean OTW percentage of 12.9% was found on uncoupled flight controls, whereas the same parameter for the coupled flight controls was 10.3%. Preliminary analyses were performed to avoid violating assumptions of normality. A paired samples t-test was conducted to compare the percentage of OTW eye fixation between uncoupled (M = 12.9, SD = 2.49) and coupled (M = 10.3, SD = 1.13); t = 0.839, p = 0.18, which did not indicate a significant difference in the percentage of OTW fixations.

Flight control configuration	*Number of take-offs*	*Mean OTW during take-off rotation dwell time percentage*	*Std Deviation*
Uncoupled	20	12.9	2.49
Coupled	26	10.3	1.13

Table 7.5 Tailstrike and take-off scenarios OTW eye fixations whole first 2 minutes of take-off roll and rotation

7.4.2 Fixation duration OTW view during take-off

A paired samples t-test was conducted to compare the duration of the OTW eye fixation in ms between uncoupled (M = 208.94, SD = 78.11) and coupled (M = 189.05, SD = 76.71); $t = 0.439$, $p = 0.693$; it showed no significant difference in the duration of OTW fixations. Preliminary analyses were performed to avoid violating assumptions of normality.

7.4.3 Pupil dilation

In addition to the overall quality of the eye-tracking data, SmartEye systems also record the specific quality of certain parameters, namely pupil dilation, heart rate variability, and electrodermal activity. Pupil dilation is scored from 0 to 1 based on the accuracy of the tracked parameter. During the initial simulation trials it became clear that the flight simulator lacks sufficient ambient light to track pupil diameter with high quality. More than half of the simulation scenarios flown lacked reliable pupil diameter data, setting the quality number to 0. For 90% of the data, the mean quality for pupil diameter has been less than 0.4. Therefore, the pupil diameter data has not been taken into account.

7.4.4 Heart rate variability

Regarding heart rate variability, four epochs were deemed unsuitable for analysis; therefore, the analysis described ahead was carried out on the remaining 36 ECG epochs. An overview of the tailstrike RMSSD values can be seen in a boxplot format in **Graph 7.6**. The RMSSD measures were analysed using a paired-samples t-test to determine whether there existed a statistically significant effect of the different flight control configuration. Preliminary analyses were performed to avoid violating assumptions of normality. It found that participants' RMSSD during entire tailstrike take-off scenarios differed, with RMSSD slightly higher whilst using the coupled flight controls (M = 35.0, SD = 3.64) than in the same scenario whilst using uncoupled flight controls (M = 33.0, SD = 3.60); this difference is significant ($t = -3.17$, $p = 0.006$). The effect size is considered to be large (Eta squared = 0.34). When the RMSSD is measured over only the 60 seconds surrounding the tailstrike event, this difference remains apparent; however, this difference is much smaller. Participants' RMSSD during the tailstrike event was higher whilst using the coupled flight controls (M = 33.5, SD = 4.15) than in the same scenario whilst using uncoupled flight controls (M = 32.0, SD = 3.78); this difference is significant (t = -3.41, p = 0.003). The effect size is considered to be large (Eta squared = 0.38). The other HRV measure captured in this experiment is pNN50, which was also analysed using a paired-samples t-test to identify whether the flight control coupling had a significant effect. Preliminary analyses were performed to avoid violating assumptions of normality. It was found that p50NN did not differ significantly between tailstrike scenarios flown with uncoupled flight controls (M = 7.66, SD = 5.260) and those flown with coupled flight controls (M = 8.55, SD = 6.74) (t = -1.20, p = 0.33). A boxplot overview of the pNN50 values can be found in **Graph 7.7**.

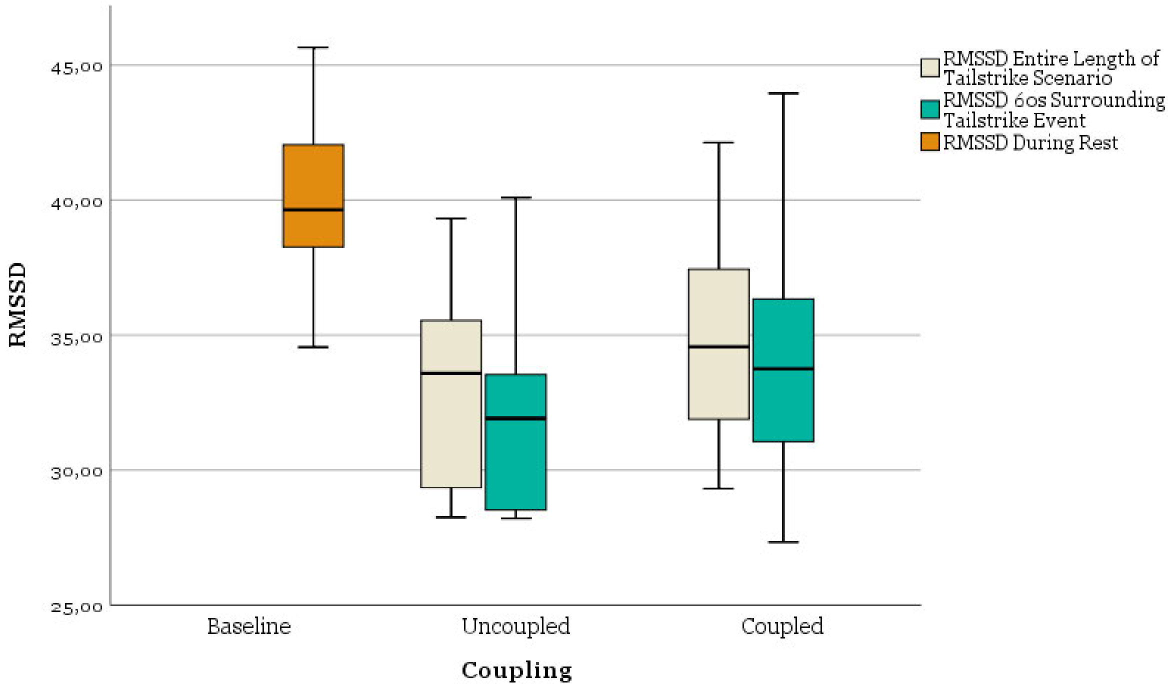

Graph 7.6 Mean RMSSD during resting conditions and tailstrike take-off events

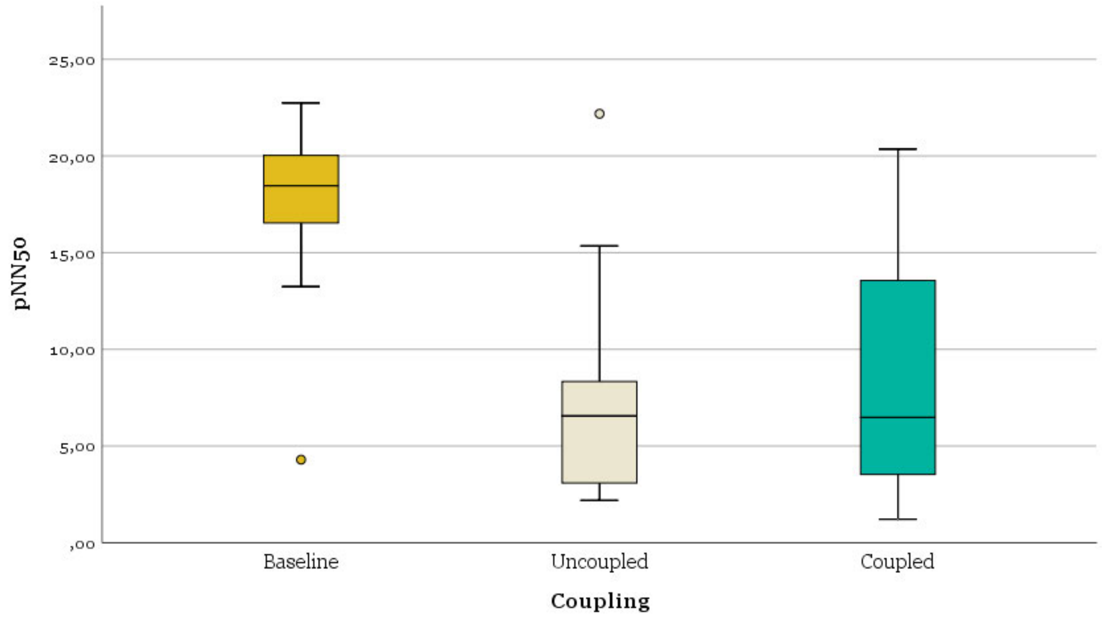

Graph 7.7 Mean pNN50 during resting conditions and tailstrike take-off events

7.4.5 Electrodermal activity

ER-SCR is used to measure electrodermal activity. The SCR peak is taken into account if the waveform onset is at least 10% of the current skin conductance level and if the rise in conductance level occurs between 1 and 5 seconds after the stimulus is provided. In the tailstrike scenarios, the stimulus is the moment where the PF is reaching 100% aft stick deflection. The amplitude of the waveform onset determines the strength of the emotional arousal (Dawson et al., 2016); therefore, the amplitude of the waveform onset is used as a measurement. Because ER-SRC is dependent on a participant's perception of the situation, not all tailstrike take-off scenarios had an ER-SCR. Of the 40 tailstrike scenarios, eight runs had no ER-SCR; in two scenarios the data was unsuitable for analysis. During the normal take-off scenarios, the stimulus is the point where the PF reaches the final stick position for the take-off rotation. During all 20 normal take-off scenarios, only half of the participants showed an ER-SCR to the take-off rotation; therefore, no accurate comparison can be made. An overview of which runs had suitable ER-SCRs can be seen in **Table 7.6**. By comparing ER-SCR amplitudes during tailstrike take-off scenarios for the different flight control types, it is found that the ER-SCR amplitudes are higher for the scenarios with coupled flight controls (M = 2.71, SD = 5.32) than for those with uncoupled flight controls (M = 1.21, SD = 1.70). A Shapiro-Wilks test for normality showed a violation of the assumption of normality $p=0.008$, therefore a non-parametric test is used. A Wilcoxon Signed Rank test found no statistically significant difference between the ER-SCR Amplitudes; $z= -1.4$, $p=0.11$.

Participant Number	*Normal Take-off Coupled*	*Normal Take-off Uncoupled*	*Tailstrike coupled*	*Tailstrike Uncoupled*
1		No ER-SCR		
2	No ER-SCR			
3				
4				No ER-SCR
5		Bad data	Bad data	Bad data
6				
7			No ER-SCR	
8		No ER-SCR		No ER-SCR
9				
10	No ER-SCR			No ER-SCR
11	Bad data			
12				
13		No ER-SCR	No ER-SCR	
14				No ER-SCR
15				
16				
17		No ER-SCR		
18	No ER-SCR			
19	No ER-SCR			
20				
Total EDA data	**5**	**5**	**17**	**15**

Table 7.6 Overview of ER-SCRs on normal and tailstrike take-off scenarios

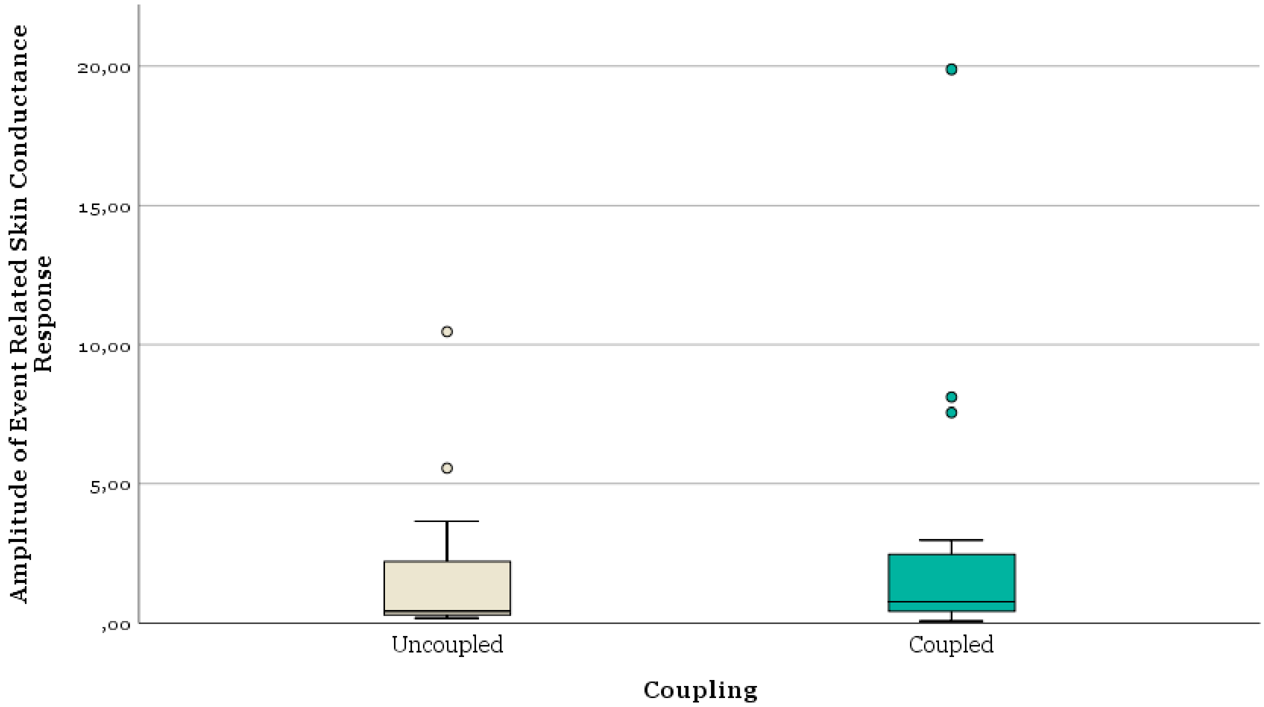

Graph 7.8 Boxplot of ER-SCR amplitude during tailstrike take-off scenarios for uncoupled and coupled flight controls

7.5 Correlations between tailstrike take-off results

7.5.1 Test for normality: Tailstrike take-off scenarios

In order to accurately test for linear relationships between the different results, a Shapiro–Wilk test was used; the results of this normality test can be found in **Table 7.7**. It yielded three variables that are not normally distributed, for which a non-parametric test was used; all other variables in **Table 7.7** are normally distributed and were subjected to a parametric test.

Shapiro–Wilk Normality Test	*Statistic*	*Degrees of Freedom*	*Significance*
Maximum Reached Pitch on Ground	.837	25	.001
Duration of 100% Aft Stick Deflection until Intervention	.845	25	.001
Total TLX Score	.975	25	.777
Total SART Score	.960	25	.407
Perceived Surprise	.927	25	.072
Perceived Startle	.940	25	.145
ER-SCR Amplitude	.788	25	.000
RMSSD	.959	25	.394

Table 7.7 Shapiro–Wilk normality test results on tailstrike take-off scenarios

7.5.2 Correlations between objective and subjective tailstrike results

The first correlation analysed is that between the maximum reached pitch attitude on ground during take-off and perceived startle and surprise. It can be theorised that the highest achieved pitch attitude (and, thus, the value closest to a tailstrike) would have a direct relationship to perceived startle and surprise, leading to a higher score on the Likert scales. Because preliminary analyses violated the assumption of normality, a non-parametric test was used; it found no correlation between the maximum reached pitch attitude on ground and perceived surprise (Spearman rank correlation coefficient; rho = -0.176, p = 0.26). In contrast, a low positive correlation was found between the maximum reached pitch attitude and perceived startle (Spearman rank correlation coefficient; rho = 3.10, p = 0.03). This means that a higher Likert-scale value on perceived startle is related to the maximum reached pitch attitude.

Another potential correlation between objective and subjective results is that between the perceived SA score on the SART and the duration of aft stick deflection. Because a participant who is more aware of the aircraft's current state will most likely perceive an improperly initiated stick input, a low duration of a 100% aft stick input may be related to the SART score. Because preliminary analyses violated the assumption of normality, a Spearman rank correlation coefficient was used as a non-parametric test. It found that no significant linear relation between the SART scores and the duration of aft stick deflection during take-off (*rho* = 0.003, p = 0.98).

7.5.3 Correlations between objective and physiological tailstrike results

As shown in the previous section, perceived startle on the Likert scale is significantly correlated with the maximum reached pitch attitude on ground during tailstrike scenarios. Therefore, it can be theorised that a linear relationship may exist between ER-SCR amplitude and the maximum reached pitch attitude on ground. A non-parametric test (Spearman rank correlation coefficient) was used to investigate this potential relationship because both variables violated the assumptions of normality in the above-mentioned normality analyses; it found no relationship between ER-SCR amplitude and the maximum reached pitch attitude (*rho* = -0.151, p = 0.41). A similar relationship can be theorised between ER-SCR amplitude and the duration of the 100% aft stick deflection during take-off. Because both variables violated the assumption of normality, a non-parametric test (Spearman rank correlation coefficient) was used to investigate the potential relationship between them; it found no relationship between ER-SCR amplitude and the duration of the aft stick deflection (*rho* = -0.02, p = -.91)

7.5.4 Correlations between subjective and physiological results

In the light of the correlations found in the hard landing chapter, a similar relationship between RMSSD and total TLX is sought in the tailstrike take-off data. The RMSSD and total TLX scores measured in the tailstrike take-off scenarios are compared to determine whether there is a significant relationship between the two variables. Preliminary analysis shows that neither variable violated the assumption of normality; therefore, a parametric test (Pearson product moment) is used. This test shows a strong negative correlation between the RMSSD and NASA TLX total score (r = -0.75, p = 0.000), which means that a higher RMSSD value, associated with less perceived stress, results in a lower TLX score. In the previous chapter, no linear relationship between the EDA data and objective data was found. In section 5.11.4, a strong relationship was found between ER-SCR amplitude and perceived startle and surprise during hard landing scenarios. Therefore, the relationship between ER-SCR amplitude and the Likert-scale scores of the startle and surprise questionnaire during tailstrike take-off scenarios is investigated. Preliminary analyses has shown that ER-SCR amplitude is not normally distributed; therefore, a non-parametric test (Spearman rank correlation coefficient) is used. It found no correlation between perceived surprise and ER-SCR amplitude (rho = 0.28, p = 0.14) nor between perceived startle and ER-SCR amplitude (rho = -0.27, p = 0.16).

7.6 Multivariate analyses of variance on tailstrike results

In the previous sections of this chapter, the coupled and uncoupled flight control configurations were compared based on a single dependent variable. In this section, their differences are tested on the entire range of variables through the use of a multivariate analysis of variance (MANOVA). The Mahalanobis distance is compared for each individual participant. According to Tabachnick and Fidell (1996), the critical Mahalanobis value for a MANOVA with eight dependent values should not exceed the critical value of 26.23. Multicollinear and singularity variables are excluded in this MANOVA. The eight dependent variables that are included in the multivariate analyses are visible in **Table 7.8**. The independent variable in this test was flight control configuration (coupled and uncoupled). Preliminary assumption testing was conducted to check for normality, linearity, homogeneity of variance and multicollinearity; no violations were observed. The result of the MANOVA test can be seen in **Table 7.8**. There was a statistically significant difference between the results of the uncoupled and coupled flight control groups on the tailstrike take-off scenarios on the combined dependent variables: F(8, 20) =

4.6, p = 0.029; Pillai's trace = 0.84; partial eta squared = 0.84. When the results for the dependent values were considered separately, the only two variables to reach statistical significance (using a Bonferroni-adjusted alpha level of 0.00625) were maximum reached pitch attitude on ground (F = 6.23, p = 0.005, eta squared = 0.29) and duration of 100% aft stick deflection until intervention (F = 23.4, p = 0.00, eta squared = 0.45).

MANOVA	*F*	*Significance*	*Bonferroni Adjustment*	*Eta Squared*
ER-SCR Amplitude	.052	.822	.0062	.004
RMSSD	.438	.519	.0062	.030
Duration of 100% Aft Stick Deflection until Intervention	19.917	.001	.0062	.587
Maximum Reached Pitch Attitude on Ground	13.388	.003	.0062	.489
Total TLX Score	.887	.362	.0062	.060
Total SART Score	1.051	.323	.0062	.070
Perceived Surprise	.854	.371	.0062	.058
Perceived Startle	.046	.833	.0062	.003

Table 7.8 Results of multivariate analysis of variance with Bonferroni adjustment on tailstrike take-off results

7.7 Discussion of the results

7.7.1 Discussion of demographic results

This experiment aimed to investigate the effects of haptic feedback on monitoring duties during tailstrike take-off events; it was conducted on an Airbus A320 fixed-base flight simulator. As discussed in Chapter 6, the original sampling aim was to recruit a sample group that consisted entirely of Airbus-rated airline pilots. Unfortunately, because there were not enough available Airbus-rated pilots to form a sufficiently large sample group, pilots rated on other modern jet aircraft were accepted to reach the minimum recruitment target of 20 participants. Of the 20 participants, four were not experienced on passive sidestick aircraft, but the results show that familiarity with the Airbus flight deck did not play a role; all of the significance tests conducted in this chapter were subdivided into Airbus-rated and non-Airbus-rated pilots, and they did not show any significant differences between the two groups. In addition to familiarity with the Airbus A320, each participant's experience in total flight hours was measured against most of the parameters measured in this experiment; it has shown that there is no relationship between total experience and the number of verbal and physical take-overs. Nor was there any relationship between the maximum recorded pitch attitude during take-off and the total amount of flight hours. The results show that there is no difference in perceived workload or SART results in relation to flight-hour experience. The physiological metrics indicated no relationship between flight-hour experience and either ER-SCR amplitude, RMSSD, or OTW eye fixations.

7.7.2 Discussion of objective results

It can be summarised from section 7.2.1 that on the coupled flight control configuration, a significantly lower number of improperly initiated take-off rotation manoeuvres resulted in an actual tailstrike. On the uncoupled flight control configuration only four of the 20 participants successfully prevented the tailstrike from happening. For the coupled flight control configuration this number was 14. Another key finding is that on the uncoupled flight control configuration the number of either verbal and physical interventions was, as in Chapter 6, extremely low. Four of the 20 participants physically intervened on the uncoupled flight control configuration, and only one participant verbally intervened before the tailstrike took place. Besides that, all of these physical interventions initiated a take-over with a 100% stick deflection. This can be seen as a startled response and possibly the result of the inability to perceive what flight control inputs were being made, until the tailstrike has occurred. In contrast, the number of physical and verbal interventions is significantly higher on the coupled flight control configuration. During the coupled tailstrike scenarios a total of 14 participants successfully physically intervened during the tailstrike scenario. Out of these 14 physical interventions, 13 participants verbally intervened before physically taking over controls. This outcome supports the claims by Field & Harris (1998) and Uehara (2013, 2015) and the results of Chapter 6, that pilots are more aware of incorrect flight control inputs and can anticipate on a possible intervention. It also supports Field and Harris' explanation that the cross-coupling between the flight control inceptors is a way in which pilots communicate (Field & Harris, 1998). When related to the three-level SA model by Endsley, discussed in section 2.1.2, one possible explanation is that, due to the coupled stick configuration, pilots perceive and comprehend (level 1 and level 2) a wrongly initiated flare manoeuvre. Their projection on future state (level 3) for these pilots is that they anticipate the availability if sufficient time to verbally intervene and perceive if proper reaction is initiated by the PF (SA feedback loop). Anticipating that the take-off is incorrectly initiated may also explain why take-over reactions in the coupled flight control configuration are less startled and have less extreme stick deflections. Another three participants verbally intervened during or right after the tailstrike occurred. Similar to the results in Chapter 6, these results can be considered a crucial aspect in take-over procedures. Due to the movement of the sticks, the PM is more aware of the current state of the aircraft and is responding to the actual position of the stick. This clearly is the case since two participants verbally intervened on just the 100% aft position of the stick. This means that there is sufficient time to verbally express concerns about the current or future state of the aircraft before the tailstrike could commence. Besides that, it can be concluded that the participants are more aware of the of the flight control inputs as only two out of the fourteen physical interventions on the coupled flight control scenarios had a flight control input exceeding 75% of the maximum stick deflection. Another finding is that the physical and verbal interventions took place on a in a much earlier stage of the rotation. This means that upon noticing that the take-off rotation is not going according to normal operating procedures, there is more time to accurately and successfully intervene. This is then followed by a significantly lower recorded pitch attitude, resulting in only 30% of the coupled tailstrike scenarios in exceeding the 11.7-degree maximum pitch attitude on ground for the Airbus A320, compared to 80% of the uncoupled flight control hard landings. The number of interventions on the uncoupled flight control configuration during the tailstrike scenarios were considered low. Only four participants intervened. A possible explanation for this low number of interventions could be that the majority of the participants did not notice the tailstrike occurring on the uncoupled flight control system. Here there are three limitations playing a role. First of all, the experiment took place on a fixed-base flight simulator. Therefore the vestibular acceleration cues of an take-off rotation is not available to the pilots. It can be assumed that the physical motion of a quickly rotating aircraft can be observed in a real take-off scenario, which cannot be felt in a fixed base simulator. Secondly, as discussed in Chapter 5, for a PM a rotation reference is often sought out-the-window. Since this simulator consists of three projectors on a screen, the quality of the projection is not as accurate compared to a real world situation. This degradation of out-the-window quality of details could mean the PMs have less visible cues to orientate the rotation speed on. Finally implementing a take-off with lower Vr reduced the angular velocity on the first part of take-off rotation, meaning the angular velocity of 3 degrees per second rotation rate is reached after 2.4 seconds of stick input. The angular velocity of the rotation is exponentially increasing over the last second. This means that noticing a high angular velocity on the take-off rotation on just the out-the-window references is therefore only observable from 2.4 seconds onwards. Since the angular rotation speed is exceeding the 3 degrees per second rotation rate from this point onwards. By providing proprioceptive feedback the position of the flight control inceptor is directly available for the PM. This could possibly mean that the majority of the physical interventions taking place on the coupled flight control configuration are triggered by the 100% aft stick deflection. This theory would also explain the relatively high number of verbal interventions that occurred before a physical intervention took place on the coupled flight control configuration.

7.7.3 Discussion of subjective results

7.7.3.a Perceived workload

The measured perceived workload in NASA TLX metric shows significant differences between the two flight control configurations. In section 7.8.1.1 it becomes apparent that for the tailstrike take-off scenarios, the total perceived workload is significantly lower whilst monitoring on the coupled flight control configuration. According to Hart and Staveland (1988), the mean TLX scores of 34 for the uncoupled and 24 for the coupled flight control configuration on the normal take-off scenarios are considered to be 'medium' to 'low'. One of the reasons for this result is the post-trial application of the TLX. The most eventful part of the scenario with a relatively high workload is the actual take-off and take-off rotation, whereas the subsequent climb-out and departure are relatively uneventful. This climb-out takes approximately 5 minutes and could therefore influence the perceived workload; in other words, it is possible that the TLX results are more a reflection of the last 5 minutes than of the actual take-off rotation. For the tailstrike take-off scenarios, a significant difference is found between the uncoupled and coupled flight control configurations: The results show that the perceived workload on the coupled flight control configuration is significantly lower. When the total TLX score is broken down into its six constituent subsections, it becomes apparent that two subsections significantly differ between the two flight control configurations on the tailstrike scenarios. First, the mental demand subsection is significantly lower, a finding that tends to be in line with the results in Chapter 6 and supports the current literature (Field & Harris, 1998; Summers et al., 1987; Uehara, 2014; Van Baelen et al., 2021). The other subsection that showed a significant difference is frustration: Measured frustration on the NASA TLX for the uncoupled flight control configuration is significantly higher than that of the coupled flight control configuration. When this mean result is compared to the other frustration levels in the previous chapter, it is found that the frustration levels are more than twice as high as in other scenarios. There is a potential relationship between the inability to perceive accurate information based on OTW references during take-off and tailstrikes that occur. Alternatively, it could be that the take-off scenarios were too long, which caused higher levels of frustration.

7.7.3.bSituation awareness rating technique

Perceived SA is measured using a self-evaluation questionnaire called the situation awareness rating technique (SART). This questionnaire consists of ten questions which combined cover three dimensions: attentional demand, attentional supply and understanding. The SART results showed no significant differences between the uncoupled and coupled flight control configurations in terms of total SART score. However, the SART is slightly outdated and involves some drawbacks; one potential reasons why SART shows no significant differences is that this experiment is a combination of the post-trial application of the SART questionnaire and the measured stimulus applied at the very beginning of the scenario. In other words, the tailstrike scenarios – which are the aim of this study – occurred at the very start of each scenario, followed by an uneventful 5-minute climb-out. During this climb-out, the PM is handling only three ATC radio commands and monitoring the flight. Other research shows that time between the stimulus and the self-assessment affects the subjective ratings because participants in self-assessments are prone to forgetting, especially in longer scenarios such as those used in this experiment (Endsley et al., 2000; Endsley et al., 1998; Salmon et al., 2009).

7.7.3.c Startle and surprise questionnaire

No significant differences were found in the Likert-scale responses to the startle and surprise questionnaire. One possible explanation is related to the number of interventions observed. Due to the limitations of using a fixed-base simulator, the majority of the uncoupled tailstrike scenarios remained unnoticed, whereas on the coupled flight control configuration, the stick position in the 100% aft position for the duration of 2.4 seconds provided information to the PM that prompted them to intervene at a much earlier stage during the tailstrike scenarios, thereby reducing perceived startle and surprise. Another limiting factor is the post-trial application of the SART. As cited in previous sections of this discussion, the tailstrike event took place at the very beginning of the scenario, after which the departure and climb-out continued for 5 minutes, potentially diminishing the effect of the perceived startle and surprise during the tailstrike.

7.7.4 Discussion of physiological results

7.7.4.a Electrodermal activity

Based on the studies mentioned in Chapter 2, analysing the activation of the sympathetic and para-sympathetic nervous system through electrodermal activity (EDA) is a common practice for measuring a participant's mental workload. The results discussed in section 7.4.5 show no significant differences in the magnitude of ER-SCR between the uncoupled and coupled flight control configurations; however, the standard deviation on the coupled flight control configuration is much higher. Even though the results are not significantly different, far more participants show an elevated ER-SCR level on the coupled flight control configuration. One of the major limitations of this result is that, due to the fact that a large number of tailstrike went unnoticed on the uncoupled flight control configuration, the number of ER-SCR on the uncoupled configuration is relatively low. Only ten participants showed an ER-SCR that can be related to the take-off rotation, whereas on the coupled flight control configuration, the number of successfully matched ER-SCRs was 15. Whereas in the previous chapter the ER-SCRs on the coupled configuration showed a lower ER-SCR amplitude, the reduced number of ER-SCRs on the uncoupled situation in this study is interpreted as an inability to detect the tailstrike. This is supported by the subjective startle and surprise questionnaire, where only limited participants scored a high value on the uncoupled control configuration. Another contributing factor is the fact that the majority of the participants physically intervened on the coupled flight control configuration before the tailstrike occurred. Therefore detecting a wrongly initiated rotation, causing a (limited) ER-SCR. What can be concluded is that the visible but insignificant differences of a higher ER-SCR measured on the coupled flight control configuration is attributable to the fact that on the uncoupled flight control configuration, the majority of the tailstrikes remained unnoticed. There were insufficient ER-SCRs on the normal take-off scenarios to make an accurate statistical comparison. This increase in mental workload measured via ER-SCRs on the coupled flight control configuration is contrary from the perspective of Wickens MRT (2005) and Endsley's three levels of SA model (1998). However, as stated in this section, the majority of the tailstrikes on the uncoupled configuration went unnoticed. The results suggest that, due to the coupling of the flight control configuration, the tailstrike became more noticeable, therefore leading to a higher ER-SCR.

7.7.4.b Heart rate variability

Based on studies mentioned in the literature review, the method of comparing RMSSD in heart rate variability HRV is a valid method for physiologically assessing a participant's mental workload. The major flaw in employing RMSSD in this study is the duration over which it was used; this metric has been used only for short time domain areas. This method tends to be in line with other research on this subject (Saus et al., 2012; Stuiver et al., 2014). A more accurate way of using HRV is by transforming it into a power frequency domain. However, in order to use this power spectral density method, a timeframe of 5 minutes or more is needed; because the tailstrike occurs within the first 50 seconds of the scenario, this method is deemed unreliable (Nickel & Nachreiner, 2003; Roscoe, 1992; Svensson et al., 1997). For this reason, the assessment of the RMSSD parameter is used to analyse HRV. The results in section 7.4.4 show a statistically higher RMSSD value during the tailstrike scenario with the coupled flight control configuration in comparison to the uncoupled flight control configuration. A higher RMSSD is associated with less stress and an increase in mental demand. The results in RMSSD values and mental demand scores on the NASA TLX during tailstrikes are strongly correlated, but no correlation was found between the RMSSD values and the answers provided in the startle and surprise questionnaire. The pNN50 values did not significantly differ between uncoupled and coupled flight control configurations, and no relation was found between RMSSD value and the maximum reached pitch attitude during the tailstrike scenarios.

7.7.4.c Eye tracking

During all take-off scenarios, the eye-tracking system recorded eye fixations based on the intersection of objects programmed into the world coordinate system. After applying a quality filter, a significant amount of the eye-tracking tracks were deemed unsuitable for use; the remaining 46 eye-tracking scenarios deemed suitable were factored into the results. There are no significant differences in the number of OTW eye fixations between the uncoupled and coupled flight control configurations. To evaluate the effect of looking for outside cues in assessing the rotation rate as discussed in Chapter 2, the OTW analysis is repeated for the first 2 minutes of take-off, focussing on the take-off rotation rate. Although the mean OTW fixations on the coupled flight control configuration is lower than on the uncoupled flight control configuration, no significant differences were found.

7.8 Conclusions

This experiment investigated the effects of coupled and uncoupled flight controls on PMs during tailstrike take-off events. Its results suggest a difference in awareness for PMs based on objective, subjective and physiological data. As reported in previous literature (Summers et al., 1987; Uehara & Niedermeier, 2015; Wolfert et al., 2019), passive sidestick control inceptors may limit the accuracy of a PM's monitoring ability. Endsley (1995) concluded that the use of several sensory modalities enhanced SA by providing tactile and proprioceptive cues to the PM, and the results of this experiment corroborate those findings.

This experiment's objective results indicated several statistically significant differences. First, far more physical interventions were observed on the coupled flight control system than on the uncoupled system: 70% of participants using the coupled stick configuration successfully intervened physically during the tailstrike, compared to 20% of those using the passive sidestick configuration. Also, the interventions on the coupled stick configuration occurred at a much earlier stage in the take-off rotation phase, leaving more time to correctly intervene.

Another conspicuous pattern is that the maximum reached pitch attitude significantly decreased when the physical intervention was preceded by a verbal intervention. Of the ten lowest maximum pitch attitudes measured in this experiment, seven involved a verbal intervention quickly followed by a physical intervention – and all seven such cases took place on the coupled configuration. It can therefore be concluded that the likelihood to encounter a tailstrike is therefore lowered with the use of an active sidestick configuration in comparison to the use of passive sidesticks.

This experiment showed that the overall mental workload on the monitoring task was significantly lower during tailstrike take-off scenarios when using the coupled flight control configuration. In contrast to the results in Chapter 6, the mental workload experienced during normal events did not significantly change depending on which flight control configuration was used. When the TLX measurements are broken down into their constituent subscales, they reveal that perceived mental demand and frustration are significantly reduced when using the coupled flight control system. Much as with the results in Chapter 6, it can be concluded that the use of coupled flight controls during tailstrike events results in a significantly less mentally demanding monitoring task.

However, these findings on mental workload are not supported by the clear differences found within the physiological data parameters. Because most participants did not notice the tailstrike occurrence while using the uncoupled flight control configuration, the EDA results show a statistically insignificant increase in ER-SCR on the coupled flight control configuration during tailstrike events. The HRV measured in RMSSD showed a statistically significant correlation with lower TLX scores on the tailstrike events. There was no statistically significant difference in OTW eye fixations or fixation durations. There have been no significant differences found in the scores of the startle and surprise questionnaire. It can therefore be concluded that the use of proprioceptive cueing during tailstrike events does not provoke a more startled or surprised response.

All of these results, combined with those presented in Chapter 6, strongly indicate that the effect of proprioceptive cueing has a powerful and beneficial effect on the PM’s ability to act in non-normal situations. Perhaps most compelling of all is the fact that even though none of the participating pilots had previously flown commercial aircraft using coupled sidesticks, they are showing significant improvements in terms of aviation safety.

Chapter 8 Summary and Future Work

8.1 Introduction

This final chapter will summarise all conclusions derived thus far, as well as enumerating their contributions to the current state of knowledge within the relevant fields. Furthermore, potential avenues for future research will be indicated, followed by a final concluding statement.

8.2 Summary

The overall aims of this thesis were:

1) Evaluate the effects of haptic feedback on the flight deck in the literature.
2) Determine whether there is a statistical association between the number of accidents/incidents and the presence of haptic feedback on the flight deck.
3) Evaluate the effects of haptic feedback on pilots' monitoring ability on a multi-crew jet aircraft.

The application of haptic feedback on flight controls is not a novel research subject in the domain of human factors within aviation. However, with only two exceptions, all published aviation research projects involving haptics have focused on the effects of the PF. Furthermore, to the author's knowledge, only one published scientific research project (Uehara, 2014) has examined the effects of cross-coupling flight controls for a PM. Up to the moment of writing, the research presented in this thesis is the first to evaluate the effects of passive and active flight control inceptors in a multi-crew experimental setup. A review of the literature clearly indicates that the absence of cross-coupling between the passive sidesticks is not the direct cause of accidents. Rather, it is found that the configuration imposes limitations upon the PM's ability to anticipate, thus limiting their ability to perceive whether actions or interventions are required.

The outcomes of the statistical studies support these findings. In both hard landing and tailstrike accidents, a significant association is found between the number of accidents and the type of flight control. Within the statistical studies, no evidence is found as to what causes this difference. However, 26% of the passive sidestick hard landing reports specifically mentioned the passiveness of the sidestick, or the dual input logic, to be contributing to the accident.

The results of the experimental studies fully support the findings in both the literature and the statistical studies. The experimental results show a significant decrease in the number and the effectiveness of take-over actions by the PM on uncoupled flight control inceptors. The experiments show that implementing a cross-coupling between the flight control inceptors allows the PM to perceive information throughout their haptic channel, drastically lowering their perceived workload, increasing their situation awareness and significantly increasing their ability to intervene and prevent accidents successfully.

8.3 Limitations of the thesis

It has proven extremely difficult to attract a broader population of licensed pilots. Unfortunately, the research project could not provide any form of compensation towards the pilots for their time, travels or expenses. This has limited the number of willing pilots to participate in this research project. At first, the aim was to have a population of 25 Airbus-rated pilots so the effectiveness of the experiments would represent a higher power. After the first phase of testing (May to October 2019), only seven participants participated, after which it was decided to invite other rated pilots (Boeing, Dash-8). When phase two started (November 2019), Thomas Cook Airlines fell into liquidation, resulting in a large number of Airbus-rated pilots, relatively close to Coventry University, willing to participate.

Another major limitation of this thesis is using a fixed base simulator. In normal flight operations, the environment plays an essential role in a pilot's perception, as can be seen in Endsley’s model (1988). In actual flight operations, the pilots perceive environmental cues, such as vestibular and aural, affecting a pilot’s situation awareness. The use of a fixed base simulator limits the number of external cues to monitor accurately, therefore putting more emphasis on the information available. A possibility is that, therefore, the effects of coupled sidesticks could be somewhat reduced in actual flight operations. The original aim of this thesis was to evaluate the effect of haptic feedback on Loss of Control Inflight (LOC-I) accidents. However, in LOC-I situations, the environment plays an even more significant role, severely limiting the fidelity of the simulations when conducted on fixed-based simulators.

During the first experimental phase, the first two participants experienced an apparent startled or surprised response to the abnormal scenarios. These responses were not apparent in the trial sessions. In response to these startled responses, a Likert scale questionnaire was developed to measure perceived startled and surprised responses. Therefore, these startle and surprise questionnaire was not applied on all twenty participating pilots, potentially losing influencing the results due to missing 10% of the pilots.

Finally, after phase two ended in January 2020, the COVID-19 pandemic introduced unprecedented challenges. The COVID-19 pandemic has severely restricted physical research on pilots due to the closure or limited operation of university buildings. Social distancing measures and travel restrictions hindered direct interactions and did not allow for human-in-the-loop experiments.

8.4 Future work

While conducting the work for this thesis, several areas for future work have been identified; these include:

1) Further investigation is needed into the effects of flight mode change from rate command to direct elevator control during the flare with passive sidestick aircraft. This factor, in combination with flight control inceptor sensitivity, could potentially be a causal factor in the elevated number of hard landings on passive sidestick aircraft.

2) This thesis conducted the first study on comparing the type of flight control and their accident rates. Further research is needed to corroborate or reject these findings.

3) The statistical study on tailstrike susceptibility showed no correlations between the aircraft design characteristics and the number of tailstrikes. However, most of the tailstrike incidents were excluded in this study due to the involvement of weather conditions or situations of high workload due to system failures. Further research on the relationship between tailstrike occurrences and aircraft-specific design characteristics in tailstrike incidents with higher workload conditions is recommended.

4) This thesis has found an apparent correlation between the Out the Window (OTW) eye fixations and perceived spare mental capacity during the approach phase. Although in automotive, the OTW and workload combination has been well established, in aviation, this phenomenon has remained unnoticed.

5) The final and potentially most crucial area for future research will be the one which links the effects of cross-coupled flight control inceptors in LOC-I situations for a PM. Further research on the potential prevention of LOC-I incidents and haptic feedback applications for the PM is recommended.

8.5 Contributions

The work presented in this thesis has contributed to human knowledge in a number of areas:

1) The proven relationship between the literature, which points in the direction of possible limitations in monitoring duties due to the passiveness of the sidestick, and the statistical associations found in the accident rates have not yet been established in the literature
2) The experimental studies show that in a multi-crew environment, the cross-coupling of the control inceptors has a more powerful effect on the pilot's monitoring ability to act in a non-normal situation than previously thought. This effect has not yet been established in the literature to this extent.
3) The number of verbal interventions preceding the physical interventions in the experimental studies related to the successful prevention of either a tailstrike or hard landing show that including another pilot changes the way pilots intervene compared to single pilot studies (Uehara,2014).
4) The experimental studies showed that passive sidesticks severely limit a monitoring pilot's ability to observe and intervene in a wrongly initiated landing or take-off. The high number of crash landings, tailstrike take-offs, incorrect physical interventions and extreme stick deflections on take-over showed that the passive sidestick and take-over functions are not intuitive. Which has not been established to this extent in the literature.
5) The experimental scenarios flown in active configuration showed drastic improvements in preventing hard landings and tail-strikes. The coupled configuration enabled the PM to intervene verbally, monitor the response, and then intervene adequately. The active sidestick configuration has shown to be intuitive since none of the participants had even used such a system before.
6) The relationship between the increase of Out the Window eye fixations during the approach phase and the reduction of perceived spare mental capacity has not been established in the literature.

References

AAIB. (2000). *Tailstrike on Landing Airbus A321-211, EI-CPE, London Heathrow Airport*.

AAIB. (2006a). *AAIB Bulletin 2/2006 Tailstrike during Take off B757 G-BYAO 12 May 2005, Manchester Airport*. Farnborough. Retrieved from https://assets.publishing.service.gov.uk/media/5423035ced915d1374000b89/Boeing_757-204__G-BYAO_2-06.pdf

AAIB. (2006b). Tailstrike on landing, Airbus A320, C-GTDK.

AAIB. (2008). SERIOUS INCIDENT: A320 G-DHJZ on Kos Airport, Greece.

AAIB. (2022). *AAIB Bulletin: Tailstrike on Go-around Airbus A350 G-XWBC 27939*. Farnborough. Retrieved from https://assets.publishing.service.gov.uk/media/62e925308fa8f5033906b7f4/Airbus_A350-1041_G-XWBC_09-22.pdf

Ackerman, K. A., Seefeldt, B. D., Xargay, E., & Talleur, D. A. (2011). Flight Envelope Information-Augmented Display for Enhanced Pilot Situation Awareness, 1–16.

Advani, S. J., Field, J. N., Training, F. C., & Recovery, U. (2011). Executive summary Upset Prevention and Recovery Training in Flight Simulators, 8–11.

Ahmed, S., Irshad, L., Gawand, M. S., & Demirel, H. O. (2021). Integrating human factors early in the design process using digital human modelling and surrogate modelling. *Journal of Engineering Design*, *32*(4), 165–186. https://doi.org/10.1080/09544828.2020.1869704

Aigoin, G. (2012). Characterising Hard Landings. *EOFDM Conference*, (January).

Airbus SE; (2017). *A330 FLIGHT CREW OPERATING MANUAL*.

A**irbus Training & Flight Operations Support Division. (2007)**. Flight Operations Briefing Notes Preventing Tailstrike at Landing, 1–8.

Arjoni, D., Villani, E., Matheus, A., & Almeida, A. (2018). EXPERIMENTAL ANALYSIS OF FLIGHT PERFORMANCE UNDER WORKLOAD EXPERIMENTAL ANALYSIS OF FLIGHT, (November).

Arnold, R. L., & Arnold, R. L. (2013). Air Transport Incident and Accidents Caused by Crew Situation Awareness Errors, 454–458.

ASCT. (2002). *IN-FLIGHT BREAKUP OVER THE TAIWAN STRAIT NORTHEAST OF MAKUNG, PENGHU ISLAND CHINA AIRLINES FLIGHT CI611 BOEING 747-200, B-18255*. Taipei. Retrieved from https://www.ttsb.gov.tw/media/4253/ci611_executive-summary_vol_1.pdf

A**ustralian Transport Safety Bureau.** (2009). *Tailstrike and runway overrun - Airbus A340-541, A6-ERG, Melbourne Airport, Victoria, 20 March 2009*. 62 Northbourne Avenue Canberra, Australian Capital Territory 2601. Retrieved from https://www.atsb.gov.au/media/5773945/ao-2009-012_final-report.pdf

Australian Transport Safety Bureau. (2016). Tail strike on takeoff involving Airbus A320, VH-VGF, (September 2017). Retrieved from www.atsb.gov.au

Aviation Week. (1987). A320 Rollout and First Flight.

Awh, E., Belopolsky, A. V, & Theeuwes, J. (2012). Top-down versus bottom-up attentional control : a failed theoretical dichotomy. *Trends in Cognitive Sciences*, *16*(8), 437–443. https://doi.org/10.1016/j.tics.2012.06.010

Babu, M.D., JeevithaShree, D.V., Prabhakarb, G., Salujab, K.P.S., Pashilkarc, A., & Biswasb, P. (2019). 'Estimating Pilots' Cognitive Load from Ocular Parameters through Simulation and In-Flight Studies.' Journal of Eye Movement Research, 12(3).

Bach, D. R., Flandin, G., Friston, K. J., & Dolan, R. J. (2010). Modelling event-related skin conductance responses. *International Journal of Psychophysiology*, *75*(3), 349–356. https://doi.org/10.1016/j.ijpsycho.2010.01.005

Baddeley, A. (2000). The episodic buffer: a new component of working memory? *Trends in Cognitive Sciences*, *4*(11), 417–423. https://doi.org/10.1016/S1364-6613(00)01538-2

BAE. (2009). BAE Active Inceptor Technology. Retrieved December 15, 2019, from http://www.baesystems.com/product/BAES_045901/active-inceptor-systems

BAE. (2016). The clear leader in active sidestick pilot controls for commercial aircraft. Retrieved from https://www.baesystems-ps.com/pilot-controls.php

Baek, **H. J., Cho, C. H., Cho, J., & Woo, J. M.** (2015). Reliability of ultra-short-term analysis as a surrogate of standard 5-min analysis of heart rate variability. *Telemedicine and E-Health*. https://doi.org/10.1089/tmj.2014.0104

Bai, S., **Guo, H., Zhou, Y., Duan, Y., Guo, X., Zhong, A**., ... **Liu, J.** (2023). Analysis of Pilot Workload in Multi-mission Phases, 10–17. https://doi.org/10.1007/978-981-99-4882-6_2

Bartley, G. F. (2001). Boeing B-777: Fly-By- Wire Flight Controls.

Baxter, G., Besnard, D., & Riley, D. (2007). Cognitive mismatches in the cockpit : Will they ever be a thing of the past ?, *38*, 417–423. https://doi.org/10.1016/j.apergo.2007.01.005

Bell, H., & Lyon, D. (2000). *Using Observer Ratings to Assess Situation Awareness. In: Endsley and Garland Situation Awareness Analysis and Measurement*. Mahwah, NJ.

Bell, M. A., Facci, E. L., & Nayeem, R. V. (2005). Cognitive Tunneling , Aircraft-Pilot Coupling Design Issues and Scenario Interpretation Under Stress in Recent Airline Accidents, 45–49.

Belcastro, C. M., Newman, R. L., Crider, D. A., Klyde, D. H., Foster, J. V., & Groff, L. (2016). 'Aircraft Loss of Control: Problem Analysis for the Development and Validation of Technology Solutions.' 2016 AIAA SciTech Conference. 4 - 8 Jan., San Diego, CA.

Bennett, S. A.,(2018). Pilot workload and fatigue on short-haul routes : an evaluation supported by instantaneous self- assessment and ethnography. *Journal of Risk Research*, *9877*, 1–32. https://doi.org/10.1080/13669877.2016.1235603

Berger, T., Gong, A., Lusardi, J. A., Ott, C. R., Ogden, L. T. C. W. R., & Miller, M. A. J. M. L. (2023). Effects of Linked vs. Unlinked Cyclic Controllers on Crew Coordination. *Vertical Flight Society 79th Annual Forum and Technology Display Conference Proceedings*, (May). https://doi.org/10.4050/F-0079-2023-18075

Bermudez, N. F., Wilt, D. F., & Deaton, J. E. (2013). Beyond Multitasking : Human Factors Implications for Single-Pilot Operations in the NextGen Environment, 220–225.

Bernadin, P. (2003). Boeing Aeromagazine Tail Strike Avoidence. Retrieved August 19, 2022, from https://www.boeing.com/commercial/aeromagazine/aero_04/textonly/tr01txt.html

BIOPAC Systems Inc. (2015). *AcqKnowledge Software Guide* (Vol. 93117). Retrieved from http://www.biopac.com

Boeing. (2003). *Boeing 777-200/300 Flight Crew Operating Manual*. Seattle, Washington.

Boeing Aircraft Industries. (1998). *Boeing 737-700 Flight Crew Operation Manual.*

B**oy, G., & Ferro, D.** (2004). Using Cognitive Function Analysis to Prevent Controlled Flight into Terrain. In *Human Factors for Civil Flight Deck Design* (2nd ed., pp. 55–68). Aldershot, UK: Ashgate.

Brady, C. (1999). The Boeing 737 Technical Site section: Tailstrike Geometry. Retrieved February 2, 2021, from http://www.b737.org.uk/tailstrikes.htm#geometry

Bromfield, M., & Landry, S. J. (2019). Loss of Control In Flight – time to re-define ? United Kingdom, (June). https://doi.org/10.2514/6.2019-3612

Brown, A., Karthaus, C., Rehak, L., Adams, B., & Rehak, L. A. (2009). *THE ROLE OF MENTAL MODELS IN DYNAMIC DECISION-MAKING Author Approved by Marie-Eve Jobidon Scientific Authority*.

Buck, A. (2019). Multiple Identity Tracking and Motion Extrapolation MULTIPLE IDENTITY TRACKING AND MOTION EXTRAPOLATION Ashley Buck and Esa Rantanen, 175–180.

CAPA. (2018). CAPA Fleet Database. Retrieved March 14, 2018, from https://centreforaviation.com/data/fleet

Causse, M., Dehais, F., Arexis, M., Pastor, J., Causse, M., Dehais, F., & Arexis, M. (2017). Cognitive aging and flight performances in general aviation pilots Cognitive aging and flight performances in general aviation pilots, *5585*(August). https://doi.org/10.1080/13825585.2011.586018

Causse, M., Sénard, J. M., Démonet, J. F., & Pastor, J. (2010). Monitoring cognitive and emotional processes through pupil and cardiac response during dynamic versus logical task. *Applied Psychophysiology Biofeedback*, *35*(2), 115–123. https://doi.org/10.1007/s10484-009-9115-0

Charles, R. L., & Nixon, J. (2019). Measuring mental workload using physiological measures : A systematic review. *Applied Ergonomics*, *74*(May 2018), 221–232. https://doi.org/10.1016/j.apergo.2018.08.028

Chihara, T., Kobayashi, F., & Sakamoto, J. (2020). Evaluation of mental workload during automobile driving using one-class support vector machine with eye movement data. *Applied Ergonomics*, *89*(June), 103201. https://doi.org/10.1016/j.apergo.2020.103201

Chiles, W. D., & Alluisi, D. E. A. (1979). On the Specification of Operator or Occupational Workload with Performance-Measurement Methods. *Human Factors*, *21*(5), 515–528. https://doi.org/10.1177/001872087902100501

Cohen, J. (1988). *Statistical Power Analysis For the Behavioral Sciences*. New York: Academic Press.

Colvin, K., & Dodhia, R. (2003). Scanning for visual traffic: An eye tracking study. *Proceedings of the 12th …*.

Corps, S. (1989). Airbus A320 Side Stick and Fly By Wire - An Update. *SAE Technical*

Paper. https://doi.org/861801

Dao, A. V, Parkinson, J. R., & Landry, S. J. (2016). Identifying Human-Machine Interaction Problems in Continuous State Data, 86–90.

Dawson, M. E., Schell, A. M., & Filion, D. L. (2016). The electrodermal system. In *Handbook of Psychophysiology, Fourth Edition*. https://doi.org/10.1017/9781107415782.010

de Mello, M. T., Esteves, A. M., Pires, M. L. N., Santos, D. C., Bittencourt, L. R. A., Silva, R. S., & Tufik, S. (2008). Relationship between Brazilian airline pilot errors and time of day. *Brazilian Journal of Medical and Biological Research*, *41*(12), 1129–1131. https://doi.org/10.1590/S0100-879X2008001200014

De Rivecourt, M., Kuperus, M. N., Post, W. J., & Mulder, L. J. M. (2008). Cardiovascular and eye activity measures as indices for momentary changes in mental effort during simulated flight. *Ergonomics*, *51*(9), 1295–1319. https://doi.org/10.1080/00140130802120267

Dehais, F., Causse, M., Vachon, F., Régis, N., Menant, E., & Tremblay, S. (2014). Failure to detect critical auditory alerts in the cockpit: Evidence for inattentional deafness. *Human Factors*, *56*(4), 631–644. https://doi.org/10.1177/0018720813510735

Dekker, S., & Hollnagel, E. (2004). Human factors and folk models. *Cognition, Technology & Work*, *6*(2), 79–86. https://doi.org/10.1007/s10111-003-0136-9

Demirel, H. O., & Duffy, V. G. (2017). Incorporating Tactile Cues into Human-Centered Virtual Product Design. *Human Factors and Ergonomics In Manufacturing*, *27*(1), 5–16. https://doi.org/10.1002/hfm.20402

Diaz-Piedra, C., Sanchez-Carrion, J.M., Rieiro, H., & Di Stasi, L.L. (2017). 'Gaze-based Technology as a Tool for Surgical Skills Assessment and Training in Urology.' Urology, 107, 26-30. DOI: http://dx.doi.org/10.1016/j.urology.2017.06.030

Ding, D., & Proctor, R. W. (2017). Interactions between the Design Factors of Airplane Artificial Horizon Displays, 84–88. https://doi.org/10.1177/1541931213601487

Dudley, R., Dorneich, M. C., Letsu-dake, E., & Rogers, W. (2014). Characterization of Information Automation on the Flight Deck Characterization of Information Automation on the Flight Deck. https://doi.org/10.1177/1541931214581061.

Durso, F. T., Hackworth, C. A., & Truitt, T. R. (1999). Situation Awareness As a Predictor of Performance in En Route Air Traffic Controllers. *Air Traffic Control Quarterly*, *6*(1), 1–20. https://doi.org/10.1518/001872007X230235

Dutch Safety Board (OVV). (2017). *Air Accident Data and Quarterly reports on General Aviation Accidents*. The Hague.

EASA. (2018). Startle Effect Management. *European Aviation Safety Agency*, 148.

Ebbatson, M., Huddlestone, J., Harris, D., & Sears, R. (2007). The application of frequency analysis based performance measures as an adjunct to flight path derived measures of pilot performance, *6*(4), 383–394.

Ebrecht, L., & Schmerwitz, S. (2015). Integration of a 3D perspective view in the navigation display-featuring pilot's mental model. *SPIE Defense+ Security*, *9471*, 94710C--94710C. https://doi.org/10.1117/12.2177402

Ellerbroek, J., Martin, M. J. M. R., Lombaerts, T., van Paassen, M. M., & Mulder, M. (2016). Design and evaluation of a Flight Envelope Protection haptic feedback system. *IFAC-PapersOnLine*, *49*(19), 171–176.

https://doi.org/10.1016/j.ifacol.2016.10.481

Ellis, K. K. E. (2009). Eye tracking metrics for workload estimation in flight deck operations. *ProQuest Dissertations and Theses*, *1467693*, 115. Retrieved from http://ezproxy.net.ucf.edu/login?url=http://search.proquest.com/docview/304901025?accountid=10003%5Cnhttp://sfx.fcla.edu/ucf?url_ver=Z39.88-2004&rft_val_fmt=info:ofi/fmt:kev:mtx:dissertation&genre=dissertations+&+theses&sid=ProQ:ProQuest+Dissertations+&+T

Endsley, M. R. (1988). Design and Evaluation for Situation Awareness Enhancement. *Proceedings of the Human Factors and Ergonomics Society Annual Meeting*, 97–101. https://doi.org/https://doi.org/10.1177/154193128803200221

Endsley, M. R. (1995a). Measurement of Situation Awareness in Dynamic Systems. *Human Factors: The Journal of the Human Factors and Ergonomics Society*, *37*(1), 65–84. https://doi.org/10.1518/001872095779049499

Endsley, M. R. (1995b). Toward a theory of situation awareness in Dynamic Systems. *Human Factors: The Journal of the Human Factors and Ergonomics Society*. https://doi.org/10.1518/001872095779049543

Endsley, M. R., & Garland, D. J. (2000). *Situation Awareness Analysis and Measurement*. Mahwah, NJ: Lawrence Erlbaum Associates, Inc.

Endsley, M. R. M. (2000). Direct measurement of situation awareness: Validity and use of SAGAT. *Situation Awareness Analysis and Measurement*, (2000), 1–21.

Endsley, M. R., (2001). Training for Situation Awareness How Do People Make Decisions , (May).

Esco, M. R., & Flatt, A. A. (2014). Ultra-short-term heart rate variability indexes at rest and post-exercise in athletes: Evaluating the agreement with accepted recommendations. *Journal of Sports Science and Medicine*.

Evans, E. T., Kramer, L. J., Etherington, T. J., Young, S. D., & Barnes, J. R. (2019). Usability Evaluation of Indicators of Energy- Related Problems in Commercial Airline Flight Decks.

FAA. (2011). Advisory Circular 23 1309.

Fairclough, S. H., & Venables, L. (2006). Prediction of subjective states from psychophysiology: A multivariate approach. *Biological Psychology*, *71*(1), 100–110. https://doi.org/https://doi.org/10.1016/j.biopsycho.2005.03.007

Faulhaber, A. K., Friedrich, M., & Kapol, T. (2020). Absence of Pilot Monitoring Affects Scanning Behavior of Pilot Flying: Implications for the Design of Single-Pilot Cockpits. *Human Factors*. https://doi.org/10.1177/0018720820939691

Federal Aviation Administration. (1996). *The Interfaces Between Flightcrews and Modern Flight Deck Systems*.

Fehrm, B. (2016, April). Leeham News & Analysis Bjorn's Corner: C Series flight controls. *Leeham News & Analysis*. Retrieved from https://leehamnews.com/2016/04/29/bjorns-corner-c-series-flight-controls/

Field, A. (2009). *Discovering Statistics Using SPSS* (Third). SAGE publications Ltd.

Field, E. (2004). 'Handling Qualities and their Implications for Flight Deck Design.' In Human Factors for Civil Flight Deck Design. Harris, D., Ed. 69-102. Surrey: Ashgate Publishing Ltd.

Field, E., & Harris, D. (1998). A comparative survey of the utility of cross-cockpit linkages and autoflight systems' backfeed to the control inceptors of commercial aircraft. *Ergonomics*, *41*(10), 1462–1477. https://doi.org/10.1080/001401398186216

Flach, J., Patrick, D., Corporation, L. M., Paassen, M. M. Van, & Mulder, M. (2003). *X A Search for Meaning : A Case Study of the Approach-to- Landing*.

Gawron, V.J. (2008). 'Human Performance, Workload, and Situational Awareness Measures Handbook.' 2nd ed. Boca Raton, FL: CRC Press.

Gazzaley, A., & Nobre, A. C. (2012). Top-down modulation : bridging selective attention and working memory. *Trends in Cognitive Sciences*, *16*(2), 128–134. https://doi.org/10.1016/j.tics.2011.11.014

Giannini, E. H. (2005). CHAPTER 6 - DESIGN, MEASUREMENT, AND ANALYSIS OF CLINICAL INVESTIGATIONS. In J. T. Cassidy, R. E. Petty, R. M. Laxer, & C. B. Lindsley (Eds.), *Textbook of Pediatric Rheumatology (Fifth Edition)* (Fifth Edit, pp. 142–173). Philadelphia: W.B. Saunders. https://doi.org/https://doi.org/10.1016/B978-1-4160-0246-8.50012-7

Glaholt, M. (2014). *Eye tracking in the cockpit: a review of the relationships between eye movements and the aviator's cognitive state*. Toronto.

Groen, E., Field, J. N., Ledegang, W., Nooij, S., Zaichik, L., Fucke, L.,. (2012). Executive summary SUPRA - Enhanced Upset Recovery Simulation An overview of the SUPRA experiments.

Grundy, J. G., Nazar, S., Malley, S. O., Mohrenshildt, M., & Shedden, J. M. (2013). The Effectiveness of Simulator Motion in the Transfer of Performance on a Tracking Task Is Influenced by Vision and Motion Disturbance Cues. https://doi.org/10.1177/0018720816639776

Grushko, S., Vysocký, A., Heczko, D., & Bobovský, Z. (2021). Intuitive Spatial Tactile Feedback for Better Awareness about Robot Trajectory during Human-Robot Collaboration. *Sensors (Basel, Switzerland)*, *21*(17). https://doi.org/10.3390/s21175748

Guilford, J. P. (1941). The phi coefficient and chi square as indices of item validity. *Psychometrika*, *6*(1), 11–19. https://doi.org/10.1007/BF02288569

Hancock, P. A., & Desmond, P. A. (2000). Stress, workload, and fatigue. Mahwah, N.J.: Lawrence Erlbaum Associates Mahwah, N.J. https://doi.org/47009885

Hanke, D., & Herbst, C. (1999). Active sidestick technology – a means for improving situational awareness. *Aerospace Science and Technology*, *3*(8), 525–532. https://doi.org/10.1016/S1270-9638(99)00107-8

Hannaford, B. (2001). Time Domain Passivity Control of Haptic Interfaces.

Harris, D. (2012). *Human performance on the flight deck. Human Performance on the Flight Deck* (2nd ed.). Boca Raton, Florida: Taylor & Francis Group.

Harris, Don, & Harris, F. J. (2004). Evaluating the transfer of technology between application domains : a critical evaluation of the human component in the system, *26*, 551–565. https://doi.org/10.1016/j.techsoc.2004.08.003

Harris, R. L., Glover, B. J., & Spady, A. A. (1986). *ANALYTICAL TECHNIQUES OF PILOT SCANNING BEHAVIOR AND THEIR APPLICATION. NASA Technical Paper*.

Hart, S. G., & Staveland, L. E. (1988). Development of NASA-TLX. *Human Mental Workload. Advances in Psychology*, (52), 139–183.

Haslbeck, A. (2013). Pilot Decision Making : Modeling Choices in Go-Around Situations, 548–553.

Haslbeck, A., & Hoermann, H. J. (2016). Flying the Needles. *Human Factors*. https://doi.org/10.1177/0018720816640394

Hegarty, M. (2004). Mechanical reasoning by mental simulation, *8*(6), 4–9. https://doi.org/10.1016/j.tics.2004.04.001

Hertz, M. T. (2013a). Situation Awareness and Situation Assessment : How Are They Related ?, 104–109.

Hertz, M. T. (2013b). Training for Situation Awareness, 257–261.

Ho, H.-F., Su, H.-S., Li, W.-C., Yu, C.-S., & Graham Braithwaite. (2016). Pilots' Latency of First Fixation and Dwell Among Regions of Interest on the Flight Deck. *Engineering Psychology and Cognitive Ergonomics*, *5639*, 414-423–423. https://doi.org/10.1007/978-3-642-02728-4

Hollnagel, E., & Amalberti, R. (2001). The emperor's new clothes: Or whatever happened to 'human error'? *4Th International Workshop on Human Error, Safety and Systems Development*, (April), 1–18.

Huddlestone, J., Harris, D., Richards, D., Scott, S., & Sears, R. (2015). Dual Pilot and Single Pilot Operations – Hierarchical Task Decomposition Analysis of Doing More with Less Dual Pilot and Single Pilot Operations – Hierarchical Task Decomposition Analysis of Doing More With Less, (May 2016). https://doi.org/10.1007/978-3-319-20373-7

Hugo, J. V, & Germain, S. S. (2017). Human Factors Principles in Information Dashboard Design.

IATA. (2016). *Unstable Approaches Risk Mitigation Policies, Procedures and Best Practices 2nd Edition*. Retrieved from https://www.iata.org/whatwedo/safety/runway-safety/Documents/unstable-approaches-2016-2nd-edition.pdf

ICAO. (2005). *Annex 2 to the Convention on International Civil Aviation - Rules of the Air*. Retrieved from http://www.icao.int/Meetings/anconf12/Document Archive/an02_cons[1].pdf

ICAO. (2012). *ICAO International Standards and Recommended Practices ANNEX 13 Attachment E.*

Isreal, J. B., Wickens, C. D., Chesney, G. L., & Donchin, E. (1980). The event-related brain potential as an index of display-monitoring workload. *Human Factors*, *22*(2), 211–224. https://doi.org/10.1177/001872088002200210

JAAIC. (1987). *Accident Report Boeing 747-SR100 JA8119*. Tokyo. Retrieved from https://www.mlit.go.jp/jtsb/eng-air_report/JA8119.pdf

Jelinek, H. F., Cornforth, D. J., Koenig, A., Riener, R., Karmakar, C., Imam, M. H., ... Minichiello, M. (1996). Task Force of the European Society of Cardiology the North American Society of Pacing Electrophysiology. Heart Rate Variability. *European Heart Journal.*

Johnston, D., Anastasiades, P., & Wood, C. (1990). The Relationship Between Cardiovascular Responses in the Laboratory and in the Field. *Psychophysiology*, *27*(1), 34–44. https://doi.org/https://doi.org/10.1111/j.1469-8986.1990.tb02175.x

Joslin, R. E. (2017). The Force Awakens, Aero Space Magazine. *Aerospace*, 24–25.

JTSB. (2014). *Aircraft Accident Investigation Report B772 Tailstrike on Landing*. Tokyo. Retrieved from https://www.mlit.go.jp/jtsb/eng-air_report/JA701J.pdf

Karim, B., Bergey, K., Chandler, R., Hasbrook, H., Perswell, J., & Snow, C. (1973). A Preliminary Study of Maximal Control Force Capability of Female Pilots. *Applied Ergonomics*, *4*(4), 1224. https://doi.org/10.1016/0003-6870(73)90227-5

Kessel, C., & Wickens, C. (1980). Processing resource demands of failure detection in dynamic systems. *Journal of Experimental Psychology: Human Perception and Performance*, *6*(3), 564–577. https://doi.org/https://doi.org/10.1037/0096-1523.6.3.564

Kim, S., Choi, B., Cho, T., Lee, Y., Koo, H., & Kim, D. (2017). Wearable bio signal monitoring system applied to aviation safety. *Proceedings of the Annual International Conference of the IEEE Engineering in Medicine and Biology Society, EMBS*, 2349–2352. https://doi.org/10.1109/EMBC.2017.8037327

Krumenacker, J. (2008). Active Stick & Throttle for F35. Retrieved from https://www.f-16.net/forum/download/file.php?id=19248

Landman, A. (2019). *Managing startle and surprise in the cockpit. TU Delft University*. https://doi.org/10.4233/uuid

Lee, J., Gordon-Becker, S., Liu, Y., & Wickens, C. (2003). *Introduction to Human Factors Engineering (2nd Edition)* (2nd ed.). Upper Saddle River, NJ: Pearson Education.

Lefevre, J. (2005). The Role of Working Memory in Maintaining Situation Awareness, 333–337.

Lehrer, P. (2013). History of Heart Rate Variability Biofeedback Research: A Personal and Scientific Voyage. *Biofeedback*. https://doi.org/10.5298/1081-5937-41.3.03

Li, G., Baker, S. P., Grabowski, J. G., & Rebok, G. W. (2001). Factors associated with pilot error in aviation crashes Factors Associated with Pilot Error in Aviation Crashes, (September 2014).

Li, W. C., Chiu, F. C., Kuo, Y. S., & Wu, K. J. (2013). The investigation of visual attention and workload by experts and novices in the cockpit. In *Lecture Notes in Computer Science (including subseries Lecture Notes in Artificial Intelligence and Lecture Notes in Bioinformatics)*. https://doi.org/10.1007/978-3-642-39354-9_19

Libyan Civil Aviation Authority. (2015). *Final Report of AFRIQIYAH Airways Aircraft Airbus A330-202, 5A-ONG Crash*. Tripoli.

Lini, S., Vallespir, B., Hourlier, S., Labat, F., & Favier, P. (2013). A Cognitive Engineering Approach for Showing Feasibility Margins on an In-Flight Planning, 430–435.

Martinovic, J., Gruber, T., & Mu, M. M. (2008). Coding of Visual Object Features and Feature Conjunctions in the Human Brain, *3*(11). https://doi.org/10.1371/journal.pone.0003781

Matthews, S., Vandel, H., & Waugh, J. (2004). Stabilised Approach and Flare are Key to Avoiding Hard Landings. *Flight Safety Digest*, (August), 1–44.

Mccoy, M. S., & Levary, R. R. (2010). A rule-based pilot performance model A rule-based pilot performance model, *7721*(2000). https://doi.org/10.1080/00207720050030761

McRuer, D. T. (1974). Mathematical Models of Human Pilot Behavior. *Aerospace*, (January).

Moacdieh, N. M., Prinet, J. C., & Sarter, N. B. (2013). Effects of Modern Primary Flight Display Clutter: Evidence from Performance and Eye Tracking Data. *Proceedings of the Human Factors and Ergonomics Society Annual Meeting*, *57*(1), 11–15. https://doi.org/10.1177/1541931213571005

Moray, N. (1979). Mental workload : its theory and measurement. New York: Published in coordination with NATO Scientific Affairs, Plenum Press New York. https://doi.org/609660769

Mosier, K. L. (2013). NASA Nextgen Flightdeck Research : A Database of Research Areas and Results, 8–13.

Mouloua, M., Hancock, P., Jones Moore, L., & Vincenzi, D. (2010). Automation in Aviation Systems Issues and Considerations. In *Handbook of Aviation Human Factors* (pp. 190–200). Taylor & Francis Group.

Mulder, Mark, Pauwelussen, J. J. A., Paassen, M. M. Van, Mulder, M., & Abbink, D. A. (2010). Active Deceleration Support in Car Following. *IEEE Transactions on Systems, Man, and Cybernetics - Part A: Systems and Humans*, *40*(6), 1271–1284. https://doi.org/10.1109/TSMCA.2010.2044998

Mulder, Max, Paassen, R. Van, Flach, J., & Flach, J. (2005). Cognitive Systems Engineering Approach to Shared Situation Awareness for Unmanned Aerial Vehicles, 7–13.

National Transportation Safety Board. (2014). Descent Below Visual Glidepath and Impact with Seawall, Asiana Airlines Flight 214, Boeing 777-200ER, HL7742, San Francisco, California July 6, 2013.

Nickel, P., & Nachreiner, F. (2003). Sensitivity and Diagnosticity of the 0.1-Hz Component of Heart Rate Variability as an Indicator of Mental Workload. *Human Factors: The Journal of the Human Factors and Ergonomics Society*, *45*(4), 575–590. https://doi.org/10.1518/hfes.45.4.575.27094

Niermann, C. A., Aerospace, G., & Guidance, F. (1959). CAN SPATIAL AUDIO SUPPORT PILOTS ? 3D-AUDIO FOR FUTURE PILOT-ASSISTANCE SYSTEMS Human Limits, *1320*.

NTSB. (2018). *NTSB Final Report Tailstrike on Landing B757-232 N698DL. 01/31/2018*. Washington. https://doi.org/10.5749/j.ctvthhd37.29

O'Leary, M., & Chappell, S. (1996). *Confidential incident reporting systems create vital awareness of safety problems*. *ICAO journal* (Vol. 51). Nasa Ames Research Center. https://doi.org/PMID: 11541832

Özcan, O. O. (2013). Exploring the Effects of Working Memory Capacity , Attention , and Expertise on Situation Awareness in a Flight Simulation Environment, 98–103.

Paassen, M. M. Van. (2013). Risk Perception in Ecological Information Systems, 436–441.

Pallant, J. (2013). *SPSS Survival Manual* (Fifth). Berkshire, England: Mcgraw-Hill.

Palmer, W. (2017). *Airbus Flight Control Laws: The Reconfiguration Laws*.

Palomeque, M. (2008). Airbus Safety First Magazine, A320 Prevention of Tailstrikes. *Safety First No.6*. Retrieved from https://safetyfirst.airbus.com/app/themes/mh_newsdesk/documents/archives/a320-prevention-of-tailstrikes.pdf

Parasuraman, R., Bahri, T., Deaton, J., Morrison, J., & Barnes, M. (1992). Theory and Design of Adaptive Automation in Aviation Systems, 48.

Parasuraman, R., & Masalonis, A. J. (2000). Fuzzy Signal Detection Theory : Basic Postulates and Formulas for Analyzing Human and Machine Performance, *42*(4), 636–659.

Patterson, F. R., Arnold, R. D., & Williams, H. P. (2013). Visual Perspective Illusions as Aviation Mishap Causal Factors, 512–517.

Perry, C. M., Kaber, D. B., Perry, C. M., & Carolina, N. (2005). Measurement of Situation Awareness Effects of Adaptive Automation of Air Traffic Control Information Processing Functions, 566–571.

Peryer, G., Noyes, J., Pleydell-pearce, K., & Lieven, N. (2005). Auditory Alert Characteristics : A Survey of Pilot Views, *15*(3), 233–250.

Pfleiderer, E. M. (2005). The Good , the Not-So-Bad , and the Ugly : Computer-Detected Altitude , Heading , and Speed Changes, 572–577.

Pihlajamäki, M., Tanila, H., Hänninen, T., Könönen, M., Mikkonen, M., Jalkanen, V., … Soininen, H. (2003). Encoding of novel picture pairs activates the perirhinal cortex: an fMRI study. *Hippocampus*, *13*(1), 67–80. https://doi.org/10.1002/hipo.10049

Pinel, P., Piazza, M., Bihan, D. Le, Dehaene, S., Unit, I., & Ge, P. (2004). Distributed and Overlapping Cerebral Representations of Number , Size , and Luminance during Comparative Judgments, *41*, 983–993.

Posada-Quintero, H. F., & Chon, K. H. (2020). Innovations in electrodermal activity data collection and signal processing: A systematic review. *Sensors (Switzerland)*. https://doi.org/10.3390/s20020479

P**ouliquen, Y., Ferrante, O., Jouniaux, P., Nicolas, G., Cabon, P., Rome, F., … Mollard, R.** (2005). A Human Factors Approach for the Analysis and the Encoding of Aviation Accidents and Incidents : A Validation Study, 578–583.

Pretorius, A., & Cilliers, P. J. (2007). Development of a mental workload index : A systems approach Technical note Development of a mental workload index : A systems approach, *0139*. https://doi.org/10.1080/00140130701379055

Proctor, R. W., & Vu, K. L. (1995). Cumulative Knowledge and Progress in Human Factors. https://doi.org/10.1146/annurev.psych.093008.100325

Puspawardhani, E. H., Suryoputro, M. R., Sari, A. D., Kurnia, R. D., & Purnomo, H. (2016). Mental workload analysis using NASA-TLX method between various level of work in plastic injection division of manufacturing company. In *Advances in Intelligent Systems and Computing*. https://doi.org/10.1007/978-3-319-41929-9_29

Rees, D. J., & Harris, D. (1995). Effectiveness of Ab Initio Flight Training Using Either Linked or Unlinked Primary-Axis Flight Controls. *The International Journal of Aviation Psychology*, *5*(3), 291–304. https://doi.org/10.1207/s15327108ijap0503_4

Roessingh, J. J. M. (2009). Transfer of Manual Flying Skills From PC-Based Simulation to Actual Flight-Comparison of In-Flight Measured Data and Instructor Ratings Transfer of Manual Flying Skills From PC-Based Simulation to Actual Flight — Comparison of In-Flight Measured Data and , *8414*. https://doi.org/10.1207/s15327108ijap1501

Rowley, J. (2007). The wisdom hierarchy : representations of the DIKW hierarchy, *33*(2), 163–180. https://doi.org/10.1177/0165551506070706

Salvendy, G. (1997). *Handbook of human factors and ergonomics* (2nd ed). New York SE - xxii, 2137 pages : illustrations ; 24 cm: Wiley New York.

Sarter, N. B. (2006). Multimodal information presentation: Design guidance and research challenges. *International Journal of Industrial Ergonomics*, *36*(5), 439–445. https://doi.org/https://doi.org/10.1016/j.ergon.2006.01.007

Savelev, A., & Neretin, E. (2019). Development of Safety Requirements for Tracking Active Pilot Controls by Signals from an Automatic Flight Control System. *Proceedings - 2019 3rd International Conference on Control, Artificial Intelligence, Robotics and Optimization, ICCAIRO 2019*, 19–24. https://doi.org/10.1109/ICCAIRO47923.2019.00012

Schriver, A. T., Morrow, D. G., Wickens, C. D., Science, A., & Corporation, T. (2016). Expertise Differences in Attentional Strategies Related to Pilot Decision Making, *50*(6), 864–878. https://doi.org/10.1518/001872008X374974.

Schubert, E., & Hüttig, G. (2013). Assessment of Manual Flying Skills by Combining Aircraft Parameters with Pilot Control Inputs, 177–182.

Schuet, S., Lombaerts, T., Acosta, D., Kaneshige, J., Wheeler, K., & Shish, K. (2017). Autonomous Flight Envelope Estimation for Loss-of-Control Prevention. *Journal of Guidance, Control, and Dynamics*, *40*(4), 847–862. https://doi.org/10.2514/1.G001729

Selcon, S. J., Hardiman, T. D., Croft, D. G., & Endsley, M. R. (1998). A comparative analysis of SAGAT and SART for evaluations of Situation Awareness. In *42nd Annual Meeting of the Human Factors & Ergonomics Society Chicago*. Chicago.

Şenol, M. B. (2020). A new optimization model for design of traditional cockpit interfaces. *Aircraft Engineering and Aerospace Technology*, *92*(3), 404–417. https://doi.org/10.1108/AEAT-04-2019-0068

Shaffer, F., & Ginsberg, J. P. (2017). An Overview of Heart Rate Variability Metrics and Norms. *Frontiers in Public Health*. https://doi.org/10.3389/fpubh.2017.00258

Shaughnessy, J. J., Zechmeister, E. B., & Zechmeister, J. S. (2000). *Research methods in psychology*. McGraw-Hill.

Shelnutt, J.B., Childs, J.M., Prophet, W.W., Spears, W.D. (1980). 'Human Factor Problems in General Aviation.' FAA-CT-80-194. Pensacola, FL: Seville Research Corporation.

Sherry, L. (2015a). Design of Cockpit displays to explicitly support flight crew intervention tasks DESIGN OF COCKPIT DISPLAYS TO EXPLICITLY SUPPORT FLIGHT CREW INTERVENTION TASKS, (September 2014). https://doi.org/10.1109/DASC.2014.6979567

Sherry, L. (2015b). Functional Complexity Failures and Automation Surprises : the Mysterious Case of Controlled Flight into Stall (CFIS), 488–493.

Skvarekova, I., Pecho, P., & Kandera, B. (2022). Analysis of the Most Critical Phase of the Flight Based on HRV Measurements of Pilots Workload. *17th International Scientific Conference on New Trends in Aviation Development, NTAD 2022 - Proceedings*, 194–200. https://doi.org/10.1109/NTAD57912.2022.10013591

SKYbrary. (2018). Defining Tailstrikes in Aviation. Retrieved from https://skybrary.aero/articles/tail-strike

Smith, K., & Hancock, P. A. (1995). Situation Awareness Is Adaptive, Externally Directed Consciousness. *Human Factors: The Journal of the Human Factors and Ergonomics Society*, *37*(1), 137–148. https://doi.org/10.1518/001872095779049444

Squire, L. R., Stark, C. E. L., & Clark, R. E. (2004). The medial temporal lobe. *Annual Review of Neuroscience*, *27*, 279–306. https://doi.org/10.1146/annurev.neuro.27.070203.144130

Stepanyan, V., Krishnakumar, K., Dorais, G., Reardon, S., Barlow, J., Lampton, A., & Hardy, G. (1998). Loss-of-Control Mitigation via Predictive Cuing. https://doi.org/10.2514/1.G001731

S**tuiver, A., Brookhuis, K. A., de Waard, D., & Mulder, B. (**2014). Short-term cardiovascular measures for driver support: Increasing sensitivity for detecting changes in mental workload. *International Journal of Psychophysiology*. https://doi.org/10.1016/j.ijpsycho.2014.01.010

Summers, L. G. ., Shannon, J. H. ., White, T. R. ., & Shiner, R. J. (1987). Fly-By-Wire Sidestick Controller Evaluation.

Svensson, E., Angelborg-Thanderez, M., Sjöberg, L., & Olsson, S. (1997). Information complexity-mental workload and performance in combat aircraft. *Ergonomics*, *40*(3), 362–380. https://doi.org/10.1080/001401397188206

Szabolcsi, R. (2014). PILOT-IN-THE-LOOP PROBLEM AND ITS SOLUTION PILOT-IN-THE-LOOP PROBLEM AND ITS SOLUTION, (October).

Tabachnick, B. G., & Fidell, L. S. (1996). Using Multivariate Statistics, 3rd ednHarper Collins. *New York*.

Taylor, L. (1988). *Air Travel: How Safe Is It?* (B. Publishers, Ed.). London.

Taylor, R. M. (1995). *SITUATIONAL AWARENESS RATING TECHNIQUE (SART): THE DEVELoPf4ENT OF A TOOL FOR AIRCREW SYSTEMS DESIGN*. Farnborough, Hants GU14 6SZ, United Kingdom.

Thomas, M., & Ormsby, B. (1994). On the Design of Side-Stick Controllers in Fly-By-Wire Aircraft. *ACM Applied Computing Review*, *2*(1), 15–20.

Uehara, Alan F., & Niedermeier, D. (2013). Limited Evaluation of the Influence of Coupled Sidesticks on the Pilot Monitoring's Awareness during Stall in Cruise. *AIAA Modeling and Simulation Technologies (MST) Conference*, 1–16. https://doi.org/10.2514/6.2013-4671

Uehara, Alan Fonseca. (2014). Use of active sidesticks in multi-crew commercial fly-by-wire airplanes. *DLR Deutsches Zentrum Fur Luft- Und Raumfahrt e.V. - Forschungsberichte*, (15), 1–155.

Van Baelen, D., Ellerbroek, J., van Paassen, M., & Mulder, M. (2018). Design of a Haptic Feedback System for Flight Envelope Protection. *2018 AIAA Modeling and Simulation Technologies Conference*, (January), 1–16. https://doi.org/10.2514/6.2018-0117

Van Baelen, D., van Paassen, M. M., Ellerbroek, J., Abbink, D. A., & Mulder, M. (2021). Flying by Feeling: Communicating Flight Envelope Protection through Haptic Feedback. *International Journal of Human-Computer Interaction*, *37*(7), 655–665. https://doi.org/10.1080/10447318.2021.1890489

Veltman, J. A. (2002). A Comparative Study of Psychophysiological Reactions During Simulator and Real Flight. *International Journal of Aviation Psychology*, *12*(1 SPEC), 33–48. https://doi.org/10.1207/s15327108ijap1201_4

Veltman, J. A., & Gaillard, A. W. (1996). Physiological indices of workload in a simulated flight task. *Biological Psychology*, *42*(3), 323–342. https://doi.org/10.1016/0301-0511(95)05165-1

Vidulich, M. ., Crabtree, M. S., & McCoy, A. . (1993). Developing Subjective and Objective Metrics of Situation Awareness. In *Proceedings of the 7th International Symposium on Aviation Psychology* (2nd ed.). Columbus, OH: Ohio State University.

Vidulich, M. A., & Wickens, C. D. (1986). Causes of dissociation between subjective workload measures and performance ; Caveats for the use of subjective assessments. *Applied Ergonomics*, *17*(4), 291–296. https://doi.org/10.1016/0003-6870(86)90132-8

Vorbach, T. (2013). Measuring Distribution of Attention as a Part of Situational Awareness - a Different Approach, 597–602.

Wang, C., Drees, L., & Holzapfel, F. (2016). Extracting measurements from operational flight data using the are example. In *AIAA Modeling and Simulation Technologies Conference*. https://doi.org/10.2514/6.2016-0175

Wickens, C., Hollands, J., Banbury, S., & Parasuraman, R. (2015). *Engineering Psychology and Human Performance* (Vol. Fourth edi). Psychology Press. Retrieved from https://search.ebscohost.com/login.aspx?direct=true&AuthType=ip,sso&db=nlebk&AN=1055279&site=ehost-live&authtype=sso&custid=s9872838

Wickens, C D. (2008). Multiple Resources and Mental Workload. *Human Factors: The Journal of the Human Factors and Ergonomics Society*, *50*(3), 449–455. https://doi.org/10.1518/001872008X288394

Wickens, C D. (2005). Attentional Tunneling and Task Management. *International Symposium on Aviation Psychology*.

Wickens, C D, & Carswell, C. (2021). Handbook of Human Factors and Ergonomics Chapter 5 Information Processing. In *HANDBOOK OF HUMAN FACTORS AND ERGONOMICS* (pp. 114–158). John Wiley & Sons, Ltd. https://doi.org/https://doi.org/10.1002/9781119636113.ch5

Wickens, C D, & Liu, Y. (1988). Codes and modalities in multiple resources: a success and a qualification. *Human Factors*, *30*(5), 599–616. https://doi.org/10.1177/001872088803000505

Wickens, Christopher D. (2015). Statistical Errors in Aviation Psychology : Commonsense Statistics in Aviation Safety Research, 348–353.

Wickens, Christopher D, & Science, A. (2014). Multiple resources and performance prediction, (May). https://doi.org/10.1080/14639220210123806

Wickens, Christopher D, & Science, A. (2015). Situation Awareness : Its Applications Value and Its Fuzzy Dichotomies, (December). https://doi.org/10.1177/1555343414564571

Wiegmann, D. a S. a. S., & Shappell, S. a. (2001). A Human Error Analysis of Commercial Aviation Accidents Using the Human Factors Analysis and Classification System (HFACS). *Aviation, Space, and Environmental Medicine*, *72*, 13. https://doi.org/10.1037/e420582004-001

Wiener, E. L., & Curry, R. E. (1980). Flight-deck automation: Promises and problems. *Ergonomics*, *23*(10), 995–1011. https://doi.org/10.1080/00140138008924809

Wilson, G. F. (1992). Applied use of cardiac and respiration measures: Practical considerations and precautions. *Biological Psychology*, *34*(2), 163–178. https://doi.org/https://doi.org/10.1016/0301-0511(92)90014-L

Wilson, G. F., Caldwell, J. A., & Russell, C. A. (2007). Performance and psychophysiological measures of fatigue effects on aviation related tasks of varying difficulty. *International Journal of Aviation Psychology*, *17*(2), 219–247. https://doi.org/10.1080/10508410701328839

Wolfert, F., Bromfield, M. A., Scott, S., & Stedmon, A. (2019). Passive Sidesticks and Hard Landings - Is there a Link? https://doi.org/10.2514/6.2019-3611

Woods, D. D., & Billings, C. E. (1997). Automation surprises. *Handbook of Human Factors and Ergonomics*, *2*, 1926–1943. https://doi.org/10.1207/s15327108ijap0204_5

Woods, David D, & Branlat, M. (2015). Chapter 10 : Basic Patterns in How Adaptive Systems Fail, (November).

Xiao, Wanyan, & Zhuang (2015). 'Mental workload prediction based on attentional resource allocation and information processing.' Bio-Medical Materials and Engineering, 26, S871-S879. DOI: 10.3233/BME-151379

Xu, F., Feng, S., John, E., Nacpil, C., Wang, Z., Wang, G., & Zhou, C. (2023). Modeling Lateral Control Behaviors of Distracted Drivers for Haptic-Shared Steering System. *IEEE Transactions on Intelligent Transportation Systems*, *PP*, 1–11. https://doi.org/10.1109/TITS.2023.3293504

Yang, X., B, Z. W., & Fu, S. (2021). *Multiple Physiological Indexes Analysisin Commercial Flight Tasks for Fatigue*. Springer International Publishing. https://doi.org/10.1007/978-3-030-77932-0

Yeh, Y. Y., & Wickens, C. D. (1984). *The dissociation of subjective measures of mental workload and performance. Public Release* (Vol. 30). Moffet Field, CA.

Yerkes, R.M. & Dodson, J.D. (1908). The relation of strength of stimulus to rapidity of habit-formation. Journal of Comparative and Neurological Psychology, 18, 459–482.

Young, M.S. & Stanton, N.A. (2005). 'Mental Workload.' In Handbook of Human Factors and Ergonomics Methods, Stanton, N., Hedge, A., Brookhuis, K., Salas, E., & Hendrink, H., eds. Boca Raton, FL: CRC Press.

Zeller, A.F. (1978). 'Three decades of USAF efforts to reduce human error accidents 1947-1977.' 35th Specialist Aerospace Medical Panel Meeting of NATO Advisory Group for Aerospace Research and Development, 6-10 Nov., Paris, France.

Appendices

Appendix I	Participant information sheet
Appendix II	Informed consent form
Appendix III	Adjusted SART Questionnaire
Appendix IV	Simulator output
Appendix V	Hard landing reports
Appendix IV	Tailstrike incidents

Appendix I Participant information sheet

RESEARCH PARTICIPANT INFORMATION

PROJECT:

Effects of Active Sidesticks on Pilot Monitoring Duties

Description of the research and your participation

You are being invited to take part in research on the effect of Active Sidestick on the flight deck. The study is being run by Floris Wolfert as part of a PhD Studentship under supervision from Dr Mike Bromfield. This research focusses on the effects of active coupled sidesticks on pilot monitoring duties. Within this experiment there will be several physiological measurements taken in order to objectively determine perceived workload and situation awareness. The monitored performances, physiological data and information from the surveys will enable the possibility to determine to what extent active coupled are of benefit for the Pilot Monitoring. Before you decide to take part it is important you understand why the research is being conducted and what it will involve. Please take time to read the following information carefully.

What is the purpose of the study?

The purpose of the study is to assess the effects of active sidesticks on the pilots' monitoring workload, performance and situation awareness.

Why have I been chosen to take part?

You are invited to participate in this study because you hold a current or frozen ATPL or have experience in flying commercial multi-crew aircraft.

What are the benefits of taking part?

By sharing your experiences with us, you will be helping the research team, Coventry University, and the wider aviation safety community to better understand the effect of active sidesticks on pilot workload, performance and situation awareness during different flight conditions.

Are there any risks associated with taking part?

This study has been reviewed and approved through Coventry University's formal research ethics procedure. There are no significant risks associated with participation. You may experience motion sickness while operating the simulator since it is static. However, if you feel dizzy inform the researcher and the simulation will be stopped so you can either rest or withdraw from the study.

Do I have to take part?

No – it is entirely up to you. If you do decide to take part, please keep this Information Sheet and complete the Informed Consent Form to show that you understand your rights in relation to the research, and that you are happy to participate.

Please note down your participant number (which is on the Consent Form) and provide this to the lead researcher if you seek to withdraw from the study at a later date. You are free to withdraw your information from the project data set at any time until the data are fully anonymised in our records on the 20th February 2019. You should note that your data may be used in the production of formal research outputs (e.g. journal articles, conference papers, theses and reports) prior to this date and so you are advised to contact the university at the earliest opportunity should you wish to withdraw from the study. To withdraw, please contact the lead researcher (contact details are provided below). Please also contact the Faculty Research Support Office so that your request can be dealt with promptly in the event of the lead researcher's absence. You do not need to give a reason. A decision to withdraw, or not to take part, will not affect you in any way.

What will happen if I decide to take part?

You will fly selected scenarios in Coventry University's transport aircraft simulator while answering questions posed by the researcher. After each scenario you will be asked to fill in two questionnaires. Video, audio, and physiological measures will be recorded. You will be briefed and debriefed on the study. The session should not be longer than 40 minutes.

Data Protection and Confidentiality

Your data will be processed in accordance with the General Data Protection Regulation (GDPR) 2016. All information collected about you will be kept strictly confidential. Your data will be referred to by a unique participant number rather than by name. Your data will only be viewed by the researcher/research team. All electronic data will be stored on a university computer. All paper records will be stored in a locked filing cabinet. Your consent information will be kept separately from your responses in order to minimise risk in the event of a data breach. The lead researcher will take responsibility for data destruction.

Data Protection Rights

Coventry University is a Data Controller for the information you provide. You have the right to access information held about you. Your right of access can be exercised in accordance with the Data Protection Act 1998 (up until 24th May 2018) and the General Data Protection Regulation thereafter. You also have other rights including rights of correction, erasure, objection, and data portability. For more details, including the right to lodge a complaint with the Information Commissioner's Office, please visit www.ico.org.uk. Questions, comments and requests about your personal data can also be sent to the University Data Protection Officer - enquiry.ipu@coventry.ac.uk

What will happen with the results of this study?

The results of this study may be summarised in published articles, reports and presentations. Quotes or key findings will always be made anonymous in any formal outputs unless we have your prior and explicit written permission to attribute them to you by name.

Contact information

If you have any questions or concerns about this study or if any problems arise, please contact:

Floris Wolfert (wolfertf@uni.coventry.ac.uk)
Mike Bromfield (ab2603@coventry.ac.uk)

Disclaimer:

Any aircraft performance data specified during the tests is applicable to the simulator flight model only and may differ from the real aircraft. The simulator is not certified by the EASA/CAA for training.

Appendix II Informed consent form

Participant Number:

Informed Consent Form

Please tick

1. I confirm that I have read and understood the participant information sheet for the above study and have had the opportunity to ask questions.

2. I agree to have biometric data, video and audio recordings taken during the experiment

3. I understand that my participation is voluntary and that I am free to withdraw at any time without giving a reason.

4. I understand that all the information I provide will be treated in confidence.

5. I understand that I also have the right to change my mind about participating in the study for a short period after the study has concluded.

6. I agree to take part in the research project.

If you wish to be informed on the outcome
of this research project, please leave your email address in this box

Name of participant: ____

Signature of participant: ____

Date: ____

Name of Researcher: ____

Signature of researcher: ______________________________________

Date: ____

Appendix III adjusted SART questionnaire

SITUATION AWARENESS RATING TECHNIQUE (SART; Taylor, 1990)

Instability of Situation
How changeable is the situation? Is the situation highly unstable and likely to change suddenly (High) or is it very stable and straightforward (Low)?

Stable 1 2 3 4 5 6 7 Unstable

Complexity of Situation
How complicated is the situation? Is it complex with many interrelated components (High) or is it simple and straightforward (Low)?

Simple 1 2 3 4 5 6 7 Complicated

Variability of Situation
How many variables are changing within the situation? Are there a large number of factors varying (High) or are there very few variables changing (Low)?

Few Variables 1 2 3 4 5 6 7 Many Variables

Arousal
How aroused are you in the situation? Are you alert and ready for activity (High) or do you have a low degree of alertness (Low)?

Not Alert 1 2 3 4 5 6 7 Very Alert

Concentration of Attention
How much are you concentrating on the situation? Are you concentrating on many aspects of the situation (High) or focussed on only one (Low)?

Single Focus 1 2 3 4 5 6 7 Many Aspects

Division of Attention
How much is your attention divided in the situation? Are you concentrating on many aspects of the situation (High) or focussed on only one (Low)?

Single Focus 1 2 3 4 5 6 7 Many Aspects

Spare Mental Capacity
How much mental capacity do you have to spare in the situation? Do you have sufficient to attend to many variables (High) or nothing to spare at all (Low)?

Nothing to Spare 1 2 3 4 5 6 7 Sufficient Capacity

Information Quantity
How much information have you gained about the situation? Have you received and understood a great deal of knowledge (High) or very little (Low)?

Very Little 1 2 3 4 5 6 7 A Great Deal

Familiarity with Situation
How familiar are you with the situation? Do you have a great deal of relevant experience (High) or is it a new situation (Low)?

Inexperienced 1 2 3 4 5 6 7 Experienced

Appendix IV Simulator Output

Column Number	Data Name/Description	Column Header	Data Ref	Units
1	Internal Timer	PC_Timer (ns)	N/A (Internal Timer)	nano seconds
2	XP Timer	XP_Timer (s)	sim/time/timer_elapsed_time_sec	seconds
3	Sim Paused	is paused	sim/time/paused	bool
4	Latitude	latitude	sim/flightmodel/position/latitude	degrees
5	Longitude	longitude	sim/flightmodel/position/longitude	degrees
6	Altitude above ground	y_agl	sim/flightmodel/position/y_agl	meters
7	Pitch/Theta	theta	sim/flightmodel/position/theta	degrees
8	Roll/Phi	phi	sim/flightmodel/position/phi	degrees
9	Yaw/Psi	psi	sim/flightmodel/position/psi	degrees
10	Alpha	alpha	sim/flightmodel/position/alpha	degrees
11	Beta	beta	sim/flightmodel/position/beta	degrees
12	Flight path/gamma	vpath	sim/flightmodel/position/vpath	degrees
13	Flight path/sigma (??)	hpath	sim/flightmodel/position/hpath	degrees
14	AoA Probe	AoA_probe	sim/flightmodel2/misc/AoA_angle_degrees	degrees
15	Normal G force	g_norm	sim/flightmodel/forces/g_nrml	g
16	Axel G force	g_ax	sim/flightmodel/forces/g_axil	g
17	Side G force	g_side	sim/flightmodel/forces/g_side	g
18	Wind velocity world coordinates x	wind_vx (m/s)	sim/flightmodel/forces/vx_air_on_acf	m/s
19	Wind velocity world coordinates y	wind_vy(m/s)	sim/flightmodel/forces/vy_air_on_acf	m/s
20	Wind velocity world coordinates z	wind_vz(m/s)	sim/flightmodel/forces/vz_air_on_acf	m/s
21	A/c velocity world coordinates x	vx (m/s)	sim/flightmodel/forces/vx_acf_axis	m/s
22	A/c velocity world coordinates y	vy (m/s)	sim/flightmodel/forces/vy_acf_axis	m/s
23	A/c velocity world coordinates z	vz (m/s)	sim/flightmodel/forces/vz_acf_axis	m/s
24	Indicated airspeed co pilot side	ind_as_cp_kts	sim/cockpit2/gauges/indicators/airspeed_kts_copilot	knots
25	Indicated altitude co pilot side	ind_alt_cp_ft	sim/cockpit2/gauges/indicators/altitude_ft_copilot	Feet
26	indicated vertical speed co pilot side	ind_VS_cp_fpm	sim/cockpit2/gauges/indicators/vvi_fpm_copilot	fpm
27	indicated pitch co pilot side	ind_pitch_cp	sim/cockpit2/gauges/indicators/pitch_AHARS_deg_copilot	degrees

28	Movement of the control inceptor in pitch	yoke_pitch	sim/joystick/yoke_pitch_ratio	ratio
29	Movement of the control inceptor in roll	yoke_roll	sim/joystick/yoke_roll_ratio	ratio
30	Flap position	flap_pos	sim/cockpit2/controls/flap_handle_deploy_ratio	ratio
31	Gear lever position	gear_pos	sim/flightmodel/movingparts/gear1def	bool
32	Override throttle position port	eng_thro_or_port	sim/flightmodel/engine/ENGN_thro_override	percent
33	Override throttle position starboard	eng_thro_or_stbd	"	percent
34	N2 port	eng_N2_port	sim/flightmodel/engine/ENGN_N2_	percent
35	N2 Starboard	eng_N2_stbd	"	percent
36	Thrust port	eng_thrust_port	sim/flightmodel/engine/POINT_thrust	Newtons
37	Thrust starboard	eng_thrust_stbd	"	Newtons
38	Nose wheel strut deflection	w_dflt_1	sim/flightmodel2/gear/tire_vertical_deflection_mtr	meters
39	Port wheel strut deflection	w_dflct_2	"	meters
40	Starboard wheel strut deflection	w_dflct_3	"	meters
41	Nose wheel strut force (moment from CoG?)	w_frc_1	sim/flightmodel2/gear/tire_vertical_force_n_mtr	Newton meter
42	Port wheel strut force	w_frc_2	"	Newton meter
43	Starboard wheel strut force	w_frc_3	"	Newton meter

Appendix V Hard landing reports

DATE	AIRCRAFT TYPE	REGISTRATION	SUMMARY
21-02-2007	B737-300	PK-KKV	The aircraft touched down hard at Juanda Airport, Indonesia, which resulted substantial damage to the fuselage, wheel wells and landing gears
28-05-2007	A320-200	C-FNVV	During a landing at Los Angeles Airport, United States, the aircraft bounced and touched down hard with a recorded 3.07g normal acceleration resulting in a damaged landing gear.
05-07-2007	A320-200	G-DHJZ	The aircraft landed heavily on Runway 32 at Kos Airport, Greece, causing substantial damage to the aircraft's main landing gear. It touched down with a high rate of descent, following a late initiation of the flare by the co-pilot, who was undergoing line training
31-08-2007	A340-400	EC-JFX	The aircraft touched down hard at Quito airport, Ecuador with a drift angle of 7^{o} resulting in damage to the undercarriage.
01-11-2007	B737-200	PK-RIL	The aircraft landed on runway 35 at Malang airport, Indonesia. The aircraft bounced twice after the initial severe hard landing resulting in substantial damage to the landing gear.
16-12-2007	Bombardier CL600	N470ZW	During the approach at TFGS Airport, Rhode Island, United States, the FO misunderstood a statement by the captain and reduced power to idle. The aircraft developed a high sink rate and

			during the flare stalled, impacting the runway at a high vertical rate.
08-01-2008	A321-200	F-GUAA	The aircraft touched down hard at Algiers Airport, Algeria following a bounced landing resulting in a 3.3g acceleration resulting in substantial damage to the landing gear struts.
07-02-2008	B717-200	VH-NXE	The aircraft sustained a hard landing at Darwin Airport, Australia, resulting in structural damage to the fuselage
18-07-2008	A321-200	G-DHDJ	During a landing at Manchester Airport, United Kingdom, the aircraft was not flared sufficiently and a hard landing occurred resulting in a crack in a wing rib gear support lug.
28-07-2008	A321-200	G-MARA	The aircraft made a hard landing in a flat attitude at Manchester Airport, United Kingdom, in which the nose landing gear sustained internal damage.
23-03-2009	MD-11F	N526FE	As result of a hard landing, the aircraft bounced repeatedly on Runway 34L at Narita International Airport, Japan. During the course of bouncing, its left wing broke and separated from the fuselage, the aircraft caught fire.
20-04-2009	767-300	CN-RNT	The aircraft touched down at New York Airport, United States, with a normal acceleration consistent with a "firm" landing. As the main gear touched down, a full nose down column was applied that produced a very high nose-down pitch rate, which resulted in a hard nose gear touchdown resulting in substantial damage to the fuselage and nose gear

06-05-2009	DC-10-30	N139WA	The aircraft experienced a hard landing on runway 10 at Baltimore/Washington, United States resulting in damage to the nose landing gear and wheels
04-08-2009	A320-200	CS-TKO	The aircraft experienced a very hard landing on Ponta Delgada's runway 30, Portugal, causing substantial damage to both main landing gears.
24-05-2010	Embraer ERJ-145	F-GUBF	The aircraft landed hard on to Ljubljana Airport, Slovenia, resulting in a deformed main landing gear shock absorber.
27-07-2010	MD-11F	D-ALCQ	During the landing phase on runway 33Left in Riyadh, Saudi Arabia, the aircraft bounced during the initial firm landing, which was followed by two hard landings. The aft fuselage ruptured and the aircraft eventually stopped on the side on the runway.
03-10-2010	B767-300	G-OOBK	The aircraft landed heavily on Runway 09 at Bristol Airport, United Kingdom. The de-rotation was rapid and damage occurred as a result of the force with which the nose landing gear met the runway.
12-12-2010	B777-200	F-GSPI	After touchdown of the main landing gear, the captain pushed the nose down firmly, the nose wheel bounced hard several times without dampening resulting in a damage nose wheel gear.
13-04-2011	A330-200	G-GZCB	The aircraft touched down hard at Caracas Airport, Venezuela resulting in a damaged landing gear strut.
30-07-2011	Bombardier CL-600	EC-ITU	The aircraft touched down hard with the nose and main landing gear on

			Barcelona Airport, Spain, resulting in substantial damage to the landing gear.
22-07-2011	B737-300	PK-GGO	The aircraft touched down on runway 17 of Malang Airport, Indonesia, resulting in substantial damage to the engines and landing gear.
26-09-2011	DC-95	YV136T	The aircraft made a hard touch down at Puerto Ordaz causing both engines' (JT8D) pylons and support structures at the airframe to crack.
14-02-2012	A319-111	G-EZFV	The aircraft made firm contact with the runway of London Luton Airport, United Kingdom. The normal acceleration recorded at touchdown was 2.99g, which is classified as a Severe Hard Landing and resulted in a gear replacement.
20-06-2012	767-300	JA610A	The aircraft experienced a bounce when attempting to land at Runway 16R of Narita International Airport and had a damage to the fuselage and gears.
29-08-2012	A320-200	EC-KDG	The aircraft produced a hard landing on Berlin Tegel Airport's runway 26R (Germany) and bounced with the tail contacting the runway resulting in substantial damage to the gear and tail section.
10-04-2013	A320-200	G-OZBY	During rejected go around on Prestwick airport, United Kingdom, the aircraft de-rotated rapidly resulting in substantial damage to the nose gear.
20-05-2013	A320-200	UR-WUB	The aircraft touched down hard at Kiev Airport, Ukraine, with a high pitch, resulting is damage to the landing gear and tail section.

25-10-2013	Bombardier CL-600	EC-JYA	The aircraft landed hard at San Sebastian Airport, Spain, resulting in a damage landing gear.
16-01-2014	A320-200	EI-EZV	The aircraft landed hard with a normal acceleration of 2.75g on London Heathrow, United Kingdom, resulting in 4 minor injured crewmembers, damage is not reported.
01-02-2014	B737-900	PK-LFH	The aircraft landed hard at Surabaya Airport, Indonesia, resulting in a broken wheel hub.
22-02-2014	B737-800	OK-TVT	The aircraft sustained damage during a hard landing in gusting winds at Teicera Airport, Portugal. The aircraft suffered substantial damage to the landing gear.
01-10-2014	Embraer 190	PH-EZV	The aircraft touched down hard at Schiphol Airport, The Netherlands, due to a wrongly set autopilot mode. The aircraft suffered substantial damage to the nose landing gear.
10-05-2014	A319	C-FZUG	The aircraft touched down hard on Montego Bay airport, Jamaica, exceeding the design criteria of the landing gear resulting in a gear replacement.
24-11-2014	747-800F	LX-VCC	The aircraft landed in Libreville, Gabon but touched down hard resulting in substantial damage to the landing gear and fuselage.
15-02-2015	A321-200	VT-PPD	The aircraft bounced during landing on Mumbai Airport, India and subsequently made a hard landing during the second touchdown resulting in damaged landing gear shock absorbers

14-03-2015	A330-300	9M-MTA	The aircraft experienced a hard landing on Melbourne Airport, Australia, of a magnitude requiring replacement of the aircraft's main landing gear.
25-04-2015	A320-200	TC-JPE	The aircraft landed hard on Istanbul Airport, Turkey causing damage to the right hand main gear and engine, the crew conducted a go around and during landed the right main gear collapsed.
14-07-2015	A320-200	VT-IEO	The aircraft was involved in hard landing incident during landing at NSCBI Airport, India, with a normal acceleration of 3.12g, resulting in a change of landing gear.
22-11-2015	B737-300	EX-37005	The aircraft touched down hard at Osh Airport, Kyrgyzstan, causing all gear to collapse and separate.
16-07-2016	A321-200	D-ASTP	The aircraft landed hard on Fuerteventura Airport, Spain, which resulted in substantial damage to the landing gear.
13-09-2016	737-300F	PK-YSY	The aircraft landed hard on Wamena Airport, Indonesia, resulting in the separation of both main landing gears
03-07-2017	A320-200	G-EZAW	The aircraft landed hard at Munich Airport, Germany, resulting in a damaged nose gear and left main landing gear.
18-09-2017	Embraer-145	XY-ALE	The aircraft encountered hard landing while landing to runway-11 of Sittwe Airport, Myanmar, resulting in substantial damage to the wings and landing gears
01-12-2017	A320-200	SX-ORG	Aircraft suffered a severe hard landing at Pristina airport, Kosovo, resulted in a full gear replacement.

Appendix VI Tailstrike incidents

Year	*Manufacturer*	*Type*	*Sub-Type*	*T/L*	*Registration*
2018	Airbus	A300	600	Landing	EP-MNK
2009	Airbus	A320	200	Take-off	DO-5379
2009	Airbus	A320	200	Landing	N448UA
2009	Airbus	A320	200	Landing	VQ-BBM
2009	Airbus	A320	200	Landing	N311US
2009	Airbus	A320	200	Take-off	LZ-BHC
2010	Airbus	A320	200	Landing	B-6612
2010	Airbus	A320	200	Landing	N646JB
2010	Airbus	A320	200	Take-off	N646JC
2012	Airbus	A320	200	Landing	EC-KDG
2012	Airbus	A320	200	Landing	JA8384
2012	Airbus	A320	200	Landing	P4-XAS
2012	Airbus	A320	200	Take-off	WU-6102
2013	Airbus	A320	200	Landing	HB-IJB
2013	Airbus	A320	200	Landing	HL7730
2013	Airbus	A320	200	Landing	JA8384
2014	Airbus	A320	200	Landing	9M-AJN
2014	Airbus	A320	200	Landing	B-6851
2014	Airbus	A320	200	Landing	ES-SAL
2014	Airbus	A320	200	Landing	LZ-MBD
2014	Airbus	A320	200	Take-off	TC-DCA
2014	Airbus	A320	200	Take-off	VP-BKB
2016	Airbus	A320	232	Take-off	VH-VGF
2017	Airbus	A320	200	Take-off	EI-DTB
2017	Airbus	A320	200	Landing	HS-ABB

2017	Airbus	A320	200	Landing	N137AA
2017	Airbus	A320	200	Take-off	N340NW
2017	Airbus	A320	200	Landing	PR-MHW
2018	Airbus	A320	214	Landing	B-6952
2009	Airbus	A321		Landing	HL7763
2009	Airbus	A321	200	Landing	HL7782
2011	Airbus	A321	200	Landing	F-GTAT
2011	Airbus	A321		Landing	OE-LBF
2011	Airbus	A321		Landing	OE-LBF2
2012	Airbus	A321	200	Take-off	SU-GBU
2013	Airbus	A321	200	Landing	N560UW
2013	Airbus	A321	200	Landing	VQ-BOC
2014	Airbus	A321	100	Landing	HB-IOC
2015	Airbus	A321	200	Landing	G-EUXF
2015	Airbus	A321	200	Landing	VT-PPD
2016	Airbus	A321	200	Landing	D-AVXB
2016	Airbus	A321	200	Landing	RP-C9928
2017	Airbus	A321	200	Landing	B-HTJ
2017	Airbus	A321	200	Landing	N315DN
2018	Airbus	A321	200	Landing	N204HA
2018	Airbus	A321	200	Landing	VN-A353
2018	Airbus	A321	200	Take-off	VQ-BCE
2019	Airbus	A321	200	Landing	SE-RKA
2013	Airbus	A330	300	Take-off	D-AIKJ
2016	Airbus	A330	300	Landing	B-18307
2013	Airbus	A340	300	Landing	4R-ADA
2013	Airbus	A340	300	Landing	LV-CEK
2009	Airbus	A350		Take-off	A6-ERG

2017	Airbus	A320		Landing	N173UP
2015	Antonov	AN24		Landing	RA-47805
2009	Boeing	B737	400	Landing	VQ-BAN
2009	Boeing	B737	800	Landing	JA56AN
2009	Boeing	B737	800	Take-off	S2-703
2010	Boeing	B737	800	Take-off	C-GJWS
2010	Boeing	B737	800	Take-off	N831NN
2010	Boeing	B737	800	Take-off	PH-HSW
2010	Boeing	B737	800	Take-off	PH-TFB
2011	Boeing	B737	800	Take-off	D-AHFO
2011	Boeing	B737	800	Landing	HA-LOC
2011	Boeing	B737	800	Landing	PR-GTN
2011	Boeing	B737	300	Take-off	YR-BGF
2012	Boeing	B737	33A	Take-off	G-ZAPZ
2013	Boeing	B737	800	Take-off	EI-DLE
2013	Boeing	B737	400	Landing	N449US
2013	Boeing	B737	800	Take-off	N831NN
2013	Boeing	B737	900	Landing	N34460
2013	Boeing	B737	300	Take-off	VH-ZXF
2014	Boeing	B737	800	Landing	EI-EFB
2014	Boeing	B737	800	Landing	G-GDFC
2014	Boeing	B737	800	Take-off	TC-AAS
2015	Boeing	B737	900	Landing	N461AS
2015	Boeing	B737	800	Take-off	N810NN
2015	Boeing	B737	800	Landing	VQ-BWA
2015	Boeing	B737	800	Landing	VT-JGE
2016	Boeing	B737	800	Landing	B-5302
2016	Boeing	B737	800	Landing	HL8253

2016	Boeing	B737	800	Take-off	N8602F
2016	Boeing	B737	800	Take-off	TC-TJP
2017	Boeing	B737	800	Landing	B-7031
2017	Boeing	B737	800	Take-off	EI-ENB
2017	Boeing	B737	800	Landing	LV-FUA
2017	Boeing	B737	900	Landing	N802DN
2017	Boeing	B737	800	Take-off	N901NN
2017	Boeing	B737	800		PH-CDE
2017	Boeing	B737	800	Take-off	TC-JVM
2017	Boeing	B737	800	Take-off	TC-SEO
2017	Boeing	B737	900	Take-off	VT-JBZ
2017	Boeing	B737	800	Landing	VT-JTD
2018	Boeing	B737	900	Landing	HL7725
2018	Boeing	B737	800	Take-off	LV-HQY
2018	Boeing	B737	800	Landing	N276EA
2018	Boeing	B737	800	Landing	N8327A
2018	Boeing	B737	800	Landing	OO-JAY
2018	Boeing	B737	800	Take-off	VH-YIR
2018	Boeing	B737	800	Take-off	VP-BVE
2018	Boeing	B737	800	Take-off	YR-BMF
2019	Boeing	B737	800	Take-off	LN-RRU
2019	Boeing	B737	900	Landing	N75436
2019	Boeing	B737	800	Take-off	SU-TMK
2019	Boeing	B737	800	Landing	VP-BNG
2010	Boeing	B744		Take-off	B-18723
2010	Boeing	B747	400	Take-off	N128UA
2011	Boeing	B757	200	Take-off	N609AA
2013	Boeing	B757	200	Landing	N698DL

2015	Boeing	B757	200	Landing	N553UA
2017	Boeing	B757	200	Landing	N633DL
2018	Boeing	B757	200	Landing	G-LSAI
2018	Boeing	B757	200	Landing	N654A
2018	Boeing	B757	200	Landing	UP-B5705
2010	Boeing	B767	300	Landing	N637TW
2010	Boeing	B767	300	Take-off	OE-LAZ
2010	Boeing	B767	300	Take-off	VH-ZXA
2011	Boeing	B767	300	Take-off	DL-121
2013	Boeing	B767	200	Take-off	XA-TOJ
2015	Boeing	B767	300	Take-off	C-FPCA
2016	Boeing	B767	300	Landing	N305UP
2017	Boeing	B767	300	Landing	N351AX
2011	Boeing	B772		Landing	B-2078
2009	Boeing	B777	300	Landing	HL7532
2012	Boeing	B777	200	Landing	JA701J
2016	Boeing	B777	312	Take-off	9V-SYG
2017	Boeing	B777	300	Take-off	VT-JEW
2018	Boeing	B777	333	Landing	C-FITW
2015	Avro	RJ85		Landing	EI-RJR
2016	Avro	RJ85		Landing	EI-RJG
2011	MD	MD11		Landing	D-ALCS
2013	MD	MD11		Landing	N618FE
2010	MD	MD81		Landing	OY-KHP
2009	MD	MD82		Take-off	OY-KHE